US Army Corps of Engineers

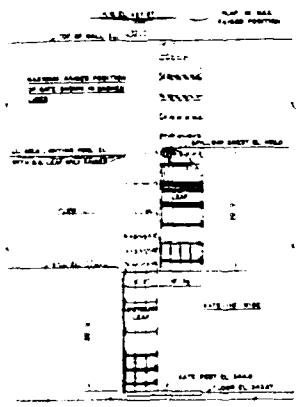

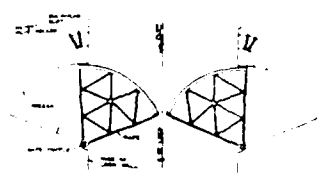

HYDRAULICS LABORATORY

MISCELLANEOUS PAPER HL-89-5

HYDRAULIC DESIGN OF NAVIGATION LOCKS

by

John P. Davis

615 Park Avenue
Prescott, Arizona 86301

September 1989
Final Report

Approved For Public Release, Distribution Unlimited

Prepared for DEPARTMENT OF THE ARMY
US Army Corps of Engineers
Washington, DC 20314-1000

Monitored by Hydraulics Laboratory
US Army Engineer Waterways Experiment Station
3909 Halls Ferry Road, Vicksburg, Mississippi 39180-6199

Unclassified

SECURITY CLASSIFICATION OF THIS PAGE

REPORT DOCUMENTATION PAGE

Form Approved OMB No. 0704-0188

1a. REPORT SECURITY CLASSIFICATION Unclassified	1b. RESTRICTIVE MARKINGS
2a. SECURITY CLASSIFICATION AUTHORITY	3. DISTRIBUTION/AVAILABILITY OF REPORT Approved for public release; distribution unlimited.
2b. DECLASSIFICATION/DOWNGRADING SCHEDULE	
4. PERFORMING ORGANIZATION REPORT NUMBER(S)	5. MONITORING ORGANIZATION REPORT NUMBER(S) Miscellaneous Paper HL-89-5
6a. NAME OF PERFORMING ORGANIZATION John P. Davis Consulting Engineer 6b. OFFICE SYMBOL (If applicable)	7a. NAME OF MONITORING ORGANIZATION USAEWES Hydraulics Laboratory
6c. ADDRESS (City, State, and ZIP Code) 615 Park Avenue Prescott, AZ 86301	7b. ADDRESS (City, State, and ZIP Code) 3909 Halls Ferry Road Vicksburg, MS 39180-6199
8a. NAME OF FUNDING/SPONSORING ORGANIZATION US Army Corps of Engineers 8b. OFFICE SYMBOL (If applicable)	9. PROCUREMENT INSTRUMENT IDENTIFICATION NUMBER
8c. ADDRESS (City, State, and ZIP Code) Washington, DC 20314-1000	10. SOURCE OF FUNDING NUMBERS PROGRAM ELEMENT NO. / PROJECT NO. / TASK NO / WORK UNIT ACCESSION NO

11. TITLE (Include Security Classification)
Hydraulic Design of Navigation Locks

12. PERSONAL AUTHOR(S)
Davis, John P.

13a. TYPE OF REPORT	13b. TIME COVERED	14. DATE OF REPORT (Year, Month, Day)	15. PAGE COUNT
Final report	FROM _____ TO _____	September 1989	291

16. SUPPLEMENTARY NOTATION
Available from National Technical Information Service, 5285 Port Royal Road, Springfield, VA 22161.

17. COSATI CODES			18. SUBJECT TERMS (Continue on reverse if necessary and identify by block number)
FIELD	GROUP	SUB-GROUP	Design, Locks, Hydraulics, Navigation, Inland waterways

19. ABSTRACT (Continue on reverse if necessary and identify by block number)

Navigation lock designs for a broad range of lifts and other conditions are described, analyzed, and compared. The emphasis is on new designs in use in waterways of the United States.

20. DISTRIBUTION/AVAILABILITY OF ABSTRACT	21. ABSTRACT SECURITY CLASSIFICATION
☒ UNCLASSIFIED/UNLIMITED ☐ SAME AS RPT ☐ DTIC USERS	Unclassified
22a. NAME OF RESPONSIBLE INDIVIDUAL	22b. TELEPHONE (Include Area Code) / 22c. OFFICE SYMBOL

DD Form 1473, JUN 86 Previous editions are obsolete. SECURITY CLASSIFICATION OF THIS PAGE

Unclassified

PREFACE

This review of the state of the art of hydraulic design of navigation locks was requested and authorized by Headquarters, US Army Corps of Engineers, in 1981.

The review was performed by Mr. John P. Davis, consulting engineer, Prescott, AZ, during the period 1981-1986.

The work was monitored by Mr. B. J. Brown, Chief, Hydraulic Analysis Branch, Hydraulic Structures Division, Hydraulics Laboratory, US Army Engineer Waterways Experiment Station (WES), Vicksburg, Mississippi, under the general supervision of Messrs. H. B. Simmons and F. A. Herrmann, Jr., former and present Chiefs of the Hydraulics Laboratory; and J. L. Grace, Jr., and Glenn A. Pickering, former and present Chiefs of the Hydraulic Structures Division. This report was prepared by Mr. Davis.

COL Dwayne G. Lee, EN, was the Commander and Director of WES. Dr. Robert W. Whalin was Technical Director.

CONTENTS

CONVERSION FACTORS, NON-SI TO SI (METRIC)
UNITS OF MEASUREMENT

Non-SI units of measurement used in this report can be converted to SI (metric) units as follows:

Multiply	By	To Obtain
cubic feet	0.02831685	cubic metres
degrees (angle)	0.01745329	radians
feet	0.3048	metres
inches	2.54	centimetres
square feet	0.09290304	square metres
tons (2,000 pounds, mass)	907.1847	kilonewtons

HYDRAULIC DESIGN OF NAVIGATION LOCK

PART I: INTRODUCTION

1. Accelerated growth of waterway traffic, the use of larger tows, the need for faster lock operation, and the use of higher lock lifts have greatly increased the demands for hydraulic design on many features of modern locks. Detailed hydraulic studies of filling and emptying systems, conditions in lock approaches, valve operation, and height and arrangement of guidewalls are required to ensure safe and reliable operation of modern locks.

Purpose and Scope

2. The purpose of this report is to present the results of research, design studies, and operation experience for guidance of hydraulic engineers in design of navigation locks. This report presents information and data that would be useful to all activities having responsibility for design of civil works projects.

Definitions

3. Definitions and explanations of the terms associated with navigation lock design are:

a. Lock chamber. Lock chamber refers to the portion of the structure encompassed by the lock walls and the gates at each end.

b. Gates. A movable barrier or barriers at each end of a lock chamber that can be opened or closed to permit a vessel to enter or exit from a lock chamber. When the gates are closed, they must be capable of withstanding the hydraulic pressure caused by the differences in water levels upstream and downstream from the lock.

c. Guide walls. Guide walls are walls that extend outward from each end of the lock chamber which serve as guide structures to aid vessels or tows in aligning for entry into the lock. For barge locks in the United States, guide walls are usually a prolongation of one of the lock chamber walls.

d. Guard walls. Guard walls are placed at each end of a lock opposite to the guide walls. The guard walls are aligned to provide flared entrances to the lock and as the name implies

provide a barrier to guard a tow from unintentionally entering areas where hazardous currents exist.

e. Sills. Lock sills are structures across the bottom of each end of the lock chamber that the gates contact to complete closure of the end of the chamber when the gates are closed. The sills usually extend upward above the lock floor by amounts varying from one to several feet, and are usually designed to withstand the full hydraulic head that would occur when the lock chamber is unwatered.

f. Lift. The lift of a lock is defined as the difference in elevation of the upstream and downstream water levels. Another term, head, is also used to denote the difference in pool levels.

g. Filling and emptying systems. The filling and emptying systems of a lock include all features such as intakes, valves, ports, culverts, and discharge outlets that are required to permit the water level in the lock to be raised or lowered. The specific features of a lock filling system vary with the adopted design. For certain low-lift locks, a filling system may consist only of valves in the lock gates that can be opened and closed to admit or discharge water. In other instances, particularly large high-lift locks, the filling system may be very complex and require an intake structure, wall culverts, complicated valve mechanisms, transverse culverts, bottom longitudinal culverts, numerous ports, and a discharge outlet structure. Depending on the lift, tonnage capacity required, importance of the waterway involved, and construction costs, the type of filling system to be adopted for a specific lock can vary in design complexity between these two cases.

h. Classification of lifts. As a result of questions regarding the meaning of the terms "high-lift locks" and "low-lift locks," the following designations have been adopted for design purposes:

Low lift	Lifts under 30 feet*
Intermediate lift	Lifts from 30 to 50 feet
High lift	Lifts over 50 feet

This classification reflects to some degree the complexity involved in hydraulic design of locks. For example, for low-lift locks, a wall culvert-side port system can be used with lifts from 10 to 30 feet, but more elaborate designs are required for lifts in the range of 30 to 50 feet. The 30- to 50-foot range requires a design that utilizes bottom longitudinal manifolds that are connected to the main wall culverts through a cross culvert at the midpoint of the lock chamber. This system provides approximate equal flow division to the upstream and downstream portions of the lock chamber by means of a vertical wall in the cross culvert. For lifts over 50 feet, it is usually desirable to provide a bottom longitudinal manifold system if satisfactory operation time and hawser stress are to be

* A table of factors for converting non-SI to SI (metric) units of measurement is presented on page 5.

tained. This system splits the flow vertically in the main ll culvert by means of a horizontal diaphragm and produces equal division of flow to four branch manifolds in the floor of each half of the lock chamber.

i. Transit time. Transit time is the total time required for a tow to move into a lock from a waiting point (arrival point), be raised or lowered, and then proceed out of the lock to a position where it will cause no interference to any other tow that needs to transit the lock.

Notation

4. The meanings of the symbols used in equations and mathematical expressions in this report are defined in the text at the places where they are first used. In addition, a complete list of the symbols used in all of the parts is presented in Appendix A for quick reference purposes.

PART II: GENERAL STUDIES FOR LOCK PROJECTS

Information and Data Required

5. In the following paragraphs, data and studies that must precede hydraulic design of a lock are discussed. The hydraulic designer is not expected to prepare studies such as capacity requirements and types of vessels to be served. However, these and other items are necessary before the various features of a lock that depends on hydraulic design can be pursued.

Type of Waterway

6. The physical characteristics of a waterway such as width, depth, and bend radii determine the type of traffic that will utilize the channels and the type of traffic, in turn, influences the design of any locks that are required. Most of the navigable inland channels in the United States have authorized depths ranging from 9 to about 15 feet. The Great Lakes connecting channels, the St. Lawrence Seaway, channels in estuaries, and several channels contiguous to the coast are exceptions as they are deep enough for vessels drawing 27 to 35 feet. Most of the vessels that ply the Great Lakes are small oceangoing ships that enter the lakes via the St. Lawrence Seaway and Great Lakes ships built specially for Great Lakes service. Since barge tows are not used on the Great Lakes, lock design for the seaway and the connecting channels is governed by requirements for lake ships and small oceangoing ships. The traffic on river channels and canals consists of barge tows and pleasure craft with drafts usually no greater than 8.5 to 9.0 feet. There are very few shallow-draft self-powered cargo vessels operating in the United States so design of locks for shallow-draft waterways is governed by requirements for tows and pleasure craft. In river estuaries near the coast, where both ships and barge traffic operate, locks that connect an estuary channel with segments of other waterways may have to be designed to accommodate barge tows, ships, and pleasure craft.

Types of Vessels

7. In designing a lock the depth on the sills, depth in the lock

chamber, the guide-wall layout, and, to some extent, the type of filling system needed are all directly influenced by the types of vessels that will use the waterway. Most of the locks in the United States are on shallow-draft waterways whose design has been governed by barge traffic and recreational traffic needs. There are no significant differences in lock design requirements for recreational craft and barge tows; however, there are conflicting design requirements for locks that are to be used by both barge tows and large ships (over 75,000 deadweight tons (dwt)). Long guide walls are required at each end of a barge lock to aid tows to align with the lock chamber, but these guide walls are an obstruction to passage of large ships. Large ships have to be moved into and out of the lock chamber with tugs, towing engines, or deck winches as they cannot maneuver into the lock with their own power. If a lock has guide walls, tugs cannot maneuver a large ship into the lock. The only solution to the problem is to provide towing engines that can move along the guide walls and lock chamber walls, towing cable systems installed at the locks, or use powered winches on the vessel's decks to move the vessel into or out of the lock. The Panama Canal Locks are the only locks with towing engines. These towing facilities reduce the transit time for vessels regardless of size and lessen the chances of accidents.

Capacity

8. The tonnage capacity required for a lock project at a specific location is determined by means of tonnage projections that are developed through economic studies of future commodity movements. Economic forecasts involve statistical studies and studies in other disciplines that are not properly a part of hydraulic engineering and are not covered in this report. Such studies usually provide estimates of annual tonnage movement of various commodities by origin and estimation for a period of 50 years in the future. The annual tonnage that can be passed through a lock project is governed by: the number and size of lock chambers, the time required for tows to transit the locks, the tonnage of the average tow, the number of days per year that the lock or locks can actually operate, the percent of time that the locks are in actual operation locking through tows, and the cost of delays to tows waiting lockage. To some extent the transit time, lock size, and number of lock chambers are mutually interdependent. Conceivably, shortening the transit time

could result in either smaller locks or possibly a lesser number of lock chambers at a specific location. Or, on the other hand, if shortening the transit time would produce extraordinary costs, it might be more economical to build a larger lock or an additional lock chamber. Therefore, when the required capacity has been established by economic studies, various plans involving different combinations of lock size, number of chambers, and operational characteristics can be studied to develop a basis for final design.

Initial Studies

9. As noted in paragraph 8, the required capacity for lockages at a given location can be met by different combinations of size of lock chamber, number of lock chambers, and different values of operation time. Sufficient preliminary studies should be made of plans with different lock sizes, a number of chambers, and operation time to provide a basis for adoption of final design features.

Lock Size

10. Lock sizes have been influenced by the sizes of barges and towing equipment and to some extent, towing equipment and practices have been influenced by lock sizes. Most of the locks built in the United States since 1950 have had usable horizontal dimensions of 84 by 600 feet, 110 by 600 feet and 110 by 1,200 feet. A number of locks with other sizes have been built which included: 56 by 400 feet; 75-foot width with lengths varying from 400 to 1,275 feet; 80 by 800 feet; 82 by 450 feet; 84-foot widths with lengths of 400, 720, 800 and 1,200 feet; and 86 by 675 feet. In addition, there have been several other smaller sizes used on smaller, less important waterways where recreational boats and small craft constitute most of the traffic. Most of the future locks will probably have widths of 84 and 110 feet and lengths varying from 600 to 1,200 feet; however, there may be locations where larger sizes may be needed. A larger lock may be necessary to transit large oceangoing ships from the Mississippi River to the new Centreport facilities at New Orleans, Louisiana; and larger locks may be necessary on the Lower Ohio River to transit larger barge tows. At this latter location, projected tonnage is so great for the decades after year 2000 that the ultimate selection of a plan

may involve use of as many as three 110- by 1,200-foot locks, a lesser number of larger size locks, or a combination of sizes.

Number of Lock Chambers

11. In the initial development stage of a waterway, the usual practice has been to provide one lock at each location; then as traffic increased, additional lock chambers were added which in most instances were larger than the original ones. On developed waterways, where traffic patterns are well-established and continued growth is assured, it is prudent to provide a minimum of two locks at each location. In the event of outage of one of the locks, at least a good portion of the traffic can still be transited. In redevelopment of the Ohio River system, a minimum of two locks has been provided at each of 19 locations. This practice is also being followed at all of the lock locations on the Rhine and Danube rivers in Austria, Germany, France, and The Netherlands. The character of the traffic may also influence the number of lock chambers needed at a specific location. If the traffic is predominantly small tows and recreational craft, two or three locks large enough to accommodate most of the tows without double lockage would provide greater capacity and more efficient operation than one very large lock. More time is required for a number of small tows to enter and moor in a large lock chamber than is required for the same number of tows to transit two or three smaller locks.

Transit Time

12. The time required for tows to transit the locks along a waterway may constitute a major part of the total trip time for a tow. Therefore, the objective in planning a lock project is to develop an overall design that reduces transit time to a minimum commensurate with cost and established engineering criteria. Transit time, as defined in paragraph 3, can be separated into seven different components: (1) time required for a tow to move from an arrival point to the lock chamber, (2) time to enter the lock chamber, (3) time to close the gates, (4) time to raise or lower the lock surface (fill or empty), (5) time to open the gates, (6) time for the tow to exit from the chamber, and (7) time required for the tow to reach a clearance point so that

another tow moving in the opposite direction can start toward the lock. The seven components of time listed above represent the total transit time for continuous lockages alternating in direction of movement. Obviously, different tow arrival situations at a lock can produce different total transit times. When a series of lockages occur with tows moving in the same direction, the transit time will be different from the alternating lockage situation. Two of the seven time components listed above (gate operating time and filling and emptying time) are dependent entirely on design of the lock. Approach time, entry time, exit time, and departure time are dependent on pilot skill and towboat capability, and also on design of approach channels, guide walls, and lock chambers. At many of the recently built locks, lock operation time for a single lockage constitutes about 25 to 40 percent of the total transit time. Thus, in attempting to reduce transit time by reducing lock operation time, a point can be reached where decreases in total transit time produce disproportionate increases in cost. Nevertheless, every minute saved in lock operation is significant economically to a project and becomes more important when growth of traffic begins to cause prolonged queuing delays. By means of many model tests and design studies, filling systems have been developed that achieve filling times of 6 to 8 minutes with locks having lifts no greater than 30 feet. These systems have been more or less standardized and can be built at acceptable cost. To reduce the filling time to less than 6 minutes would require excessively large culverts, valves, intakes and outlets and would materially increase the size and cost of walls. For lifts in the range of 30 to 50 feet, an 8-minute filling time can still be achieved, but the design becomes more complex and slightly more costly. For lifts in excess of 50 feet (up to 100 feet), it becomes difficult to obtain a filling time under 10 minutes.

Location

13. The general locations of locks are usually established by hydraulic studies of the physical conditions of the waterway involved. Within a general area or short reach, the final exact location of a locks project is usually determined by foundation conditions and by means of a general river model. The proper location of a lock with respect to channel alignment, river currents, and other structures is very important as it affects directly the time

required for a tow to move from an arrival point to the lock. Lock location and factors that must be considered are covered in US Army Corps of Engineers literature.

Basis of Design

14. In the foregoing paragraphs of this part the data needed, the studies required, and the factors that have to be considered in determining a sound basis for design of a lock have been presented. When proper consideration has been given to all of these factors, the location, the lock size, the number of chambers needed, and the desired operation time will be known. Design of the hydraulic features of the lock, such as culverts, intakes, outlets, valves, height of walls, and arrangement of guide walls, can proceed.

PART III: TYPES OF LOCKS

Lock Structures

15. Most of the locks in the United States are built of concrete. There are a few built with concrete gate bays and sheet-pile tieback walls or sheet-pile cell walls, and several locks have been built that have concrete gate bays with earth embankment walls. A few very old locks that are constructed of stone masonry are still in use on some of the older canalized river projects.

Concrete Lock Structures

16. Lock structures built of concrete are used at almost all locations where lifts exceed about 10 feet. Most designs utilize concrete gravity walls founded on either piling or rock. Where extremely poor foundation conditions exist such as soft mucky material, the drydock or bathtub design is sometimes used as it provides some insurance against undesirable differential settlement. One high-lift lock founded on rock has been built with buttress-type walls. Most of the concrete locks have filling systems with longitudinal culverts in the walls and with intakes either in the lock walls or the floor of the upper entrance. Discharge outlets have been placed in the lock walls or in transverse culverts downstream from the downstream gate bay. At most of the concrete locks, but not all, guide walls and guard walls are also built of concrete. There are several locks with timber guide walls and floating caisson guide walls. A typical concrete lock is shown in Figure 1.

Sheet-Pile Cellular Locks

17. At locations where the lift is no more than 10 feet and where heavy traffic (with large tows) is expected, the lock chamber walls between gate bay monoliths can be formed by sheet-pile cells. This type of structure requires that an end filling system be used. Such a system may utilize loop culverts around the gates with valves in the culverts, slide valves or butterfly valves in miter gates if miter gates are used, or filling by means of gradually opening sector gates where sector gates are used. Sheet-pile cell locks offer

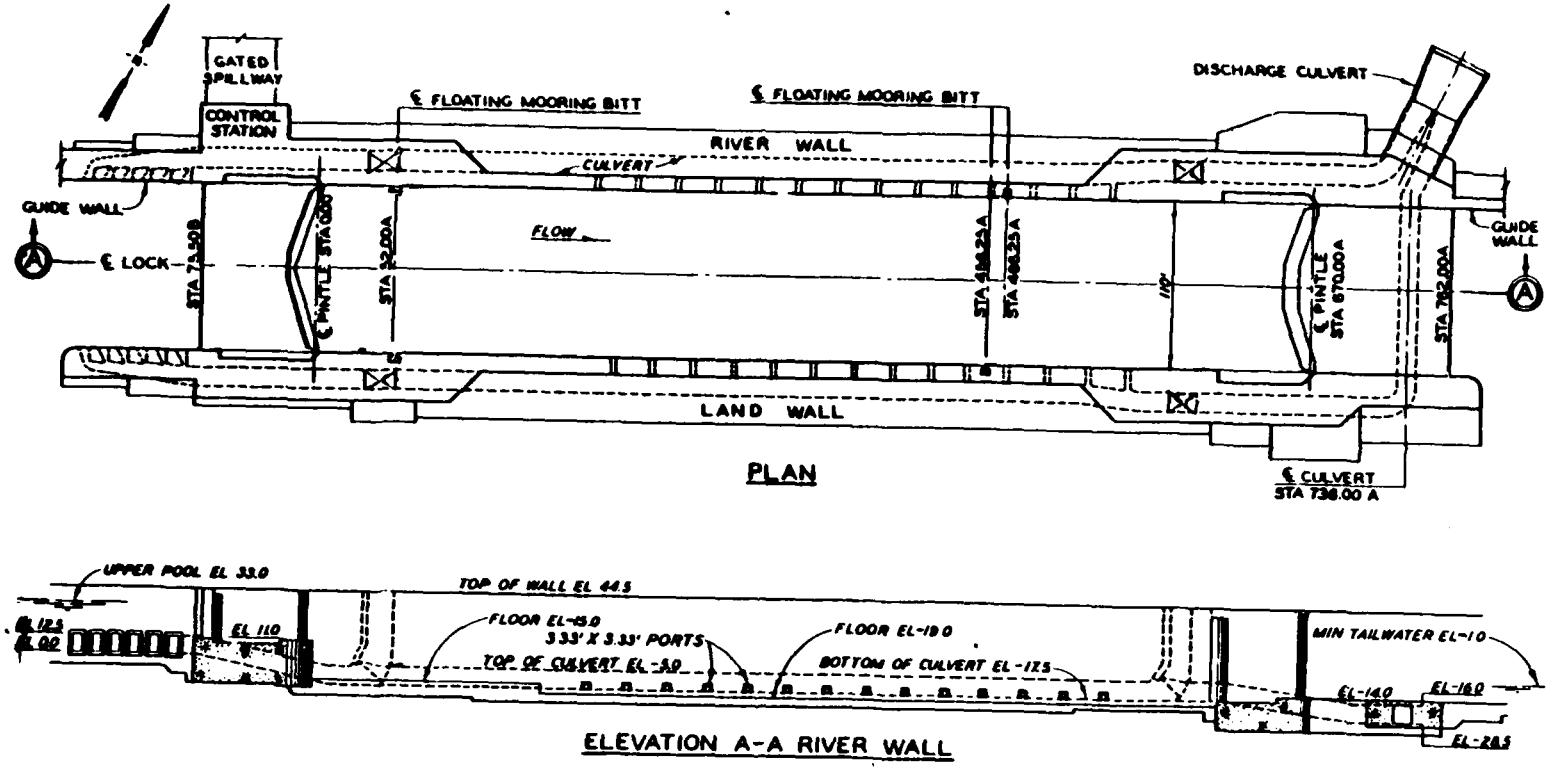

Figure 1. Typical concrete lock

advantages in lower first cost where traffic may not be great enough to warrant a more expensive structure and at places where a temporary lock may be needed. However, this type of lock will involve a shorter useful economic life and higher maintenance costs. Figure 2 illustrates a sheet-pile cellular lock.

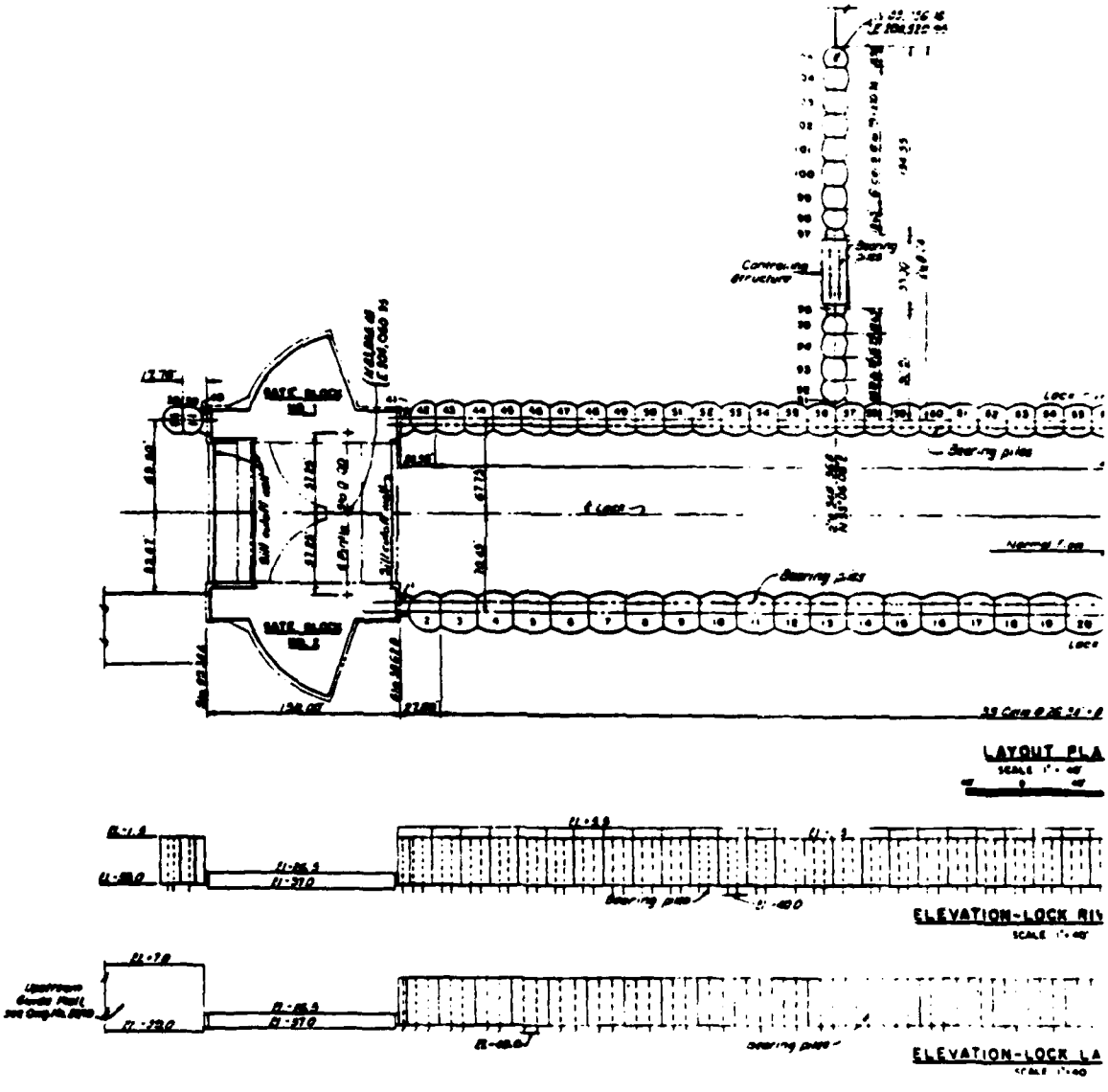

Figure 2. Typical sheet-pile cellular lock

Sheet-Pile Lock with Tieback Anchorage

18. An alternative type of sheet-pile lock that utilizes walls between

gate bay monoliths is built of M-Z steel sheet piling supported laterally by wales and tierods, near the top of the wall, connected to embedded anchorages. Horizontal struts are usually placed across the bottom of the lock to prevent inward movement of the sheet piles at the bottom, and the tie-rods connected to the anchors prevent movement of the top of the wall. This type of lock is generally only suitable for low heads where traffic is not heavy and operation time is not a critical factor. Sheet-pile locks are filled and emptied through sector gates, loop culverts, a combination of sector gates and culverts, or valves in miter gates. If reversal of head is involved, sector gates should be used. If no head reversal occurs, the lock gates may be of the mitering type, but loop culverts or valves in the gates would have to be provided for filling and emptying. Figure 3 shows a sheet-pile lock.

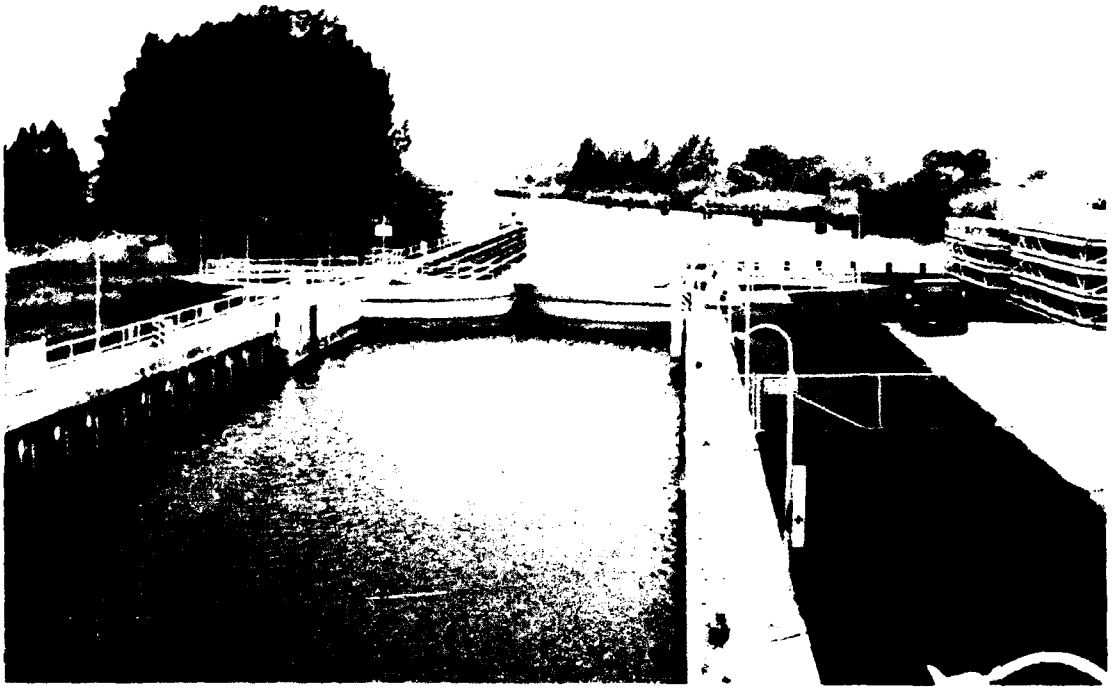

Figure 3. Lock with sheet-pile walls

Earth Wall Locks with Concrete Gate Bays

19. At locations where the lift rarely exceeds 1 or 2 feet and where the maximum lift is less than 5 feet, a reasonably satisfactory lock can be designed by using earth embankments for chamber walls with concrete gate bays

forming the ends of the lock. Such locks have been built in the Gulf Intracoastal Waterway at several locations to prevent saltwater intrusion into agricultural areas and to prevent adverse or dangerous currents during abnormal tide conditions. The earth embankments walls are essentially levees, with riprap protection on the side slopes. The bottom of the channel (the chamber) is also protected with riprap from scour by towboat propellers. A timber guide wall with a walkway is provided for tows to moor during lockage. Because of the low lifts involved where this type of lock is used, filling and emptying through the gates by means of slide valves in miter gates or by gradual opening of sector gates is acceptable. If reversal of head occurs, sector gates should be used; but if the head always occurs from the same direction, miter gates can be used. A lock of this type is shown in Figure 4.

Selection of Lock Type

20. In the foregoing paragraphs of this part, brief descriptions of four types of lock structures have been presented along with some of the factors that influence their designs and selection. The final selection of the type of lock to be built at a specific location on a waterway must be governed by the following factors: (1) capacity required, which is dependent on operation time and on type, size, and number of vessels; (2) foundation conditions; (3) planned economic life; (4) first cost; (5) maintenance and operation costs; and (6) reliability and safety. On important busy waterways, concrete lock structures have been generally accepted as the most reliable and desirable from all engineering and economic considerations. On waterways where traffic is not heavy and at locations on such waterways where the lift is very low, sheet-pile locks or possibly earth wall locks may be suitable.

Figure 4. Earth wall lock with concrete gate bays

PART IV: FEATURES OF LOCKS

21. In the preceding parts of this report, different kinds of locks were discussed and the terminology applicable to locks was defined. In this part, further details of the important features of locks are presented. The principal features of a lock for barge traffic are: guide walls, guard walls, sills and gates at each end, operating machinery, lock-chamber walls, and control and communications equipment. Depending on the type of lock under consideration there may be additional features such as intakes, culverts, valves, discharge ports, discharge outlets, emergency closures, floating mooring bits, and sometimes either a fixed or movable bridge.

Guide Walls

22. Guide walls, essentially continuations of a lock wall, are placed at each end of a lock to aid a towboat pilot in aligning the tow for entry into the lock chamber. The face of a guide wall is flush with the face of one of the lock chamber walls so that a tow lying alongside a guide wall can move straight ahead to enter or leave the lock chamber. As the name implies, a guide wall provides a towboat operator with a structure to help guide the tow to the lock entrance. It provides visual aid, can be used to pull the tow into alignment, and can be used for temporary mooring. If there is only one lock chamber at a lock project the guide wall may be placed on either side of the lock, depending on the configuration of the channel, proximity to a spillway, and occurrence of adverse river currents. Many of the single lock projects in the US have guide walls on the landward side. There are some operating advantages in having the guide wall at each end of a lock on the same side of the lock chamber. At projects where parallel locks are to be built, the proper location of guide walls becomes more complex. No general rules can be established and the only satisfactory means of determining the proper location is by studies on a general river model of the channel, lock approaches, and the locks and dam. Guide-wall lengths are usually made the same as the usable lock chamber length. In some instances, it may be necessary to increase the length of a guide wall if unusually hazardous situations develop during high river stages. At low-lift and medium-lift locks, the elevations of the guide walls are frequently at the same elevation as the top

of the lock walls. At high-lift locks, the upstream guide wall is usually at the same elevation as the lock walls; but the downstream wall will be based on tailwater elevations.

23. Guide walls may be constructed as concrete gravity walls, timber walls supported by pile clumps, or floating caisson structures. Virtually all concrete lock structures have concrete gravity guide walls. A few high-lift locks at multipurpose projects have concrete (caisson) floating guide walls at the upstream end. A plan of a typical concrete guide wall at the upstream end of a lock is shown in Figure 5, and a photograph of a lock with concrete guide walls is shown in Figure 6. Timber guide walls have been used where the lift is low (5 to 10 feet) and where traffic consists of smaller tows. The first cost is low (relatively) but maintenance is high. Timber has a better fendering quality which may make it more desirable. The usual type of construction for timber guide walls consists of heavy timber walers supported by clumps of timber piling. A timber walkway and mooring bolards are provided (attached to the pile clumps) for linesmen to use. Figure 7 shows a timber guide wall at a low-lift lock. Some of the high-lift locks on the Snake River have floating guide walls. A typical floating caisson guide wall is shown in Figure 8.

Guard Walls

24. Guard walls are placed at each end of a lock on the opposite side from the guide walls. They are usually much shorter than guide walls and are angled outward from the end of the lock so that a misaligned tow would strike the guard wall at an angle instead of hitting the end of the lock wall head-on. Guard walls are built of concrete or timber similar to guide walls. Short, floating guard walls are usually uneconomical. There are situations when two parallel locks are built adjacent to a spillway, where a guard wall may be as long or longer than a guide wall. Figure 6 shows this type of arrangement.

Lock Sills

25. The sills of a lock are the structures across the bottom at each end of the lock chamber that the gates contact when they are closed to complete closure of the end of the lock. In all modern locks, the sills are

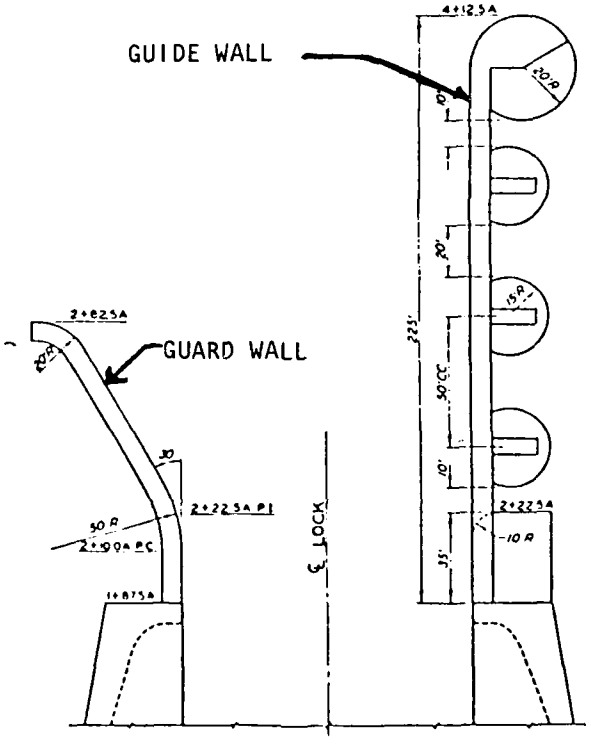

Figure 5. Typical concrete guide wall (upstream)

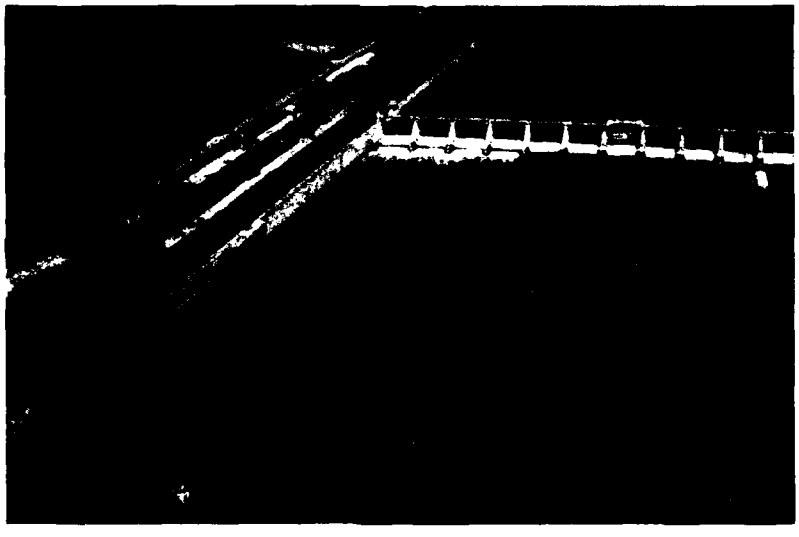

Figure 6. Guide wall and guard walls, parallel locks

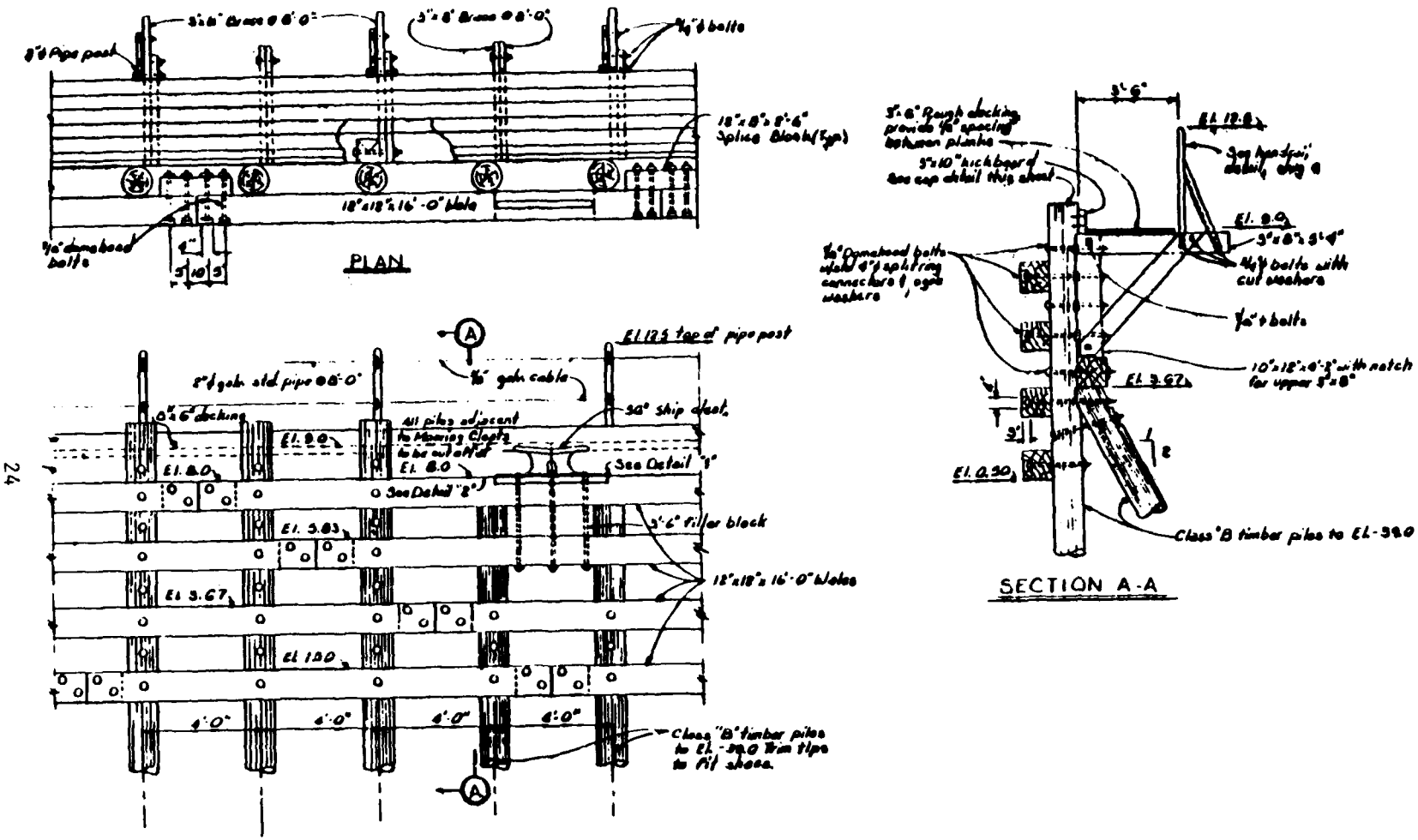

Figure 7. Timber guide wall

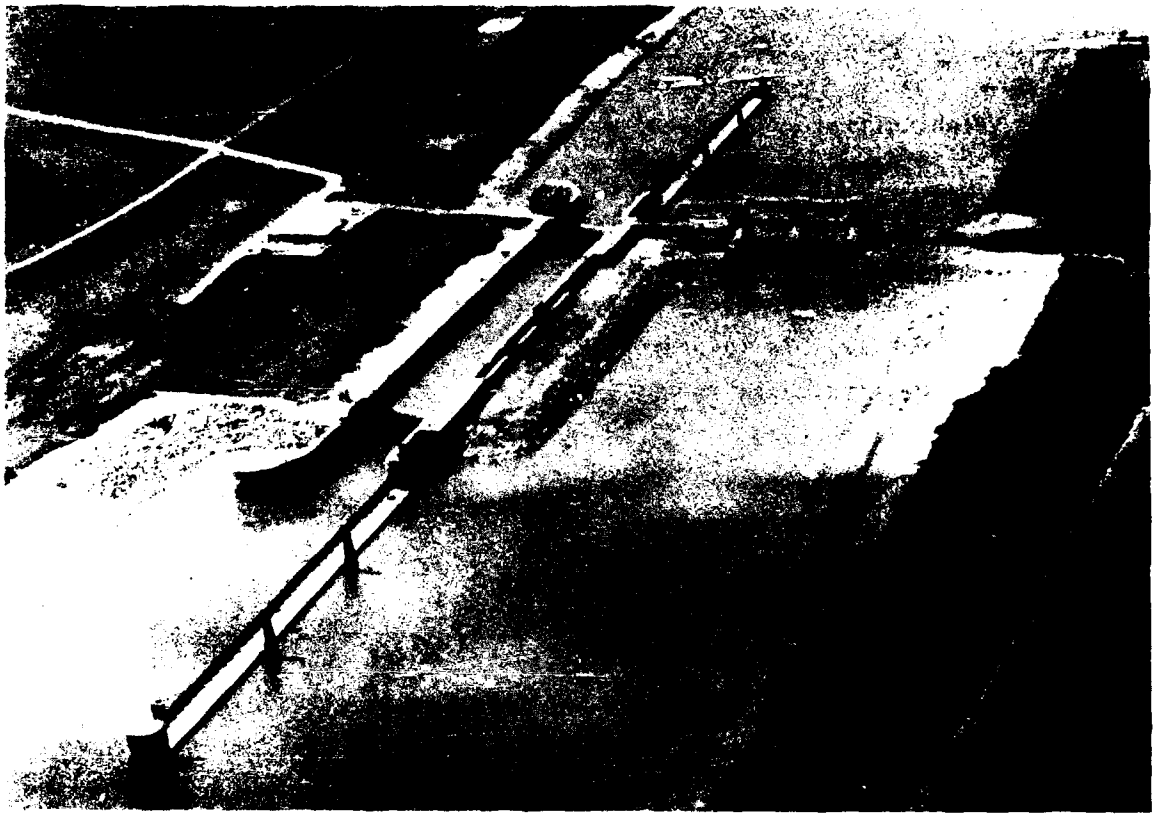

Figure 8. Floating caisson guide wall

concrete and form part of the gate block (gate bay) at the ends of the lock chamber. There are no specific characteristics of lock sills that involve hydraulic design, except for their depth below minimum pool levels. Guidance on sill depth is presented in Part VI.

Lock Gates

26. Eight different types of gate structures are being used for lock gates:

a. Miter gates.
b. Submergible vertical-lift gate.
c. Overhead vertical-lift gate.
d. Submergible tainter gate.
e. Vertical axis sector gate.
f. Rolling gate.
g. Tumbler gate.
h. Rising sector gate.

Miter gates

27. A miter gate has two parts or leaves which has led to the designation of "miter gates" even though the two leaves only provide a closure at one end of the lock. The miter gate derives its name from the fact that the two leaves meet at an angle pointing upstream to resemble a miter joint. Horizontally framed miter gates possess many advantages over other types and have been used on more locks than any other kind. Miter gates are rugged, do not involve complicated construction problems, are easily serviced, and are fast operating. Their only drawbacks rise from their inability to operate under head and to withstand very much reverse head. Figure 9 illustrates a typical miter gate installation.

Submergible vertical-lift gate

28. Submergible vertical-lift gates can sometimes be used to advantage at the upstream end of a lock. If the lift is high enough, a single leaf gate can be designed so that when it is lowered it drops along the downstream vertical face of the upstream sill block. If the lift is not as great as the upstream sill depth, the gate may have two leaves that telescope together when they are lowered. It is not advisable to try to use a submergible

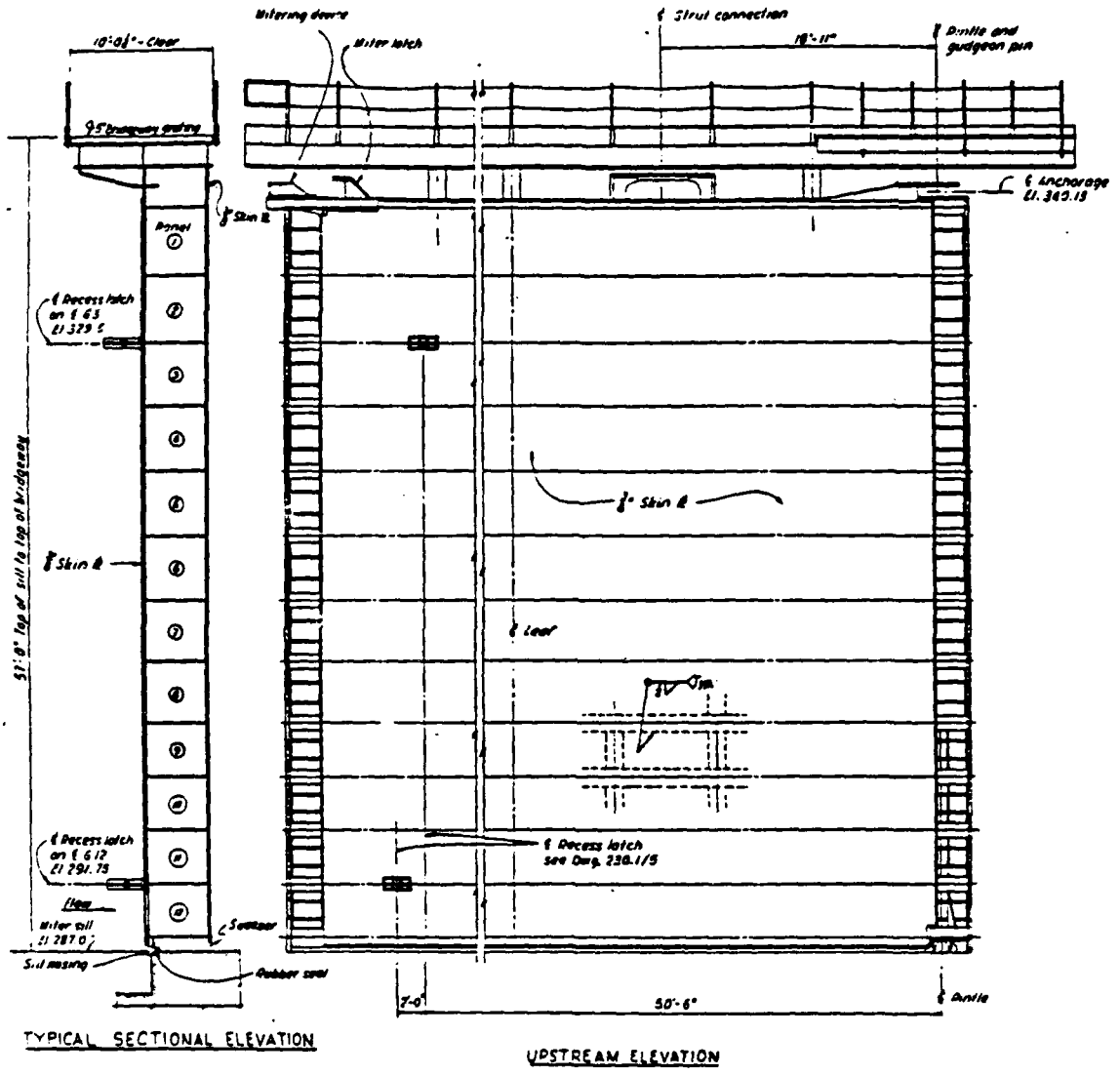

Figure 9. Miter gate

vertical-lift gate in a situation where the leaf or leaves would have to rest in a bottom recess when the gate is lowered. Debris and silt would cause operation problems and lead to high maintenance costs. A vertical-lift gate can be designed to resist reverse head as well as direct head and can be designed to operate under either direct head or reverse head. The disadvantages are high maintenance and operation costs, difficulty in controlling skew and misalignment, and greater vulnerability to damage from collision than miter gates. Figure 10 shows a typical submergible double leaf vertical-lift gate.

Overhead vertical-lift gate

29. The overhead vertical-lift gate has been used as the downstream gate at several locks where the lift is great enough to provide sufficient overhead clearance when the gate is in the raised position. This type of gate has been used at the downstream end of the John Day, Ice Harbor, and Lower Monumental Locks. Overhead lift gates at these locks are very rugged and heavy. They possess the same general advantages as the submergible lift gates, but require a longer operation time--2 to 3 minutes. Operation and maintenance problems are not as great with overhead lift gates as with submergible gates. Figure 11 shows a typical overhead vertical-lift gate.

Submergible tainter gate

30. Submergible tainter gates have the same advantages as submergible lift gates, but are subject to the same limitations with regard to their use in a low- or medium-lift situation. The lift must be great enough to permit the gate to submerge to below the sill without resting directly on the lock floor. There are fewer operating and maintenance problems with submergible tainter gates than with vertical-lift gates. A typical submergible tainter lock gate is shown in Figure 12.

Vertical axis sector gate

31. A vertical axis lock sector gate, like a miter gate, requires two gates at each end to effect closure of a lock chamber. Sector gates might be compared with a pair of tainter gates where the trunions are mounted on a vertical axis. Sector gates are used in pairs and are designed to rotate around a vertical axis and meet at the center line of the lock chamber. Since the hydrostatic pressure is toward or away from the gate axis, there is very little unbalanced hydraulic force opposing opening or closing under any condition of head. Figure 13 shows a plan of a typical sector gate. Since sector gates can be opened or closed under a head, they can be used as a means of

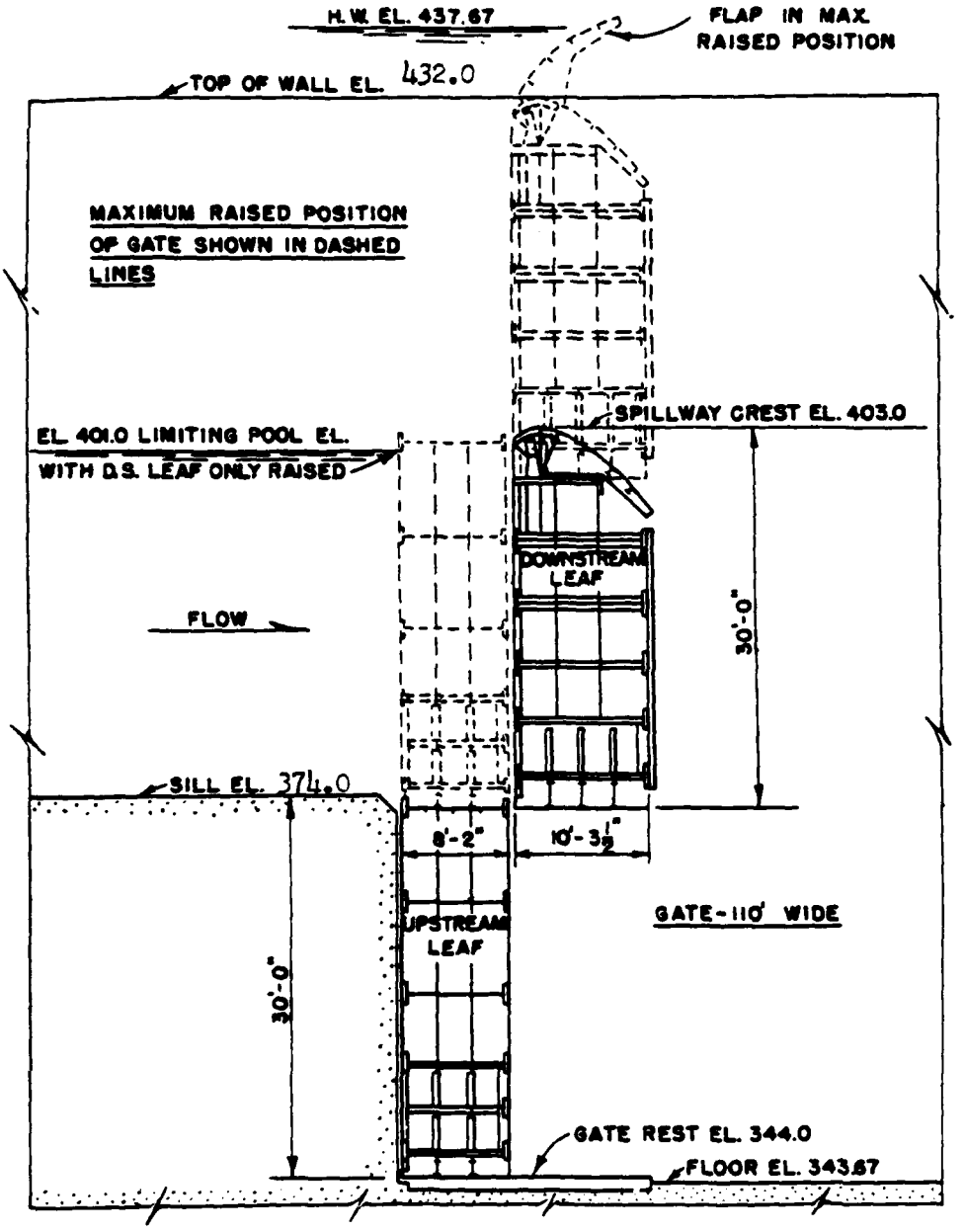

Figure 10. Submergible vertical-lift gate

Figure 11. Overhead vertical-lift gate

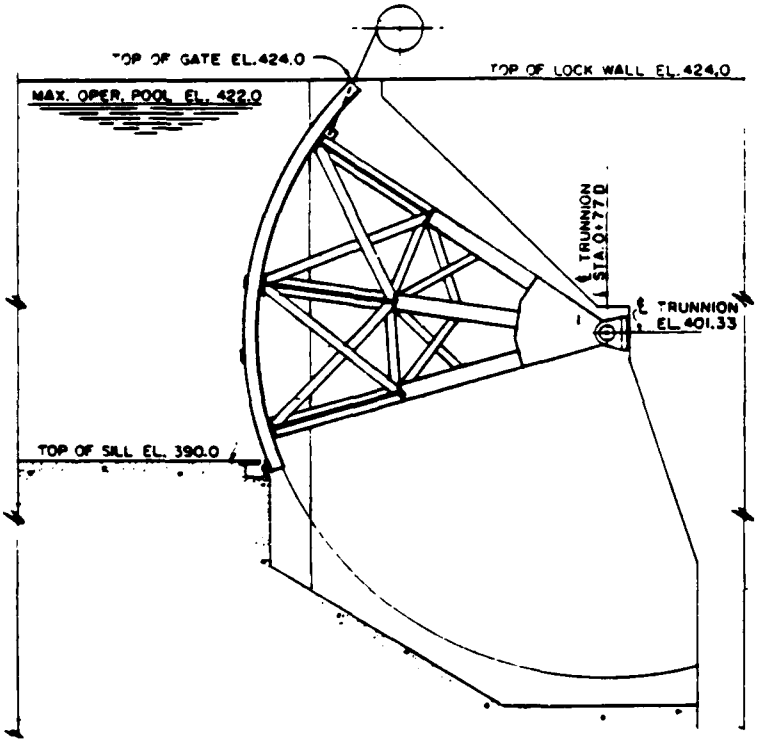

Figure 12. Submergible tainter gate

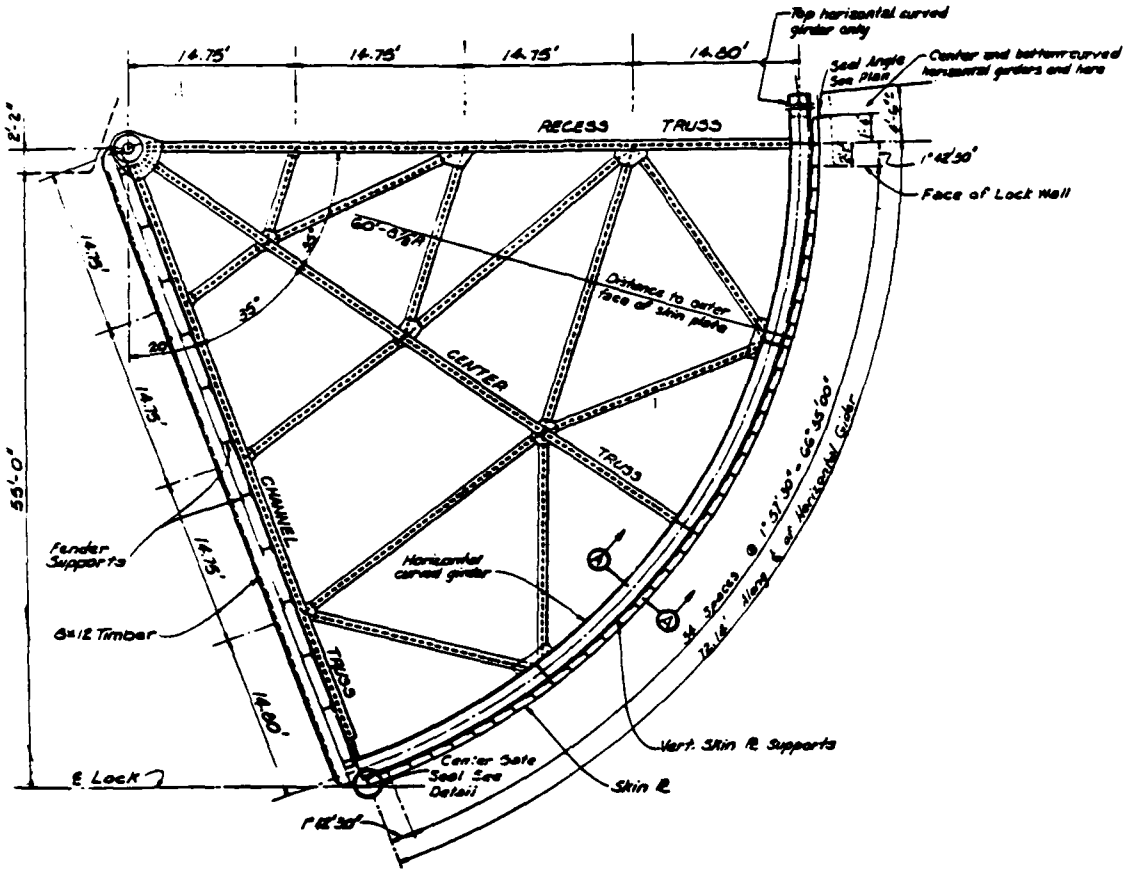

PLAN OF TOP HORIZONTAL FRAME

Figure 13. Sector gate

filling and emptying locks with very low lifts. Sector gates can be designed to withstand head from either direction and are very useful at a tidal lock or at any situation where reversal of head occurs. The two principal disadvantages are their cost and the amount of horizontal space required.

Rolling gate

32. A rolling gate consists of a structural steel frame with a skin plate, arranged to roll horizontally across the lock chamber from a recess in one lock wall. The structure moves on flanged wheels riding on rails embedded in the lock sill. When the gate is in the closed position, each end extends into a recess in its respective wall. When the gate is opened, it is pulled back into a recess in one wall that is long enough to receive the entire gate length. This type of gate was used in early canalization of the Ohio River before miter gates were developed that span 110-foot-wide locks. Several other early lock projects used this type of gate, but it has been entirely

supplanted by other gate types in recent years. Rolling gates are still being used on recent large lock projects in Europe. Use of this type of gate complicates design of a filling system. A typical rolling gate structure is shown in Figure 14.

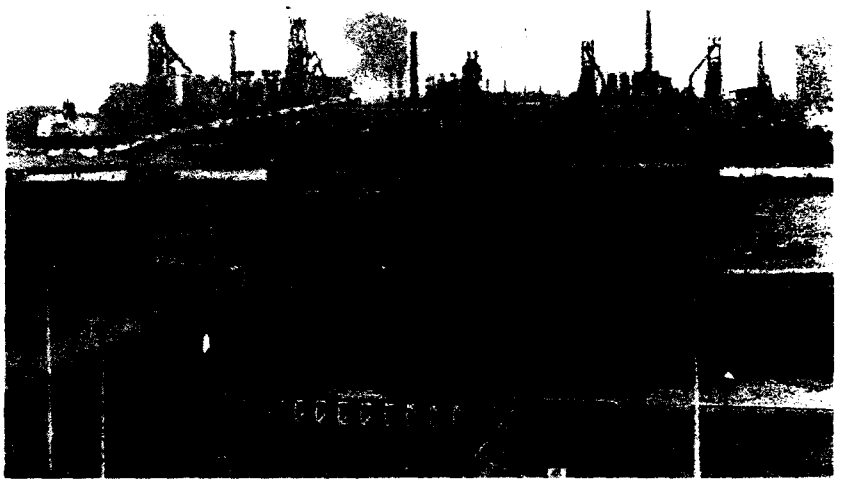

Figure 14. Rolling gate

Tumbler gate

33. A tumbler gate is a single gate leaf with a horizontal hinge across the lock sill. In the open position, the leaf lies flat on the bottom of the lock chamber. To close the gate, the free edge of the gate is pulled upward in an arc and is retained in the vertical position by a locking mechanism.

Rising sector gate

34. The rising sector gate is a relatively new gate design. It is currently being used in Europe for locks that are approximately 75 feet wide and also as a flood barrier gate in England. This type of gate is essentially a segment of a circle attached to horizontal axis trunion arms mounted on pivots at each end. When the gate is in the raised position, the curved surface of the segment closes the space between the sill and the water surface. When the gate is lowered, it is rotated 90 degrees so that the segment then occupies a recess in the sill. In this position the gate causes no obstruction to traffic. Since this gate is untried for large locks, its reliability, usefulness, and cost are unknown.

Intakes

35. The intakes of a culvert filling system are designated as separate features of a lock because of their importance in design of a filling system and because most of the locks in the US utilize filling systems that have culverts. An intake structure must be designed to conduct water from the upstream pool at a lock into the culvert system with a minimum of head loss and without producing serious vortices. Most of the intake structures have several ports that gradually converge as they lead into a culvert in the wall. Some locks have intake ports placed in the lock approach floor that lead vertically downward and then turn outward into the lock chamber wall. In other designs the intakes have several ports placed in the lock walls (upstream from the gates) that lead horizontally into wall culverts. Further details on intakes are presented in Part VIII. An intake is shown in Figure 15.

Culverts

36. Culverts are a principal feature of the filling system on many locks. The culverts conduct flow from the intakes through the lock walls to ports connecting the culvert to lock chamber or, in some designs, into smaller culverts with ports across the bottom of the chamber. In some designs wall culverts conduct flow to the midpoint of the lock chamber where it enters a crossover culvert that connects with longitudinal floor culverts with ports. In the US, all locks built in the last 40 years have rectangular or square culverts. Round culverts were used in some of the older locks and are still being used occasionally in Europe.

Valves

37. Valves to control flow into and out of the lock chamber, of several different types have been used in the past, but in recent years almost all permanent locks (culvert filling systems) have utilized reverse tainter valves. The following different types of valves are used:

a. Slide valve.

b. Wagon valve (wheeled vertical-lift valve).

c. Stoney valve.

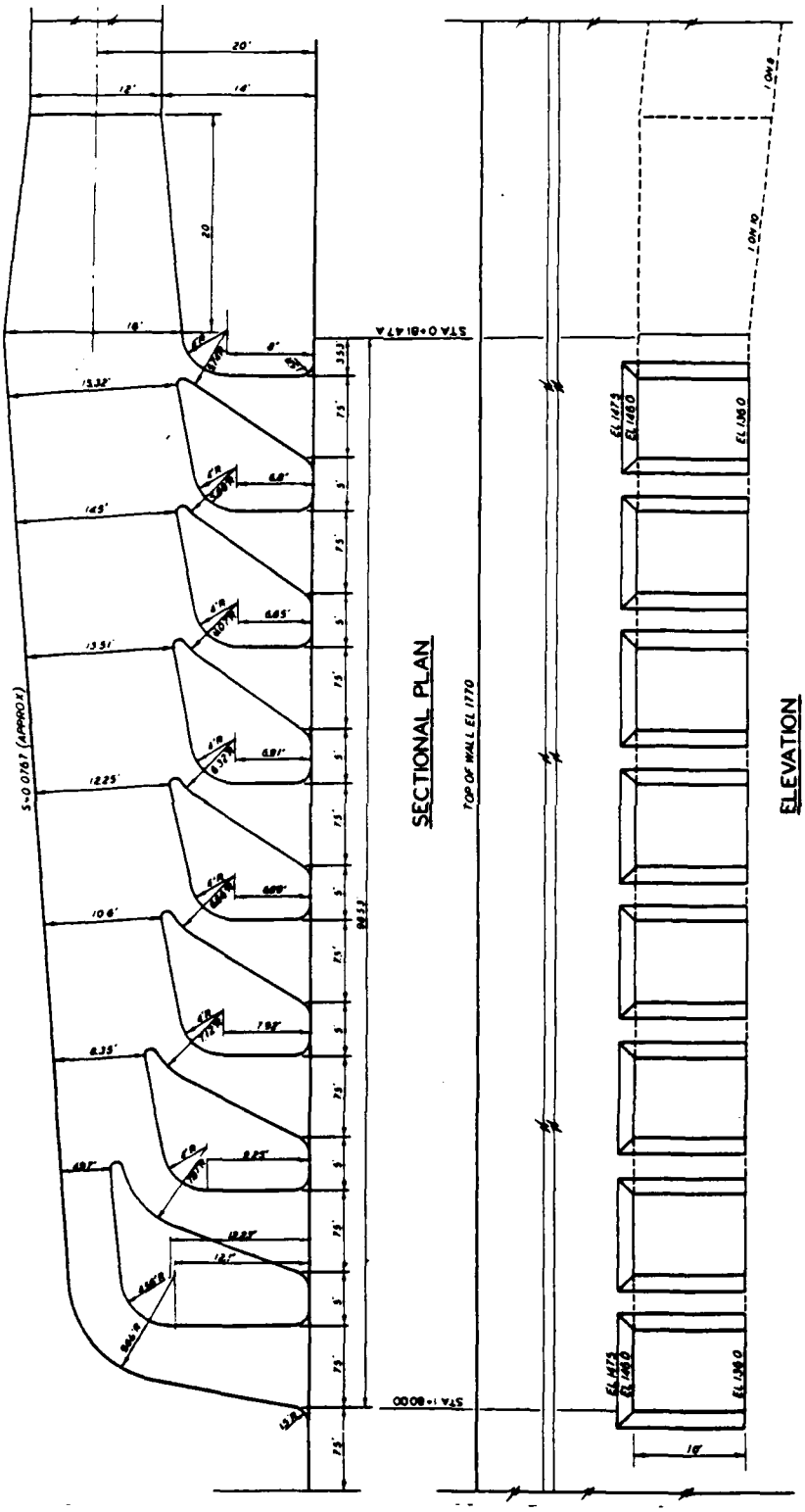

Figure 15. Intake for low-lift lock

d. Butterfly valve.

e. Tainter valve.

f. Reverse tainter valve.

A reverse tainter valve is shown in Figure 16. Design of valves is presented in Corps of Engineers literature.

Discharge Outlets

38. The culverts that conduct water out of the lock chamber usually terminate in a structure that is designed to dissipate the energy of the flowing water and reduce velocities. Such a structure may consist of a number of horizontal ports that extend through the lock wall into the downstream lock entrance; or a culvert may terminate in a rectangular basin with an end sill located on the riverward side of the downstream end of the lock. Figure 17 shows a typical outlet structure of the former type.

Operating Machinery

39. The operating machinery at a modern lock includes the hydraulic rams used to operate the gate and valves; the oil pumps and receiver system; the necessary controls; standby electric power source; and communications equipment required to operate the lock. Very little use is made of direct electrically driven mechanisms for gate or valve operation, as the hydraulic systems have superior advantages.

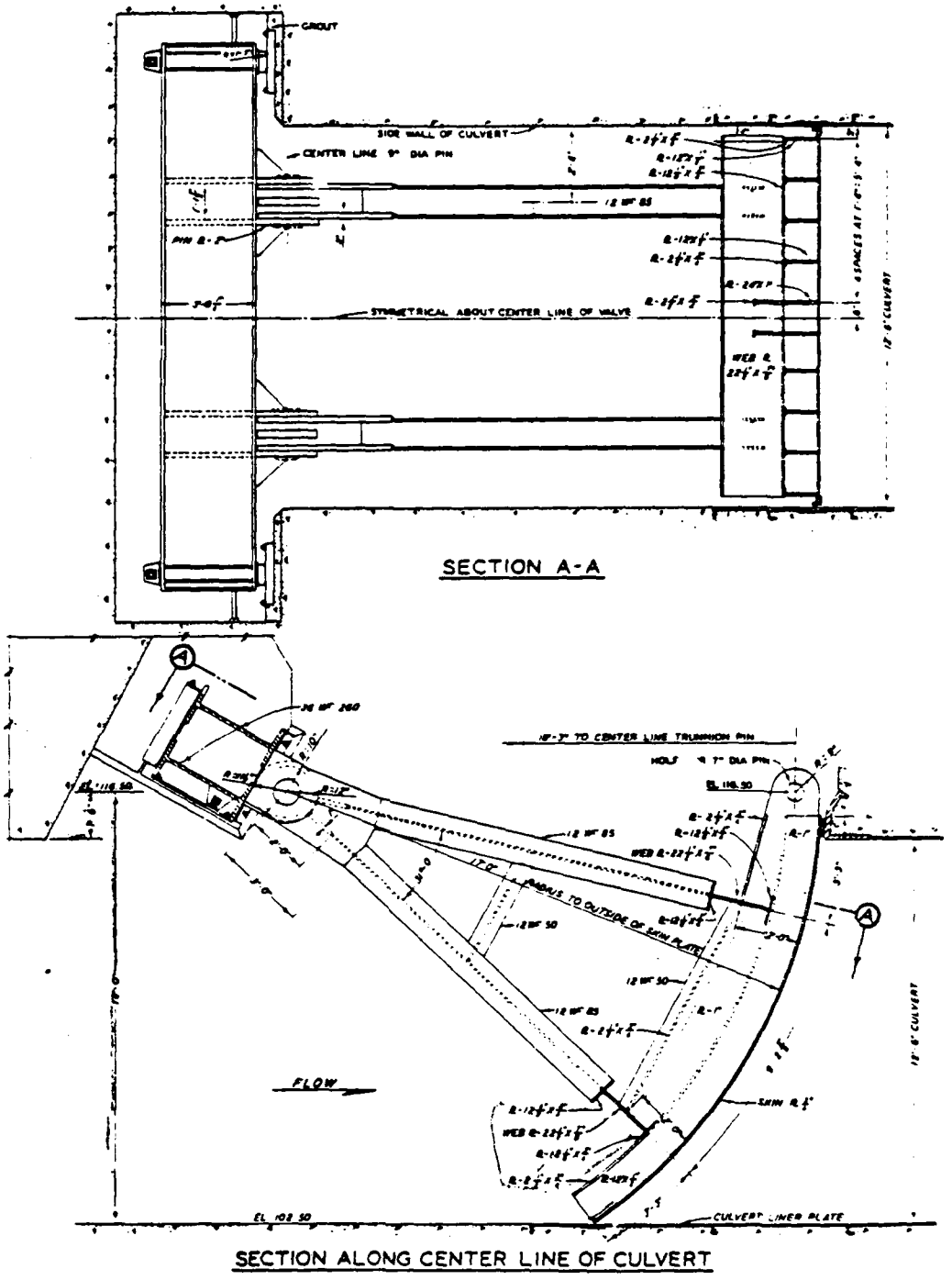

Figure 16. Reverse tainter valve

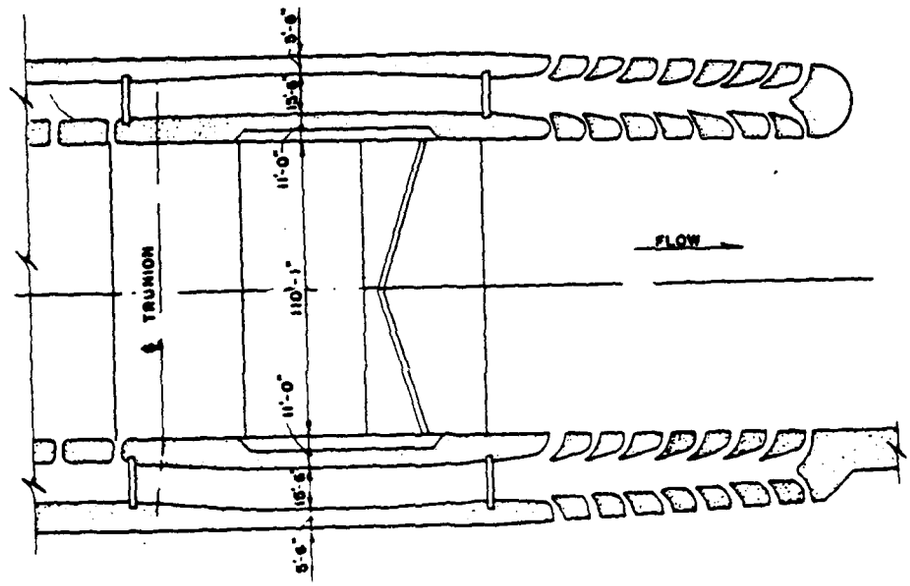

Figure 17. Discharge outlet manifold

PART V: FILLING AND EMPTYING SYSTEMS

40. The purpose of this part is to present a brief description of the classes and types of filling systems that have been used in lock design. There are three classes of systems and a number of different types in each class. The first class is designated "end filling system" because water from the upstream pool enters the lock only at the upstream end of the chamber. Filling systems of this class were the first ones to evolve when locks began to be used on canals. The second class involves use of longitudinal culverts in the lock walls or in the floor to distribute flow more evenly into the lock chamber. This class is termed "culvert system." The third class embodies combinations of end filling systems and culvert systems. In the development of US waterways, all three of the above classes have been used; however, the "combination class" has not been used very recently and use of the "end filling" class is limited to very low-lift projects.

End Filling Systems

41. There are six different types of end filling systems and also the possibility of combining one type (loop culvert) with each of the other systems.

Valves in lock gates

42. This type was used very early in the development of waterways and is still being used on modern low-lift locks in Europe. Ports in the lock gates (miter, vertical lift, or rolling gates) are equipped with slide valves that can be opened to admit water into or out of the lock chamber. Butterfly valves in the lock gates have also been used. Figure 18 shows a view of a miter gate with slide valves. In some instances, ports through lock sills with butterfly valves have been used.

Culverts around the lock gates (loop culverts)

43. This type of system has had more recent usage in the US for small locks than other types of end systems with the exception of sector gates. It is used in Europe for a number of relatively new large Maritime locks. Culverts with either slide valves or butterfly valves that conduct flow around the gates are placed in the gate blocks at each end of the lock. The lock is filled or emptied by operating the valves.

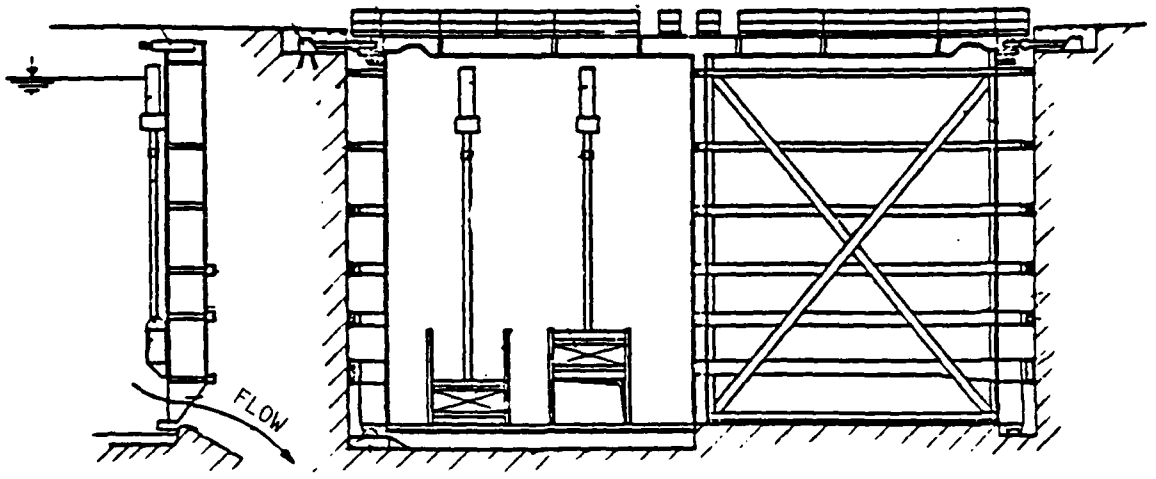

Figure 18. Miter gate with slide valve

Sector gates

44. Sector gates were described in Part IV, and it was noted there that since they could be opened or closed under head, they were sometimes used to fill or empty a lock. Sector gate filling systems can be used where the lift is no greater than about 5 feet for a high percentage of the time. Further, there is usually a greater filling time required and extra length of lock chamber needed for this type of system (Figure 13).

Submergible vertical-lift filling system

45. This type of system has been model-tested but never gave satisfactory results in the tests. Several locks have submergible vertical-lift gates at the upstream end; but it has been found that their use for filling requires too much time to be of practical use. Descriptive information on this type of gate is given in Part IV and Figure 10 shows a typical submergible vertical-lift gate.

Submergible tainter gate filling system

46. This type of system produces the same performance characteristics as the submergible vertical-lift gate system. It differs only in the structure design and has the same inherent deficiencies as far as its use for filling is concerned, as the submergible lift gate. A typical submergible tainter lock gate is shown in Figure 12.

Rising sector gate filling system

47. The rising sector lock gate was described in Part IV. This gate can be raised or lowered under head to admit water to the lock chamber.

Either type of operation produces severe turbulence in the upstream end of the lock chamber and requires a significantly longer filling time than a culvert system. Like all other end systems, it is limited to use with very low lifts.

Combination of loop culverts with gates

48. It was noted earlier that some locks have been built that filled and emptied by a combination of loop culverts and gates. The most practical combination type consists of sector gates with loop culverts to augment the filling and emptying operations. While some improvement in filling may be obtained with such an arrangement, this system does not perform adequately for lifts over 10 feet and is only marginally satisfactory for lifts between 5 and 10 feet. Figure 19 shows a diagrammatic plan of a lock with a sector gate-loop culvert filling system.

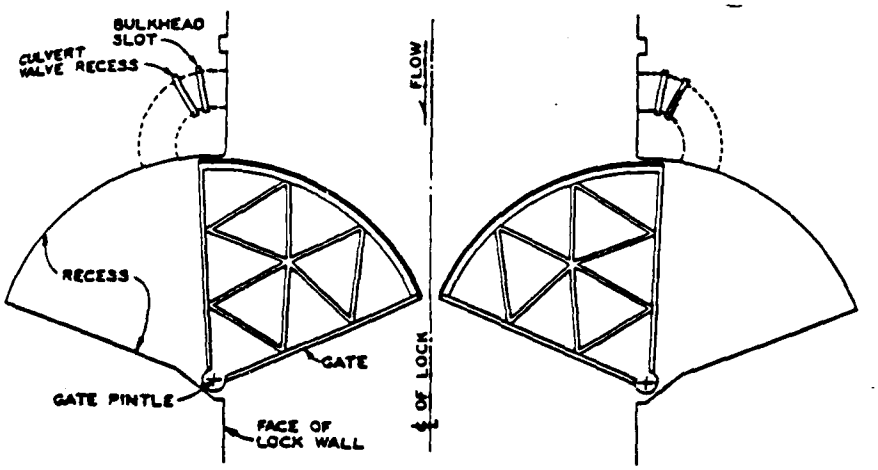

Figure 19. Sector gate and loop culvert system

Combination of submergible lift gate and wall culvert system

49. Two locks have been built that have wall culvert filling systems and submergible lift gates at the upstream end that are used to augment filling operations. The submergible lift gates were built primarily to provide the capability to pass ice and debris and to serve emergency purposes. However, model tests showed that filling time could be appreciably reduced by starting to lower the lift gate when the lock water surface was about 3 feet below the upper pool level. This operation reduced filling time without causing excessive hawser stress. Complicated controls and extra cost make use of this combination system unattractive when considered only for filling purposes.

Culvert Filling Systems

50. There are seven general types of culvert filling systems. In all of these systems, the objective is to achieve a design that will distribute the flow into the lock evenly throughout the entire filling operation. In theory, this can only be accomplished with a very elaborate arrangement of culverts, manifolds, and ports that would be impracticable and too costly to consider. One type of system, the bottom longitudinal system with vertical division of flow, comes very close to obtaining an even split of discharge to each half of the lock chamber. In all of the other types, it is impossible to obtain equal division of flow into the upstream and downstream portions of the lock chamber during the entire filling period; but within a certain range of lifts, depths, and filling times, some of the less-than-ideal types come sufficiently close to producing balanced flow conditions to be quite satisfactory.

Wall culvert side port system

51. This type of filling operation is presently the most widely used system in the US for locks in sizes up to 1,200 by 110 feet with lifts up to about 30 feet; on smaller locks, it can be used successfully for slightly higher lifts. Figures 20, 21, and 22 show the manifold and port details of wall culvert side port filling systems for 1,200- by 110-foot, 600- by 110-foot, and 600- by 84-foot locks, respectively. The arrangement of intakes, culverts, valves, ports, and discharge outlets appears to be very simple. This appearance is deceptive as enormous amounts of research, prototype testing, and analytical study have been required to arrive at the present state of the art. As shown in Figure 20, rectangular culverts in each wall extend over the full length of the lock. Multiport intakes are connected to the upstream ends of the culverts and discharge outlet manifolds are connected to the downstream ends. A number of ports in each wall of the lock chamber connect the wall culverts to the lock chamber. The location of ports in one wall is staggered in relation to the ports in the opposite wall. Reverse tainter valves upstream from the most upstream port in each culvert control flow into the lock. Valves downstream from last ports control flow out of the lock. The problem that is inherent with all wall culvert side port systems occurs as a result of transient flow conditions caused by the inertia of the mass of the water in the culverts. As the valve in a culvert begins to open,

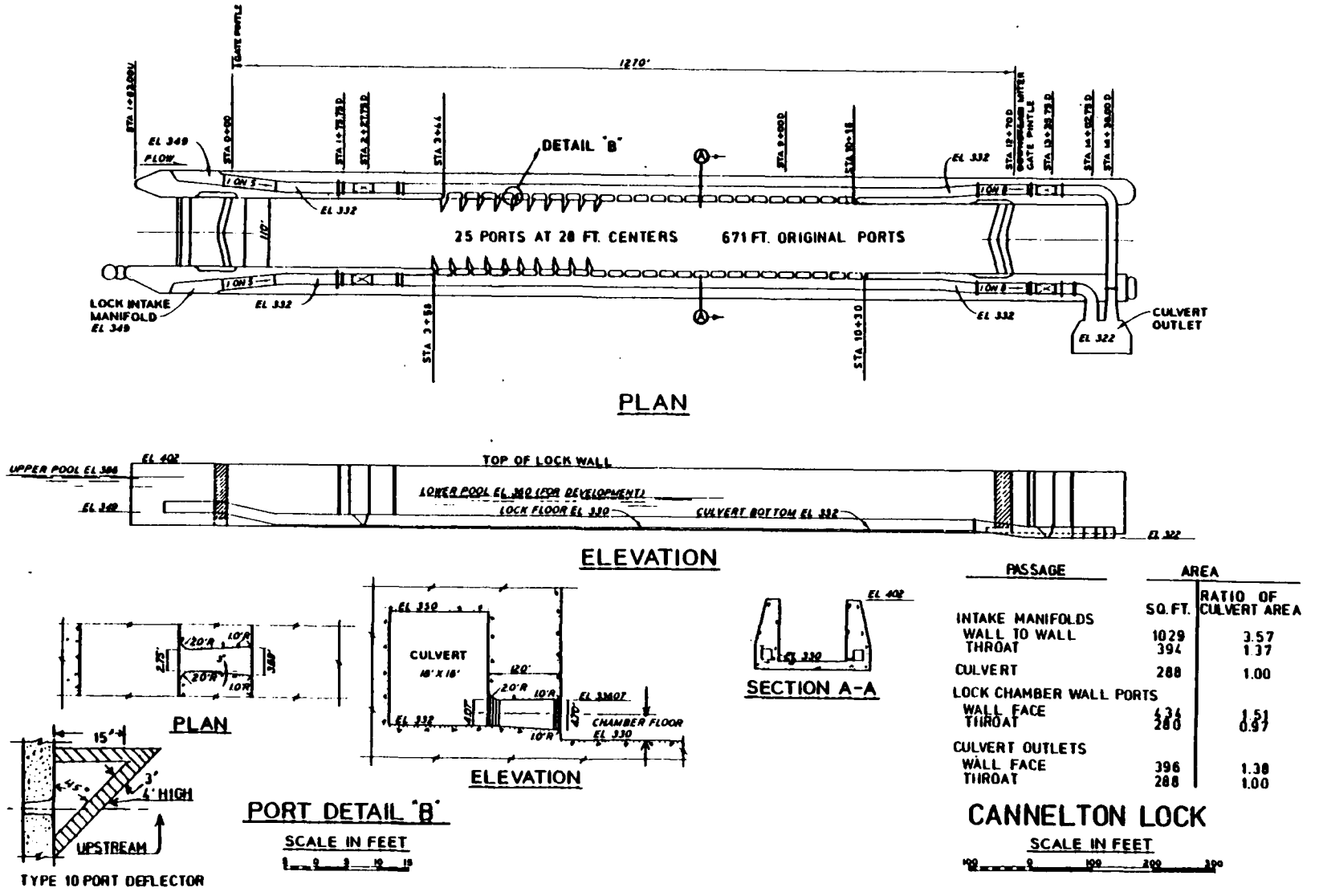

PASSAGE	AREA SQ. FT.	AREA RATIO OF CULVERT AREA
INTAKE MANIFOLDS		
WALL TO WALL	1029	3.57
THROAT	394	1.37
CULVERT	288	1.00
LOCK CHAMBER WALL PORTS		
WALL FACE	434	1.51
THROAT	280	0.97
CULVERT OUTLETS		
WALL FACE	396	1.38
THROAT	288	1.00

Figure 20. Wall culvert system, 1,200- by 110-foot lock

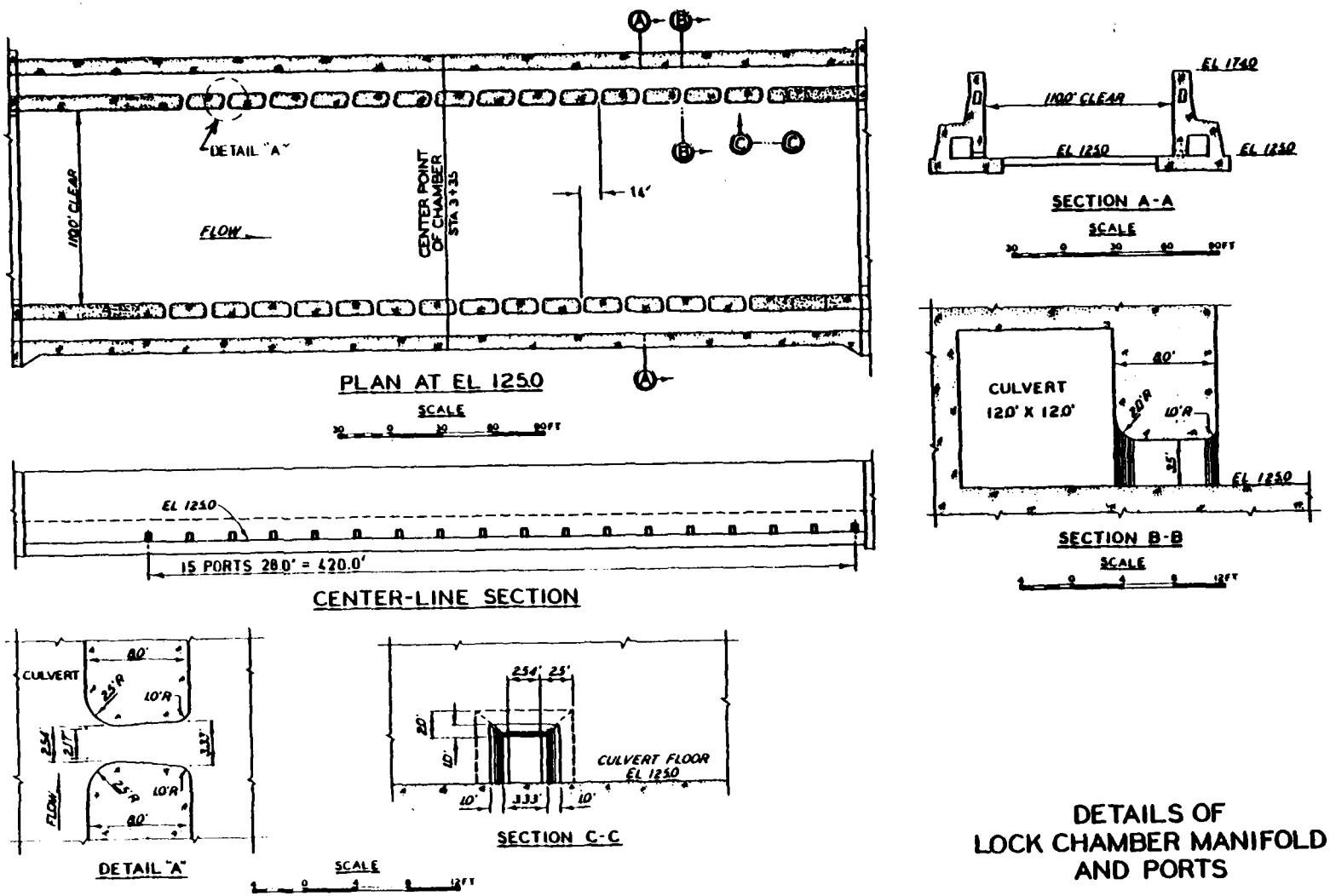

Figure 21. Wall culvert manifold, 600- by 110-foot lock

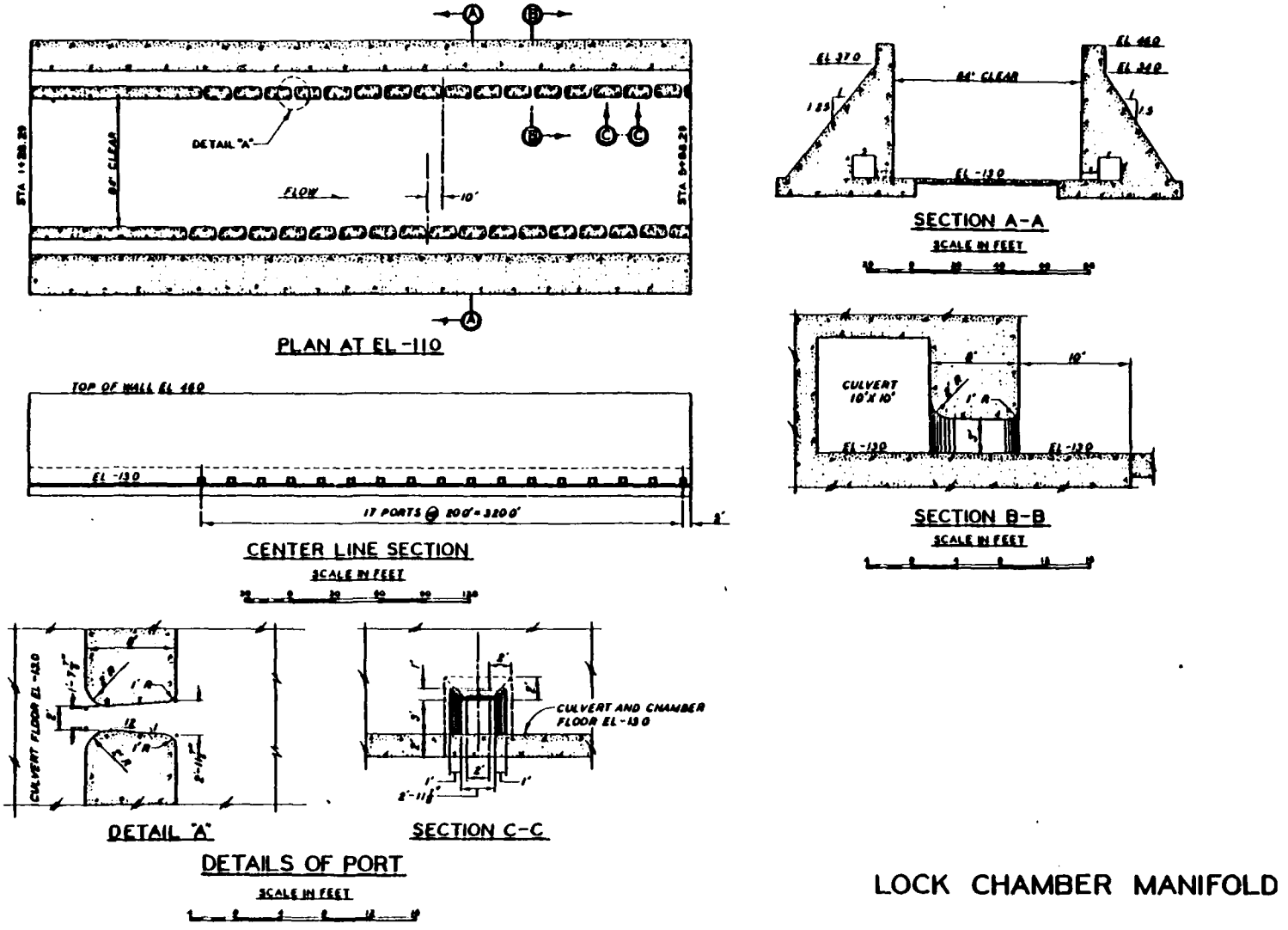

Figure 22. Wall culvert manifold 600- by 84-foot lock

flow will first start through the port nearest to the valve and will then start at successive downstream ports in sequence until all ports are discharging. As flow past the upstream ports increases, pressure in the culvert drops and flow through several of the upstream ports may actually reverse. The length of time during which this transient condition exists is relatively short; but in this short time, the sequential increase in flow through the upstream ports causes a surge to build up in the upstream end of the lock chamber. The surge moves rapidly downstream where it may be either partially damped or reflected by flow from the downstream ports and shortly afterwards, reflected by the downstream gate. Reducing the amplitude of this surge is the principal objective in arranging location, size, shape, number, and spacing of the ports. The typical wall culvert side port systems shown in Figures 20-22 all have intakes with ports in the vertical face of the lock wall upstream from the upstream gate. Reverse tainter-type valves are used and the discharge outlets may consist of horizontal ports in the lock wall downstream of the lower gate that discharge either into the lock approach or into areas on the outside of the approach area. Usually, but not always, the design of a wall culvert side port system is governed by the requirements for the filling operation. Because of this, the design that performs satisfactorily for filling may require a slightly longer time for emptying. More detailed information is given in Part X.

Wall culverts with
small ports--multiport system

52. This system was developed by the Tennessee Valley Authority and is very similar to a conventional wall culvert side port system. It differs only in the size and number of the ports and in their depth in relation to the lock floor. Figure 23 shows a multiport filling system. Model tests by the Corps of Engineers indicate that this system has no advantage over a conventional wall culvert side port system and that hydraulic characteristics are about the same. Also, there appears to be no cost advantages for the multiport system.

Wall culverts with inter-
meshed lateral floor culverts

53. This type of filling system is shown in Figure 24. It is similar in hydraulic action to the wall culvert side port system but can be used for somewhat higher lifts. As shown in Figure 24, the ports connecting the culverts directly to the lock chamber in the side port system connect to the

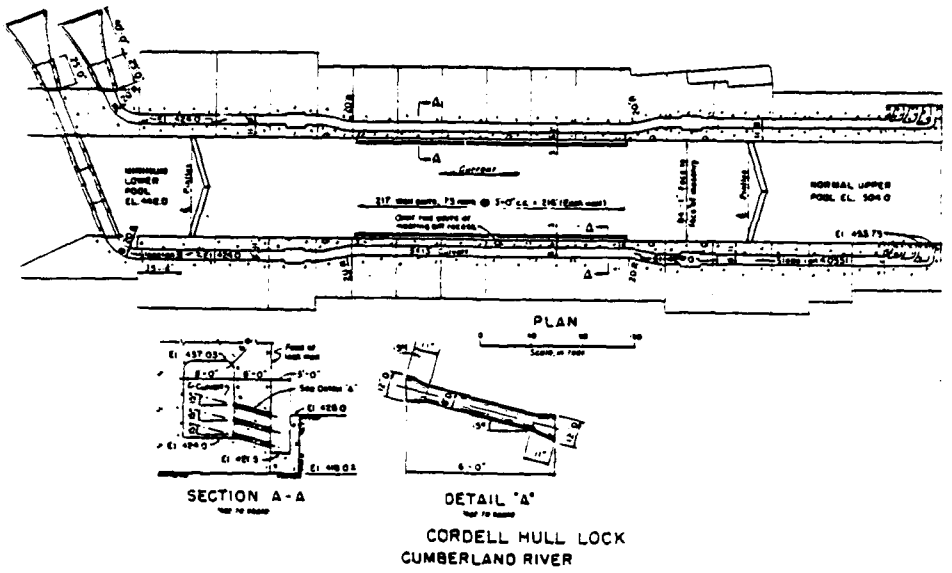

Figure 23. Multiport system

transverse culverts. Flow that enters the transverse culverts is discharged into the lock through ports in the sidewalls (or tops) of the transverse culverts. The locations of the transverse culverts in one wall are staggered in relation to the locations of the culverts in the opposite wall. This system will usually produce a more quiescent water surface than the wall culvert side port system. However, the transient conditions and problems of sequential increase in the flow through ports in the side port system also occur with this type of system. Hydraulic action during filling is quite similar--about the only difference is a slight damping of the buildup of long-period surges. This system and a modification of it, which is described later, were regarded as the best available until development of the wall culvert bottom longitudinal system.

Wall culverts with two groups of lateral culverts--split lateral system

54. In this system the transverse culverts on the lock floor are not intermeshed. They are arranged so that one wall culvert connects with one group of lateral culverts in one end of the lock and the other group in the opposite end of the lock is connected to the other wall culvert. This system achieves a much better distribution of flow than the intermeshed system, especially for medium and high lifts. The one principal disadvantage arises from

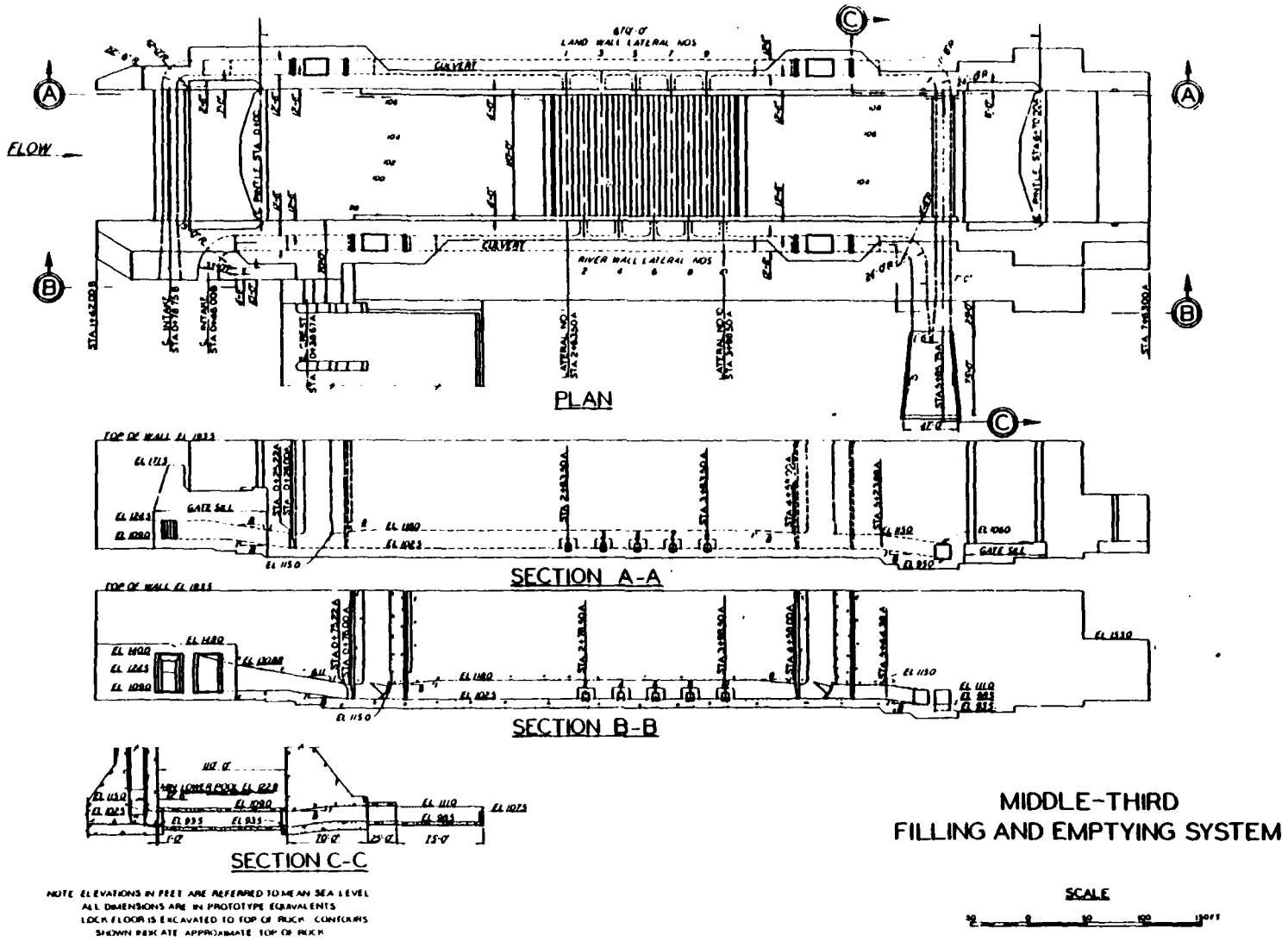

Figure 24. Interlaced bottom lateral system

the fact that any lack of synchronization of the filling valves causes unbalanced flow that creates dangerous surges. Two potentially serious accidents have occurred because of the failure of filling valves to open in unison. In these incidents, tows in the lock broke their mooring lines and only timely and immediate action by vessels' crews prevented serious consequences. Fail safe devices have been developed that will stop movement of both valves if a difference in opening of more than 0.5 foot develops at any time during valve opening. These devices minimize the chances of serious accident; however, there is still the problem of filling with one valve when the other is out of service. For these reasons and because cost difference between a split lateral system and wall culvert bottom longitudinal system is not great, the split lateral system is no longer used.

Longitudinal floor culverts with ports in the top

55. This system has longitudinal culverts under the lock floor that extend the full length of the lock from the upstream face of the upper sill block through the downstream sill block. Ports are placed in the tops of the culverts and flow in the culverts is discharged vertically upward into the lock chamber. There are no intake or outlet structures similar to those in a wall culvert side port system. Flow into each culvert is controlled by butterfly valves in the upstream sill block. Butterfly valves are also placed in the downstream sill block to control flow out of the lock. This system was first used on the Weitzel Lock at Sault Ste. Marie, Michigan, in 1881. The Sabin and Davis Locks at the Soo, which are still in use, utilize this system. As with the wall culvert side port systems, buildup of surge by sequential flow through the ports (beginning upstream and proceeding downstream) creates high hawser stresses. This system is no longer used, but in 1881 it represented a major advance in filling system design.

Wall culverts with horizontally split crossover culvert and longitudinal floor manifolds

56. The system shown in Figure 25 has intakes, wall culverts, valves, and discharge outlets that are all similar to corresponding features of a wall culvert side port system. Instead of discharging into the lock through wall ports, flow is conducted to the midpoint of the lock to a crossover culvert, and then enters longitudinal floor culverts that extend upstream and

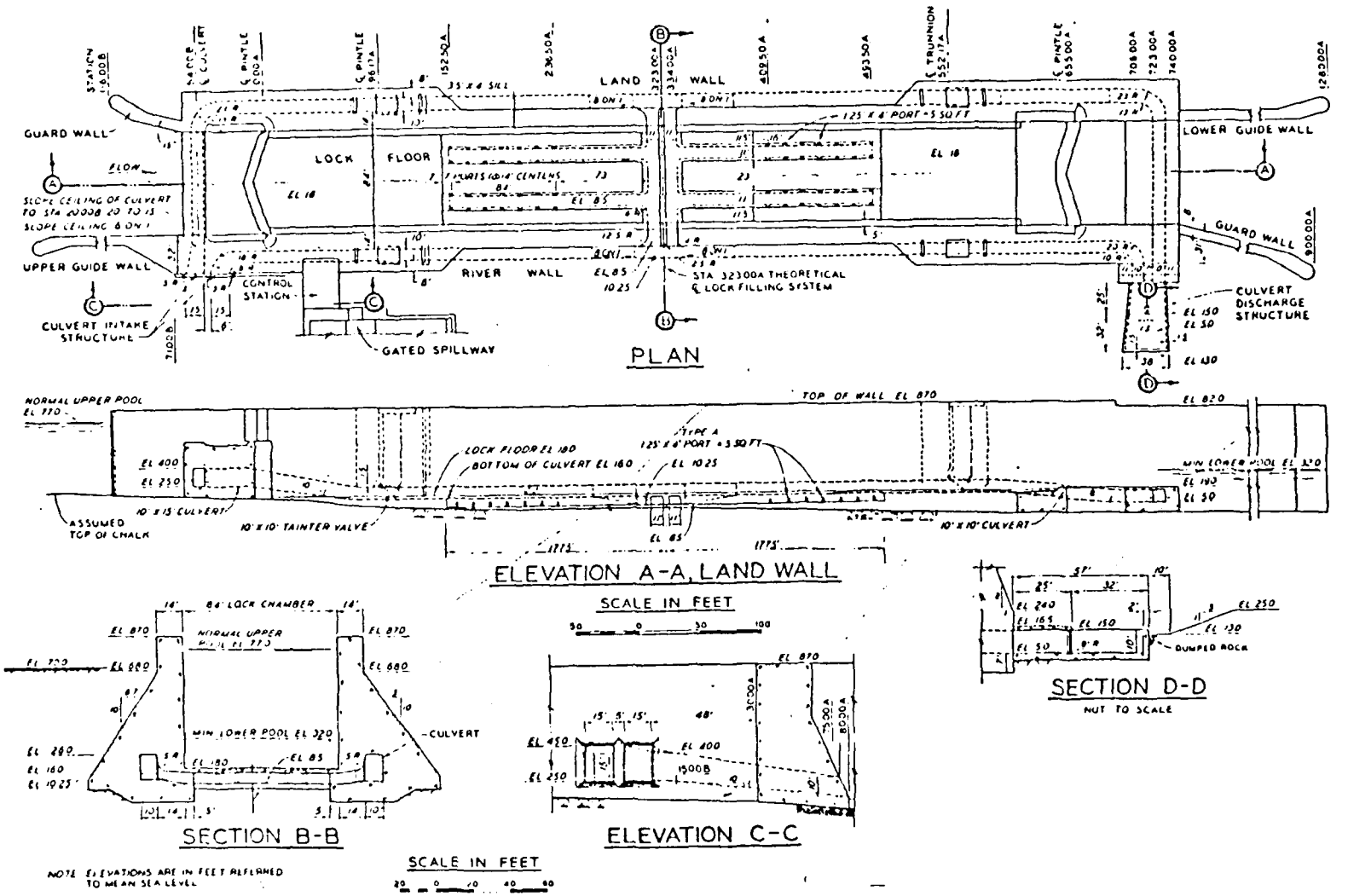

Figure 25. Horizontally split bottom longitudinal system

downstream from the crossover culvert. Flow enters the lock chamber through ports in the sides of the longitudinal culverts. The success of this system depends on how evenly the flow is divided between the upstream and downstream longitudinal culverts after it enters the crossover culvert. Turning the flow 90 degrees (where it enters the crossover culvert) causes very unequal velocity distribution in the crossover culvert, which in turn produces an unequal division of flow. However, although this scheme is not ideal, it has been made to give reasonably good results for a 600-foot-long lock with a lift of 69 feet. This system is not generally recommended for a length greater than 600 feet or lifts greater than 60 feet.

Wall culverts with vertical
split crossover culvert
and longitudinal floor manifolds

57. Figure 26 illustrates this system, which was developed for the 105-foot lift Lower Granite Lock on the Snake River. This system achieves an almost perfect division of flow to each half of the lock by means of a horizontal diaphragm that extends completely across the crossover culvert into the wall culverts. Thus, flow in each wall culvert is divided (vertically) before it begins to turn into the crossover culvert. Flow is conducted to a four-branch manifold in each half of the lock and enters the lock chamber through ports in the sides of the manifold culverts. When the valves start to open, flow will start simultaneously in eight ports in each half of the lock chamber. Lack of valve synchronization or one-valve operation has no adverse effects on the distribution of the flow, on hawser stress, or on turbulence. This system permits the most rapid operation and safest operating conditions of any high-lift lock in the world today. The Lower Granite Lock at a lift of 99 feet fills in 8 minutes with a valve time of 1 minute and 20 seconds.

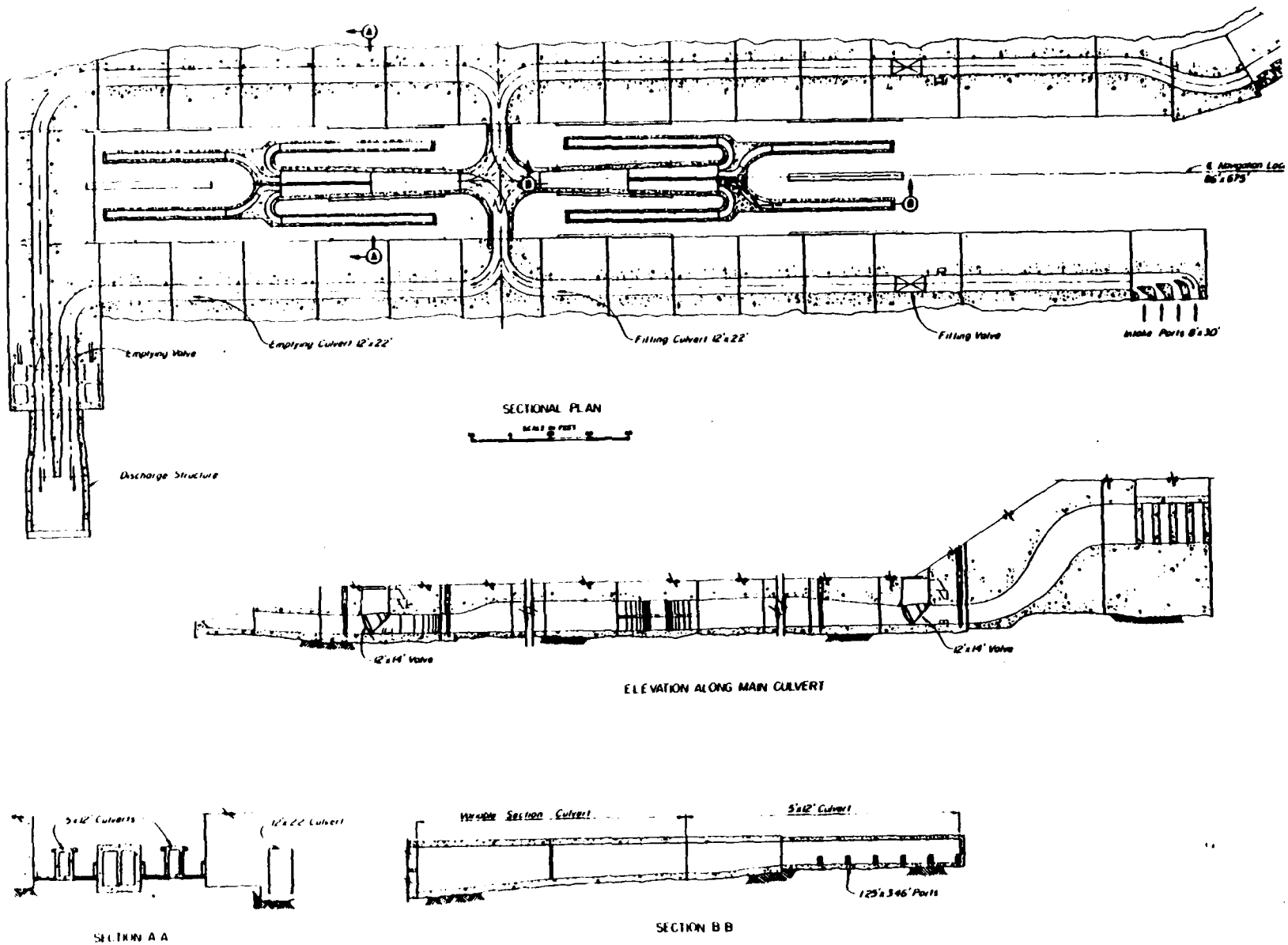

Figure 26. Vertically split bottom longitudinal system

PART VI: DESIGN GUIDANCE

58. The guidance suggested below has been established to aid in design of navigation locks on inland waterways in the United States. This guidance is considered to be applicable to all projects unless it can be shown that at a specific project, conditions and requirements are sufficiently different to warrant changes. For locks that must be designed to accommodate oceangoing vessels and barge tows, design features and criteria will vary with the location and with the particular navigation requirements involved.

Capacity

59. Locks should be designed to accommodate the traffic which can reasonably be anticipated during the life of the structures. For economic planning purposes, the expected useful life of navigation locks is usually considered to be 50 years. Projections of annual tonnage for a 50-year period, starting with the date of project completion, can be used to establish the capacity needed. Such projections are normally prepared by economic units during initial planning studies of a project.

Lock Size

60. Unless an inland waterway channel is unrestricted in width and curvature, the maximum horizontal dimensions of any locks required will probably be governed by the maximum size tow that can safely navigate in the channel. This does not mean that a lock must necessarily be built to accommodate the largest tow or vessel that can use the waterway but it does provide an upper limit on the size. It has already been pointed out that capacity requirements can be met in different ways--for instance, one large lock or perhaps more than one smaller lock. To serve all situations, a number of different lock sizes have come into common usage and are in harmony with most of the barges and towing equipment currently in use. For locks built for commercial traffic, the horizontal dimensions listed below are standard sizes and represent usable dimensions that are not to be encroached on by fenders, protective booms, gates, sills, or any other feature.

Lock Width ft	Usable Lock Length ft
84	400
84	600
84	720
84	1,200
110	600
110	800
110	1,200

Standard size of locks that must be designed to accommodate oceangoing vessels and barge traffic, and locks that serve Great Lakes vessels have not been established. Sizes of locks required to serve these needs must be determined by studies of large ship characteristics and other factors that are not usually encountered with barge traffic.

Hawser Stress

61. Limiting values of mooring line stresses that vessels are subjected to during filling or emptying of a lock chamber were established originally by consideration of tests on breaking strength of used 2.5-inch-diameter manila hawsers. The original criteria assumed that a tow would be moored with two lines that could safely resist a pull in any direction of about 5 tons. At the time the guidance was established, adequate means of measuring hawser stress under prototype conditions had not been developed and models were used to determine hawser stress for filling system design. However, in measurement of hawser stress in a lock model, prototype conditions cannot be exactly duplicated. In a model test the ship or tow model is more nearly restrained than in prototype conditions and because of strain in the mooring lines in the prototype, stresses are normally less than model stresses. Therefore through many years of prototype observation and model testing, it has been found that when a lock is designed to not exceed the hawser stresses given below as determined in a model, the lock will be satisfactory for barge tows as well as small craft.

Barge tows

62. For various sizes and numbers of barges in any location in the lock

chamber, the prototype hawser stress as measured in a model should not exceed 5 tons (2,000-pound tons). Further, surface turbulence must not cause hazard or distress to small craft.

Single vessels (ships up to 50,000 tons)

63. Prototype hawser stress should not exceed 10 tons as measured in a model.

Single vessels greater than 50,000 tons

64. Hawser stress for larger vessels can be allowed to exceed 10 tons, since they will be required to have more mooring lines than either barge flotillas or the smaller single vessels. Model tests made to date indicate that if a lock filling system is designed to meet the preceding criteria, hawser stress (measured in a model) will not exceed approximately 25 tons for vessels up to 170,000 dwt.

Filling and Emptying Time

65. Lock filling systems should be designed to operate as rapidly as possible commensurate with the importance of the waterway, capacity needed, and cost. On busy important waterways, economic and queuing studies show that every minute that filling and emptying time can be reduced will usually produce benefits in excess of any added costs within certain limits. Depending on the lift and size of the lock under design, a filling time of 6 to 10 minutes can be achieved without causing excessive costs. Locks should be designed so that the filling and emptying times presented below will not be exceeded unless it can be shown that at a specific project a longer filling time is warranted.

a. Low lift locks, 6 to 10 minutes
b. Intermediate lift locks, 7 to 10 minutes
c. High lift locks, 8 to 12 minutes

Gate Operating Time

66. For locks equipped with miter gates, tainter gates, and double-leaf vertical-lift gates, the operating machinery should be designed to open or close the gates in 1 minute. Where sector gates are utilized, the operation time is normally governed by requirements for lock filling if filling or

emptying is accomplished through the gates. If sector gates are not used in filling or emptying, they should be designed to operate in 1 minute.

Depth on Lock Sills

Shallow-draft locks

67. The minimum lock sill depth for shallow-draft large locks should be approximately two times the design draft of the tows that use the waterway. If there are locations where compliance with this requirement will result in much greater sill depth most of the time, the criterion may be relaxed. In such a situation, the requirement of two times the design draft should be available for 95 percent of the time and an absolute minimum of 1.7 times the draft should be available 100 percent of the time. For a design vessel draft of 9 feet, the 95 percent depth would be 18 feet and the minimum depth would be 15 feet. These criteria have been based on studies of model tests conducted at the De Voorst Laboratory[1] in The Netherlands and on operating experience at numerous locks in the US. The extra depth over the sills provides space for the water in the lock chamber to be displaced as the tow enters, and enables large tows to enter and leave safely and more rapidly. For some lock projects, this criterion may also govern the floor elevations, as operations and maintenance needs usually specify that the lock floor be at least 2 feet below the sills. With certain types of filling systems (side port), the required chamber depth may be greater than two times the vessel draft plus 2 feet. For some other types of filling system (bottom culvert systems), the tops of the bottom culverts may be the controlling factor, and the elevation of the lock floor will be governed by the height of the culverts. In this situation, the tops of the bottom culverts should be no higher than the lock sills. In a situation where it is believed that providing a minimum sill depth of 1.7 times the draft will impose an unreasonable restriction on the project, a deviation may be considered, provided a complete evaluation of the effects of such a change is furnished. The evaluation should include the following: (1) a comparison of construction costs and annual costs, with and without the deviations; (2) increases in vessel transit time and cost of such increases over the life of the project; (3) decrease in lock capacity; (4) expected dates when additional capacity will be needed with and without the required sill depth of 1.7 times the vessel draft; and (5) effects on

safety and increase in operating hazards with and without the required draft.

Deep-draft locks

68. At locks that are designed for vessels having drafts greater than 16 feet the criteria discussed in paragraph 67 should not apply, as other factors become important. There is presently no situation in the US where a lock would be designed for some specific vessel draft between 16 and 25 feet. Under existing conditions, vessels having drafts between 16 and 25 feet would only be used in locks with 25 to 30 feet of depth on the sills. Almost all of this traffic (Great Lakes vessels) consists of single vessels that have entirely different characteristics from barge tows. Vessels in sizes from 15,000 to 30,000 dwt do not usually fill the horizontal space in a modern lock. Even if such a vessel has a draft of 20 to 25 feet (with 30-foot sill depth) it does not encounter the entrance and exit problems experienced by a very large barge tow in a barge lock. For vessels with deep drafts (25 feet and greater), lock sills should be placed low enough to provide ample allowance for squat, trim, and sinkage if the vessels are to be permitted to enter or leave the lock under their own power. If vessels are to be moved into the lock by towing engines or winches, it may be possible to reduce the sill depth slightly. In this situation, the vessel squat would be considerably reduced. For large vessels, over 100,000 dwt, a minimum clearance between the sills and the hull of the vessels of about 5 feet should be provided. Vessels of this size would not be permitted to enter or leave a lock under their own power.

Depth in Lock Chamber

69. Depth in a lock chamber is governed by the depth on the sills and by requirements for the filling system cushion depth. For operation and maintenance purposes, the lock floor should be at least 2 feet lower than the lock sills. This depth may or may not be great enough to satisfy filling system design submergence requirements. For instance, considering a design draft of 9 feet, the required sill depth would be 18 feet and with the required 2-foot clearance (sill to lock floor) the lock chamber depth would be only 20 feet. If the lock under consideration had dimensions of 110 by 1,200 feet with a 25-foot lift, the required water cushion depth (side port system) would be about 23 feet for an 8-minute filling time and 5-ton hawser pull. In this instance, the lock floor would have to be lowered an additional 3 feet to meet

design requirements for the filling system. The other situation, where the sill depth did control the depth in the lock chamber, was discussed previously. In that instance, the required lock chamber depth was controlled by the height of the bottom culverts. As stated earlier, the tops of the bottom culverts should be no higher than the minimum lock sill elevation.

Increased Gate Height

70. In the example of lock chamber depth given in the previous paragraph, the question might arise as to why the sill should not be lowered an additional 2 feet to provide a 21-foot sill depth, since there would be no significant cost difference. The cost of additional gate height would be offset by reduction in the cost of the lowered gate sill, and it might appear that some decrease in tow entry and exit time would be obtained. However, as sill depth-draft ratios are increased beyond a value of two, gains in tow efficiency do not increase proportionately. Furthermore, lowering the sill increases the gate height and thereby increases the hydraulic loads on the gate. The increase in direct static and temporary loads on the gate structures poses no serious design problems. But when miter gates are used, an increase in temporary reverse load may make the design of operating machinery more difficult. Because of this problem (where miter gates are used), requirements for operating machinery design should be considered before a decision is made to increase the depth on the gate sills over the minimum specified.

Hydraulic Loads on Gates

71. Lock gates and gate operating machinery should be designed so that the gates will be under positive control of lock operating personnel at all times insofar as possible. In the case of miter gates, the operating machinery and the gate leaves should be designed so that the gates will remain completely closed when they are in the closed position; remain in the gate recesses when they are open; and be under positive control of the operator at all times when they are being either opened or closed. These operation requirements impose severe design conditions for miter gates when reverse head or loading from the reverse direction occurs. With other types of gates, the design should be such that the gate can be opened or closed to any position

and held at that position as long as necessary under a minimum head of 2.5 feet from either direction. In some situations it may be necessary to design a gate to be operated under full direct or reverse static head. Such a situation constitutes a special case that would have to be fully investigated as to the hazards involved, the need for such a design, and the proper design criteria to be used. Reverse heads can occur from a number of causes but the most frequent cause is lock overfilling or overemptying. Overfilling or overemptying of a lock results from the momentum of the water moving in the culverts. On a filling operation, the momentum causes the lock water surface to rise higher than the upstream pool level momentarily. This rise is designated overfill. After the lock water surface reaches a maximum value, flow in the culvert reverses, the lock water surface falls, and then again rises above the upper pool level. But the overfilling on this second cycle is much less than the first rise. This pendulation of flow continues through several cycles with rapidly decreasing amplitude until it is damped out by friction in the culvert system. Overemptying is the same phenomenon, but occurs when the lock chamber is emptied and results in the lock water surface being momentarily lower than the downstream pool level.

Loading conditions

72. The hydraulic loading conditions that are of primary interest in gate design are the loads produced by differences in water level from one side of the gate to the other, i.e., head across the gate. Two water-level conditions must be considered--a static condition with water levels quiescent on each side of the gate and a temporary condition wherein the water level on one side may be temporarily increased or decreased. The temporary condition may add to the static head and thus make the total direct head on the gate greater, or a temporary condition may decrease the direct static head. This latter situation is of no interest to a designer unless it produces a reverse head. If there is no head on the gate under static conditions, a temporary condition can occur that will produce a reverse head. This can happen at the upper gate (gates) if the lock is full and the upper pool level is temporarily lowered very rapidly. It can also happen at the lower gate (gates) if the lock water surface is at the same level as the normal lower pool and the lower pool is suddenly raised temporarily. Thus any occurrence that temporarily lowers the normal upper pool level or raises the lower pool level temporarily can produce reverse temporary heads on the upper or lower gates. Any sudden

temporary increase in the upper pool level can increase the total head on the upper gate if the upper gate is closed or on the lower gate if the upper gate is open.

Static hydraulic load

73. The maximum static hydraulic load on the upstream gate is the load due to the difference in elevations of the maximum upstream pool level and the gate sill. This difference in elevations is designated direct static head. The maximum static load on the downstream gate is the load caused by the difference in elevation of the maximum upstream pool level and the minimum downstream pool level (direct static head).

Temporary hydraulic load

74. Temporary loads that add to the maximum direct static load on both upper and lower gates can be caused by wind waves, seiches, surges, ship waves, tides, propeller wash, or a combination of these factors. Also, reverse heads and reverse hydraulic loads almost always occur as a result of temporary conditions. Reverse head at the upstream gate can occur from lock overfilling; from powerhouse or spillway gate operation; from a filling operation of an adjacent lock; or from the negative wave caused by reflections of a seiche, surge, wind wave, or wave from propeller wash or ship passage. Reverse head at the lower gate can be caused from the lock overemptying; from an emptying operation of an adjacent lock; from a seiche, surge, wind wave, propeller wash, sudden increases in powerhouse or spillway discharge, or any combination of these phenomena. Reverse head can cause miter gates to be momentarily forced open and then slammed shut. When they slam shut, the gates may be damaged; also, they may not miter properly. Then when they are subjected to design static head in a subsequent filling or emptying operation, further damage or even failure may result.

Evaluation of temporary hydraulic load

75. Conditions should be evaluated for each specific lock under consideration. The full value of temporary loads of durations greater than 30 seconds are considered as additions to static loads if they increase the head on the gate. If the temporary load produces a reverse head on the gate of a duration greater than 30 seconds, its full value should be considered for design purposes. The actual hydraulic load exerted on a gate from temporary loading conditions of less than 30 seconds duration can be obtained from Reference 2.

Design data

76. The following design guidance is suggested for temporary hydraulic load evaluation:

a. A temporary hydraulic load of 2.5 feet for durations exceeding 30 seconds should be used if the evaluations described in the preceding paragraphs produce values of either direct or reverse temporary head no greater than 2.5 feet. This criterion is a minimum value and applies to structural design of all gates, gate leaves, and operating machinery except miter gate operating machinery.

b. A temporary hydraulic load of 1.25 feet for durations exceeding 30 seconds should be used as a minimum value for design of miter gate operating machinery.

c. In situations where a temporary reverse loading significantly greater than 2.5 feet can occur for durations greater than 30 seconds, miter gates should not be considered.

d. The most serious temporary loading condition usually occurs as a result of reverse heads that are produced by overfilling and overemptying of the lock. Since overfilling and overemptying can possibly occur on every lock operation, provision should be made to reduce the reverse heads to nondamaging values. This can be accomplished by starting closure of the filling valves before the chamber is full. Automatic controls should be designed that will operate the valves so they will be about 95 percent closed at the time the lock chamber is full. The initial adjustment of the controls can be made by trial and error.

Height of Lock Walls and Approach Walls

77. The height of the walls for a lock depends on a number of factors. The importance of the waterway, the extent of protection desired for navigation, the characteristics of the waterway, the type of dam, the type of lock structure, the balance between annual costs and the benefits for uninterrupted transportation during high stages--all influence the selection of wall height. On important waterways, locks should be designed so that they will be usable at all times except during large floods. Freeboard between top of lock walls and upper pool level can vary from a minimum of 4 to 5 feet on waterways with little stage fluctuation to over 20 feet on streams with nonnavigable dams where ranges in stage may be great. If the characteristics of the waterway are such that a navigable dam will be advantageous, lock walls and operation equipment can be designed to withstand submergence. The factors mentioned above should be given consideration in the determination of the elevation of

the tops of the main lock walls and the upper guide walls. The elevation of the top of the downstream guide walls is usually based upon a study of tailwater conditions. However, at some locations where the lifts are not great, it may be advantageous for the downstream guide wall to be level with the lock wall and upstream guide wall.

Guide Walls and Guard Walls

78. The hydraulic characteristics of the waterway in the vicinity of the upstream and downstream lock approaches and the nature of the traffic expected to use the waterway will determine the needs for structures to facilitate entrance to and exit from locks, and to reduce hazards caused by adverse currents. Approach walls, which are extensions of the main lock walls, are known as guide walls and are required for all locks that serve barge traffic. In investigations to determine the layout and design of approach walls for a lock, it should be recognized that vessels or tows entering or leaving locks at low speed lack maneuverability and steerageway and are vulnerable to adverse currents. Approach walls, which are used to guide long tows and large vessels into the lock and to provide mooring facilities for tows longer than can be accommodated in a single lockage, are referred to as guide walls. Shorter walls on the opposite side that are designed only to minimize entrance or exit difficulties or to prevent a vessel from entering hazardous areas are designated guard walls. Guide walls may be placed on either side of the lock, depending on the general layout of the lock and dam and on current conditions. At some locations, the guide wall is placed on the riverside of the lock, so that it will provide a barrier to prevent vessels from being pulled toward the dam during its approach to the lock. When the lock is on the outside of a bend in the river, it may be necessary to locate the guide wall on the landside of the lock approach. In this case, a guard wall on the riverside of the upstream lock approach will usually be required to protect against currents resulting from operation of the spillway. A downstream guard wall may also be required to protect against turbulence and currents resulting from spillway discharge.

79. Decisions, in regard to the layout and arrangement of approach walls, should be based on studies made on a general model. All hydraulic factors should be given consideration in the layout of these walls. It may be

advisable to make the upstream guide or guard wall permeable (slotted) in order to avoid a concentration of flow at the upstream end of the wall. Floating upstream guard and guide walls have been used at a number of projects and have proven to be generally satisfactory. Where great water depths are involved, floating guide walls have cost advantages. Model studies have indicated that submerged dikes upstream from a lock, or a submerged fill in the upper approach where depths permit, will often reduce currents and improve approach conditions. Model tests can be made to determine the optimum depth of curtain wall on permeable guard walls. The usable length of guide walls should be equal to the usable length of the lock chamber in order to accommodate a tow that will just fill the lock. Conditions at the upstream portion of a lower guide wall may, in some instances, be hazardous because of turbulence or high velocities resulting from the discharge of water from the lock chamber. The usable length of a lower guide wall should be measured from the point where velocities become less than 6 feet per second or where excessive turbulence ceases.

Types of Guide and Guard Walls

80. Three different types of guide and guard walls are in general usage. For most locks situated on rivers, concrete gravity walls are used. Concrete wall types and designs may differ according to foundation conditions. For instance, a concrete gravity wall may be founded on (1) bearing piles; (2) on rock; (3) on sheet-pile cells filled with rock or gravel.

81. On some inland canals, where tows and vessels are not large, guide and guard walls may be built of timber construction. On this type of wall, heavy horizontal timber wales and rubbing timbers are supported on pile clumps. A walkway for linesmen and tie-up bollards are added to complete the structure. The first cost may be low compared with concrete, but the annual maintenance cost will be high.

82. Floating concrete guide walls are used successfully at the upstream end of locks located at a reservoir where water depth may be great and difficult foundation conditions exist.

Emergency Closures for Locks

83. All locks on a busy modern waterway should be equipped so that flow through the lock chamber can be quickly stopped in the event of failure of the lock gates. The possibility of such failure may appear to be remote, but with increases in tow sizes and increases in traffic, accidents also increase. Instances of tows ramming gates happen frequently. The most vulnerable situation develops where a tow upon entering a lock knocks out the gates that are in the closed position before the gates behind the tow can be closed. In one instance, an out-of-control vessel actually knocked out the gates in both ends of a lock. In the past 15 years, there have been two instances where accidents knocked out lock gates (miter gates) and free flow through the lock chamber existed for some time. In both of these instances, closure was eventually made by means of stop logs; but considerable time was lost in mobilizing and actually getting the closures in place.

Losses from uncontrolled flow through a lock

84. The losses that may be caused by uncontrolled flow through a lock depend principally on the conditions of development upstream and downstream of the lock. In a highly developed area, such as areas along the middle reaches of the Ohio River, enormous monetary losses and other hazards could result from unrestricted flow through a lock. The three principal sources of loss are as follows:

a. Loss of pool upstream from the lock.

b. Possible flood damage downstream from the lock.

c. Loss to shipping on both pools, particularly in the upstream pool.

The loss of pool upstream from the lock can cause loss of domestic water supply, loss of condenser water for steam electric generation stations, and losses to tows and vessels by virtue of their being beached on an uneven muddy channel bottom with attendant damage. Unrestricted flow into the downstream pool may create enough of a sudden rise in stage to cause some vessels (small craft) and barges to break their moorings and drift uncontrolled into the channel. Also, a sudden and unexpected rapid increase in river stage can cause flood damage to equipment and installation that would not be damaged by a normal river rise. To contrast the situation on the Ohio River, consider

the situation along the Snake River in Washington and Oregon. The Snake River dams create relatively large deep reservoirs that are used to produce hydropower. Free flow through a lock at one of these projects would not constitute a major portion of the total riverflow and there would be minimal effects from loss of reservoir storage except for monetary losses to power production. While this loss might be large in terms of dollars, it would not be catastrophic and it would not create the general disruption that loss of one of the Ohio River pools would cause.

Requirements for
emergency closure facilities

85. The requirements for emergency closure facilities are as follows:

a. Reliability. Any closure facility should be designed so that it is available for use at any time under any condition. Any and all appurtenant equipment (cranes, hoists, trucks, and auxiliary power source) should also be readily available at all times and should be periodically checked to ensure operating capability.

b. Operation time. The time required to close off uncontrolled flow through a lock should be as short as possible, depending on the location and the specific situation involved. At some locations immediate response is necessary, as flow should be stopped in a matter of 2 or 3 hours (Ohio River). At other locations, the time factor may not be so critical. The time required to make closure may govern the type of facility to be provided.

Maintenance and operation costs

86. In selection of a closure structure, consideration should be given to the anticipated maintenance and operation costs at the site under study. For instance, at a lock with a high upstream sill (high lift), a submergible vertical-lift gate or tainter gate that would be placed at the downstream edge of the upper sill might meet all requirements at that location. If the same submergible vertical-lift gate is used at a low-head lock, the maintenance costs might be very high because of accumulation of silt. In this latter situation, the gate would have to remain submerged on the bottom of the lock chamber where silt and debris would be trapped and this would require regular periodic costly removal work.

Usefulness for routine maintenance

87. The usefulness of an emergency closure structure for routine maintenance should also be considered. In some instances it may be possible to design the emergency closure facility so that it can be used in ordinary

dewatering operations and eliminate the need for an extra set of stop logs.

Types of emergency closure structures

88. The following types of emergency closure structures have been used successfully:

a. Overhead vertical-lift gate.

b. Submergible vertical-lift gate.

c. Submergible tainter gate.

d. Stop logs placed with crane and hoist.

e. Stop logs placed with overhead locomotive crane.

f. Sector gates.

g. Poiree dam.

h. Needle dam.

89. All of these types have special advantages and some disadvantages that tend to limit their usefulness under some conditions.

a. The overhead vertical-lift gate can be used where great clearance is not required; but this qualification generally rules out its use on all but a very few inland waterways.

b. The submergible vertical-lift gate and the submergible tainter can be used at locks where there is sufficient lift to allow these gates to be submerged downstream from the upper sill without resting directly on the floor of the lock. They possess the advantage of being fast operating and can be operated under flowing water.

c. Stop logs placed with a crane and hoist can be used under all conditions and can be considered the most universally adaptable system and probably the least costly of any of the eight listed. This system was developed first at the Port Allen Lock and requires a stiffleg derrick to handle and place the logs into position so they can be lowered into the recesses in the lock wall by hoists. Stop logs cannot be placed one-at-a-time in flowing water. When this is attempted, water flowing over and under the log produces vortex trails that cause erratic movement and the log will jam in the recess. In the Port Allen system, the first stop log is placed in the recesses above the flowing water and retained in this position by dogging devices until the second log is placed on top of the first and fastened to it. The two logs (acting as a single unit) are then lowered in the recesses, by the hoist at the recess in each wall, so that the third stop log can be placed on top of the second log. This procedure continues with the stop logs being gradually lowered into the flowing water, but never permitting flow to go over the top. No erratic movements are produced. When the last stop log is added, the entire unit (all stop logs fastened together) is finally lowered through the last increment of depth, and all flow except leakage is stopped. The principal

advantages with this system are as follows: (1) no overhead structure is required; (2) there are no permanently submerged structures or operating mechanisms to maintain; and (3) the system is reliable and the stop logs, hoists, and stiffleg derrick require very little maintenance. The disadvantages of the method are that it requires (1) too much time to effect closure; (2) space for storage of stop logs near the upstream end of the lock; and (3) a stiffleg derrick. This last item may change as it may be possible to move and handle the stop logs with motorized cranes.

d. The system of placing stop logs from an overhead locomotive crane has been used at a number of the new Ohio River locks. The same procedure of lowering the stop log units so that flow never goes over and under the stop logs at the same time, which was developed for Port Allen Lock, is used at these locks. The only difference is in the equipment used to handle and place the stop logs. At the Ohio River locks that use this system, the overhead bridge on the gated spillway piers continues on over the upstream end of the lock (upstream of the upstream gates). The locomotive crane that moves along this bridge to place stop logs in the spillway bays is used to place the stop logs in the recesses in the lock. The advantages are essentially the same as the advantages of the Port Allen system. The disadvantages are about the same as for the Port Allen system with possibly another added disadvantage. The added disadvantage arises from the requirement for vertical overhead clearance at the lock. In the case of the Ohio River locks, this required clearance is 55 feet above the 2 percent duration flow line. This might make it necessary to set the elevation of the spillway piers higher than would normally be required and increase the cost of the piers.

e. Sector gates possess important advantages: (1) they can be closed in flowing water; (2) they require no special equipment, personnel, or mobilization activity; and (3) they can be closed in a matter of minutes. Balanced against these advantages are the following disadvantages: (1) very high first cost and continued maintenance of a submerged structure; (2) extensive horizontal space requirements; and (3) possible differential settlement complications if a wide lock is involved.

f. The last two types, Poiree dams and needle dams, have no specific advantages over the other types except possible first cost. Their disadvantages are that they (1) require a much greater length of time to place; (2) create dangerous hazards to personnel in placing the needles or planks; and (3) require an entire crew to transport, handle, and place the needles.

Overhead Clearance for Structures Over Locks

90. If, for any reason, it becomes necessary to place a permanent nonmovable structure over a lock, the same overhead clearance must be maintained

that is required for other structures that cross over the waterway. At some projects, bridges across the lock are needed. If it is a high-lift lock, it is sometimes possible to place the bridge across the lock at the elevation of the top of the lock walls immediately downstream of the downstream gates. If a bridge is needed at the upstream end of the lock, the bridge is usually a bascule bridge that offers no restriction to navigation when it is raised. Minimum overhead clearance for all structures over inland waterways is the responsibility of the US Coast Guard. This organization should be consulted before proceeding with any plan that involves placing a structure over a lock.

PART VII: HYDRAULIC ANALYSIS OF LOCK FILLING AND EMPTYING SYSTEMS

91. This part presents the methods developed, data available, and general theory involved in hydraulic analysis of lock filling systems. Appendix A contains a notation, equations, and list of symbols used throughout this text, except where calculations involve the use of Appendix B. Appendix B is an excerpt from Internal Flow Systems, by David S. Miller,[3] which presents design curves and data to be used herein in analyzing head losses in bends in lock culverts. Figures 27 and 28 are definition sketches to aid in understanding the material and equations. The material in this part makes considerable use of prototype studies made for this report on Lower Granite and McNary Locks. These prototype studies are contained in Appendix C.

92. An analysis of the filling and emptying system of a lock includes:

a. Allowable filling time for permissible hawser stress for different lifts, for different sizes of tows, and different valve times.

b. Determination of culvert size.

c. Calculation of head losses for various portions of the culvert system and for filling and emptying valves.

d. Determination of pressures at different locations, with special importance given to the area immediately downstream from the valves.

e. An investigation of cavitation tendencies and the proper elevation for the filling valves.

f. Turbulence conditions in the lock chamber.

g. Tendencies for vortex formation at the intakes.

93. Model tests have been used extensively to study and evaluate the items listed above. Prototype tests have been made at several locks to enable comparisons to be made of model with prototype data, and to verify model tests. Of the seven items listed above, filling and emptying time and pressures can be estimated reasonably well with analytical methods by utilizing data from model and prototype tests on head losses. Studies made during preparation of this report have provided head loss curves for intakes, manifolds and loss coefficients for bulkhead slots, valve wells and flow resistance for lock model filling operations. Loss coefficients have been computed for flow through the manifold on a lock emptying operation and some data have been developed on discharge outlet exit loss for model locks. Head loss curves for

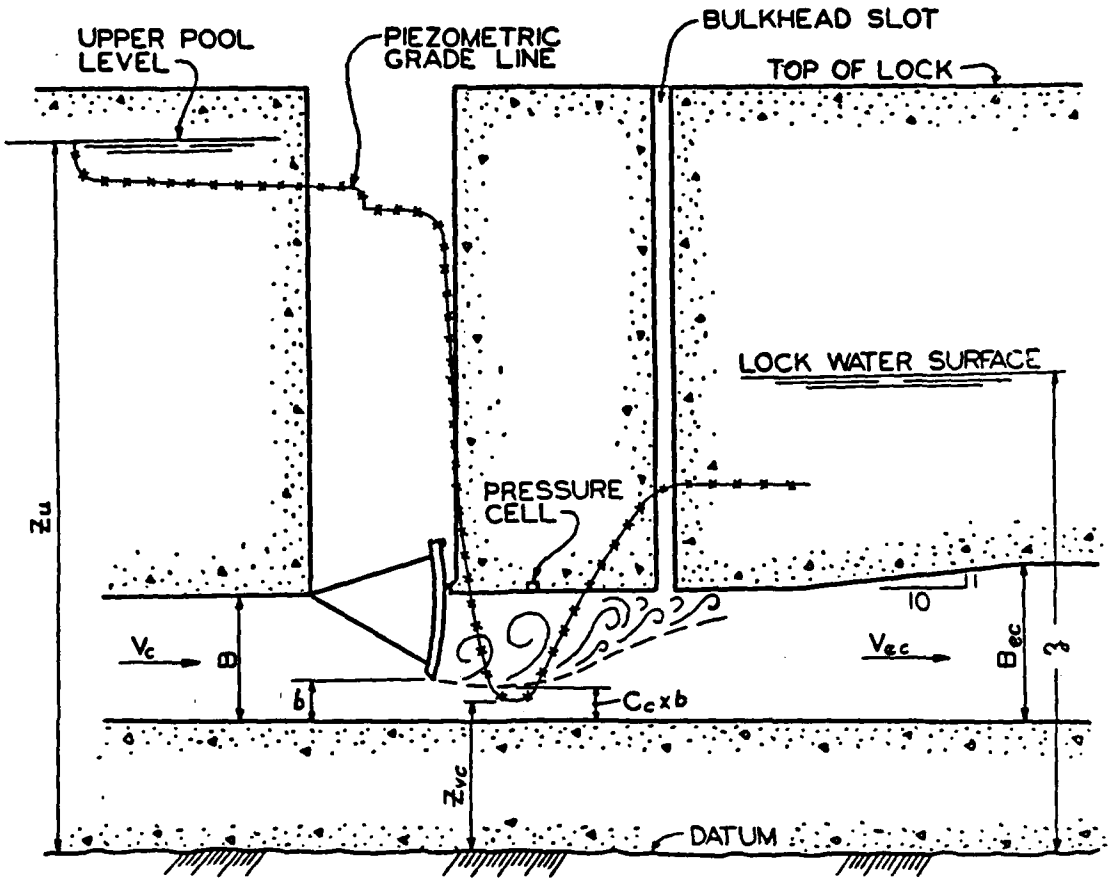

Figure 27. Definition sketch (see Appendix A for definitions of symbols)

prototype lock reverse tainter valves have been completed and loss coefficients for flow resistance in prototype culverts, bulkhead slots, and valve wells have been analyzed. Relation between total head loss for model locks and prototype locks are presented for both filling and emptying operations in this part.

94. Pressures can be calculated when head loss coefficients, filling times, and filling curves are computed. The accuracy of any pressure determination will, of course, depend on the accuracy of head loss coefficients and filling curve data. Determination of critical pressures on model tests for high lift locks are not always reliable. Cavitation tendencies and attendant problems can only be investigated reliably if critical pressures are reasonably accurate.

95. There are no analytical methods of determining turbulence conditions in the lock, whether vortices will form at intakes, or the magnitude of

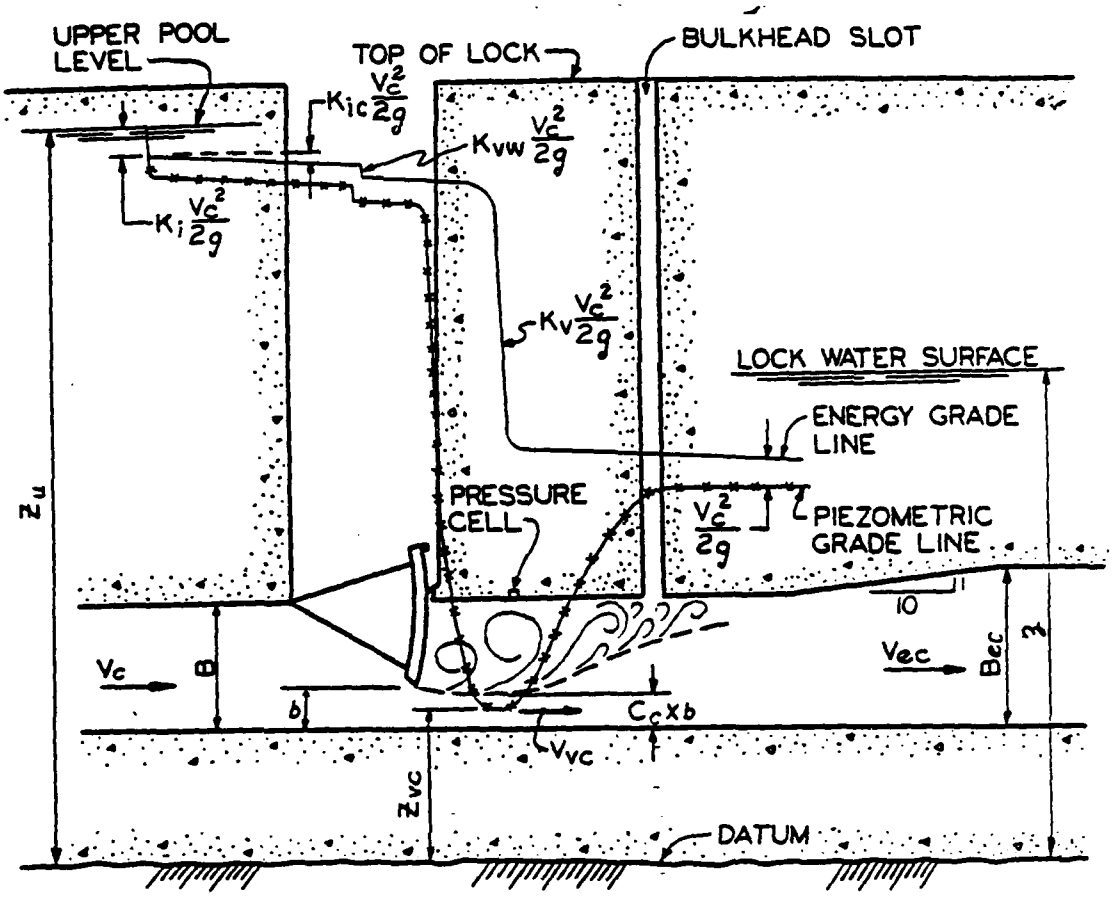

Figure 28. Definition sketch (head losses) (see Appendix B for definitions of symbols)

hawser stresses. Of these three items, hawser stresses and turbulence conditions can only be determined by model tests. While model tests are useful to indicate whether or not a given design will show vortex tendencies, there appears to be no valid relationship between a barely discernible vortex in a model and conditions that may occur in the prototype. However, as will be explained in Part XIII, certain rule-of-thumb guides have been developed to minimize occurrence of serious vortices.

96. In working with models to determine hawser stresses, it must be noted that when a hawser stress of only 5 tons is achieved in a model it does not necessarily follow that the hawser stress on the prototype lock will be no greater than the value measured in the model. On a performance basis it has been found that when the model hawser stress is no greater than 5 tons, the prototype lock will perform very well and no surging or severe turbulence will

occur. Prototype hawser stress data from tests at two locks show only approximate conformance to model measurements. But the maximum prototype values were not enough greater than model values to be of any real significance except at the end of the filling cycle when the overfill was permitted to spill through partially open upper miter gates.

97. Filling and emptying times obtained in model tests are always greater than prototype values. Losses in models are greater because of lower values of Reynold's number in flow in model lock filling systems.

Analytical Studies

98. Two of the three principal elements used in any analysis of lock systems, model and prototype tests, have been discussed briefly in the foregoing paragraphs. Theoretical hydraulic studies have also been pursued in the research and development work on lock design. Theoretical studies alone have many limitations insofar as practical design problems are concerned and designers turned to scale models to augment theory. Then, as research continued and the need developed for larger, higher lift, faster operating locks, it became necessary to make prototype tests to better evaluate model results. During the past 40 years, model tests have been made in the United States for many locks of many different sizes with lifts ranging from a minimum of 3 or 4 feet to a maximum of 113 feet. Virtually all conceivable types of systems, (end filling of various designs, side ports, transverse bottom culverts, bottom longitudinal culverts, and various combinations) have been considered and tested. In Europe, similar research has been pursued, but with different objectives in some cases. Also, features such as designs to minimize salt-water intrusion into freshwater areas and water saving devices have been studied, tested, and built. It was noted earlier that while model tests are a very useful tool, there are limitations. On intermediate-lift and high-lift locks, it is difficult to predict critical pressures in the culvert downstream from the filling valves with a reliable degree of accuracy in a model. Further, the difficulty involved in determining accurate head loss coefficients and valve loss curves for high lift locks makes determination of pressures by theoretical calculations questionable. Thus, prototype tests become a valuable means of securing data that can be used with confidence for high lift lock studies.

99. In subsequent paragraphs the basic hydraulic theory of filling a lock will be presented with development of the necessary mathematical expressions and equations. The use of data from prototype tests at Lower Granite Lock and McNary Lock to develop discharge hydrographs into the locks, head loss coefficients, contraction coefficients, valve loss curves, inertia head corrections, and pressures is described and explained.

Discharge Under Falling Head

100. The filling or emptying of a lock chamber, regardless of the type of system considered, is essentially a problem of discharge under falling head.[4] If the upper and lower pools at a lock are denoted as Z_u and z, respectively, the head on the lock is then

$$H = Z_u - z \tag{1}*$$

Consider flow through an opening or orifice, from elementary hydraulics,

$$V = C\sqrt{2gH} \tag{2a}$$

and

$$Q = CA\sqrt{2gH} \tag{2b}$$

where

V = velocity of the flow

C = discharge coefficient

g = acceleration of gravity

Q = discharge

A = area of the opening or orifice.

Flow into a lock chamber in an elemental time period of dt produces a volume equal to Q dt which can be designated by $CA\sqrt{2gH} \times dt$. This volume may also be indicated by the change in water level in the lock chamber and is

* Equation numbers refer to the sequence of equations in Appendix A, in which the equations are arranged in topical order.

equal to $-A_s\ dH$ where A_s is the area of the lock water surface and dH is the elemental change in the elevation of the lock water surface in the time dt. The negative sign (-) is used here to indicate that the lock water surface is rising and the head, H, is becoming less. Then with reference to Figure 29,

$$CA\sqrt{2gH}\ dt = -A_s\ dH \tag{3}$$

and

$$dt = \frac{-A_s\ dH}{CA\sqrt{2gH}} \tag{4}$$

Rearranging Equation 4 gives

$$dt = \frac{-A_s}{CA\sqrt{2g}}\ H^{-1/2} dH$$

Then integrating between limits of t_1 and t_2

$$\int_{t_1}^{t_2} dt = \int_{H_1}^{H_2} \frac{-A_s}{CA\sqrt{2g}} \times H^{-1/2}\ dH$$

gives

$$t = \frac{-A_s}{CA\sqrt{2g}} \left(\frac{H_1^{1/2}}{1/2} - \frac{H_2^{1/2}}{1/2} \right)$$

and there results

$$t = \frac{2A_s}{CA\sqrt{2g}} \left(\sqrt{H_1} - \sqrt{H_2} \right) \tag{5}$$

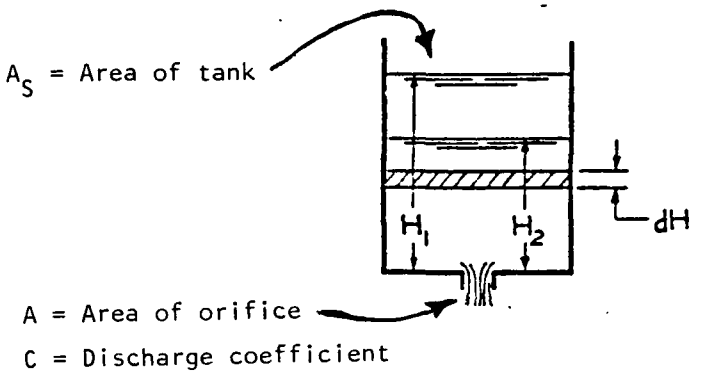

Figure 29. Discharge under falling head

The negative sign (-) has been omitted and t represents a finite time period. Equation 5 gives the interval of time, t, required to fill a vessel under falling head conditions, from a constant level source through a fixed size opening or orifice, through a depth from level z_1 to z_2. The discharge coefficient C reflects only the losses in the submerged opening through which the flow is discharged and the area A of the opening remains constant during the time interval t.

101. Equation 5 is applicable only where changes in momentum are of no significance and the only head losses are those commonly attributed to orifice flow. In the case of flow through an orifice, from one container to another, it is assumed that the thickness of the wall separating the two containers is not great relative to the size of the opening or of the containers, so that the opening cannot be considered either a conduit or culvert. In this situation the length of the path of flow through the opening is small, the volume of water being accelerated at any instant is small, and the inertia head (head required to accelerate the flow) is negligible. It is apparent then, that Equation 5 cannot be used to calculate filling time for a lock unless it is modified. Equation 5 would only be applicable to a hypothetical condition of a lock with valves that open instantaneously and with no appreciable length of culvert. Further discussion of the effects of inertia head in locks with culvert filling systems are presented later in this part.

Lock Operation Time

102. In actual lock design one of the first problems encountered is the preliminary determination of valve and culvert sizes and operation times. It

was noted earlier that Equation 5 cannot be used directly for this purpose. Modifications to Equation 5 have been developed that provide a reasonably satisfactory means of determining operation time for locks with end filling systems and locks with wall culvert systems. For locks with end systems the modifications developed for Equation 5 are described as follows:

a. In a filling or emptying operation, when a lock chamber is full, H_2 (in Equation 5) is zero; hence the expression in parentheses $(\sqrt{H_1} - \sqrt{H_2})$ becomes $\sqrt{H_1}$ which may then be written as H where $H = Z_u - z_l$.

b. t can be replaced with T which now represents operation time (filling or emptying).

c. Another term, Ut_v where U is the valve time coefficient, must be added to the right-hand side of Equation 5 which, provides an approximation of the effect on operation time of adding a portion of the valve opening time t_v.

d. The discharge coefficient C has been replaced with the overall lock coefficient C_L, which represents not only hydraulic losses through the opening, but also includes the effects of the changing conditions that occur during the valve opening period. Equation 5 as modified for valve opening is:

$$T = \frac{2A_s}{C_L A\sqrt{2g}} \sqrt{H} + Ut_v \tag{6}$$

In Equation 6, U is an empirical coefficient that is used to determine the proportion of the valve opening time, t_v, that must be included in the right-hand member of Equation 5 to obtain the operation time T. The coefficient U is dependent on the valve opening schedule and the hydraulic losses in the system and is readily obtained for lock models during model tests. Values of U, either model or prototype, cannot be determined analytically, but prototype values of U can be developed by consideration of prototype data from locks having similar valve schedules and filling systems. Data on lock operation times are obtained for several different values of valve time, t_v, and are plotted as abscissae versus filling or emptying times as ordinates. The value of U is then defined by the ratio of $\Delta T/\Delta t_v$, which gives Equation 7.

$$U = \frac{\Delta T}{\Delta t_v} \tag{7}$$

Figure 30 shows a plot of such data. It can be seen that by extrapolating the curves (straight lines) back to zero valve time, the operation time for the hypothetical condition of instantaneous valve opening can be obtained.

103. In Equation 6 there is no correction for inertia head or head loss from flow through culverts, so it is useful only in design of a lock with an end filling system, i.e., no appreciable length of culverts. For lock designs that utilize culverts with significant length, where inertia corrections must be considered, modifications to Equation 6 are necessary. At the beginning of a lock filling or emptying operation, part of the available head, H , is required to start the mass of water in the culverts moving. As the velocity of flow increases, potential energy is changed to kinetic energy and the conversion continues as long as the flow is accelerating. With lock filling systems, the velocity in the culverts usually increases from the beginning of the valve opening to the time when the valve is nearly open. As the valve approaches the fully open position, the acceleration begins to decrease rapidly; and very soon after the valve is fully open, the acceleration decreases to zero. The flow then begins to decelerate. The deceleration continues to increase until it reaches a value that remains nearly constant throughout the remainder of the operation. During this period of deceleration, kinetic energy is being given up, which increases the head that produces velocity in

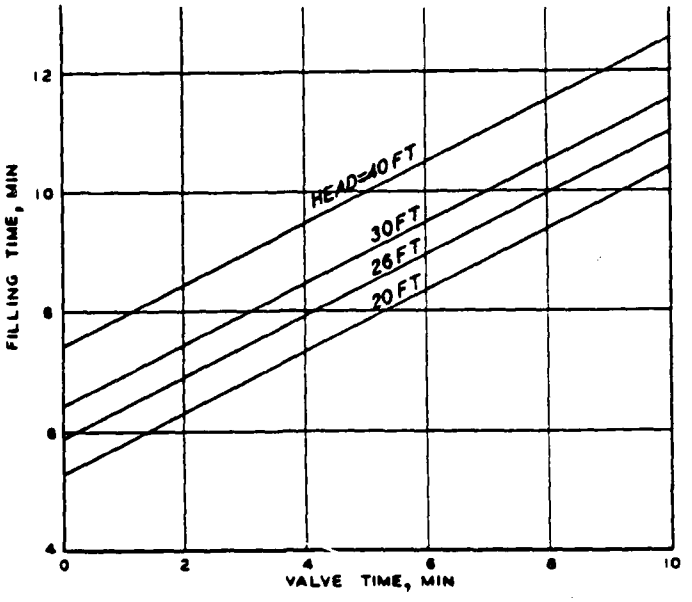

Figure 30. Valve time coefficient curve

the system. It is this deceleration that produces the overfill or underfill that is readily observed in model and prototype locks. It then becomes apparent why Equation 6 cannot be used for locks with culverts, as the value of H in the expression

$$\frac{2A_s}{C_L A\sqrt{2g}}\sqrt{H}$$

does not represent the true head that is actually producing discharge at any instant. The symbol A in this expression has been used to designate the area of a single opening or orifice. As a lock with more than one valved opening is considered--say, two culverts with valves--the symbol A will be replaced with $2A_c$ where A_c represents the area of one culvert. During the valve opening period, the head that is producing flow will be less than $Z_u - z$ at any instant, which will increase the operation time. However, in the period of deceleration, the head that is producing flow will be greater than $Z_u - z$, which will reduce operation time. The expression is now $H = Z_u - z \pm H_m$ where H_m is used to designate inertia head.

104. These statements can be better understood if Equation 4 is reexamined. In this equation

$$dt = \frac{-A_s\, dH}{CA\sqrt{2gH}} \qquad (4 \text{ bis})$$

the numerator is an actual volume for an increment of change in water level represented by dH, and measurement of the value of dH is unaffected by inertia. However, the denominator, $CA\sqrt{2gH}$, is the rate of flow, Q, wherein $C\sqrt{2gH}$ represents the velocity of flow in the culverts. In this expression, it can be seen that the velocity varies as the $\sqrt{H}$. When a portion of H is being used to accelerate the mass of water in the culvert, there will be less effective head to produce velocity and hence less discharge. With reduced discharge a greater increment of time, dt, will be required to cause the lock water surface to rise through the increment dH.

105. Pillsbury[5] developed an equation that gives the approximate time required to fill or empty a lock after the valves are fully open that takes

into account inertia effect for the part of the filling or emptying operation that occurs after the valves are fully open. Using the same notation as was used in the foregoing paragraphs, Pillsbury's equation is:

$$t = \frac{2A_s}{C2A_c\sqrt{2g}} \left(\sqrt{H_1 + d} - \sqrt{H_2 + d} \right) \tag{8a}$$

In this equation, t is the time required for the lock to fill or empty from H_1 to H_2 after the valves are fully open where $2A_c$ is the area of the culverts at the valves and A_s is the area of the lock water surface. The symbol d represents lock overfill or overempty. Pillsbury's studies included development of a complex method to estimate d which is not presented in this report. A good approximation of d can be obtained from the relationship shown in Figure 31, in which values of the parameter j have been plotted versus model values of overfill, d_f. It can be shown that d varies directly as the product of the length and area of the culverts and inversely as the area of the lock chamber. Since the overfill or overempty represents only the inertia head that exists after the valves are open, other methods have to be used to account for inertia effects during the entire filling or emptying operation. The basic equation for inertia head is

$$H_m = \frac{L}{g} \frac{dV}{dt} \tag{10}$$

where the value of L is a measure of the culvert length. Derivation and use of this equation are covered later. Figure 32 shows the relation between model and prototype values of overfill or underfill. By transposing Equation 8a, the value of C, which is the discharge coefficient for the culvert system (excluding valve losses) can be obtained. This transposition gives

$$C = \frac{2A_s\left(\sqrt{H_1 + d} - \sqrt{H_2 + d}\right)}{2A_c\sqrt{2g}\ (t_2 - t_1)} \tag{8b}$$

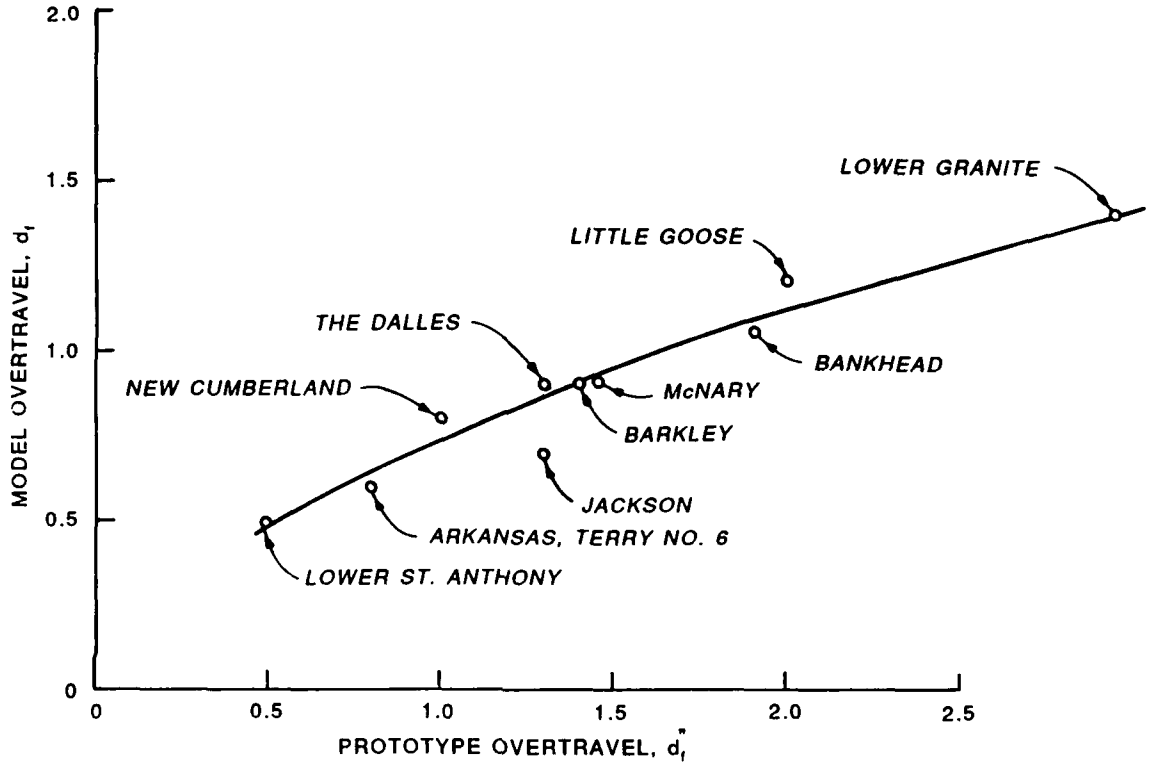

Figure 31. Overfill versus j

106. It is emphasized that in this equation, C is not the same as C_L and also is not identical to the C of flow through an orifice, even though it is used similarly. The C in Equations 8a and 8b express the relation between the theoretical velocity and the velocity that actually occurs with losses that exist in the system. Thus the head loss coefficient for a culvert system may be determined from C with Equation 29 as follows:

$$k = \frac{1}{C^2} \tag{29}$$

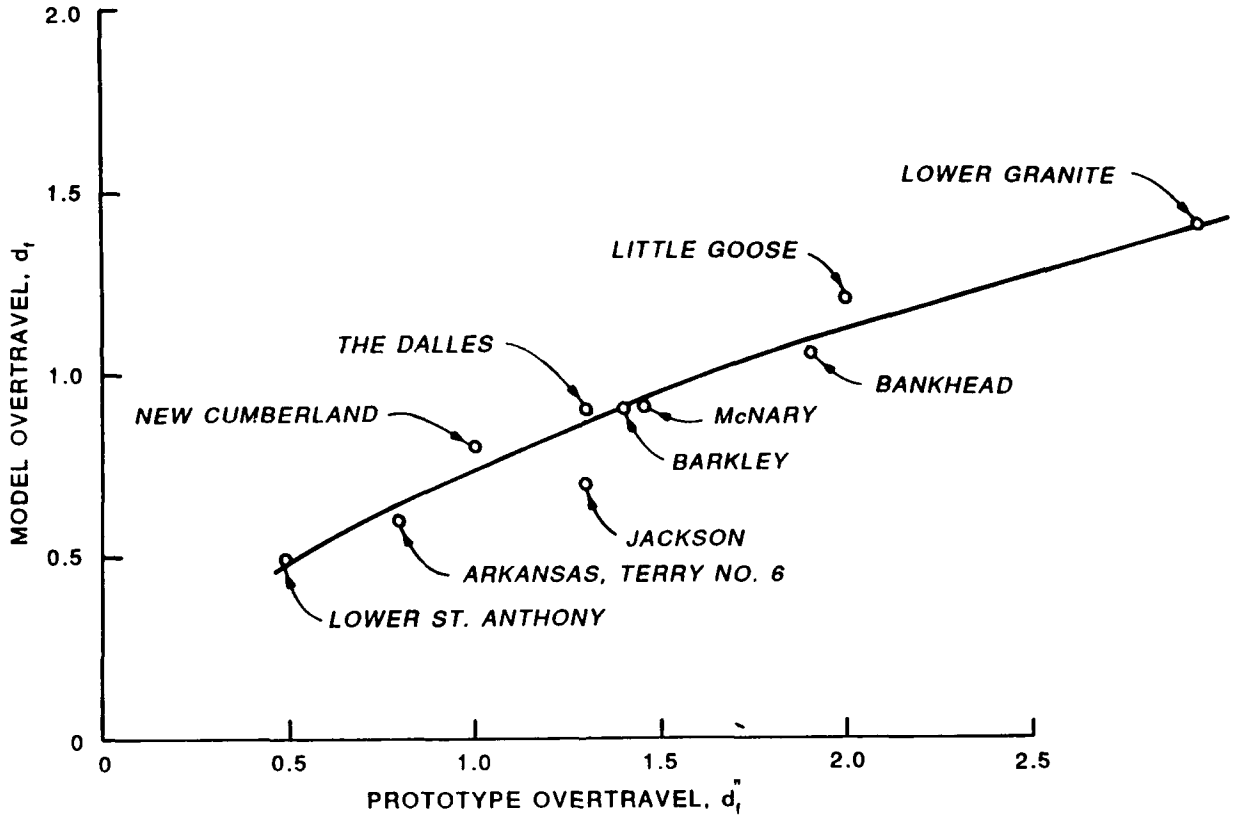

Figure 32. Model overtravel versus prototype overtravel

where

$$k = \frac{H_{L_c}}{V^2/2g}$$

107. It can be seen that Pillsbury's equation can be obtained by adding d to H_1 and H_2 in the expressions (H_1 - H_2) of Equation 5. When the same modifications are made to Equation 8a that were made to Equation 5 for valve opening time and A is designated as $2A_c$ (culvert area at valves) there results

$$T = \frac{2A_s}{C_L 2A_c \sqrt{2g}} \left(\sqrt{H + d} - \sqrt{d} \right) + Ut_v \qquad (9a)$$

In Equation 9a, C_L represents the overall coefficient for an entire filling or emptying operation (mentioned earlier) and includes the effects of head losses in all segments of culverts, intakes, discharge ports, and valve operations. This equation is sometimes given with the term Ut_v transposed to the left side. In this form, the term on the right side of the following equation

$$T - Ut_v = \frac{2A_s}{C_L 2A_c \sqrt{2g}} \left(\sqrt{H + d} - \sqrt{d} \right) \qquad (9b)$$

is the time required to fill a lock having a culvert filling system, with the hypothetical condition of instantaneous valve opening. This hypothetical condition was discussed previously in developing Equations 5 and 6 and in determination of the coefficient U . Equation 9a expresses the approximate relationship between:

operation time	T
valve time	t_v
surface area of lock chamber	A_s
area of culverts at valves	$2A_c$
lock coefficient	C_L

head	H
overfill and overempty	d (d_f and d_e)
valve coefficient	U

By rewriting Equation 9b, culvert area is defined by

$$2A_c = \frac{2A_s(\sqrt{H + d} - \sqrt{d})}{C_L\sqrt{2g}\ (T - Ut_v)} \tag{9c}$$

108. In all of the foregoing analyses the symbols and equations that have been presented are general in nature because they are applicable to either filling or emptying operations and also to model or prototype data. However, as the analyses proceed, subscripts are used to indicate whether filling or emptying is being considered and an additional symbol (") is used to designate whether model or prototype values are being used. This last additional symbol (") is necessary because there are significant differences between model and prototype values of C_{L_f}, C_{L_e}, C_f, C_e, d_f, d_e, and T_f and T_e. The following designations are used:

Model	Prototype	Model	Prototype
C_{L_f}	C''_{L_f}	d_f	d''_f
C_f	C''_f	d_e	d''_e
C_{L_e}	C''_{L_e}	T_f	T''_f
C_e	C''_e	T_e	T''_e

Since most of the data available to evaluate the parameters in Equations 9a and 9c were obtained from model tests, methods have to be devised to obtain prototype values before filling and emptying times, overfill and underfill, and culvert size can be determined for a prototype lock. The methods that have been developed to relate T_f and T''_f, C_f and C''_f, C_{L_f} and C''_{L_f}, and d_f and d''_f and the corresponding parameters for emptying are described later.

Area of Culverts

109. In the beginning stage of design of a lock it is necessary to determine the dimensions of the culverts for a lock of a given size and given lift for a specified filling time and valve time. The type of filling system that is to be used will usually determine the minimum filling time that can be accepted, based on hawser stress and turbulence in the lock chamber during filling or emptying. For instance, a wall culvert side port system can be used for lifts from 5 to 30 or 40 feet, depending on the lock size, but cannot be used for high lifts. Hawser stress data have been obtained in model studies for three different size locks with wall culvert side port systems for lifts from 10 to 40 feet that relate operation time T, lift H, hawser stress F, and cushion depth s (submergence). These data have been used to develop generalized curves relating these four variables. Thus for a given size, lift, allowable hawser stress, and cushion depth there is a minimum limiting operation time for both filling and emptying. Use of the curves and generalized data on hawser stress are presented later. The filling operation, in almost all cases, governs the size of the culvert and other design details such as location, size, and spacing of the ports.

110. Required culvert area for a lock of a given size, lift, and filling time can be determined by

a. Equation 9c, using values of C_{L_f}, U, t_{v_f}, and d_f from models.

b. Equation 9c, using values of C''_{L_f}, U, t''_{v_f}, and d''_f from prototype locks.

c. Using relationships between the total port area and the culvert area for a given size lock.

This last method has no theoretical basis and is a more or less rule of thumb procedure developed from model tests. It has been found that port size and spacing are dependent to a large extent on lock width; that the port manifold should have enough ports to occupy 50 to 60 percent of length of the lock chamber; and that the total area of the port throats (for one culvert) should be about 90 to 95 percent of the area of the culvert. This procedure is only applicable to wall culvert side port filling systems. If a design study is initiated by using the rule of thumb procedures to determine culvert size, the size should also be calculated by Equation 9c using both model and prototype data. Use of Equation 9c with prototype data should be given more weight

than either of the other two methods, but the difference between the size determined by Equation 9c with model data and 9c with prototype values will be very small. Equation 9c defines culvert area as follows:

$$2A_c = \frac{2A_s(\sqrt{H + d_f} - \sqrt{d_f})}{C_L\sqrt{2g}\left(T_f - Ut_{v_f}\right)} \qquad \text{(9c bis)}$$

with subscripts to denote model filling operation in terms of the other variables U, T_f, d_f, C_{L_f}, t_{v_f}. Valve time, t_{v_f}, is variable but it can be fixed when the type of system to be used for a specific lock is selected and an estimate of the filling time T_f has been made. Equation 9c is not a very exact statement of the relationship between the parameters that are involved. The value of d_f, the overfill, is utilized to allow for the effects of inertia head, but it does not provide an accurate measure of the inertia effects on head during the valve opening period when the mass of water in a culvert is being accelerated. In spite of this deficiency, Equation 9c can be used to determine culvert area with an acceptable degree of accuracy. Obviously, to use Equation 9c to determine culvert area, U, T_f, C_{L_f}, and d_f must be evaluated. A rigorous mathematical solution to evaluate the four variables is not practical or necessary. Using experimental data from model tests and performance observations from model and prototype studies, approximate values that are sufficiently accurate can be determined.

111. Locks designed in the United States in the last 40 years have had model valve time coefficients, U, ranging from about 0.45 to 0.70. Unless an unusually long valve time is used or an extremely variable valve motion curve (such as a fast-slow-fast schedule) is adopted, the value of U for conventional locks in the United States will normally fall between 0.50 and 0.60. Table 1 shows valve time coefficients for 14 locks built since 1955. It is recommended that U values shown in the following tabulation be used.

Type Lock	Valve Motion	$\frac{t_v}{T}$	$\overline{\quad}$	ılue Empty
Wall culvert side port	Approx. uniform	0.25-0.70	0.53	0.58
Bottom lateral	Approx. uniform	0.25-0.70	0.65	0.65
Bottom longitudinal	Approx. uniform	0.25-0.70	0.58	0.58

There is insufficient data at present to determine U values for prototype locks. It appears at this time that model and prototype values would be about the same.

112. Before attempting to make a preliminary determination of culvert size for a lock, a tentative layout must be made in order to obtain the approximate length of the culverts and the general configuration of the proposed system. If the project being considered has a lift no greater than 30 feet, the choice of a filling system may usually be narrowed to only one--a wall culvert side port system. If the lock is no longer than 670 feet, the side port system could be used for lifts of up to 40 feet. At lifts of 40 feet the four-manifold bottom longitudinal system may be desirable, depending on expected traffic and construction costs. At lifts greater than 40 feet, the side port system should not be considered. For 1,270-foot locks with lifts greater than 30 feet, the 8-manifold bottom longitudinal system similar to Lower Granite Lock should receive primary consideration. It was stated earlier that limiting values for minimum filling times for three sizes of locks with side port systems had been developed in generalized model tests. The generalized model tests relating hawser force, lift, cushion depth, and operation time were developed during model studies of wall culvert side port systems for the Arkansas River low-lift locks, the Cannelton Lock on the Ohio River, and the Jonesville Lock on the Ouachita River. The curves shown in Figures 33-35 are for the recommended design for each of the locks. The model test reports on these locks (References 6-8) contain curves similar to those shown in Figures 33-35 for other port arrangements. Figures 36-38 present data for the emptying operations. The curves for the 600- by 84-foot Jonesville Lock should be used with caution because it appears that the culverts used in the model tests were too small.

113. Using the generalized curves for low-lift locks and performance data from high-lift locks with bottom lateral systems and bottom longitudinal systems, the three curves shown in Figure 39 were developed. These curves, lock chamber volume versus average discharge into the lock chamber during a filling operation, may be used to obtain a preliminary value of T_f for a lock of a given size and lift with any of these three filling systems. By entering the curves with lock volume, the allowable rate discharge is obtained and T_f is then calculated by dividing the volume by the discharge. Operation time, T , from a model of a lock is always greater than for the

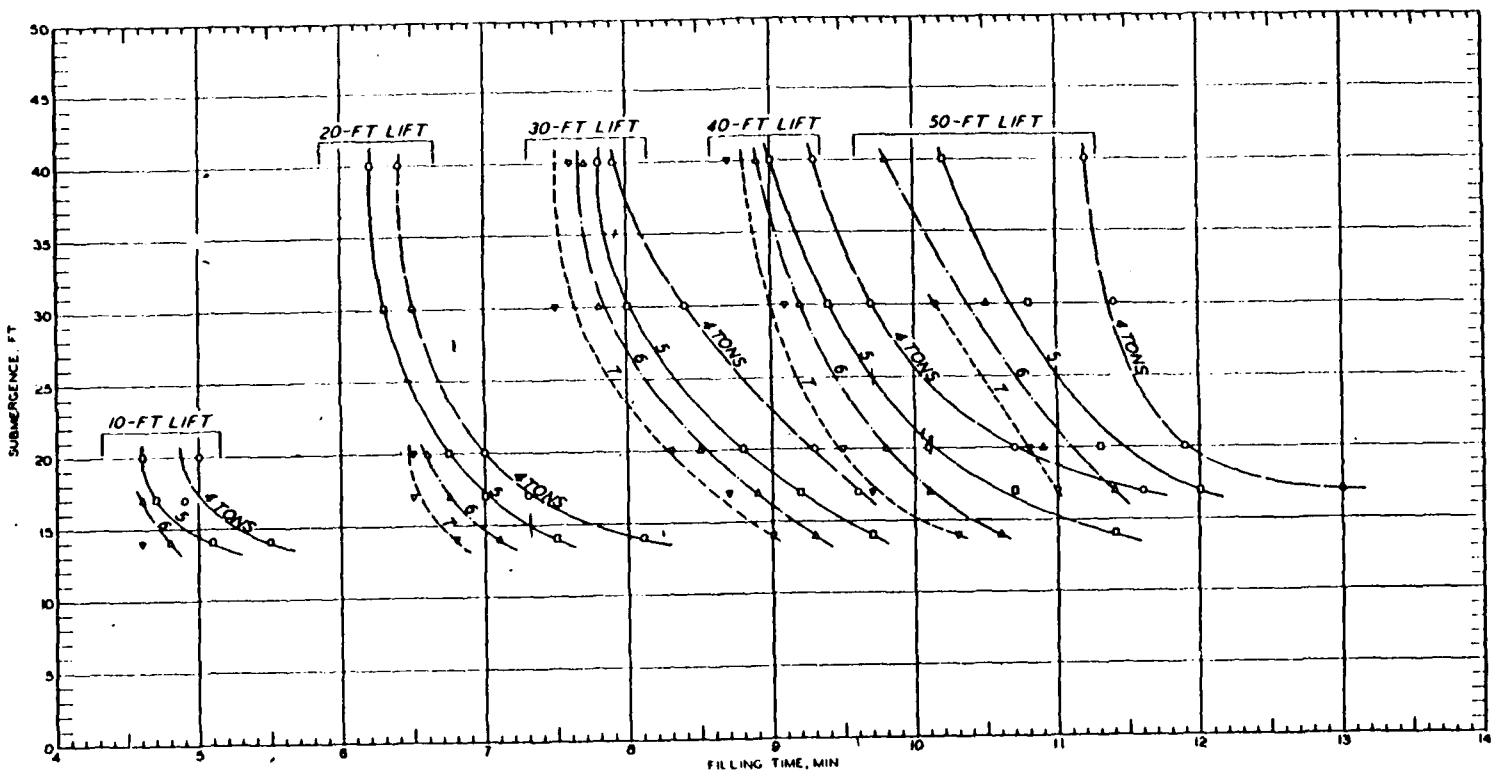

NOTE HAWSER STRESSES WERE MEASURED ON 8-BARGE TOW (15,530 TONS DISPLACEMENT) POSITIONED 55FT FROM UPSTREAM MITER GATE PINTLES
SUBMERGENCE IS THE DIFFERENCE IN ELEVATION BETWEEN LOWER POOL AND THE LOCK CHAMBER FLOOR

Figure 33. Permissible filling times, 600- by 110-ft lock

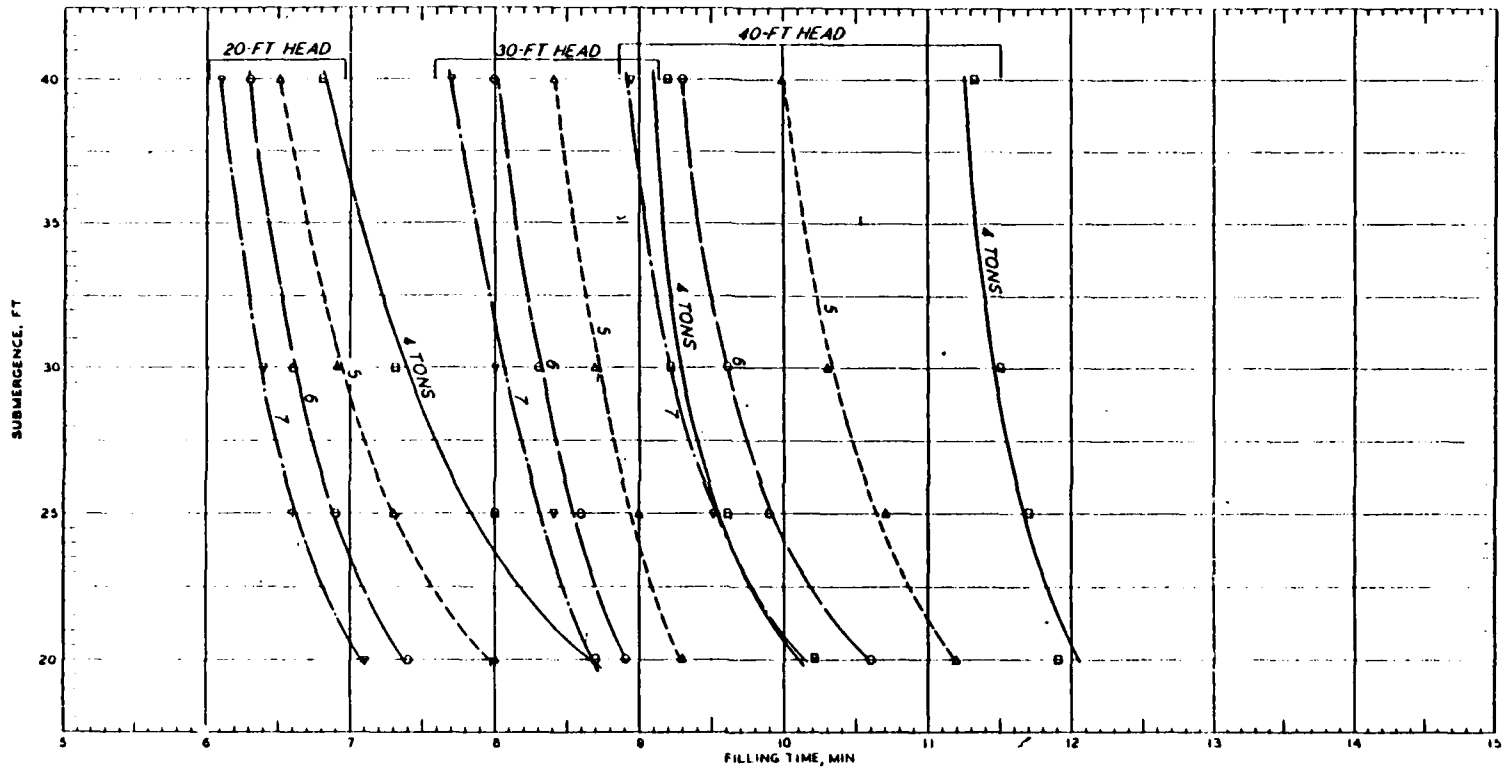

NOTE HAWSER STRESSES WERE MEASURED ON 18-BARGE TOW (33 900 TONS DISPLACEMENT) POSITIONED 35 FT FROM UPSTREAM MITER GATE PINTLES

SUBMERGENCE IS THE DIFFERENCE IN ELEVATION BETWEEN TOWER POOL AND THE LOCK CHAMBER FLOOR

CULVERT AREA WAS 288 SQ FT

PERMISSIBLE FILLING TIMES TO KEEP HAWSER STRESSES WITHIN 4-, 5-, 6-, AND 7-TON LIMITS

TYPE A PORTS, TYPE 100 ARRANGEMENT

Figure 34. Permissible filling times, 1,200- by 110-ft lock

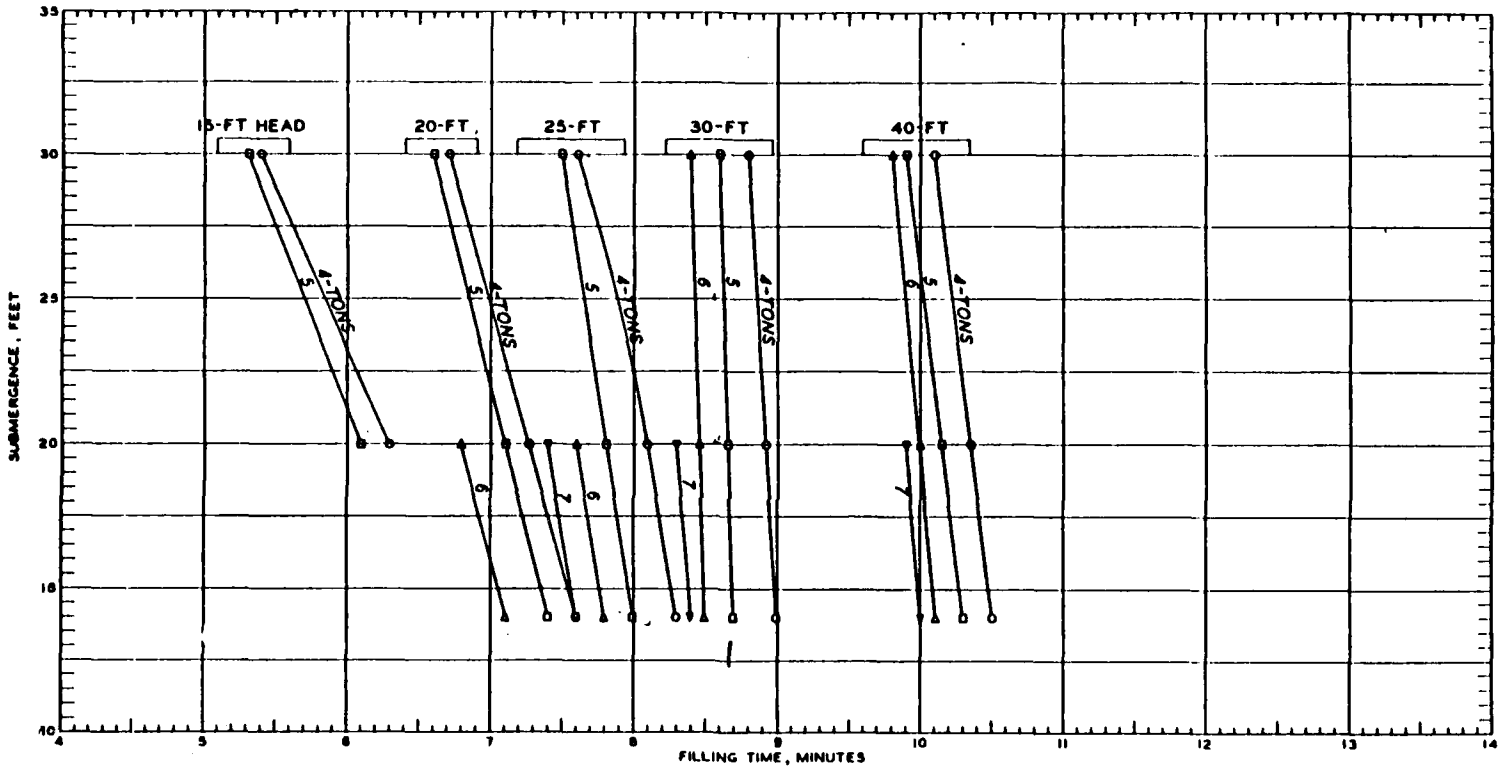

NOTE: HAWSER STRESSES WERE MEASURED ON 6-BARGE TOW (11,110 TONS DISPLACEMENT) POSITIONED 35 FT FROM UPSTREAM MITER GATE PINTLES.

SUBMERGENCE IS THE DIFFERENCE IN ELEVATION BETWEEN LOWER POOL AND THE LOCK CHAMBER FLOOR.

PORTS WERE 2 FT WIDE BY 3 FT HIGH AT THE THROAT.

PERMISSIBLE FILLING TIMES TO KEEP HAWSER STRESSES WITHIN 4-,5-,6-, AND 7-TON LIMITS
TYPE 3 PORT ARRANGEMENT

Figure 35. Permissible filling times, 600- by 84-ft lock

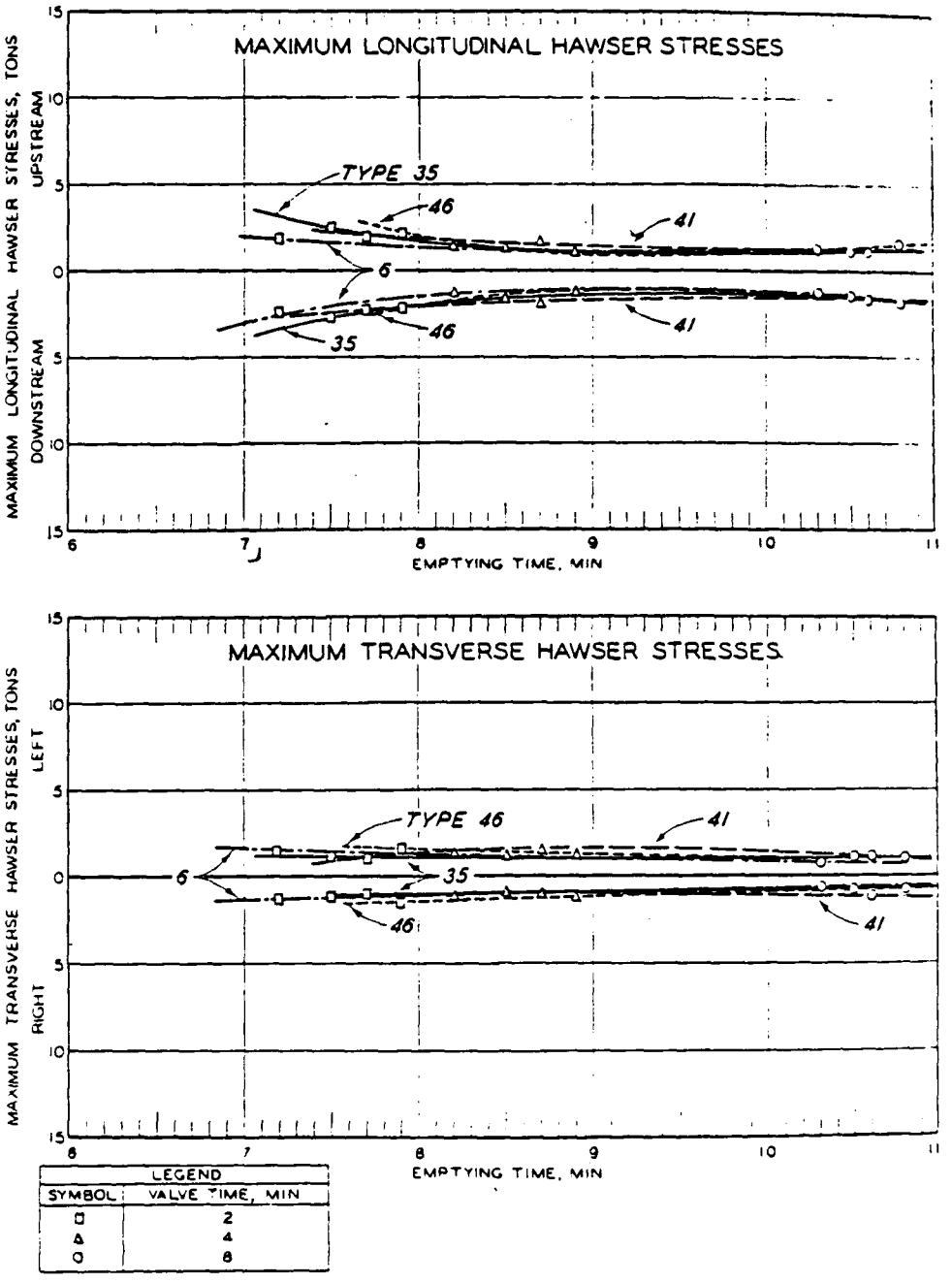

Figure 36. Hawser stress during emptying, 600- by 110-ft lock

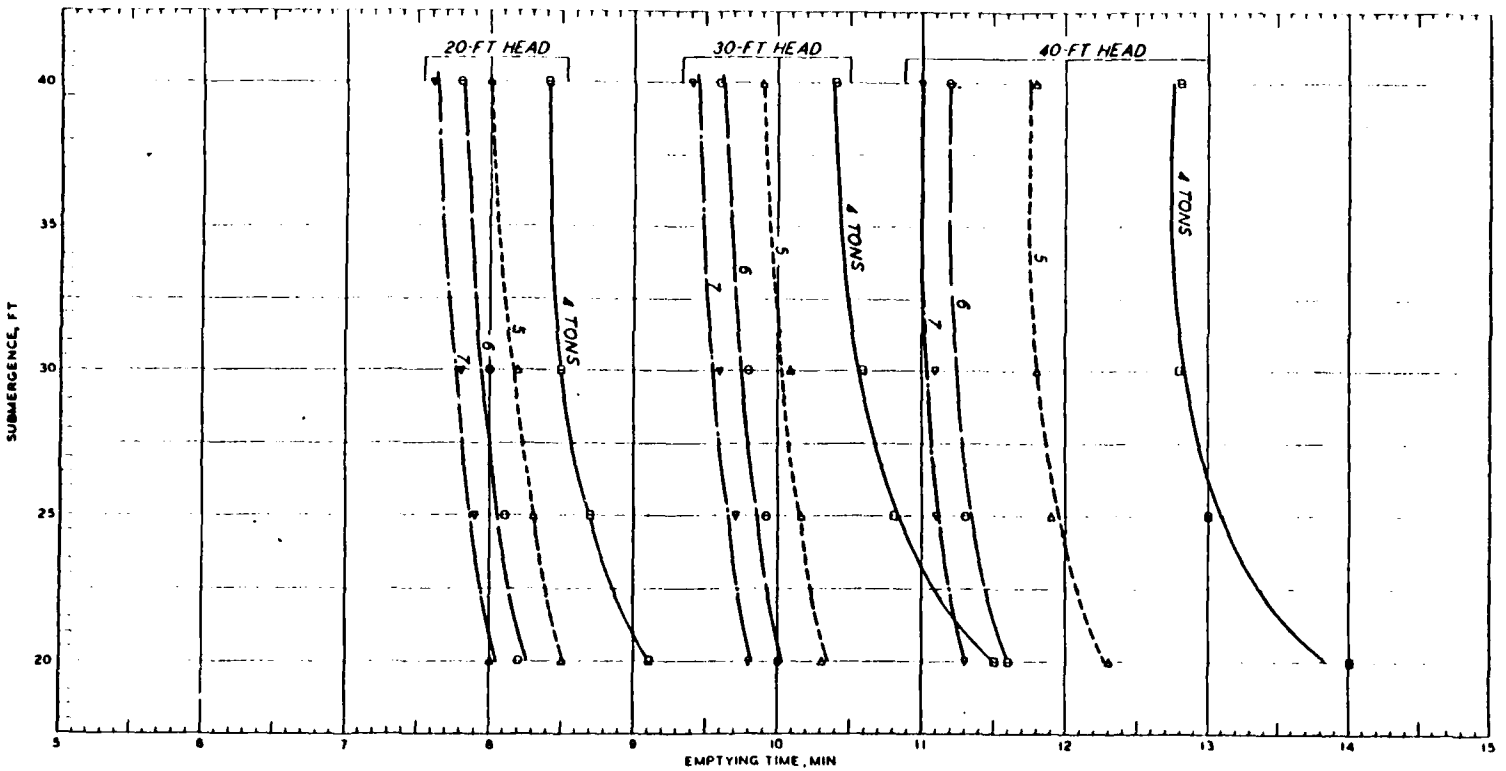

NOTE HAWSER STRESSES WERE MEASURED ON 18-BARGE TOW (33,900 TONS DISPLACEMENT) POSITIONED 35 FT FROM UPSTREAM MITER GATE PINTLES

SUBMERGENCE IS THE DIFFERENCE IN ELEVATION BETWEEN LOWER POOL AND THE LOCK CHAMBER FLOOR

CULVERT AREA WAS 288 SQ FT

PERMISSIBLE EMPTYING TIMES TO KEEP HAWSER STRESSES WITHIN 4-, 5-, 6-, AND 7-TON LIMITS

TYPE A PORTS, TYPE 100 ARRANGEMENT

Figure 37. Permissible filling times, 1,200- by 110-ft lock

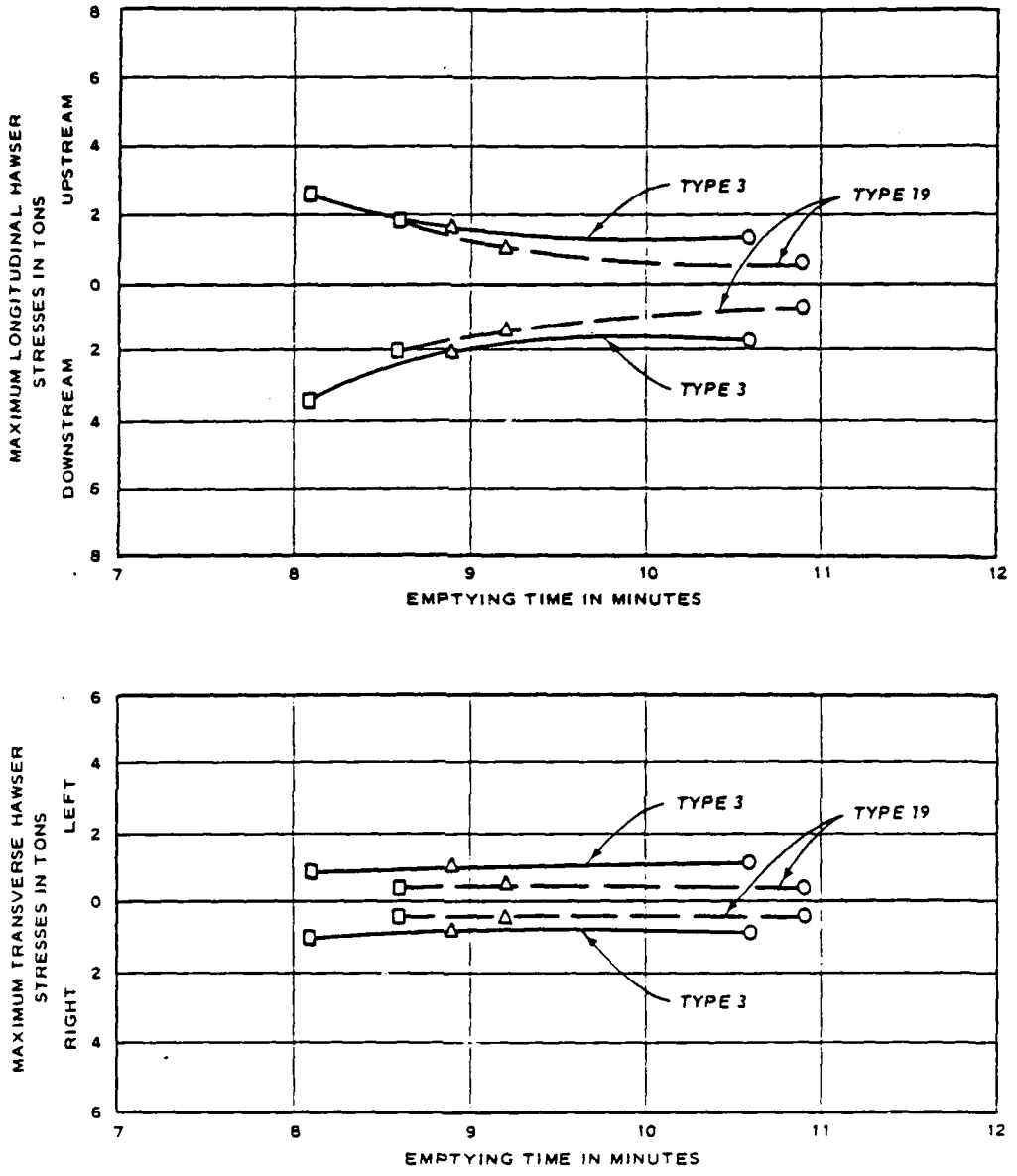

Figure 38. Emptying characteristics, 600- by 84-foot lock

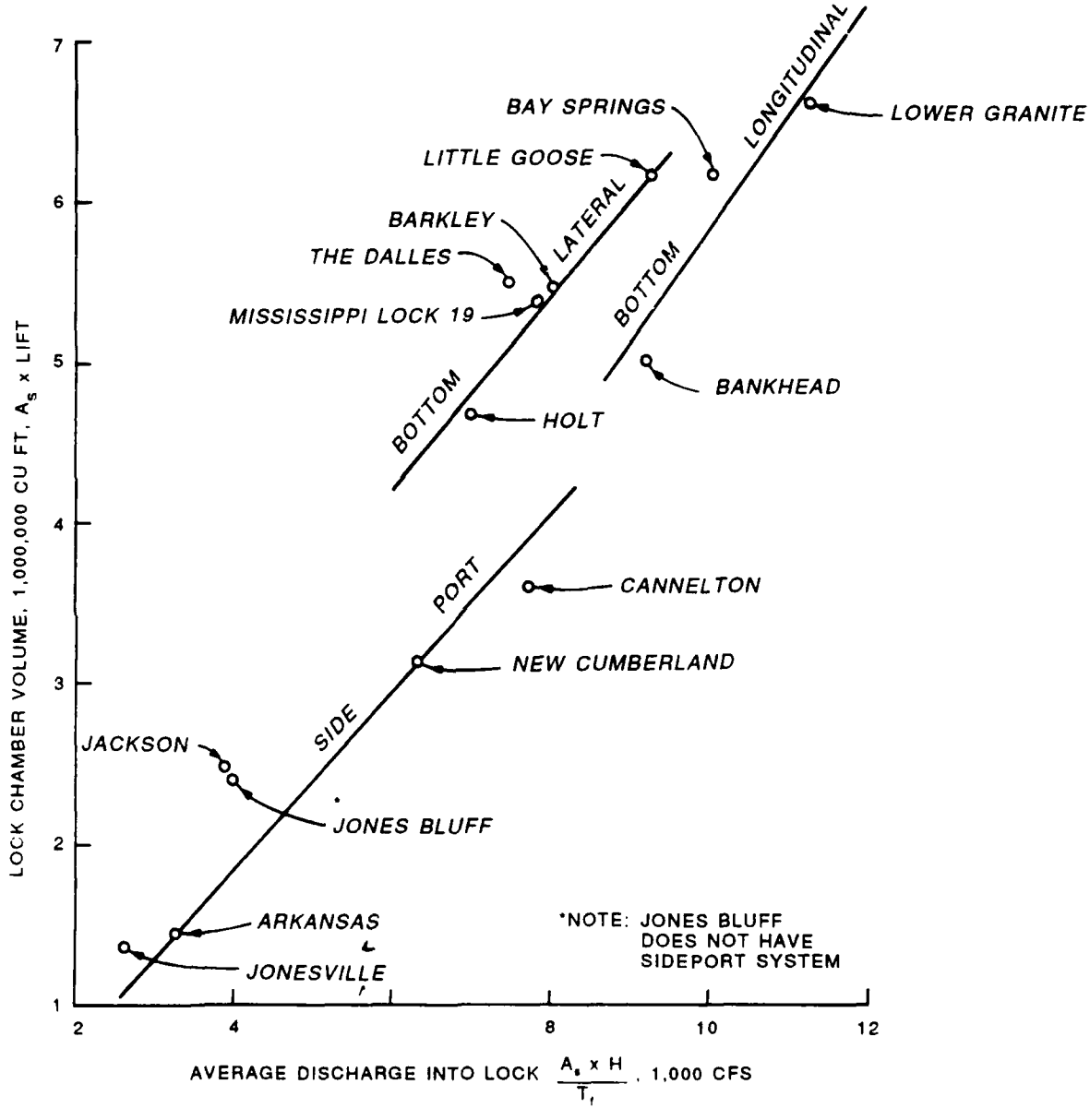

Figure 39. Lock volume versus average discharge (model filling time)

prototype lock. Figure 40 shows the relation between model and prototype filling times for several locks. With a wall culvert side port system, the depth in the lock chamber is a critical factor. In developing the curve in Figure 39 for the side port system, the values of T_f used were values obtained from the model test reports for the recommended designs for each lock and in each case represented the approximate optimum combination of operation time and cushion depth for a given lift and a limiting hawser force. Values from the curve in Figure 39 for side port systems should be compared with values from the generalized curves shown in Figures 33-35. For locks of sizes that are different from the three covered in these figures, filling time can

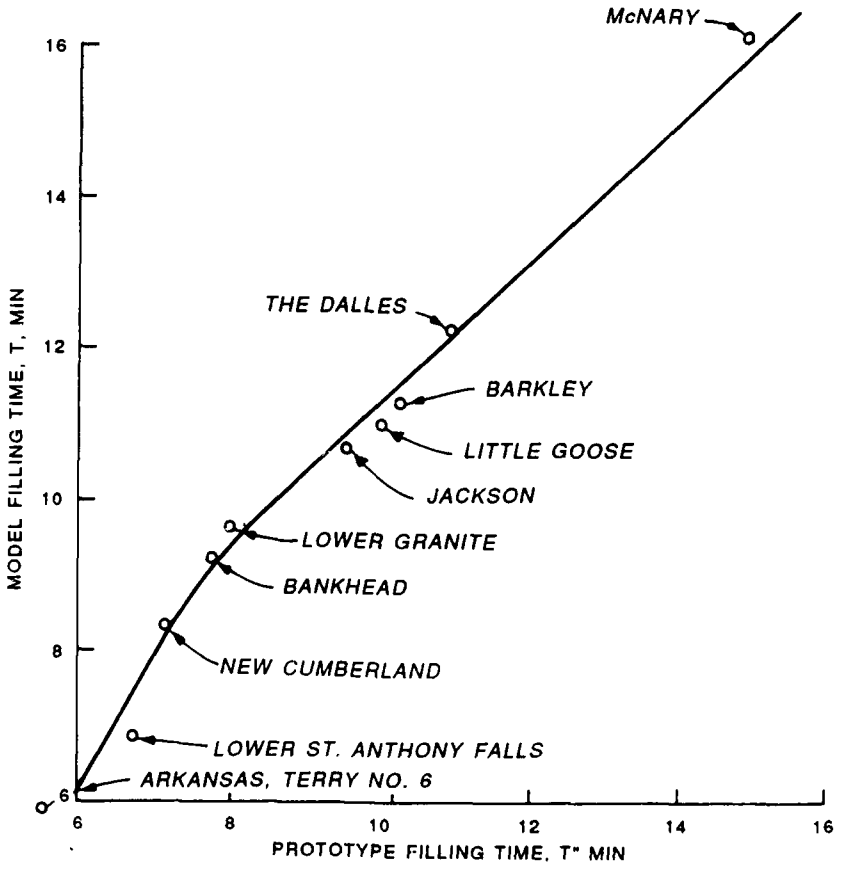

Figure 40. Prototype filling time versus model filling time

be interpolated from these figures by adopting a limiting hawser stress and cushion depth to use in the figures used in the interpolation. With bottom longitudinal design, the minimum depth required for navigation must be provided over the tops of the bottom culverts, and this minimum depth is adequate insofar as turbulence and hawser force are concerned.

114. As was explained earlier, the overall lock coefficient, C_L, is similar to a discharge coefficient but is not identical and is influenced by factors other than losses from the intake, culvert, and manifold. In paragraph 108, the parameters of Equations 9b and 9c were given specific designations to distinguish between filling or emptying operations, to show whether the data are for a model or a prototype lock, and to indicate whether coefficient values are overall lock coefficients or discharge coefficients. Throughout the remainder of this report, the four different lock coefficients and the four different discharge coefficients of paragraph 108 will be utilized. For clarity these eight are defined as follows:

C_{L_f} = overall lock coefficient for model for filling operation

C_{L_e} = overall lock coefficient for model for emptying operation

C_f = discharge coefficient for model for filling operation (after valves are fully open)

C_e = discharge coefficient for model for emptying operation (after valves are fully open)

C''_{L_f} = overall lock coefficient for prototype lock for filling operation

C''_{L_e} = overall lock coefficient for prototype lock for emptying operation

C''_f = discharge coefficient for prototype for filling operation (after valves are fully open)

C''_e = discharge coefficient for prototype for emptying operation (after valves are fully open)

This same system of distinguishing between model and prototype values will be followed with head loss coefficients.

115. There is no way to calculate directly the value of C_{L_f}, C_{L_e}, or the corresponding values for a prototype lock that is being designed. It is known, however, that the values shown in the following tabulation are reasonably satisfactory for preliminary determination of culvert area with model data.

Type of System	C_{L_f}
Wall culvert side port	0.68 to 0.74
four-manifold bottom longitudinal	0.60 to 0.68
eight-manifold bottom longitudinal	0.52 to 0.65

If a situation develops where the length of the culvert between the intake and the manifold is longer than customary, these values will be reduced because of the increased head loss. These values may seem to be objectionably low. However, it must be recognized that while the overall lock coefficient is a useful parameter, it is not an indication of hydraulic efficiency. In tests of different size culverts during Cannelton Lock model studies it was found that C_{L_f} varied considerably with variation in culvert size. Figure 41 shows the results of the Cannelton tests. As the culvert area was varied, the values of C_{L_f} and T_f changed as follows:

A_c sq ft	C_{L_f}	T_f min.	t_{v_f} min.
288	0.736	7.9	4.0
240	0.733	9.1	4.0
213	0.777	9.6	4.0
200*	0.805**	9.9*	--
300*	0.725**	7.6*	--
320*	0.756**	7.0*	--

* Extrapolated from curves on Figure 41.
** Calculated with extrapolated values of C_{L_f}, T_f, and d_f.

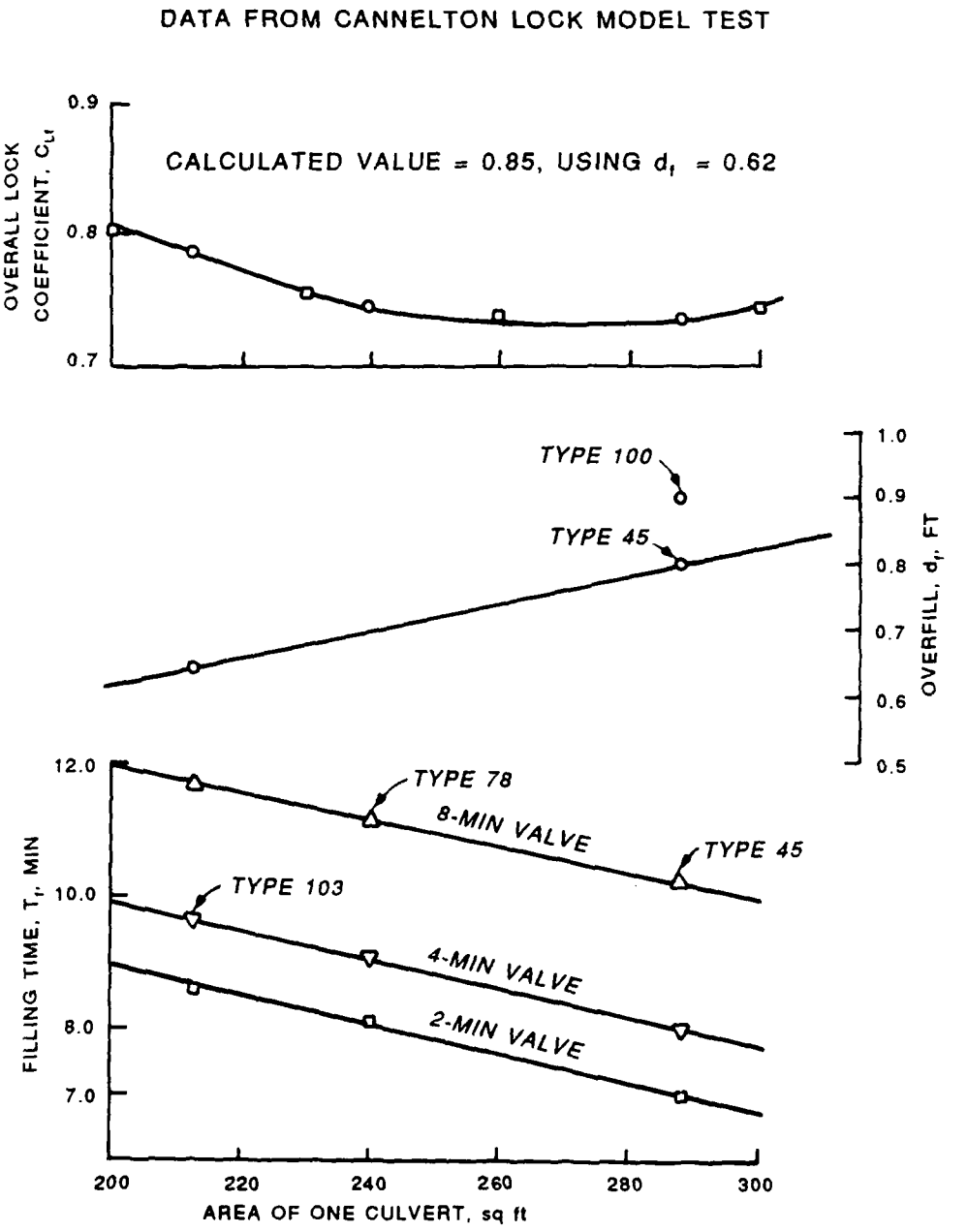

Figure 41. Culvert area versus T_f , d_f , and C_{L_F}

This tabulation shows that C_{L_f} is not constant and can even increase as the culvert area decreases. This appears to contradict the fact that normally, in any conduit system, hydraulic losses usually increase as the size is reduced. It must be remembered though, that (1) a lock manifold system is not a normal conduit for conveyance of flow; (2) C_{L_f} is not a pure discharge coefficient; and (3) C_{L_f} is materially affected by the transient flow conditions that exist during the filling operation when inertia head changes rapidly. Calculations of model and prototype values of C_{L_f} and C_f from observed data show that a reasonably constant difference exists between them. Values of C_{L_f} and C_f that were computed from model data for several locks are plotted in Figure 42. The value of C_f averages about 3.5 percent greater than C_{L_f} over the range of values shown. In Figure 43 a plot of C''_{L_f} and C''_f values indicates that the relationship is similar, but the C''_f values average only about 2.0 percent greater than the C''_{L_f} values.

116. For a given preliminary layout of a filling system, the value of C_f and of C''_f may be regarded as essentially constant. Head loss coefficients may be estimated from the physical characteristics of the filling system by procedures that will be given later and discharge coefficients can then be calculated by rewriting Equation 29 so that:

$$C_f = \frac{1}{\sqrt{k_f}} \tag{30}$$

where

$$k_f = \frac{H_{L_c}}{V_c^2/2g} \tag{32}$$

Then by using Figure 42 or 43 an approximate value of C_{L_f} or C''_{L_f} can be obtained. The C_{L_f} value can be used to check the value selected originally from the data in paragraph 115. Figures 44-46 give values of coefficients for model and prototype locks for emptying operations.

117. The valve time, t_{v_f}, can be determined on the basis of the type system chosen and the operation time, T_f, can be obtained from Figure 39. If a side port system is being considered and the operation time is estimated

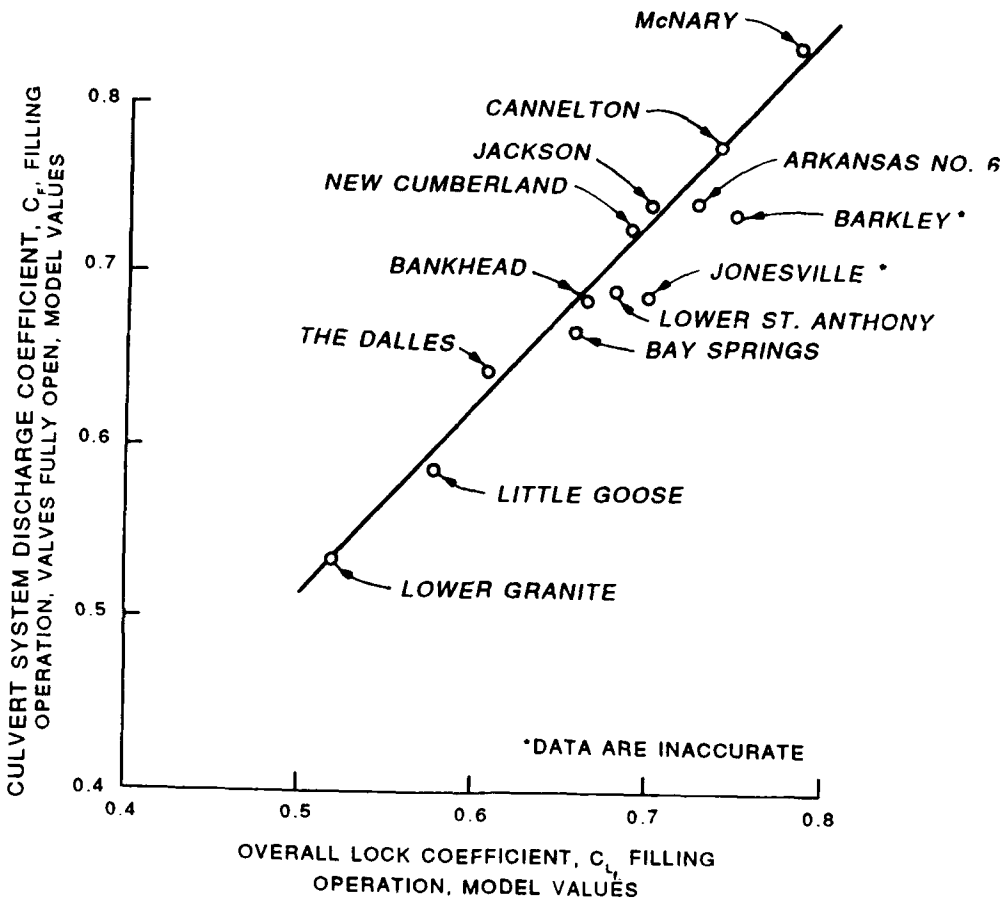

Figure 42. C_{L_F} versus C_f values (model)

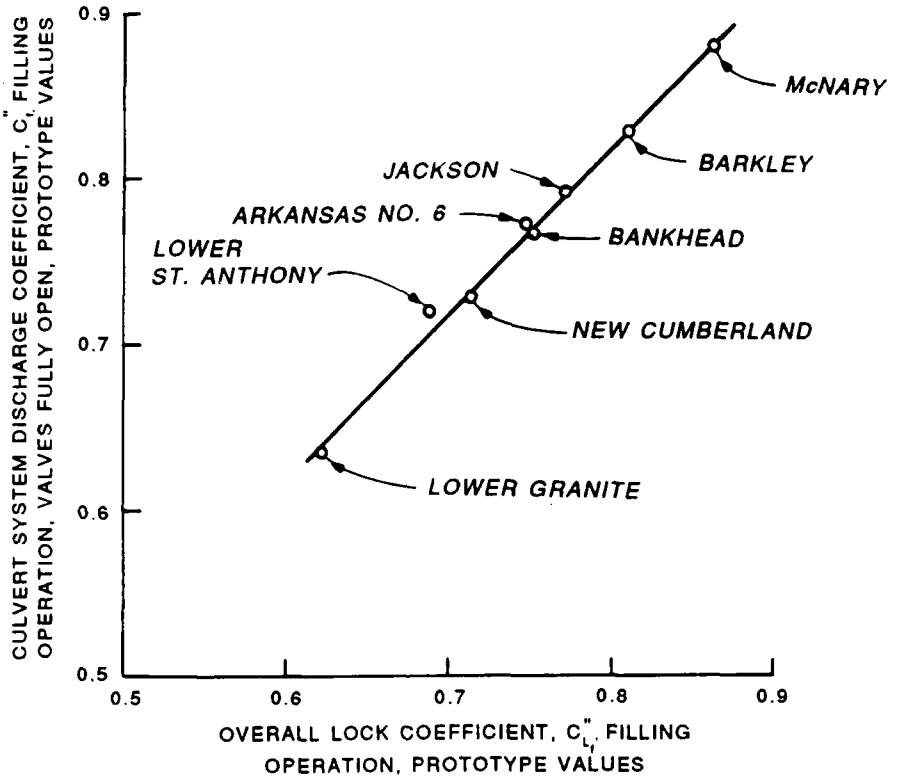

Figure 43. C''_{L_f} versus C''_f values (prototype)

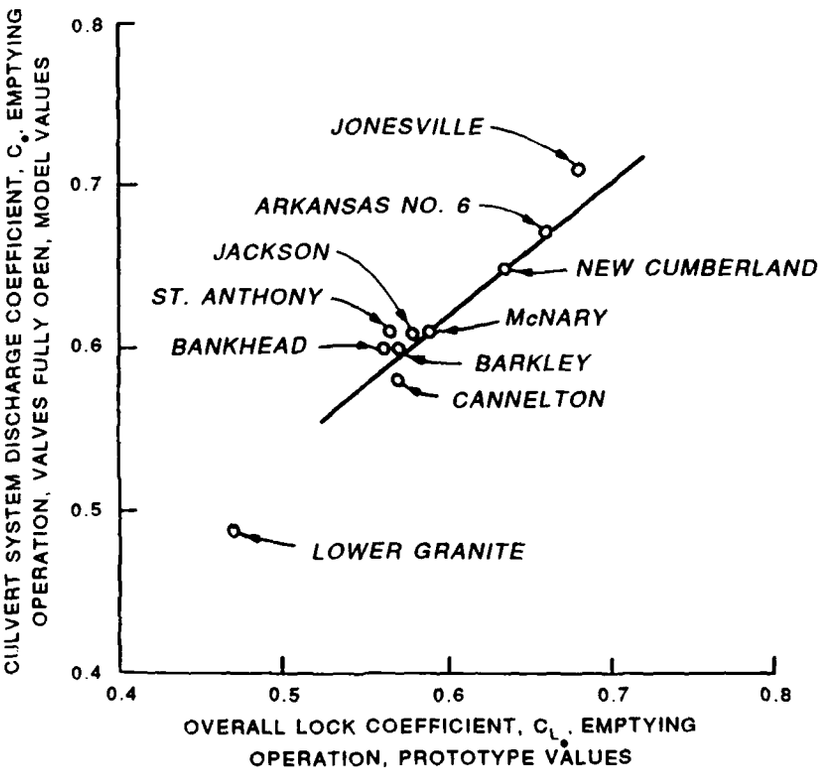

Figure 44. Coefficients for emptying (model locks)

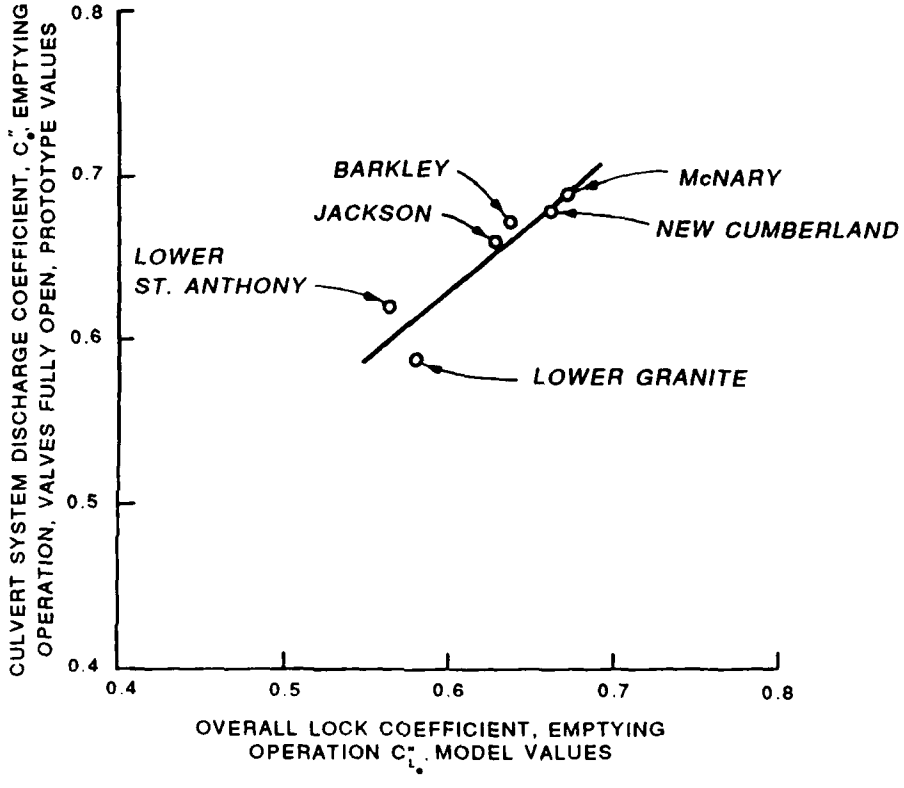

Figure 45. Coefficients for emptying (prototype locks)

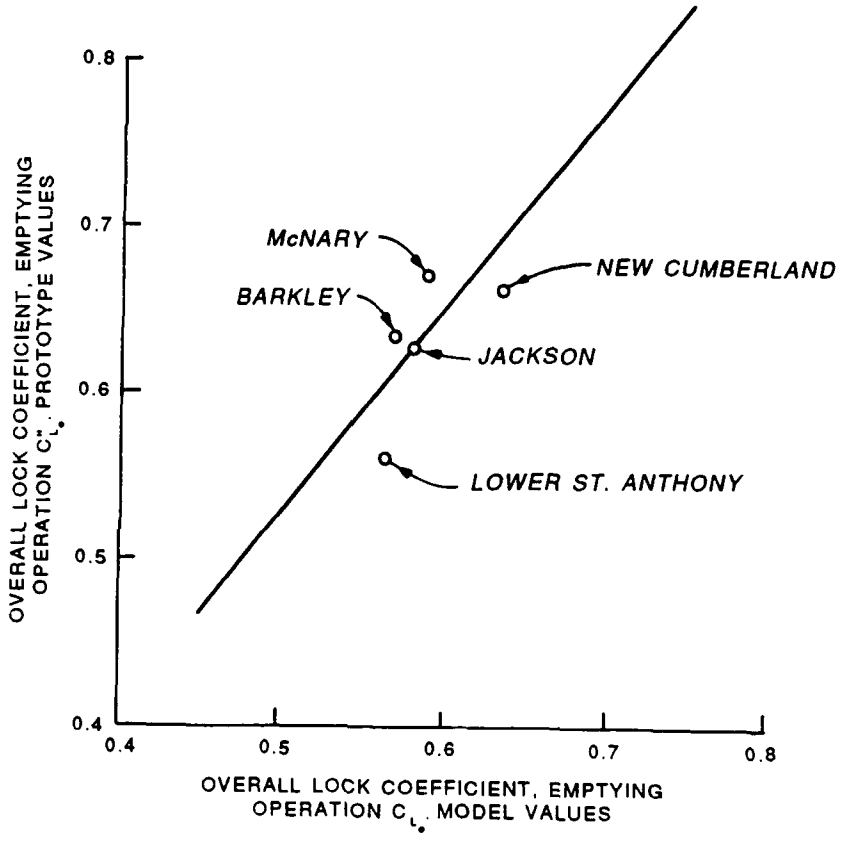

Figure 46. Model and prototype values for overall lock emptying coefficients

to be greater than 6 minutes, the minimum value of t_{v_f} would be 2.0 minutes and 4 minutes would probably be required. If the bottom longitudinal system is to be used the valve time would normally be no greater than 2.0 minutes and 1 minute would probably be a more reasonable value.

118. In paragraph 105, overfill and underfill were discussed and in Figure 31, a curve defining d_f or d_e in terms of an inertia parameter designated "j" was presented. Since,

$$j = \frac{2A_c L_c}{A_s} \tag{14}$$

where L_c is the length of the culvert, it is necessary to arrive at a trial value of A_c which will be designated as A_c^*. A value of A_c^* can be calculated from

$$2A_c^* = \frac{2A_s H}{\sqrt{2g}\left(T - Ut_v\right)} \tag{9e}$$

At the start of a lock design study H and A_s are known. The operation time, T_f, the valve time coefficient, U, and the valve time t_{v_f} can be estimated by procedures described earlier. With a value for $2A_c^*$ and the length of the culverts from the preliminary layout, a first trial value of d_f can be obtained from Figure 31. By using the values of U, T_f, d_f, and C_{L_f} determined previously and the preliminary layout, a tentative size for the main culverts can be calculated with Equation 9c). At this point the value of $2A_c$ can be used to recalculate a new value of j, and a new value of d_f can be read from Figure 31. The new d_f value can then be used to go back and check the first calculated value of A_c. In all probability the difference in A_c that results from use of the new d_f value will be insignificant.

119. With reference to paragraph 116, calculation of C_f can proceed when the tentative arrangement of the culverts, intakes, and manifolds have been made. By utilizing the curves and data from paragraph 134, "Head Losses," the loss coefficients for the intake, the culvert (resistance and bends), the valve (fully open), bulkhead slots, and the lock chamber manifold

can be calculated. These loss coefficients are designated as follows and apply to the filling operation of a model unless designated differently.

Symbol	Coefficient
k_f	Loss, upper pool to lock chamber (filling valve open)
k_i	Loss at intake
k_r	Resistance loss in culvert
k_b	Loss in culvert bends
k_{vw}	Loss at value well for fully open valve
k_s	Loss at each bulkhead slot (usually 2 slots)
k_{m_f}	Loss in manifold (including exit into lock)

Then,

$$k_f = k_i + k_r + k_b + k_{vw} + k_s + k_{m_f}$$

This summation of loss coefficients does not contain a coefficient for loss during the valve opening period. Derivation of these loss coefficients is given in paragraph 134; however, for purposes of continuing with the explanation of design procedures, the loss coefficient curves and adopted loss data of paragraph 134 will be utilized without explanation of their derivation here. For clarification, it is noted that in Tables C-8, C-9 and C-10, which contain computations for culvert loss coefficients and a valve loss curve, k_f is designated as k_c when the valve is fully open. Then the total loss coefficient at any instant during valve opening becomes $k_c + k_v$ and varies with position of the valve.

120. Figure 47 shows values of intake head loss coefficients versus the ratio of total intake port throat area to culvert area, k_i versus $\Sigma A_p/A_c$. This curve can be used for conventional multiport intakes that usually have from four to eight square or rectangular ports in the vertical faces of the lock walls upstream from the upper lock gates. More details are given on design of intakes in Part VIII. Figure 47 shows that as the intake throat area is made larger, k_i is reduced, but as $\Sigma A_p/A_c$ approaches a value of 2.0, further decrease in k_i is quite small. Values of $\Sigma A_p/A_c$ in the range of 1.50 to 2.25 are considered good design practice, and a final selection may be influenced to some extent by other design factors.

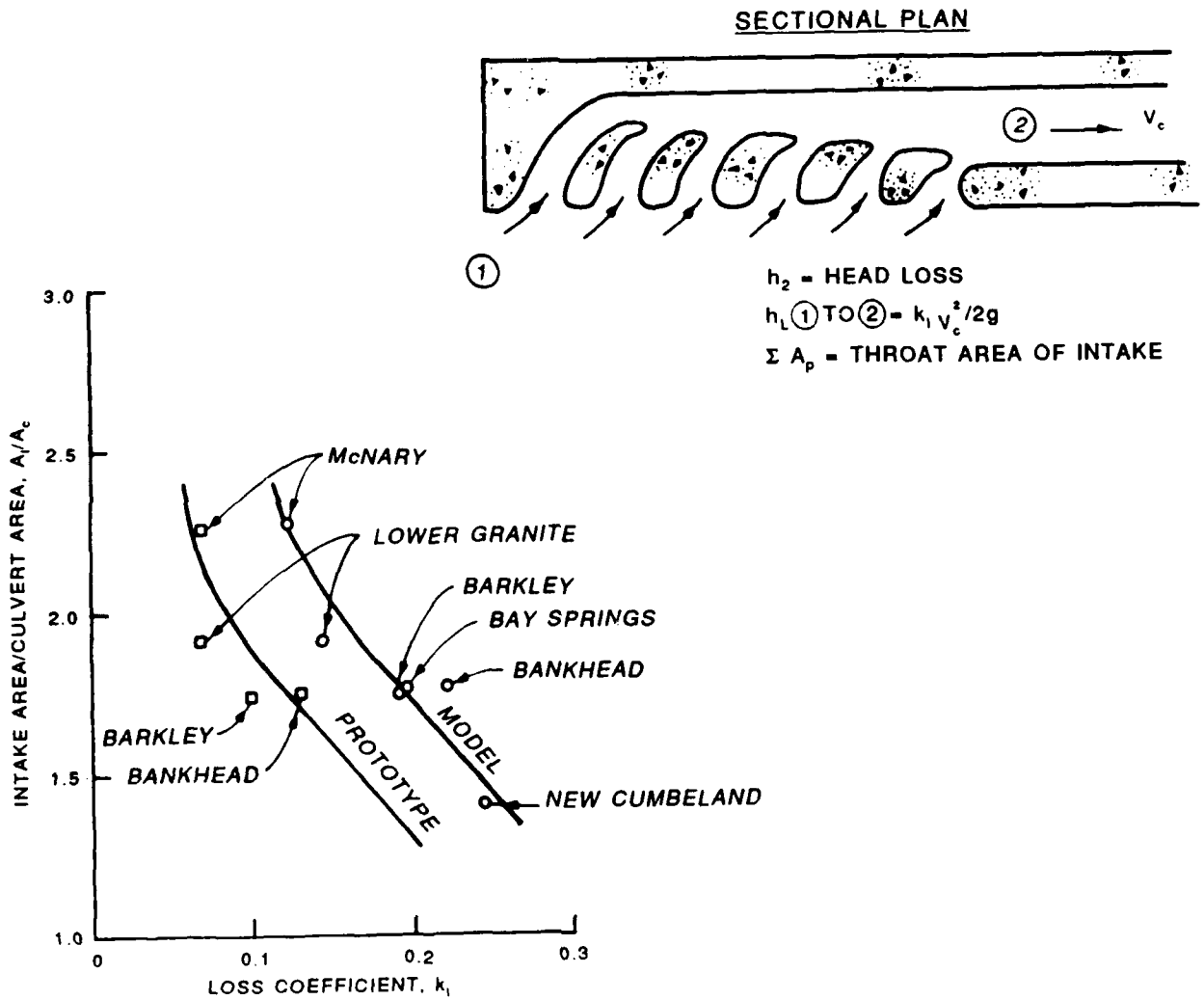

Figure 47. Intake head loss coefficient, k_i

121. The resistance loss coefficient for the culvert can be computed by

$$k_r = \frac{Lf}{D_h} \tag{35}$$

where f is the resistance factor from the Colebrook-White diagram, D_h is equal to 4R (for rectangular culverts), and L is the length of the culvert from the intake to the first port in the manifold. (Note: This value of L is not the same value used to determine inertia head--the L for inertia head is the length from intake to midpoint of the manifold.) In studies for this report, values of f for lock models range between 0.014 and 0.020 depending on the model scale, material used in the model, and the value of Reynolds number, N_R, that existed during model test runs. A prototype value of f, based on a meager amount of data, of 0.009 has been adopted as being representative of locks built in the United States in the last 25-30 years.

122. On most locks, requirements for the filling operation govern the culvert size and manifold design. Since the manifold has to be designed to distribute flow into the lock chamber to minimize surging and turbulence, it cannot operate as efficiently as an intake (on emptying) as it does during a filling operation. Thus, the emptying of a lock involves greater head losses than during filling and hence emptying times are normally greater than filling times. The same general procedures that were used to determine filling system losses are necessary to estimate loss coefficients for an emptying system. Emptying losses include k_{m_e} (manifold serving as an intake), k_r, k_s, k_{vw}, and k_{o_e} (outlet loss).

123. Loss coefficients for any bends in culvert alignment can be determined by the curves and data presented in Appendix B. Explanation and discussion of the bend loss data are given in paragraph 134.

124. Values to be used for loss coefficients for bulkhead slots range from 0.02 to 0.04. These values are the results of analysis of model and prototype data from conduit tests and are to be used for both model and prototype studies until sufficient prototype data become available to provide more reliable values.

125. The valve well loss coefficient, k_{vw}, for both model and

prototype has been established as 0.05 for the conventional reverse tainter valve when in the fully open position. Losses that occur during the opening period are covered elsewhere in this report.

126. Figures 48-50 show model values of manifold loss coefficients for three different filling systems. These curves may be used to obtain manifold head losses. For side port and bottom lateral systems, the culvert at the valve is usually the same size as the culvert at the manifold and k_{m_f} can be used directly with $V_c^2/2g$. But with bottom longitudinal systems, the main wall culverts and the manifold culverts may have significantly different areas, and a manifold loss coefficient will have to be converted to a loss coefficient referenced to the main culvert velocity head. This conversion can be done by consideration of the square of the ratio of the areas, as k_{m_f}, in terms of main culvert velocity head (reference section) is

$$k_{m_f} = \left(\frac{A_c}{A_m}\right)^2 \times k_{m-m_f} \tag{37}$$

where k_{m_f} is the manifold loss coefficient in terms of the reference section, i.e., the main wall culvert velocity head; A_m is the ΣA of the manifold culverts that receive flow from one wall culvert; and k_{m-m_f} is the loss coefficient based on the velocity head in the manifold culvert.

127. The summation of all of the six separate head loss coefficients, k_f, can be used to obtain the discharge coefficient, C_f, by using Equation 30,

$$C_f = \frac{1}{\sqrt{k_f}} \tag{30}$$

128. In the studies of lock coefficients C_{L_f} and lock discharge coefficients C_f that were covered beginning in paragraph 115, it was shown by Figure 42 that a reasonably constant relationship existed between C_{L_f} and C_f. Using Figure 42 with the value of C_f determined from k_f with Equation 30, a value of C_{L_f} can be obtained. If this new value of C_{L_f} is within 3 percent of the value used earlier, the value of $2A_c$ that was computed according to paragraph 118 will probably be satisfactory. If the

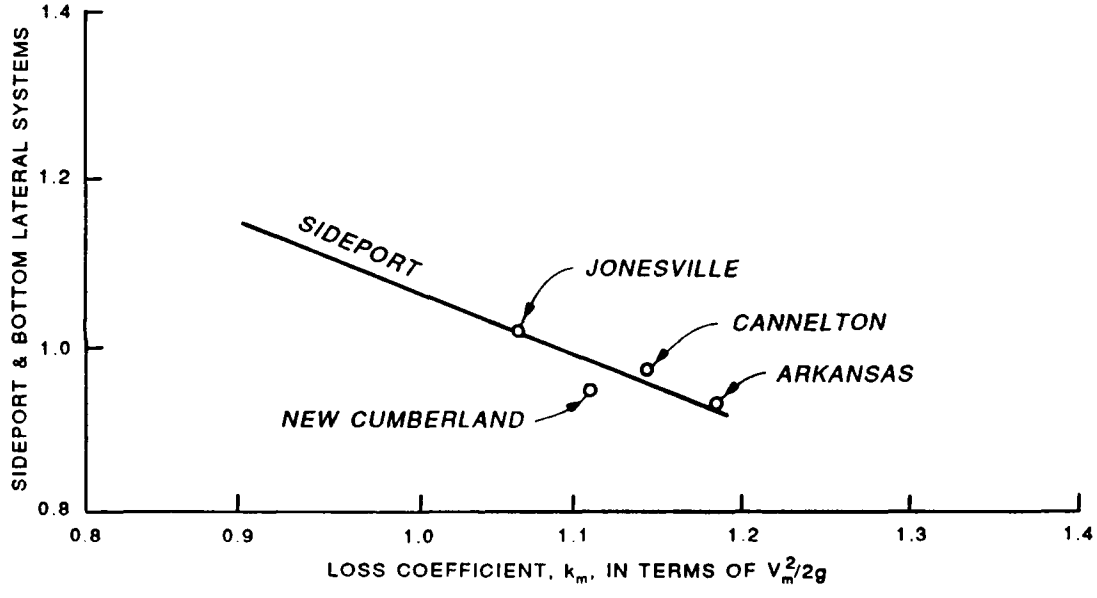

Figure 48. Manifold loss coefficients (side port systems)

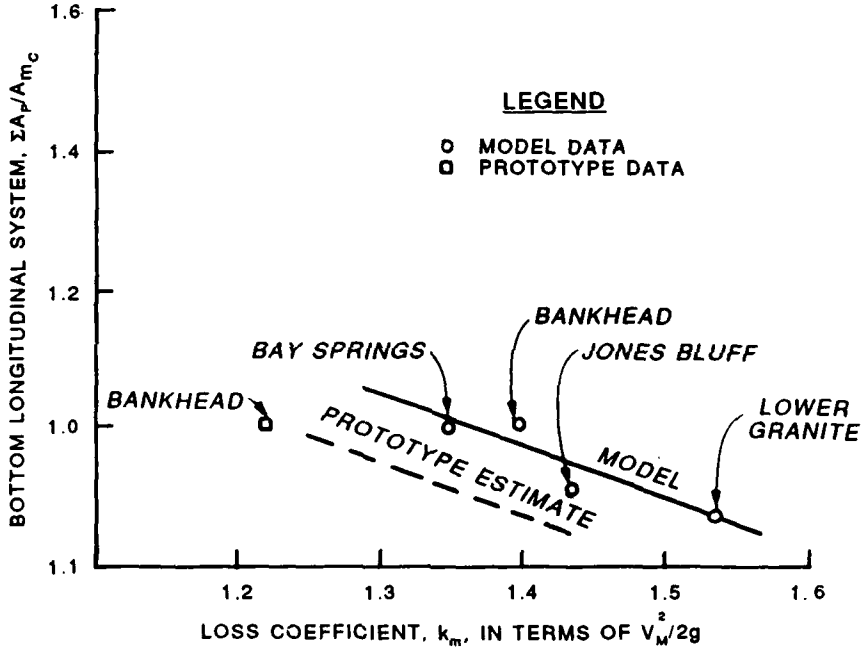

Figure 49. Manifold loss coefficients (longitudinal systems)

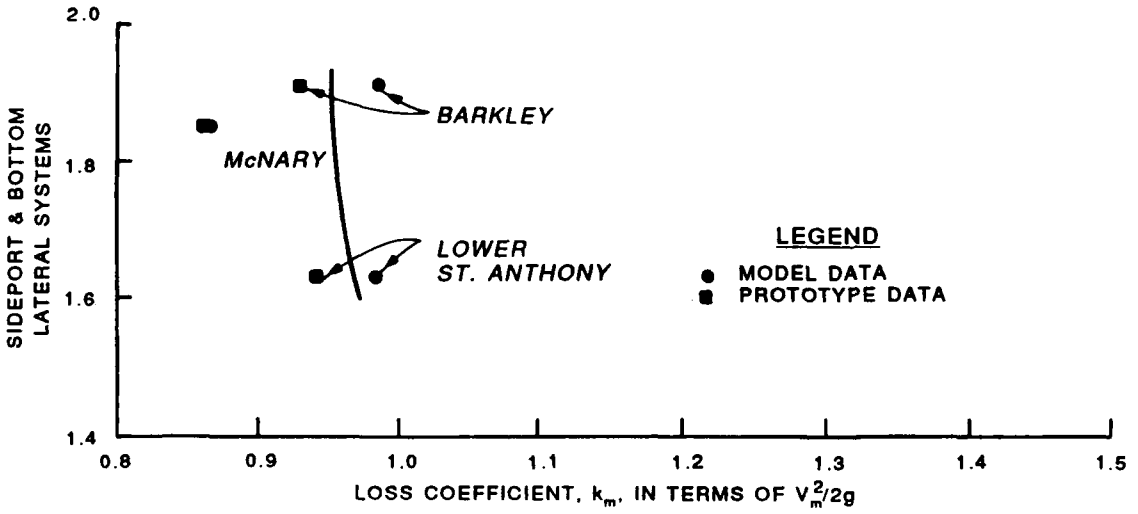

Figure 50. Manifold loss coefficients (lateral systems)

value of C_{L_f} that was originally used varies appreciably from the value obtained by use of C_f and Figure 42, another set of computations should be made for $2A_c$ using the C_{L_f} value obtained from Figure 42.

129. In the preceding paragraphs, procedures for determining losses during filling have been described and manifold loss curves were presented. Losses during lock emptying operations also have to be determined, and Figure 51 provides a means of estimating loss coefficients when the filling system manifold is serving as an intake.

Inertia Head

130. In paragraphs 103-111, the effects of the momentum of the water moving in a lock culvert were discussed. An equation developed by Pillsbury[5] can be used to estimate overfill, d_f, and to approximate its effects on operation time. Pillsbury's analysis is not sufficiently accurate because it does not provide a means of determining inertia effects during the valve opening period.

131. For water flowing in a conduit of uniform cross section, the inertia head at any instant is

$$H_m = \frac{L}{g} \frac{dV}{dt} \tag{10}$$

where H_m is the inertia head (feet of water), L is length of uniform conduit in feet, and dV/dt is the rate of change of velocity or the acceleration in feet per second per second in the conduit. Equation 10 is developed as follows. At any instant when the flow is increasing in the culvert, the head H is equal to the head loss H_L minus the head required to accelerate the mass of water in the culvert. If the flow is decreasing, the head H is equal to H_L plus the head that is producing the deceleration. Designating the acceleration or deceleration head as H_m gives

$$H = H_L \mp H_m \tag{15a}$$

(H_m is negative when flow is accelerating and is positive when flow is decelerating.)

Referring to Figure 52 and considering Newton's Second Law, $F = Ma$ and

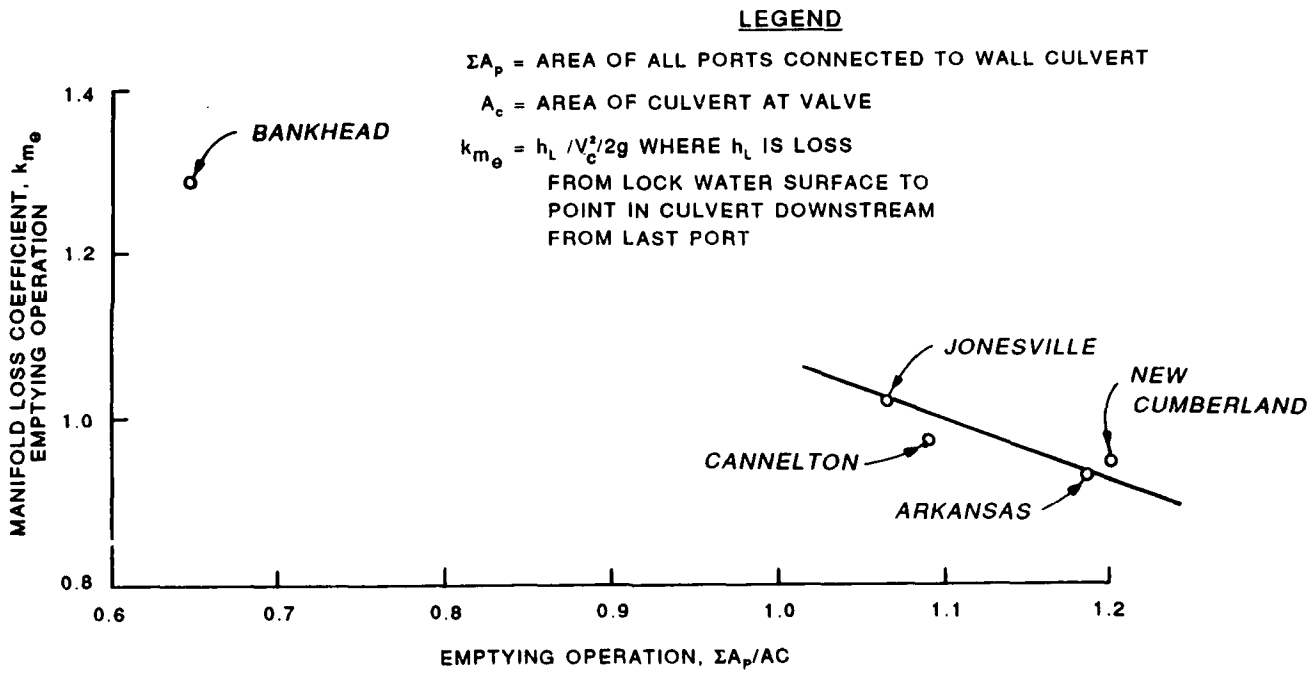

Figure 51. Loss at manifold during emptying operation

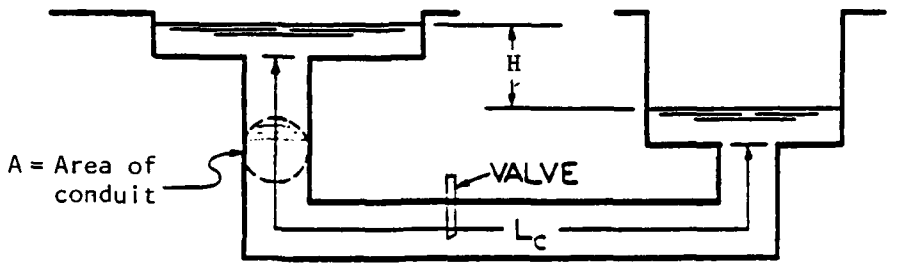

Figure 52. Schematic of lock culvert

According to Equation 15a,

$$H = H_L \mp H_m \quad \text{and} \quad H_L = \frac{V^2}{2g} + \frac{kV^2}{2g} \mp H_m = H - H_L$$

The force producing flow is HwA, where w is the unit weight of water and A is the area of the conduit. With L being the length of conduit, wAL/g is the mass, M, in $F = Ma$. Since dV/dt is a, the force resisting flow is:

$$wA\left(\frac{V^2}{2g} + \frac{kV^2}{2g}\right) \mp \frac{wAL}{g}\frac{dV}{dt}$$

$$HwA = wA\left(\frac{V^2}{2g} + \frac{kV^2}{2g}\right) \mp \frac{wAL}{g}\frac{dV}{dt}$$

then $$H = \left(\frac{V^2}{2g} + \frac{kV^2}{2g}\right) \mp \frac{L}{g}\frac{dV}{dt}$$

since $$H = \frac{V^2}{2g} + \frac{kV^2}{2g}$$

$$H = H_L \mp \frac{L}{g}\frac{dV}{dt}$$

and

$$\mp \frac{L}{g}\frac{dV}{dt} = H - H_L$$

then replacing $H - H_L$ with H_m

$$H_m = \mp \frac{L}{g} \frac{dv}{dt} \tag{10}$$

132. Since in Equation 10 L must be the length of a conduit with uniform cross section, and the culverts in most locks are not always uniform, a means of correcting the culvert length to allow for lack of uniformity must be considered. This problem is addressed by O'Brien and Hickox.[9] For a culvert with varying cross section of length L , the equivalent length L_c' (uniform cross section) may be approximated by

$$L_c' = L_1 \frac{A_c}{A_1} + L_2 \frac{A_c}{A_2} + L_3 \frac{A_c}{A_3} \cdots L_n \frac{A_c}{A_n} \tag{11a}$$

In the preceding equation, L_1 is the length of culvert with cross-sectional area of A_1 , L_2 is the length of culvert with cross-sectional area of A_2 , and so on for the entire culvert length. A_c is the cross-sectional area at the reference section (of one culvert)--in this case at the valve. The use of Equations 10 and 11a to calculate inertia head in a lock culvert is complicated by one other factor. The valve well operates as a surge tank and has some effect on determination of inertia head. However, it does not appear that serious error is introduced if effects of the open valve well are ignored. Values of the inertia head at finite intervals of time can be calculated by replacing dV/dt by $\Delta V/\Delta t$ in which the change in velocity in the culvert is determined at some short interval of time (10 seconds) and replacing L_c (length of culvert) by L_c' . In determining L_c' the areas at each end of each section of culvert are averaged and used with the length of each section in Equation 11a. Culvert discharge must be known at any instant during a filling operation before inertia head can be calculated. In the case of a prototype lock, discharge can be obtained from a carefully determined lock filling curve.

133. It is necessary to know the value of inertia head during a filling operation before prototype head losses in the culverts and valves can be determined. If inertia head is not considered, the actual head producing discharge will be in error and hence all head loss values will be incorrect.

Inertia head values have to be calculated if a lock filling curve is to be developed during lock design studies. Calculation of a lock filling curve using known or assumed values of head losses, physical dimensions of culverts, etc., and a valve operation schedule is a trial and error step procedure in which inertia head must be calculated for each trial in each step. An example of this calculation will be presented later in this Part.

Head Losses

134. Head losses in lock filling systems are the hydraulic losses that occur as a result of water flowing through gated openings, into and through conduits, through valves, through conduit transition sections and ports, and into or out of a lock chamber. For a steady flow condition, such losses can be represented as a discharge coefficient for the entire system by Equation 2b, $Q = CA\sqrt{2gH}$. This discharge coefficient can be converted to an actual head loss coefficient by Equation 29, $k \approx 1/C^2$. This loss coefficient, k , can be used with the velocity head $V^2/2g$ to determine head loss H_L in the system. The velocity in $V^2/2g$ is the mean velocity through a reference section of the conduit--with a lock the section at the valve is usually used. In lock design it is necessary to know or estimate the loss coefficients for valved openings in end filling systems or for various segments of a culvert in a culvert filling system. In this report k has been used generally to represent head loss coefficients. Subscripts are used with k to designate a loss coefficient for a specific segment of the culvert system. For instance, k_i is the loss coefficient for the culvert intake, k_r is the loss coefficient for resistance to flow in the portion of conduit being considered, k_b is the coefficient for any bends in the culvert, k_s is the coefficient for bulkhead slots, and k_{vw} is the coefficient for the valve well (valve fully open). These coefficients may be combined for the culvert upstream from the valve and indicated as

$$k_i + k_r + k_b + k_s + k_{vw} = k_{uv}$$

Then the head loss upstream from the valve is

$$H_{L_{uv}} = k_{uv} \frac{V_c^2}{2g} \tag{27}$$

where $H_{L_{uv}}$ is the total head loss from the upper pool Z_u to the valve skin plate and V_c is the mean velocity in the culvert at the section where the valve is located. Other combinations and designations of loss coefficients may be convenient, such as letting

$$k_{ic} = k_r + k_b + k_s$$

Also

$$k_{uc} = k_i + k_r + k_b + k_s$$

may represent the total loss upstream from the valve well. Losses at other locations in the system are designated similarly. This example is of particular interest because it is necessary to calculate losses upstream of the valve to determine pressure downstream from the valve over the vena contracta. Loss coefficients can be determined in a lock model study by establishing steady flow (in the culvert system) and accurately measuring the pressure drop for the various segments that are of interest. Unfortunately, model loss coefficients are greater than prototype coefficients because the roughness of the material used in constructing a model is not much different than the material in the prototype and also because of differences in Reynolds number of model and prototype. Prototype tests have been made on several locks and more tests should be made, but it must also be noted that certain test conditions that can be readily accomplished in a model cannot be exactly duplicated in a prototype test. For instance, it may be very difficult if not impossible to test a condition of steady flow in a prototype lock culvert. In published reports on prototype measurements of head loss made at McNary,[10] Lower St. Anthony Falls,[11] and Barkley Locks[12] there were no corrections for or assessment made of inertia effects.

Determination of Head Losses

135. Estimates of head losses of various segments of a lock filling and

emptying system must utilize loss data and loss curves developed from lock designs that have been modeled and tested. Using model and prototype data, head loss curves have been developed for filling and emptying as follows:

Filling Operation		Emptying Operation	
Intakes	Model and prototype	Manifold (acting as intake)	Model (only)
Bends	Model and prototype	Valve	Prototype (only)
Valve	Prototype (only)	Valve well	Model (only)
Valve well	Model (only)	Bends	Model and prototype
Manifold	Model (only)		
Resistance	Model and prototype	Resistance	Model and prototype
		Discharge outlet	(Data not usable for either model or prototype)

Until more data become available, model head loss values for bulkhead slots, valve wells, and lock manifolds have to be used for prototype locks. In most locks, the close proximity of intake to culvert bulkhead slots, bends, transitions, and valve wells makes separating the total loss into individual components extremely difficult and in some cases impossible. Individual losses from each component are not necessarily additive--especially if such components are close together. This is amply demonstrated by the studies covered by Miller[3] in Appendix B. Thus, while overall head losses (upper pool to lock chamber) can be measured in both prototype and model locks and can also be calculated fairly accurately by means of Equations 8b and 29, the resolution of the overall loss into values for various components involves many judgmental estimates. Loss data that should be used are tabulated as follows:

	Model	Prototype
Intake	Figure 47	Figure 47
Bulkhead slot	0.02-0.04	0.02-0.04
Valve well	0.05	0.05
Resistance	$f = 0.015$	$f = 0.009$
Manifold		
Side port	Figure 48	Figure 48

	Model	Prototype
Bottom Longitude	Figure 49	Figure 49
Bottom Lateral	Figure 50	Figure 50
Manifold (emptying)	Figure 51	Figure 51
Valve loss curve		
Expanded culvert	Figure 53	Figure 53
Uniform culvert	Figure 54	Figure 54

The loss curves of Figures 47-51 were developed by calculating discharges from lock water-surface elevations (given in model or prototype tests); determining the head loss between the piezometers involved; making corrections for inertia; and then expressing the loss in terms of $V^2/2g$ at the valve section. For several locks, intake losses (from Figure 47) were combined with calculated losses for resistance, bends, bulkhead slots, valve well, and manifold loss from Figures 48, 49, or 50. The summation of these losses was then compared with overall loss determined by Equations 8b and 29 for the same test runs used to calculate loss from individual components, and with overall head loss from upper pool to lock water surface. Thus three values of overall head loss estimates were computed. The results of these calculations are given in Table 2. In the calculation of loss based on actual discharge and on Equations 8b and 29 the observations used were taken from the recession side of the lock filling curve, when the inertia head approximated the observed overfill. The inertia head correction for each component of the culvert system was calculated by prorating the overfill according to the ratio of culvert length of the component to the total culvert length involved in the filling operation. The data in Table 2 indicate that using a summation of estimates of losses for individual components of a filling system provides an overall head loss coefficient that is sufficiently accurate for design purposes.

Losses at Valves

121. Head loss curves for reverse tainter valves at Lower Granite and McNary Locks that were computed for this report are presented in Figures 53 and 54, respectively. These curves show values of the head loss coefficient,

600
400
300
200
100
80
60
40
30
20
10
8.0
6.0
4.0
3.0
2.0
α Loss Coefficient (k_v)

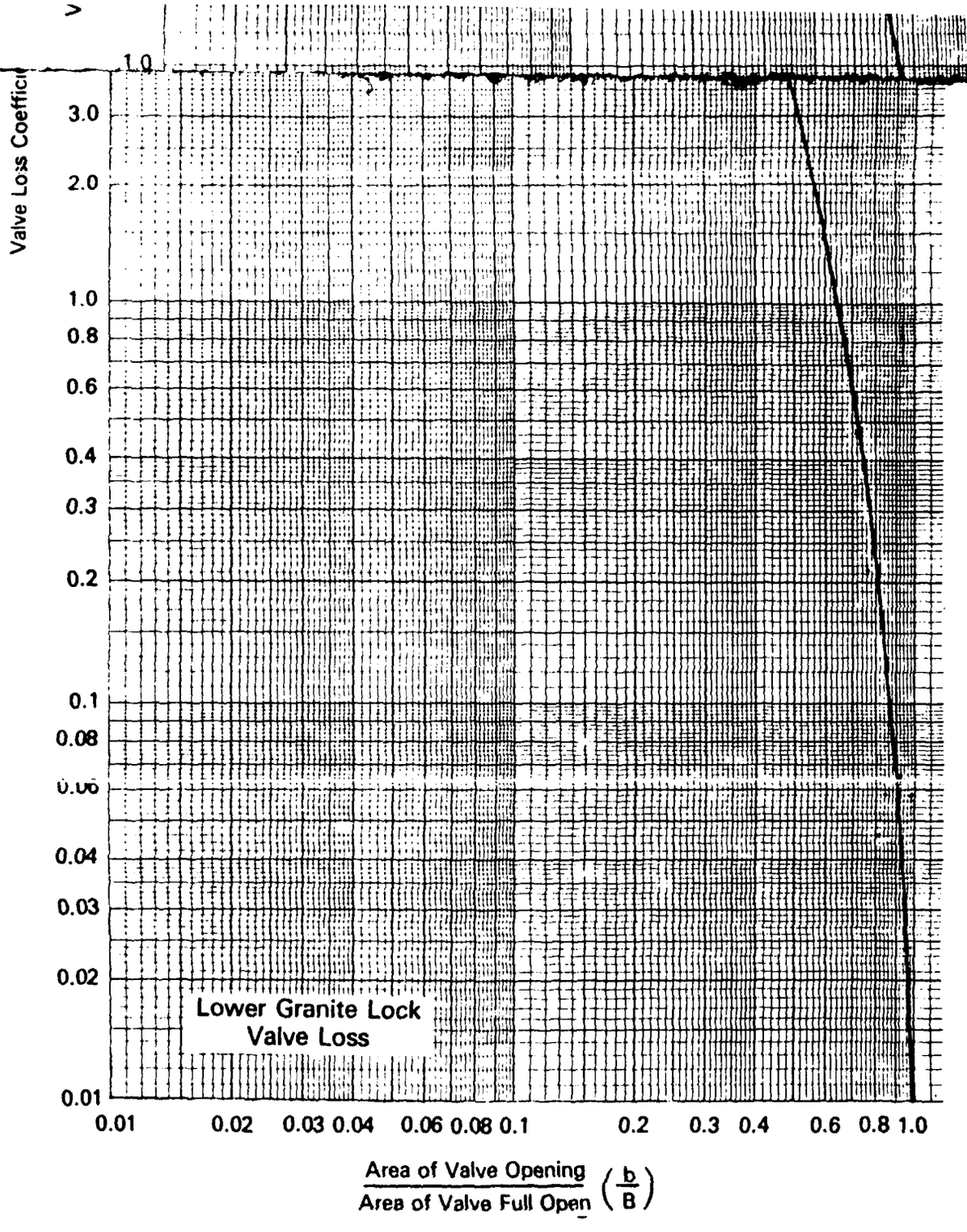
Valve Loss Coefficient
1.0
3.0
2.0
1.0
0.8
0.6
0.4
0.3
0.2
0.1
0.08
0.06
0.04
0.03
0.02
0.01
Lower Granite Lock
Valve Loss
0.01
0.02
0.03
0.04
0.06
0.08
0.1
0.2
0.3
0.4
0.6
0.8
1.0
Area of Valve Opening / Area of Valve Full Open (b/B)

Figure 53

600
400
300
200
100
80
60
40
30
20
10
8.0
6.0
4.0
3.0
2.0
1.0
0.6
Valve Loss Coefficient (k_v)

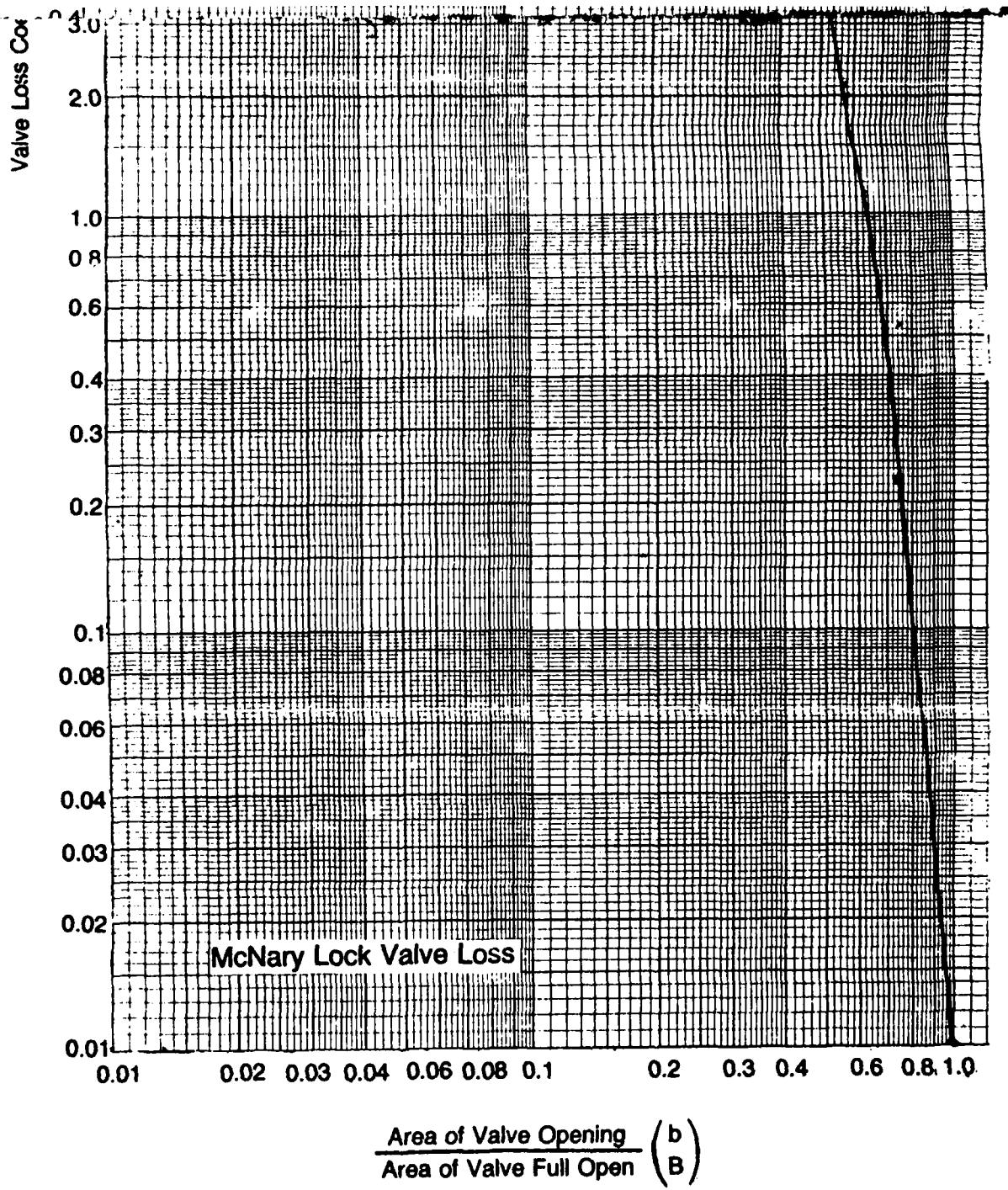
Valve Loss Co
3.0
2.0
1.0
0.8
0.6
0.4
0.3
0.2
0.1
0.08
0.06
0.04
0.03
0.02
0.01
McNary Lock Valve Loss
0.01
0.02
0.03
0.04
0.06
0.08
0.1
0.2
0.3
0.4
0.6
0.8
1.0
Area of Valve Opening / Area of Valve Full Open (b/B)

Figure 54

k_v , versus percent of valve opening where

$$k_v = \frac{H_{L_V}}{V_c^2/2g} \tag{33}$$

In previous studies of valve losses, data from various sources, including material from Weisbach's[13] tests in 1850, were plotted and used as though all of it were applicable to a reverse tainter valve in any lock. Some consideration was given to the lip angle of the valve as it opened. In preparation of this report the valve curve of Figure 53 was developed which gives entirely different values than the curves in either Reference 14 or 15. In further studies of prototype data on McNary Lock (Figure 54), it was found that (utilizing the Lower Granite calculation procedure) the McNary curve differed from the Lower Granite curve. These differences are accounted for by the differences in culvert configuration downstream from the valve. At Lower Granite Lock the culvert roof is expanded upward on a slope of one vertical on ten horizontal to a height of 22 feet. The expansion begins about 56 feet downstream from the valve well. At McNary Lock there is no expansion of the culvert. The head loss from any valve occurs principally from the expansion of flow downstream from the vena contracta. Since expanding the culvert apparently affects the expansion of the jet from the valve, it appears that a single valve loss curve cannot be developed that can be used with different culvert configurations. However, very little research has been done on this problem and there may be other factors that affect valve losses in addition to the culvert expansions.

Prototype Studies

136. In preparation of this report, detailed studies were made of prototype tests on two locks and some data were used from several other lock prototype studies. The principal objectives of the study were to (1) investigate head loss coefficients including valve losses; (2) determine valve contraction coefficients; and (3) develop more reliable methods of computing minimum pressures downstream from a partially open valve.

Lower Granite Lock prototype tests

137. The tests at Lower Granite Lock were made to determine effects of air vents on lock filling and to investigate cavitation phenomena that had caused severe shock "booms" at other high-head locks. The tests included

a. Measurement of pressures 7 feet upstream from the upstream edge of the riverward filling valve well.

b. Measurement of pressures downstream from the downstream edge of the riverward filling valve well.

c. Observation of lock water surface at 15-second intervals.

d. Observation of valve opening time and determination of valve opening versus time relation.

e. Observation of overfill.

Both filling valves started opening at the same time and were fully open in 80 seconds. Ten test runs were made in March 1976 with a head of about 98 feet and with different numbers of air vents open and one and two valves operating. In the summer of 1976, eight additional tests were made of which several were run with reduced head, i.e., a 10-foot-higher lock water surface.

138. Test 10 was selected for study. In this test both valves were operated, all air vents were closed, the lock water surface was at an elevation of 638.1 feet referred to the National Geodetic Vertical Datum (submergence of valves of 32 feet) and the head was approximately 98 feet.

a. A discharge hydrograph of flow into the lock chamber was developed by plotting the 15-second water-surface elevations to a very large scale versus time and drawing a smooth curve through the plot. Elevations were read from this curve at 3-second intervals to an estimated accuracy of 0.01 foot. Discharges over 6-second time increments were then computed from volumetric change in the lock chamber and were plotted versus time to a rather large scale. A smooth curve was drawn through this plot and discharge values were read from the curve and recorded as adjusted discharges. These data are shown in Table C-4.

b. The data used to determine equivalent culvert lengths were taken off construction plans and are shown in Table C-5. In Table C-6 equivalent culvert lengths for the entire system, L'_c, and for the culvert upstream from the valve skin plate, L'_{uv}, are calculated with Equations 11a and 11c, respectively.

c. Using the equivalent culvert length L'_c discharge data from Table C-4, and valve opening patterns from Table C-7 head loss values for the culvert system are computed in Table C-8. Head losses are computed at 6-second intervals beginning 120 seconds after the valves start opening, i.e., 40 seconds

after the valves are fully open. In Table C-8, ΔV_c is computed by Equation 13; inertia head is calculated by Equation 12a; the total head loss is given by Equation 15a; and k_c, culvert head loss coefficient, is determined by Equation 32. Culvert head loss values were determined every 6 seconds from a time of 120 seconds to a time of 327 seconds and averaged. The head loss coefficient with the valve full open is 1.222 based on culvert area at the valve.

d. On Table C-10, values of the valve loss coefficient, k_v, are computed. This calculation gives values of k_v at 6-second intervals during the valve opening period. In this computation, the total head loss for the system, H_L, is determined at 6-second intervals. Then the head loss for the culvert system is determined using the loss coefficient value k_c of 1.222 previously computed in Table C-8. The valve loss coefficient k_v values are calculated by subtracting the culvert head loss values from the total head loss values. The k_v values are then obtained by Equation 33:

$$k_v = \frac{H_{L_v}}{V_c^2/2g} \tag{33}$$

The column headings on Table C-10 are self-explanatory. Figure 53, valve loss curve, is a log-log plot of the k_v values versus the corresponding percent of valve opening values of Table C-10.

e. The observed pressures upstream from the valve well were used to compute the head loss coefficient for the culvert system from the upper pool to the valve skin plate. The calculations are shown in Table C-9. It should be noted here that the inertia head correction is based on the equivalent culvert length from the intake to the valve well. A value of $0.05\ V^2/2g$ has been adopted for loss through the valve well with the valve fully open. This loss coefficient value has been assigned to the culvert system instead of to the valve. In previous studies, the loss through the valve well for a fully open valve was considered a valve loss.

f. The pressure data from the pressure cell downstream from the valve was used in calculating valve contraction coefficients and velocities at the vena contracta.

McNary Lock prototype tests

139. The prototype test data contained in Reference 10 was used to calculate values of k_c, and to calculate a valve loss curve (Figure 54) by the same procedures used with the Lower Granite tests. Observations of discharge, pressure, and lock water surface in Test 4 were used to determine the loss coefficient and valve loss data. A value of k_c of 1.294 was determined

from Test 4 data. However, the value of the head loss coefficient for the upstream conduit, k_{uc}, of $0.31V^2/2g$ that was determined in Reference 10 was used, as a few trial calculations indicated that this value was nearly the same as the trial calculations produced.

Pressures Downstream from Valves

140. At the high-head locks on the Columbia and Snake Rivers, extremely low pressures develop during filling operations that cause severe explosion-like booms. Field observations and tests and model tests have been made to try to determine the exact cause of the phenomena. No clear picture has yet emerged as to exactly how the shock booms occur. The booms accompany occurrence of subatmospheric pressures that apparently produce cavitation. Several facts are known: (1) the phenomenon occurs when the valves are from about 40 percent to 70 percent open; (2) if the valve is submerged so that the average piezometric level remains above the culvert roof the booms occur; (3) if the culvert roof is placed at an elevation so that the average piezometric level remains below the culvert roof by 5 to 10 feet, a small amount of air can be admitted through vents in the culvert roof and no booms or shocks will occur; (4) model tests made so far to predict the magnitude of the average low-pressure gradient in the prototype have not proven reliable; and (5) no proven method of determining the amount of submergence required or the elevation of the average piezometric level required to completely suppress the low cavitation pressure has been developed. Expanding the culvert cross-section area downstream from a valve raises pressure (over the vena contracta). In model tests for John Day Lock, the location of the expansion was fixed, the culvert submergence was fixed, and then several tests were made to determine the amount of expansion required to produce an average piezometric level at least 10 feet above the culvert roof. In the prototype lock, the booms and shocks are severe, even though the average piezometric level remains above the culvert roof. In model tests for Lower Granite Lock, a series of tests were made to determine a design that would ensure that the average piezometric level would remain about 5 feet below the culvert roof during the critical valve opening period so that air could be admitted to overcome the low pressures and cavitation problems. In these tests the upward expansion of the culvert was located at distances from the valve well from about 25 to

67 feet. A plot of the average pressure gradient shows a straight-line increase in pressure from the 67-foot location to the 25-foot location. However, at the 67-foot point the rate of decrease in the pressure was beginning to approach the value obtained with no roof expansion. The data just described were used to fix the location of the roof expansion for the lock. Since it was deemed desirable to hold the average low-pressure gradient about 5 feet below the culvert roof, the location of the beginning of the expansion was set about 56 feet from the valve well. In the prototype tests discussed earlier, it was found that the average gradient fell below the 5 feet predicted in the model. In follow-up model tests, the exact conditions of head and tailwater (higher tailwater and reduced head) that existed at the time of the prototype tests were duplicated. In these tests the model showed the average pressure gradient to be at the culvert roof. The prototype tests showed pressure 10 to 11 feet below the roof.

Prediction of culvert pressures

141. In the foregoing paragraphs the inability of model tests to predict low pressures was pointed out. However, the model is still the best tool hydraulicians have to address the problem. For the present, it is recommended that after careful model studies have been made for a high-head lock, the average low pressures measured during the valve opening period be adjusted downward by 5 to 10 feet.

142. Pressures can be calculated for a proposed lock with a fair degree of accuracy providing accurate values of loss coefficients, valve losses, discharge, and corresponding lock water-surface elevations are available. The loss coefficients and valve loss curve have to be based on the physical layout of the culverts and valves in the proposed lock and similarities to existing locks where these data are known. The discharges (hence culvert velocities) and lock water-surface elevations have to be determined by means of a step-by-step calculation of a lock filling curve. An example of this for McNary Test 4 conditions is presented later. With these data, pressure can be calculated at any instant by means of Equation 46:

$$Z_{vc} = Z_u - k_{uv} \frac{V_c^2}{2g} - \frac{V_{vc}^2}{2g} \pm H_{m_{uv}} + \Psi \left(\frac{V_c^2}{2g} - \frac{V_{ec}^2}{2g} \right) \qquad (46)$$

where Ψ is the pressure reduction factor for an expanded culvert. The

velocity at the vena contracta V_{vc} is determined by rearranging Equation 48 so that

$$V_{vc} = \frac{V_c}{C_c b/B} \tag{49}$$

This equation requires values of the contraction coefficient C_c, which will be covered later. The last term in Equation 46 was developed empirically from the model tests on Lower Granite Lock discussed earlier. The difference in velocity heads between the culvert section at the valve and the expanded culvert section is used with the coefficient Ψ to estimate the pressure increase caused by the expansion. In Figure 55, the coefficient Ψ is shown as a percentage increase in pressure over the pressure that would be obtained with a flat roof versus distance from the valve well. In this plot it is assumed that prototype pressures will vary with location of the expansion, in the same relation that model pressures vary with location of an expansion, even though the values of pressure in model and prototype are not the same. At the present time there is not sufficient information available to prove the validity of the assumptions or the curve on Figure 55. Further prototype tests are needed on locks with culvert expansions at different locations to verify the relation. With reference to Figure 55, if the expansion begins at the valve well, the pressure would be increased by 100 percent of the difference in velocity heads. When the expansion begins 90 to 100 feet downstream, the value of Ψ would be zero and there would be no pressure increase over the pressure with a flat roof. Table 3 lists comparative data on observed and computed pressures downstream from the valves of prototype locks.

Contraction coefficients

143. In the studies for this report it was found that available contraction coefficient data for reverse tainter valves could not be used to calculate prototype velocities at the vena contracta with known pressures and could not be used to determine pressures with calculated vena contracta velocities. By use of observed prototype data from McNary and Lower Granite tests, contraction coefficients were computed by means of Equations 47 and 48.

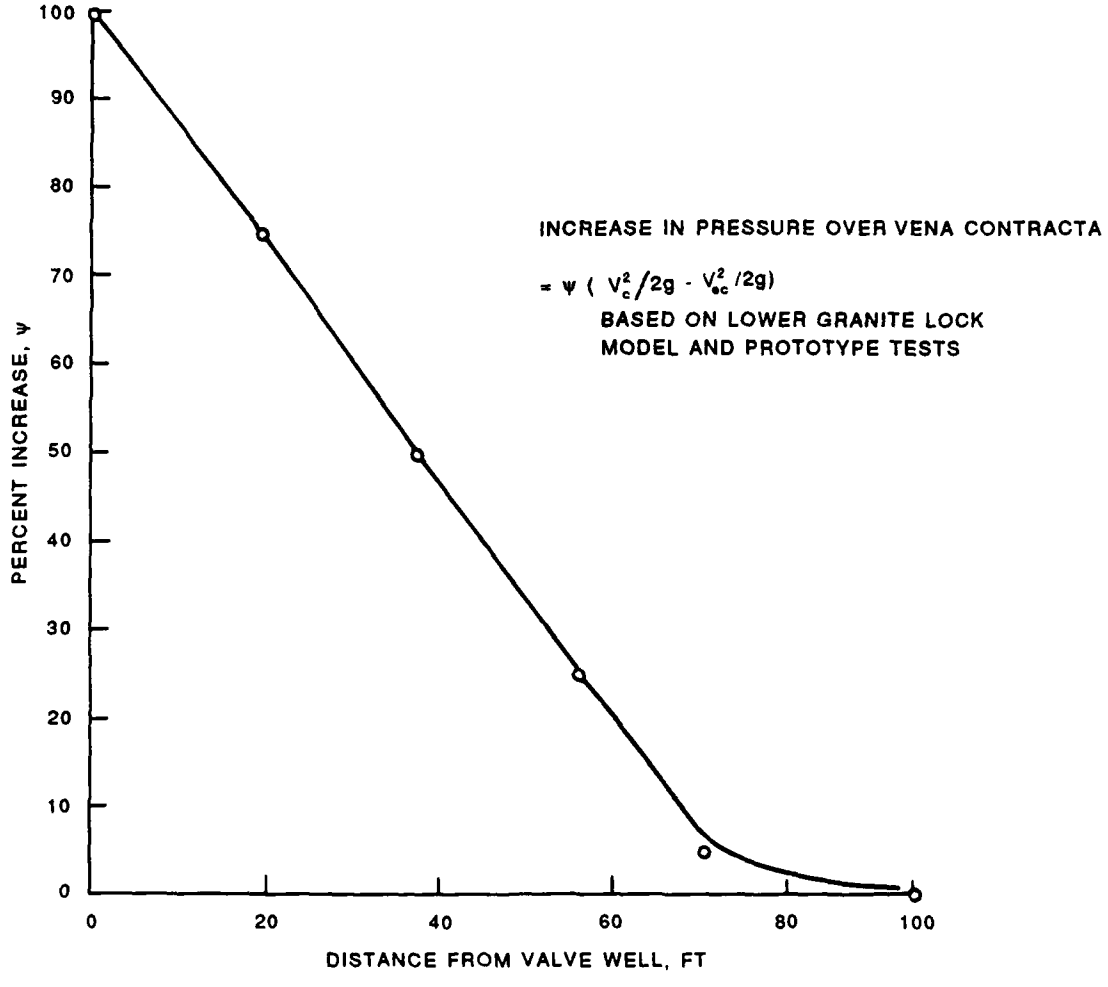

Figure 55. Increase in pressure over vena contracta

$$V_{vc} = \sqrt{2g\left[(Z_u - k_{uv}\frac{V_c^2}{2g} - Z_{vc} + H_{m_{uv}} + \Psi\left(\frac{V_c^2}{2g} - \frac{V_{ec}^2}{2g}\right)\right]} \quad (47)$$

$$C_c = \frac{V_c}{\frac{b}{B}V_{vc}} \quad (48)$$

Figures 56-59 were developed in the contraction coefficient study. The curve in Figure 56 was developed from Lower Granite data with Equation 48 and was used as a base curve for comparison of computed coefficients. Weisbach's data is plotted in Figure 59 along with others for comparison. Weisbach's contraction coefficient was computed from the equation for loss at a sudden expansion

$$C_c = \frac{B}{b(\sqrt{k_v} + 1)} \quad (52)$$

which can be derived from Borda's equation. But, little is known about the actual test condition in Weisbach's study. Further, there is not much reason to believe that the conditions of his tests were applicable to conditions existing downstream of a reverse tainter valve. For these reasons and because the use of the sudden expansion equation requires use of a valve loss curve, the validity of this method is subject to question. Therefore, it is considered that the plots of McNary and Lower Granite data shown in Figures 57 and 58 represent the best interpretation of contraction coefficient data to date. The importance of Figures 57 and 58 arises from the fact that within the range of valve opening of primary interest (0.4 to 0.7 percent) an average can be used that represents reasonably well all of the test data calculations.

Calculation of Lock Filling Curve

144. Calculation of a filling curve for a lock with a wall culvert filling system is one of the most basic and important features of hydraulic design of a lock. Before the filling curve study can be made, a tentative

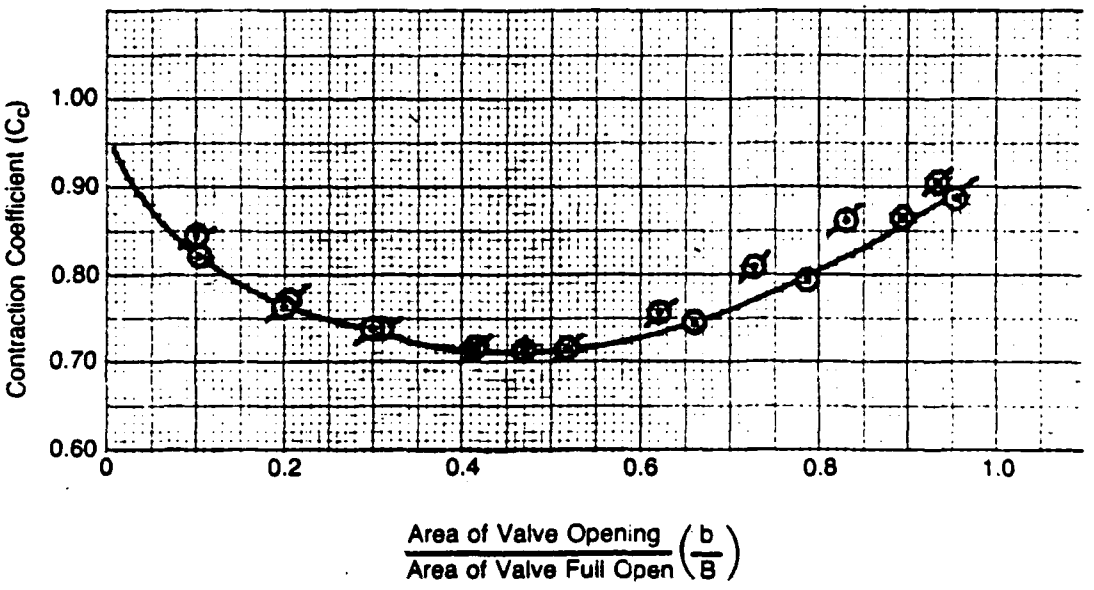

● $C_c = \frac{V_c}{b/B \times V_{vc}}$ (Lower Granite Test 10 – 1^m–20^s Valve, 2 Valves)

$C_c = \frac{B}{b(\sqrt{k_v} + 1)}$ (Lower Granite Data, Test 10)

V_c = Mean Velocity in Culvert at Valve

V_{vc} = Mean Velocity in Vena Contracta

k_v = Valve Loss Coefficient = $\frac{H_{L_v}}{V_c^{\,2}/2g}$

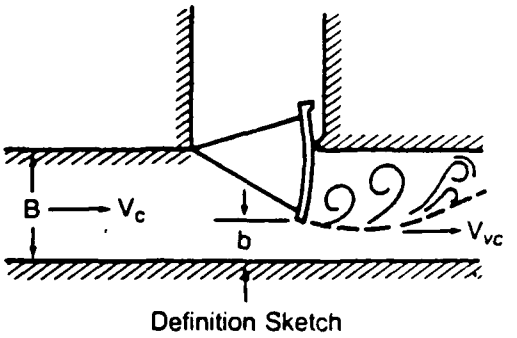

Definition Sketch

Figure 56. Lower Granite Lock contraction coefficients

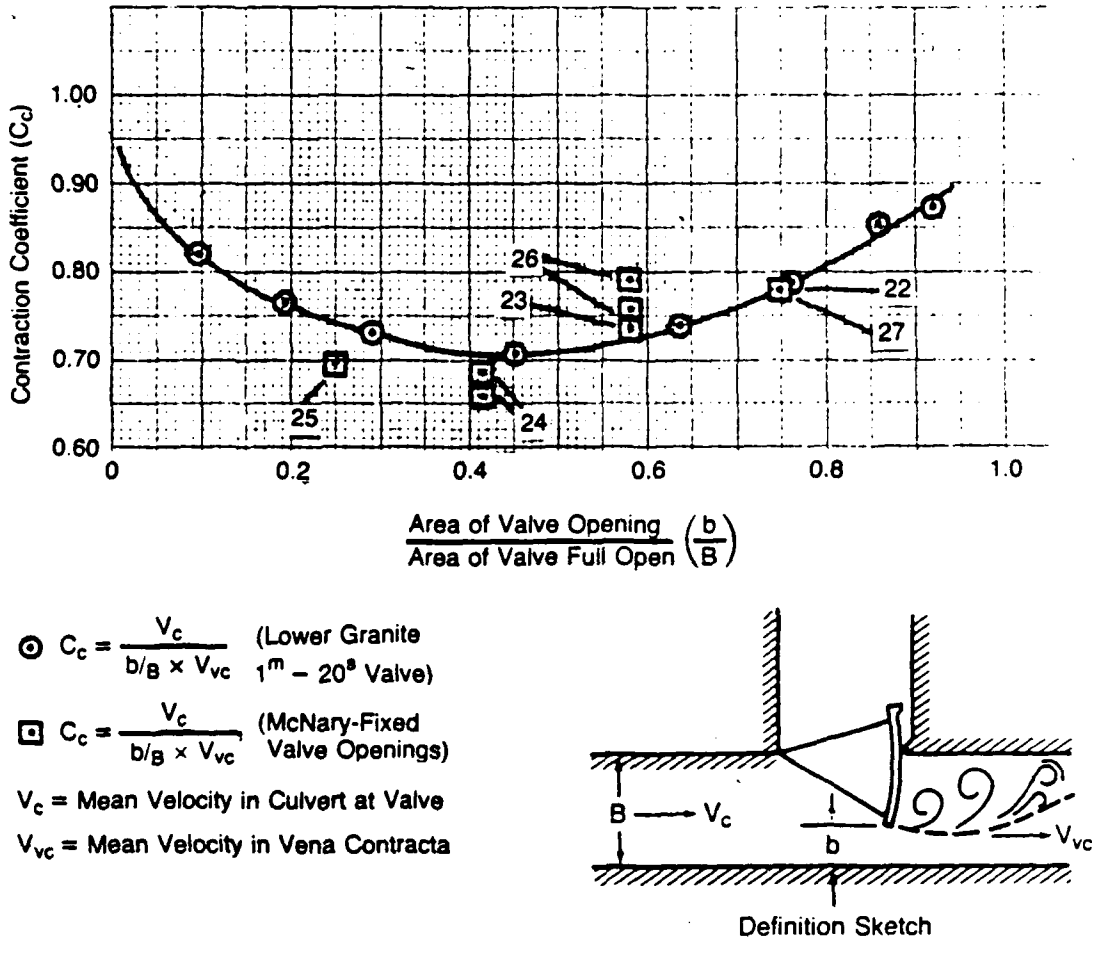

Figure 57. Lower Granite and McNary Locks contraction coefficients (fixed valve openings for McNary)

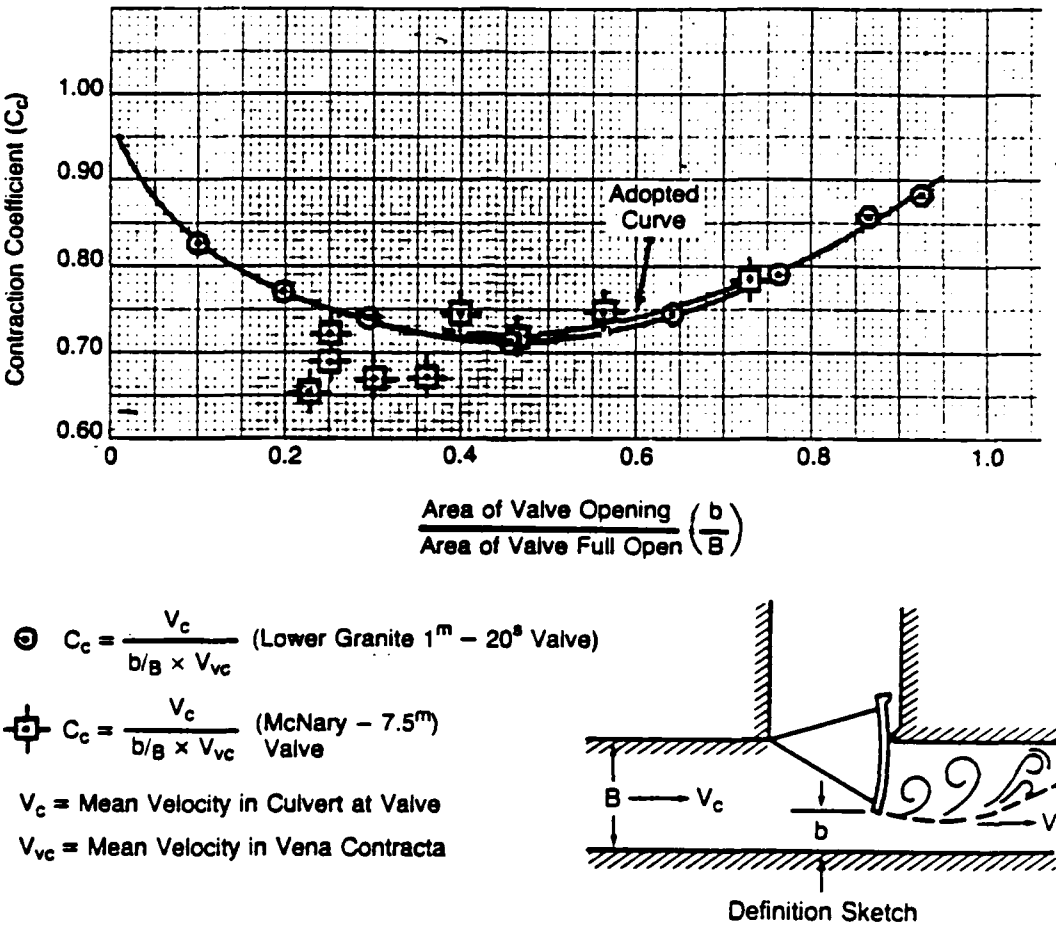

Figure 58. Lower Granite and McNary Locks adopted contraction coefficient curve

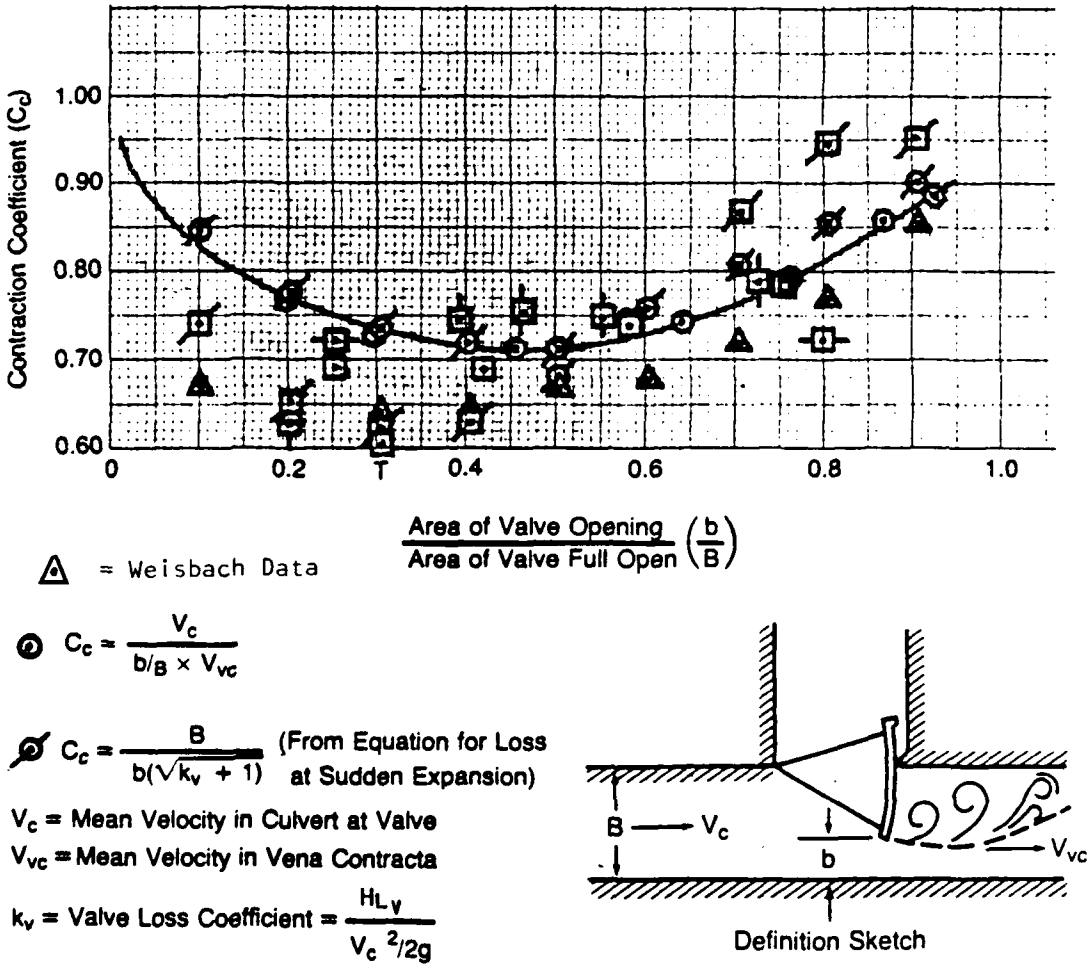

Figure 59. Contraction coefficients, plot of all data

design for the system must be developed and certain other factors must be determined. For instance, head loss coefficients for the culvert system must be estimated from prototype tests on existing locks (Reference 12 and Appendix C). A valve loss curve for the type of valve and the configuration of the culvert downstream from the valve must be available. And finally, length and cross-sectional dimension of each section of the culvert, from the intake to the discharge manifold, must be developed so that the "equivalent" length of the culvert system can be determined to permit calculation of the inertia head in the system.

145. When these data have been developed, calculation of the filling curve can proceed. The procedure involves trial and error step-by-step computations. When the transient conditions that occur are expressed in a differential equation, the equation cannot be integrated and no exact solution is possible.

146. An example of a trial and error computation of a filling curve for McNary Lock on the Columbia River is presented in Table 4 and is described in subsequent paragraphs. In this example, the valve opening curve (Figure 60), the upper pool elevation, and the initial lock water-surface elevation are the same as the values that existed during Prototype Test 4, made by the US Army Engineer Waterways Experiment Station in 1957.[10] The culvert loss coefficients and the valve loss curve used in the example in Table 4 were developed in an analysis of this prototype test which is presented in Appendix C of this report. Figure 61 shows the results of the calculations in Table 4. In this example, conditions of Prototype Test 4 were used in order to provide a better test of the accuracy of the procedure. It is recognized that in an actual study of a new lock, culvert loss coefficients would have to be estimated from loss curves and data in this report. The equivalent length of the culverts would be different from McNary Lock and the valve opening schedule would probably be different. However, if the McNary valve design is used in a proposed lock, and if the culvert downstream from the valve is of a uniform size for a minimum distance of 100 feet, the McNary valve loss curve (Figure 54) would be applicable.

147. The basic data from McNary Prototype Test 4 that have been used in the filling curve computations in Table 4 are listed below:

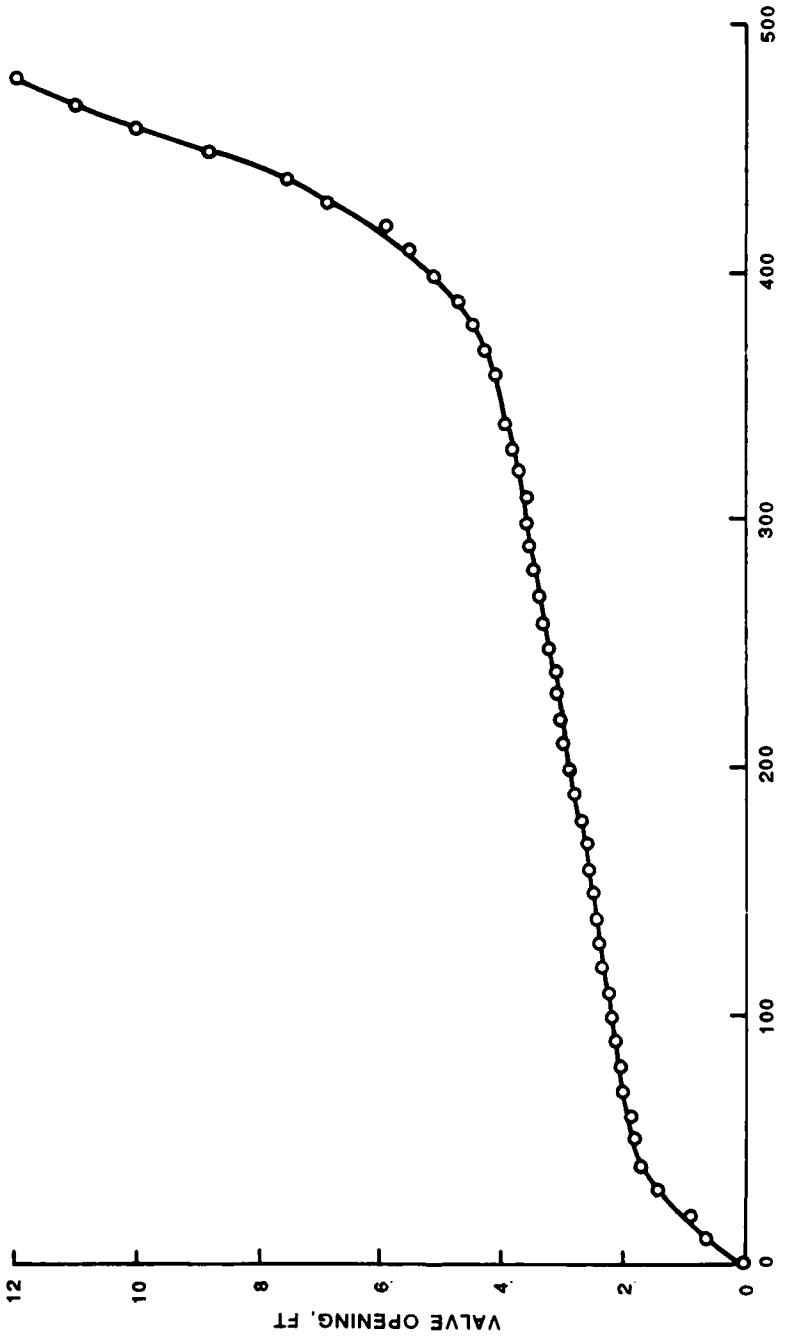

Figure 60. Valve opening curve for McNary Lock

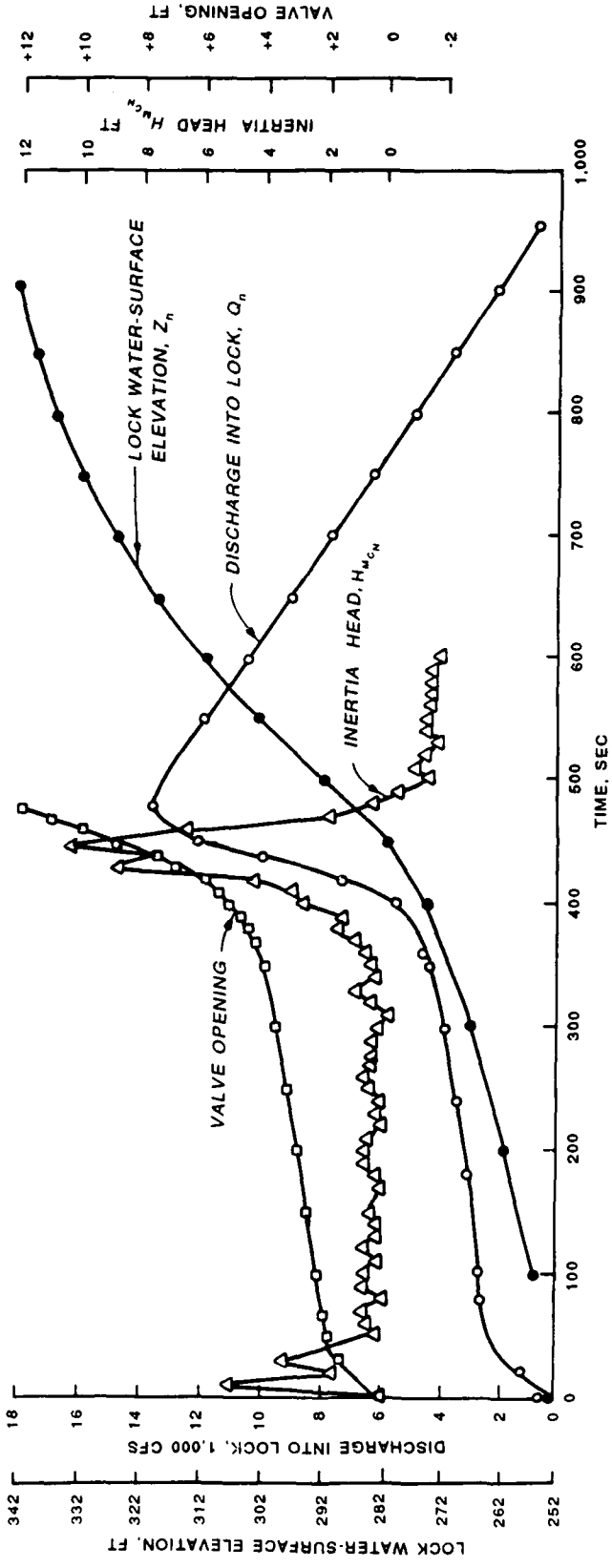

Figure 61. McNary Lock, calculated values, test 4 conditions

Upper pool elevation, feet	$Z_u = 340.14$
Initial lock water surface, feet	$z_1 = 251.80$
Equivalent length of culvert, feet	$L'_c = 468.70$
Time increment	$\Delta t = 10$ seconds
Area of lock chamber	62,267 square feet
Valve schedule	Same as Test 4
Valve loss curve	New curve developed in this study from Test 4 (Figure 54)

The equations used are given below for ready reference.

$$\Delta z = z_n - z_{n-1} \tag{39a}$$

$$z_n = z_{n-1} + \Delta z \tag{39b}$$

$$q_{a_n} = \frac{\Delta z \, A_s}{2\Delta t} \tag{41}$$

$$V_{c_{a_n}} = \frac{q_{a_n}}{A_c} \tag{42}$$

$$V_{c_n} = 2V_{c_{a_n}} - V_{c_{n-1}} \tag{43}$$

$$H_{m_{c_n}} = \frac{\Delta V_{c_n}}{\Delta t} \frac{L'_c}{g} \tag{12a}$$

$$H_n = Z_u - z_n \tag{1}$$

$$H_n = Z_u - z_{n-1} - \Delta z$$

$$H_{L_n} = H_n \pm H_{m_n} \tag{15}$$

$$V_{c_n} = C_n \sqrt{2gH_{L_n}} \tag{2a}$$

148. The trial and error computations mentioned earlier use a constant value for Δt and start each new step with an estimated value of Δz that is assumed to occur in the increment of time Δt. The symbol i (column 1 in Table 4) is used to designate the sequential number of each successive computational step. However, it must be noted that each step of the computation, i.e., each line across the table may require more than one set of calculations in 13 of the 19 columns before sufficiently accurate values of culvert velocity, head loss, and inertia head are obtained. Therefore, the final line of calculations in each step will bear the sequential number in column 1 designated by i. In column 2, t represents the elapsed time from beginning of the computation to any step i under consideration. In column 1, i has been assigned the value of 1 when $t = 0$ and initial conditions are known, namely:

$$q_{c_a} = 0$$

$$V_{c_a} = 0$$

$$\Delta z_n = 0$$

$$H_L = 0$$

$$H_m = 0$$

z = initial lock water-surface elevation

Since i is 1 when $t = 0$, the value of t at any succeeding final computational step is then $(i - 1)\,\Delta t$.

149. In column 3, b/B represents the amount of valve opening (percent of total opening) at any time-step. Values of valve opening are obtained from the curve of valve opening versus time for the McNary valve schedule. Column 4 shows the valve loss coefficient k_v that is read from the new McNary valve loss curve (k_v versus b/B). The total loss coefficient k for any step i is the sum of k_v plus k_c; the loss coefficient k_c is

constant, but k_v varies with the amount of valve opening and becomes zero when the valve is fully open (b/B = 1.00). Values of the discharge coefficient C_n, which are the reciprocal of the values of $\sqrt{k_v + k_c}$, are shown in column 5.

150. The calculation proceeds across Table 4 from left to right starting with values of b/B, k_v, and C_n from known data corresponding to time t, in column 2.

151. Starting with the step designated by i = 2, at the end of the first time increment (t = 10 seconds), values in columns 3, 4, and 5 can be readily obtained. In column 6, Δz_n is the estimated increment of increase in lock water surface in the increment of time Δt. As already noted, when i = 1, Δz_n, t, q_{a_n}, $V_{c_{a_n}}$, H_{L_n}, and H_{m_n} are zero. The symbol n is used as a subscript (without being assigned finite numbers) to indicate relative sequence of beginning and ending of increments of H and V_c. By utilizing n for a general subscript, Δz_n at any computational step is the difference between z at the step under consideration (designated by subscript n) and z at the preceding step designated by n-1. In column 7 q_{a_n} (average discharge for one culvert) is determined by considering the change in volume in the lock chamber produced by Δz_n in an increment of time Δt. The discharge through one culvert is assumed to be one-half of the total discharge into the lock chamber as determined from the change in volume produced by Δz in time increment Δt. The average velocity in one culvert over the time increment Δt is q_{a_n}/A_c and is designated $V_{c_{a_n}}$ in column 8.

152. As $V_{c_{a_n}}$ may be represented approximately by

$$V_{c_{a_n}} = \frac{V_{c_n} + V_{c_{n-1}}}{2}$$

V_{c_n} may be determined by rearranging the terms in this equation so that $V_{c_n} = 2V_{c_{a_n}} - V_{c_{n-1}}$. Thus at the end of the first increment of time, Δt, the average velocity $V_{c_{a_n}}$ is known and V_{c_n} at the beginning of the first

time-step, when $i = 1$, is zero. Then $V_{c_{n-1}}$, when $i = 2$, is zero and hence V_{c_n} is $2V_{c_n} - 0$. In succeeding time-steps $V_{c_{n-1}}$ will not be zero but the relation is still valid. Continuing on with the computations, then, V_c for the end of any increment of time, Δt, becomes the V_c for the beginning of the next increment of time. Thus V_{c_n} for $i = 3$ is $V_{c_{n-1}}$, for $i = 4$. In column 9 values of $V_{c_{n-1}}$ are shown which are the same as the values previously computed in column 10 for the step immediately preceding the one under consideration.

153. Column 11 contains successive differences in V_{c_n} values which are designated ΔV_{c_n} and column 12 shows values of $\Delta V_{c_n} / \Delta t^n$ at any time-step i.

154. In column 13, values of inertia head in the culvert, H_m at any time step i, are computed from $H_{m_n} = \Delta V_{c_n} / \Delta t \times L_c' / g$. The head, H_n at any value of i, is shown in column 14 and is the elevation of the upper pool Z_u minus z_{n-1} minus Δz_n. The head loss in the culvert system H_{L_n} is shown in column 15 and is equal to H_n minus the inertia head correction when the flow is accelerating. When flow is decelerating, H_{L_n} is equal to H_n plus the inertia head correction H_{m_n}.

155. In column 16, the value of H_{L_n} in column 15 is used to calculate a check value of velocity by Equation 2a, $V = C \times \sqrt{2gH}$. Using the subscripts and symbols of this computation, the equation becomes $\Psi_{c_n} = C_n \sqrt{2gH_{L_n}}$. This check value of velocity is designated by the symbol Ψ_{c_n} to distinguish it from the original value of V_{c_n} shown in column 10. If Ψ_{c_n} is within 1.0 percent of V_{c_n}, the assumed value of Δz_n is considered satisfactory and the line of computations for another step can be started. If Ψ_{c_n} does not check V_{c_n} within 1.0 percent, another trial value of Δz_n is assumed and the computation is repeated. Successive trials are made until Ψ_{c_n} checks V_{c_n}. When a satisfactory check value of Ψ_{c_n} is obtained, a Δz_n value for the next step, i, is assumed and the process is continued. The computations proceed line by line with i denoting the number of each step (final line of computations) in sequence until the values of $q_{a_n} = 0$, $V_{c_{a_n}} = 0$, and $z_n = Z_u$ are reached. At this point the lock chamber will be filled, the total filling time in column 2 will be known, and the values of z_n (at 10-second intervals in column 18 when plotted versus t

will produce the filling curve. The values of V_{c_n} in column 10 may be used in subsequent calculations to determine the pressures (hydraulic grade line) at various points in the system.

Other Design Details

156. In the foregoing parts of this report, general design procedures have been covered, but there remain a number of design details that must be considered before a satisfactory filling and emptying system can be developed.

Culverts

157. Culvert shapes are usually square or rectangular and the rectangular shapes have height to width ratios varying from about 1.10 to 1.15. In wall culvert side port systems, the culverts are usually of uniform rectangular size from the intake, through the manifold section on through the emptying valves. In some cases structural conditions may require that a culvert be higher than it is wide. Normally, there is no reason to use a culvert section with a width greater than the height. Such a shape, if used at the valve section, can create undesirable mechanical problems at the valve. Circular-shaped culverts have been used at several locks in Europe and were used on the old 600-foot lock at Louisville, Kentucky, on the Ohio River and on some of the locks on the upper Mississippi River. Circular culverts offer no particular advantage over square or rectangular culverts, but pose difficulties in construction and in providing for filling and emptying valves.

158. In bottom longitudinal systems, wall culverts are usually made rectangular from some point upstream from the filling valve to the point where the culverts turn to enter the area under the lock chamber. It may be desirable to expand the culvert area at some point downstream from the valve to obtain satisfactory pressure conditions. In the case of the Eisenhower Lock, the culvert was expanded 2 feet vertically to create a more uniform pressure gradient along the manifold section. At Lower Granite Lock, the culvert was expanded vertically from 14 feet at the valve to 22 feet in a distance of 76 feet. In the final design this transition began at a point 56 feet downstream from the downstream edge of the valve recess. The 22-foot culvert height was maintained through the curving section where the culverts enter the area under the lock chamber. However, the 2-foot-thick horizontal diaphragm in this section reduced the net vertical dimensions of the water passages from

22 to 20 feet (two 10-foot by 12-foot passages). This expansion and contraction produce no serious problems or great head losses.

159. The horizontal location of a culvert in a lock wall with respect to the face of the lock chamber may be governed by structural requirements. In the case of side port systems the wall thickness (between culvert and the face of the lock chamber wall) governs the length of the ports and is important to the filling system. No hard and fixed rules are applicable, but wall thickness of about 8 feet (length of port) is a desirable minimum.

160. On bottom longitudinal systems with four- and eight-branch manifolds in the bottom of the lock chamber, wall thickness of the manifolds (at the ports) cannot be designed to give port length of 8 feet because of space requirements. Also, in this situation, port lengths of 6 to 8 feet are unnecessary for satisfactory performance of the filling system. The thickness of the manifold culvert walls (port length) of Lower Granite Lock is only 3 feet. Figure 62 shows a typical plan and section of a culvert at the manifold section of wall culvert port system.

161. Culvert elevations are governed by submergence requirements for the ports in a wall culvert port system; by pressure conditions at the valves; and by minimum depth requirements in the lock chamber for a bottom longitudinal or bottom lateral system. In the case of bottom longitudinal systems the wall culverts can be at a higher elevation than the bottom culverts, but there cannot be very much difference in elevation without creating undesirable bends and transitions. Further, at locks where a bottom longitudinal system is required (usually high lift), the valves will have to be placed low in order to control pressures and air intake which means that the valves and wall culverts must be almost as low as the bottom manifold system.

162. Generally, bends in culverts, whether horizontal or vertical, should be made as flat or as gradual as possible. The deflection for a miter bend should be no greater than about 10 degrees. For circular bends of 90 degrees, the ratio of radius to width r^*/w^* should be at least 1.5 to 2.0 to avoid severe head losses. For a 180-degree bend the r^*/w^* ratio should be on the order of 3 to 5. Figures 9.6-9.8 of Appendix B show head loss coefficients for bends of different r^*/w^* ratios.

163. Culvert expansions should be made gradually to minimize losses. For instance, an upward expansion of a rectangular culvert should be no greater than about 1 vertical to 9 or 10 horizontal. Expansion at a greater

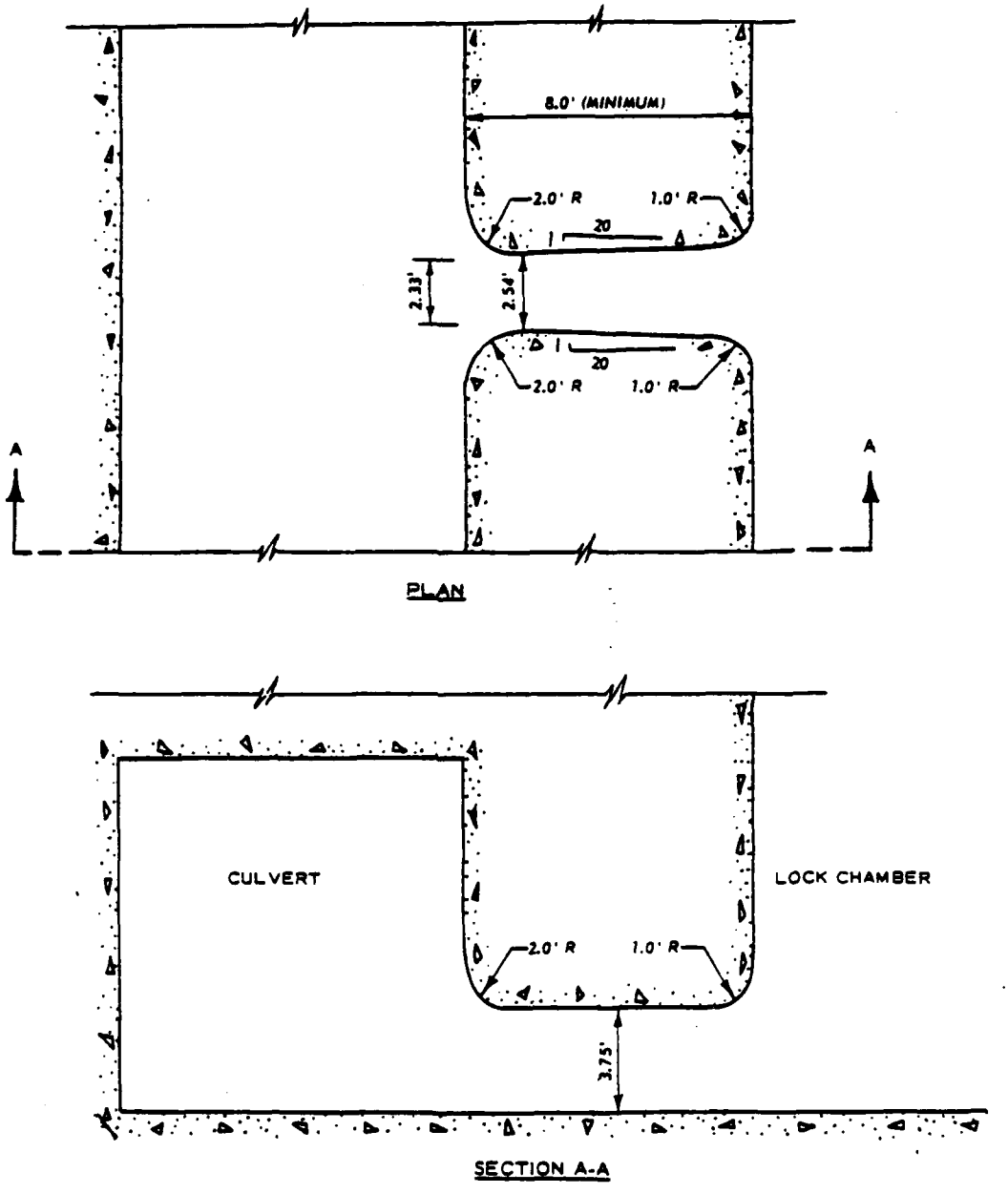

Figure 62. Port for 110-foot-wide lock

rate, particularly where high velocities occur, will cause excessive head loss and turbulence.

164. Contractions in culvert cross sections are also a source of head loss but do not cause nearly as much loss as expansions. Any contraction should not be made with completely abrupt boundary changes, but should have a transition section between the two sections of culvert. Curves in the culvert walls should be used instead of miter bends if the transition section is relatively short.

165. Bulkhead slots are usually placed in culverts upstream and downstream of valves so that the valve can be unwatered for maintenance. To reduce unwatering time and cost, the slots should be placed close to the valve, i.e., immediately upstream and downstream from the valve shaft. However, the downstream slot should be placed far enough downstream to avoid the cavitation that develops during the valve opening period. Otherwise the concrete around the embedded metal of the slot can be seriously and rapidly damaged. To avoid the worst cavitation damage, the downstream bulkhead slot should be placed downstream of the vena contracta when the valve is 50 to 70 percent open. Locating the slot about three culvert heights downstream will usually place it out of the area most susceptible to cavitation damage. The upstream bulkhead slot should be placed at least two culvert heights upsteam of the upstream edge of the valve shaft.

166. Culvert liners (steel plate) are used in high-lift locks to protect the culvert surfaces immediately downstream from the valve. With reverse tainter valves, the culvert liner on the bottom extends downstream for a distance of about 2.0 to 2.5 culvert heights from the valve body seal line on the culvert floor. The sidewall liner in the valve shaft covers the area from the floor upward to the curving vertical seal plate of the valve body. The top liner extends downstream from the top seal nose and terminates vertically above the downstream edge of the culvert floor liner. The liner on the culvert floor, sidewalls, and top is terminated at a point far enough downstream to cover the area exposed to the most severe cavitation damage during the valve opening period. From observation of culvert models of high-lift locks, the most vulnerable area is usually 2.0 to 2.5 culvert heights downstream from the bottom seal line of the valve body.

Valves

167. With only two exceptions, all of the locks built in the

United States since 1940 have had reverse tainter valves. At older locks various types of valves were used. Vertical lift valves of several different types (wheeled valves and slide valves), butterfly valves, vertical cylindrical valves, and regular tainter valves have all been used at some of the old locks. The reverse tainter valve was developed during 1937-38 and has proven to be superior to other types. Several different designs of reverse tainter valves have been developed and a number of tests have been made to determine the magnitude of dynamic loads, load reversals, and vibration tendencies. The single skin plate design developed for the Holt Lock has the best hydraulic characteristics of any developed so far.

168. Vertical slide valves are used at most of the locks built recently in Germany and Austria. German engineers have developed a slide valve that will operate under head from either direction.

169. Reverse tainter valves can be operated by direct electirc motor drive or by hydraulic cylinder mechanisms. At most of the recently built locks, the valves are operated by hydraulic cylinder. Valve opening curves (opening versus time) are slightly concave upward. Straight-line operation might be of some advantage but exact straight-line motion is difficult to achieve without encountering complicated kinematic design problems.

Manifolds for wall port systems

170. In a wall culvert port system, water is discharged into the lock chamber through short rectangular passages between the culvert and the lock chamber. The portion of wall culvert in which the water passages or ports are located is known as the manifold section of the culvert. The number, size, location, spacing configuration, and elevation of the port with respect to the lower pool level are all critical factors in design of a wall port system. The ports should occupy about 50 to 60 percent of the length of the lock chamber and should be centered around the midpoint of the chamber. As a result of many model tests and much research, the total throat area of the ports in one culvert manifold should be from 90 to 98 percent of the culvert area, preferably about 95 percent. Making this ratio, $\Sigma A_p/A_c$, smaller than 0.95 increases filling time and making the ratio larger tends to produce less desirable lock chamber conditions. Port sizes are influenced to a large extent by lock size and culvert size. For instance, on a 1,270- by 110-foot lock, port sizes of 10.0 to 11.0 square feet give satisfactory results. For a 670- by 110-foot lock, a port size of 9.0 to 10.0 square feet will give good results;

and in 655- by 84-foot locks, ports of 6 to 7 square feet in cross section are satisfactory. There are no very precise rules for establishing exact sizes of ports for locks with different lifts, different sizes, and different amounts of submergence.

171. The location of the filling valves in a wall port system can affect the operations of the most upstream ports. For this reason, it is good practice to place the valves at least four to six culvert heights upstream from the most upstream port in the manifolds. During the valve opening period low pressures created by the jet at the vena contracta produce low pressures that extend at least six to seven culvert heights downstream from the valve. This low pressure tends to reduce flow through ports that are too close to the valve and may actually cause a slight reversal of flow during the later part of the valve opening period. Many tests have been made of different port shapes. The design shown in Figure 62 does about as well as any of the designs ever developed. The entrance to the port should have rounded corners on the top and sides; should be long enough to direct the major part of the port flow at 90 degrees to the lock chamber; and should be flared to aid in dispersing the jet and reducing exit losses. The optimum flare angle should be about 3 degrees or roughly a 1 to 20 horizontal deflection for each sidewall of the port. In most cases at locks designed for shallow-draft vessels (barge locks) the ports should enter the lock chamber at or slightly below the lock chamber floor and the bottom of the port should be at the same level at the culvert floor. If for foundation requirements, the lock floor has to be placed at a much lower level than is needed for proper submergence, the culverts and the ports do not need to be lowered to the floor level. This situation existed at the Eisenhower and Snell Locks on the St. Lawrence Seaway. At the Eisenhower Lock the depth in the lock chamber at the minimum lower pool elevation was 57 feet. Since the St. Lawrence locks are designed for 27-foot draft vessels, the lock floor is 30 feet below the bottom of a 27-foot vessel. The floor of the culvert manifold was placed 26 feet above the lock floor, and the ports were angled downward at a 1 vertical on 5 horizontal slope. The top of the jet as it expands after issuing from the port does not strike the bottom of a vessel.

172. Submergence requirements for barge locks with wall port manifolds were discussed previously. The curves on Figures 33-35 give permissible filling times for various combinations of lift, hawser stress, and submergence for

three sizes of locks. For locks of widths and lengths falling within the range tested, widths of 84 to 110 feet and lengths of 670 to 1,270 feet, design data may be obtained by interpolation of these curves. For any proposed lock that significantly exceeds the 110-foot width or the 1,270-foot length, Figures 33 and 34 should either not be used or used with extreme caution.

173. Port spacing is influenced more by lock width than by any other feature. By staggering (offsetting horizontally) the port in one wall with respect to the ports in the opposite wall and providing proper port spacing an arrangement can be developed that permits the expanding jet issuing from a port to cross to the opposite lock wall without directly colliding with an opposing jet. Thus, the energy of the jets, as they exit from a port, is expended as they disperse and comingle with jets from the opposite manifold. The objective is to dissipate most of the energy through boundary friction in the areas of contact between opposing jets. If the jets are permitted to collide, head-on, there will be upwelling, severe turbulence, and unstable conditions that will cause surging in the chamber.

174. The following port spacing for the two widths of locks that are most widely used in the United States are:

110-foot width	28-foot spacing
84-foot width	20-foot spacing

If these data are extrapolated, reasonable values can be obtained for lock widths as follows:

75-foot width	18-foot spacing
120-foot width	32-foot spacing

These data apply only to locks designed specifically for shallow-draft traffic. The test data obtained for the Mississippi River Gulf Outlet (MRGO) Lock should not be considered applicable to a 150-foot-wide barge lock since the design was partially governed by oceangoing vessels of 45-foot draft with a displacement of 170,000 dwt. Under this situation, the 48.28-foot minimum depth in the lock chamber provides much greater submergence than would normally be provided for a barge lock.

175. Since the port spacing, port size, number of ports, manifold length, and culvert size are all interrelated, a tentative procedure for establishing the number of ports would be as follows:

Consider 655- by 84-foot lock.

Manifold length 55% of 655 = 360.25 feet

Port spacing	= 20.0 feet
Number of ports = 360.25/20	= 18
Port size	= 6.0 square feet
Port to culvert ratio	= 0.95
Total port area = 6 × 18	= 108.0 square feet
Culvert area = 108/0.95	= 113.76 square feet
Use culvert 10 feet wide by 11.5 feet high	= 115.00 square feet
Then $\Sigma A_p/A_c$	= 0.94

This procedure is rule of thumb and should be tested out with procedures described in the section, "Area of Culverts." However, the rule of thumb procedure provides a basis or starting point for design of a wall port low-lift lock.

176. Ports angled upstream in the upstream half of culvert manifold have been used to reduce turbulence and hawser stress in several designs. Cannelton Lock has the ports in the upstream half of the lock chamber angled upstream by about 7 degrees. This plan was adopted in lieu of a plan with straight ports with baffle walls enclosing an area at the port exit. It is difficult to predict or predetermine turbulence conditions when angled ports are used unless the lock under design has the exact features and condtiions of a similar lock that has been model tested.

177. Baffles for wall port systems consist of placing low concrete walls on the lock floor around the exit of each port or else placing the culvert floor low enough so that the port can discharge into a shallow recess in the lock floor at the port exit. The baffles that were designed for Cannelton (but not used) formed a rectangular enclosure about 15 feet square that extended vertically from the chamber floor to the top of the port. The upstream ports had triangular-shaped enclosures that were designed to help direct the jets from the ports directly (90 degrees) across the lock chamber. Figure 63 shows details of port baffles or deflectors.

Manifolds for bottom longitudinal systems

178. In a bottom longitudinal system, flow from the two wall culverts enters a cross culvert that is connected to the manifolds in the bottom of the lock at the midpoint of the chamber. Obtaining an equal division of flow to the manifolds in the upstream and downstream halves of the lock chamber is the critical problem in design of a bottom longitudinal system. In the first designs of this type system, a culvert was placed across the lock at the

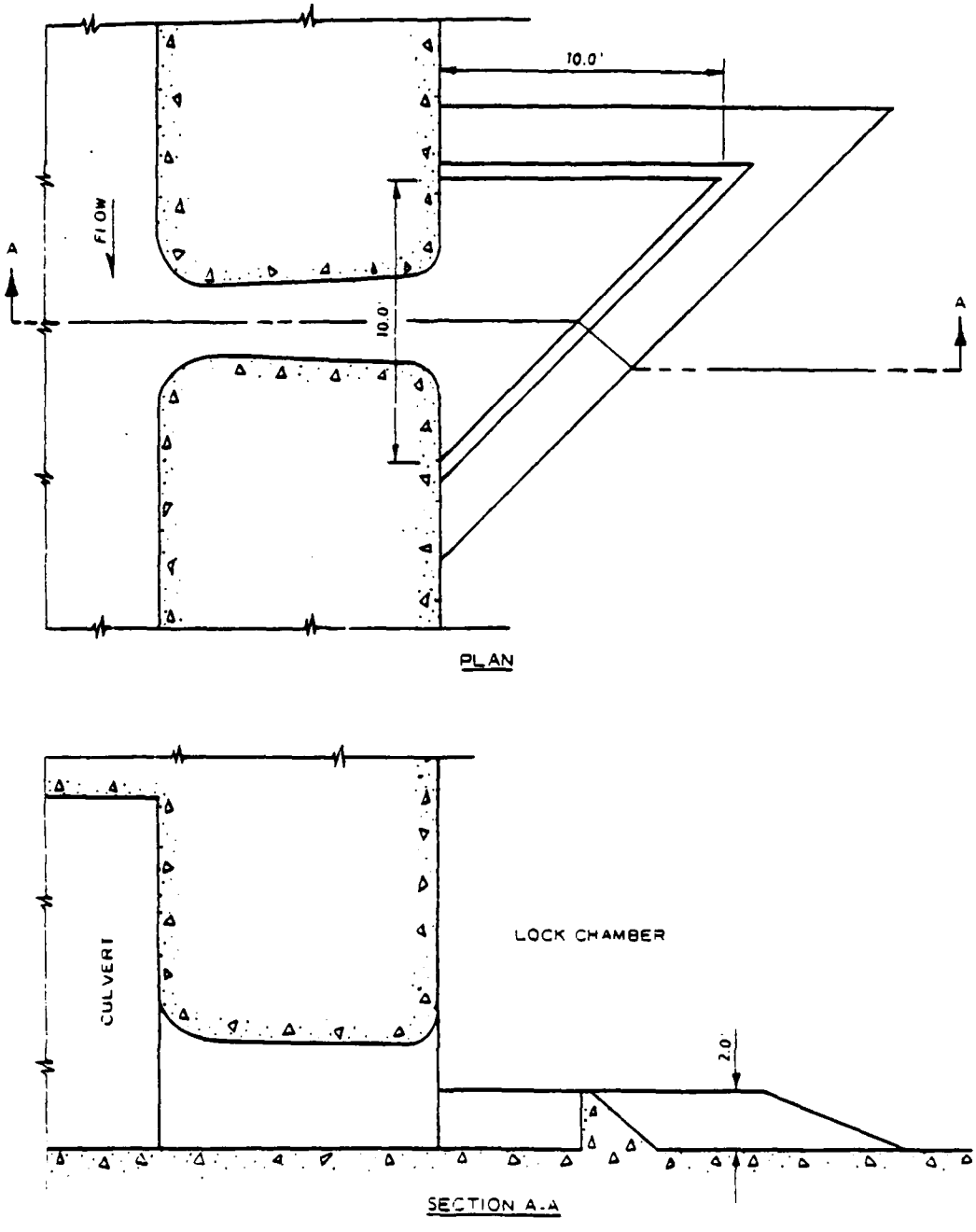

Figure 63. Port deflection for 110-foot-wide lock

midpoint of the chamber that connected directly to the culvert in each wall. Four longitudinal culverts (two extending upstream and two downstream) were placed in the bottom of the lock chamber and connected directly into the cross culvert. These four longitudinal culverts served as manifold culverts and had ports in each side. These first tests were made in 1962-64 for the Millers Ferry Lock. After numerous trial arrangements, the two manifold culverts in each half of the lock chamber were connected with a cross culvert at their outer ends, but the cross culvert at the middle of the lock was closed off to flow from one side of the lock to the other. A splitter wall was added at each end of the middle cross culvert to direct the flow from the main wall culverts to the upstream and downstream manifold culverts. This arrangement worked fairly well for the 48-foot-lift, 84- by 655-foot lock at Millers Ferry. In subsequent testing for the Jones Bluff Lock, the crossover culvert at the lock midpoint was again made continuous (from one wall culvert to the other) and a vertical splitter wall was placed in the middle that extended the entire length of the crossover culvert. The crossover culverts at the ends of the bottom manifold culverts were eliminated.

179. Turning the flow from the main wall culverts into the crossover culvert and obtaining equal division of flow during an entire filling operation cannot be accomplished with this system. The entrances to the crossover culvert were adjusted so that a 50-50 divisio of flow was obtained with a steady flow that approximated the peak flow during a filling operation. This entrance design was considered about as good as could be obtained and was used on Millers Ferry Lock. The upstream and downstream passages of the crossover culvert were 7.0 feet high by 11.0 feet in width. This configuration was carried on to each of the longitudinal manifold culverts. Each of the manifold culverts had five ports, spaced 14 feet on centers in each side. The crossover culverts at the ends had nine ports in the outer wall and twenty-seven 8-inch-diameter ports in the tops of the culverts. The ports in the vertical walls of the manifold were 4.0 feet high and 1.25 feet wide. The entire manifold system occupied about 35 percent of the lock chamber length. Even though it does not provide balanced flow conditions at all times during a filling operation, the system performs very well and does not cause excessive hawser stress with one valve operation.

180. Subsequent studies of bottom longitudinal filling systems were pursued at the US Army Engineer Waterways Experiment Station, Vicksburg,

Mississippi, and at the North Pacific Division Laboratory in Bonneville, Oregon. An improved version of a four-branch manifold system with flow divided by a vertical wall at the crossover culvert was developed for Bankhead Lock (110- by 670-foot lock with 69-foot lift). This design includes an improved entrance to the crossover culvert (from the wall culverts) and a different arrangement of the longitudinal manifold culverts. The crossover culvert has a vertical splitter wall, and a short section of wide longitudinal floor culvert is connected to each of the passages in the crossover culvert. Two longitudinal manifold culverts join the short, wide floor culverts that branch out in the shape of a tuning fork in each half of the lock. Twelve pairs of ports are placed in each culvert on 15.0-foot centers. The ports are 1.5 feet wide by 3.5 feet high. A baffle wall with a tee-shaped overhang is placed along the center line of the lock to reduce turbulence and upwelling during filling. The manifold section is symmetrical with respect to both width and length of the lock chamber. The manifold culverts occupy about 51 percent of the lock chamber length and are centered on the quarter points. Flow distribution is good, and turbulence and surging conditions are very satisfactory. The area at the valve is 196 square feet; the crossover culvert area is 200 square feet; and at the manifolds, the area is 250 square feet. Thus, the ratio of manifold to culvert area is 1.28. The total port area (per wall culvert) is 252 square feet, giving an $\Sigma A_p/A_c$ ratio of 1.29. However, the ratio of port area to manifold area is only 250/252, or 0.99. This design represents about the optimum that can be obtained with the vertical splitter arrangement at the entrance to the crossover culverts. Use of this system with higher lifts or larger lock chambers is not recommended.

181. The design developed for the Lower Granite Lock on the Snake River is superior to any other design ever developed in the United States for high-lift locks. The Lower Granite design was developed at the North Pacific Division Laboratory from 1966 to 1970. Flow in the main wall culverts is divided equally between the upstream and downstream halves of the lock during the entire filling period by a horizontal diaphragm. The diaphragm across the wall culvert forms two passages, one of which curves upstream from the center of the lock, and the other downstream. Symmetrically arranged passages are provided on the opposite wall culvert, and the passages that turn upstream from the wall culverts enter a short longitudinal culvert extending upsteam to connect to a four-branch manifold. Similar culvert arrangements are provided

in the downstream half of the lock. The four-branch manifold in each half of the lock is laid out in the form of an H. Equal division of flow is provided to each of the four culverts in each manifold at all times during a filling operation. With this balanced flow condition, at the instant either one or both valves start to open, flow from 16 ports will begin simultaneously. Each of the two four-branch manifolds is centered symmetrically to the midpoints of each half of the lock. The eight manifold culverts each have 12 ports that are 1.25 feet wide and 3.46 feet high. Baffles, in the form of a horizontal diaphragm, overhang each port about 2.0 feet.

182. This system represents about the best that can be achieved for any situations of high-lift large lock chamber.

Bottom lateral systems

183. Prior to development of bottom longitudinal systems, a filling system known as the bottom lateral system was used for large medium-lift locks (1,270-foot locks with lifts over 30 feet), and for smaller high-lift locks. In this system, lateral or transverse culverts are connected to openings in the wall culverts to conduct flow from the main wall culvert into the lock chamber via ports in the sidewalls of the lateral culverts. Essentially, the system involves placing transverse culverts with ports in their sidewalls over the exits of the ports in a wall port system. Since the wall ports are normally staggered in relation to each other, adjacent laterals will not be connected to the same wall culvert. If the first lateral downstream from the valve is connected to the left wall culvert, the next one (adjacent one) will be connected to the opposite wall culvert. This arrangement is designated as an intermeshed lateral system. Th head loss from the main wall culvert to the lock water surface is greater than with a wall port system, and to offset this increased loss, the entrance area of the laterals and hence the laterals, are made larger than the area of the ports in a wall port system. The number, location, and size of the laterals are the critical factors in design of this type system.

184. A variation of the bottom lateral concept places the laterals in two separate groups. One group is connected to one culvert only and is centered (roughly) about the one-third to the one-quarter point of the lock. The other group is connected to the other culvert and is centered about the one-third to the one-quarter point in the opposite end of the lock. This system, designated as a split lateral system, produces good lock chamber

conditions for long low- to medium-lift locks and short high-lift structures. The system has one very serious flaw. Operation of the filling and emtpying valves must be perfectly synchronized at all times. Any difference in rates of opening of the valves causes more flow to enter one end of the lock chamber, and thus sets up serious surges. One-valve operation is also difficult, and filling must be very slow. Fail-safe devices must be placed on the valve operating equipment so that if one valve stops or slows, the other valve will automatically stop also. For these reasons, further use of this system has been curtailed. Also, with the development of the bottom longitudinal system, there was no longer any real advantage to further use of the split lateral concept.

185. Where space limitations make use of a culvert in only one lock wall desirable, a bottom lateral system may offer some advantage in cost for locks that do not exceed 670 feet in length.

186. There are no fixed criteria on spacing of intermeshed bottom laterals. Spacing for intermeshed systems have varied from 17 feet for a 500-foot lock to 19 feet for a 675-foot lock. The close spacing of the laterals may have been influenced by the desire to place the laterals in the middle one-third of the length of the lock chamber. In model studies this location produces the least surging and turbulence, but in prototype locks, Holt Lock, for example, concentrating the laterals in the center portion with a 17-foot spacing produces an upwelling in the middle of the lock that tends to break up tows. It appears that lateral spacing should probably be about 20 to 25 feet and that the laterals can occupy more than the middle third of the chamber without worsening lock chamber conditions. Where bottom laterals are connected to only one culvert, such as the 670-foot auxiliary locks on the Ohio River, the lateral spacing is greater--usually 30 to 40 feet. Lateral culvert designs using a gradually decreasing cross section (tapered) and full cross section over the whole length have been used. The objective in either case is to obtain reasonably uniform flow through all of the ports in the lateral. The port spacing, size, and number depend on the amount of port area desired. The combined area of all of the laterals (at their entrances) is usually greater than the culvert area by 25 to 40 percent. Also, the total area of the ports in a lateral is usually, but not always, made greater than the area of the lateral entrance. Making combined areas of the ports smaller results in a more uniform pressure gradient, but increases the head loss and

the filling time. Ports from adjacent laterals will discharge into the trench area between the laterals and should be staggered so that the jets do not collide. Extensions should be placed on the port exits to straighten the jet as it emerges from the lateral.

PART VIII: INTAKE DESIGN

187. While the procedures discussed in the following paragraphs on design of intakes are primarily concerned with the design of hydraulic systems using culverts located in the lock walls, many of the general principles discussed are equally applicable to the design of systems utilizing longitudinal culverts or lateral culverts in the lock floor. Manifolds designed for flow in only one direction can be made more efficient than those subject to flow in opposite directions such as occurs in a combined filling and emptying system. This is illustrated by the fact that head losses are greater for the lock manifold during emptying than during filling. Since ports and transitions in a single-purpose manifold can be shaped specifically for the one direction of flow, streamlining need not be compromised to accommodate reversed flow conditions.

Intake Area

188. The area of a lock intake is made considerably larger than the area of the culvert. There are many reasons for this. A larger intake reduces entrance head losses, tendencies to draw air, and danger of damage to the trash racks by impact of floating drift or ice. By using several small intake openings with a larger aggregate area, instead of one large port, the flow is spread over a wider area and hence the tendency for the formation of vortexes and the entrainment of air into the culvert flow is further reduced. For structural reasons several small intake ports are preferable when the openings are located in a lock wall since trash racks of a reasonable size can be used. Locating the top of the intake well below the minimum upper pool level, ensures a positive pressure gradient and further improves the hydraulic operation. If the intake ports are exposed to floating drift or ice, the gross intake velocity should be limited to 8 or 10 feet per second to avoid damage to the racks by impact. Figure 47 shows that as the ratio of total throat area to culvert area ($\Sigma A_p/A_c$) is made larger the head loss decreases. But, as the ratio approaches a value of 2.0, any further decrease in the loss coefficient is small. Values of A_p/A_c ranging from about 1.3 to over 2.0 have been used. Values in the range of 1.5 to 2.0 are good design practice. The port openings at the wall face are all of uniform dimensions, i.e., port

number 1 has the same vertical and horizontal dimensions as the lost port. The total combined area of the ports at the wall face is usually made from 2.5 to 3.5 times the area of the culvert ($\Sigma A_{p_w} / A_c$ = 2.5 to 3.5).

Examples of Intakes

189. Examples of single and twin intake manifolds located in the approach walls of a lock are shown in Figure 64. The successive ports in the downstream direction being subjected to increasing pressure head differentials are made progressively smaller at the throat to obtain approximately uniform distribution of flow. The culvert converges between successive ports but expands abruptly below each port in the downstream direction. This is done to increase the velocity in the culvert until it approaches the velocity of inflow from the ports at each point of confluence, thus reducing impact losses. Curvatures at port entrances and throat as well as the general layout of the manifolds shown in Figure 64 are also applicable to designs for different numbers of ports.

Intake Model Tests

190. Several approach wall intake manifolds have been tested in scale models with the purpose of developing flow control at the throat such that all ports will carry equal fractions of the total discharge. The flow through each port in the initial design was measured and if the distribution was not uniform the throat areas were adjusted in proportion to the deviation. The relative areas of the throat sections developed in several intake manifolds by this "cut and try" process are shown in Figure 65. In the absence of specific model test data or analogous prototype designs these data can be used in the design of intake manifolds for a project lock. Due to the fact that approach flow conditions may be different in the project lock than existed in the model tests on which the design data are based, some variation from uniform flow may still occur. Whether another adjustment in area is necessary can be determined if the project lock is to be tested in a model--the criterion being the attainment of satisfactory flow conditions in the approach.

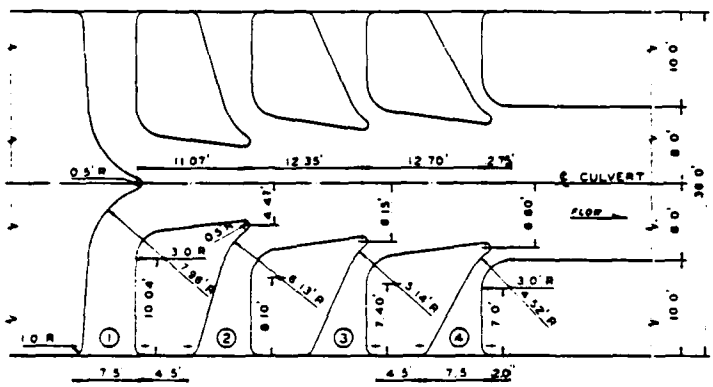

a. Twin manifolds

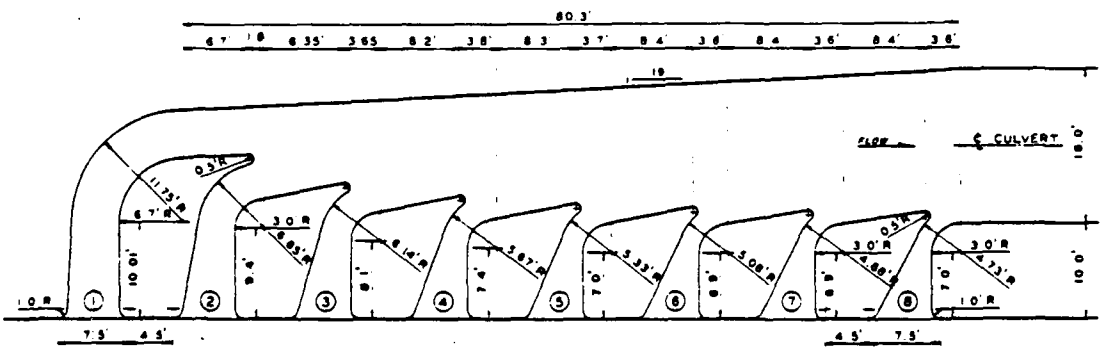

b. Single manifold

Figure 64. Intake manifolds, horizontal sections

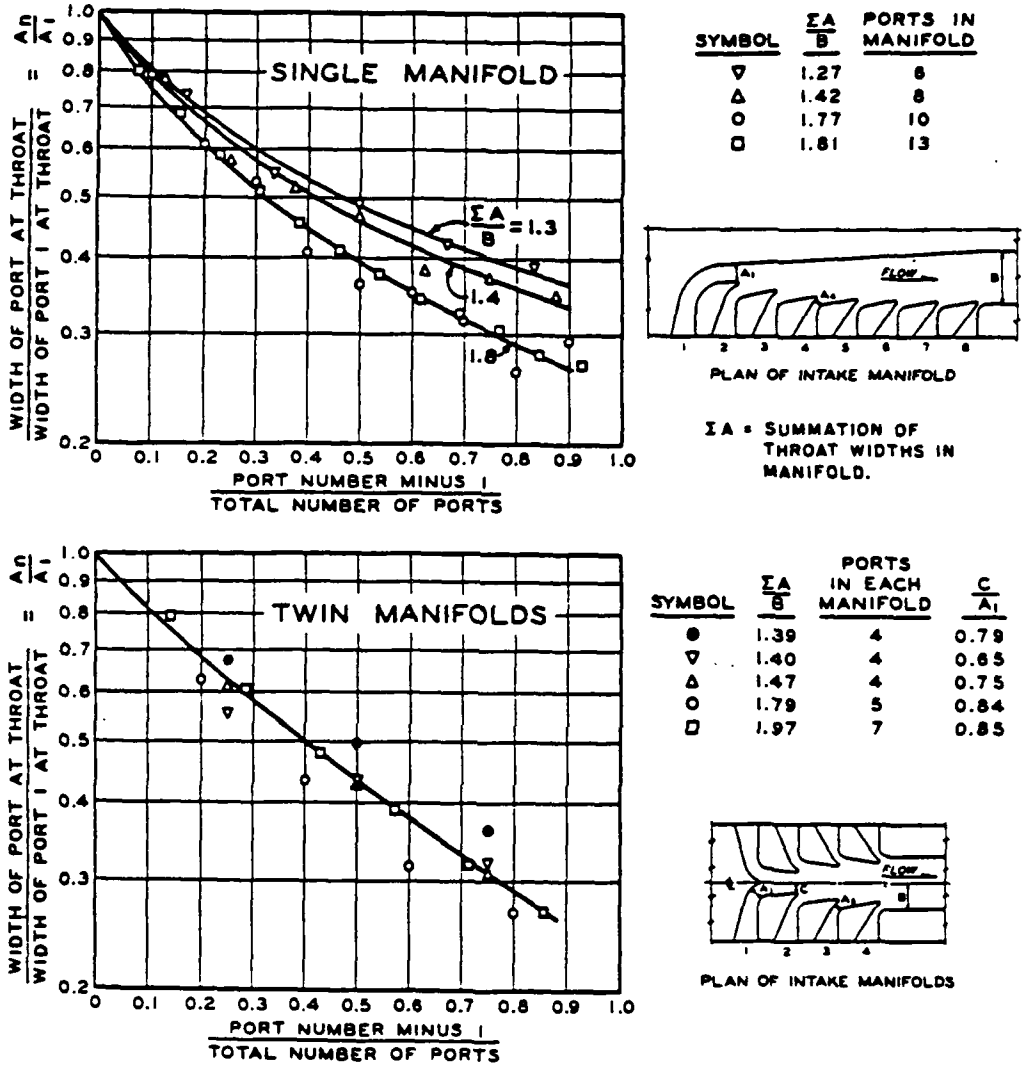

n = number of any port under consideration
N = total number of ports

NOTE: Data are based on model tests of intake manifolds for the Dardanelle, Greenup and Markland, Pickwick, and Port Allen Locks. When flow measured in any port deviated from the average for the manifold, the width of the port was adjusted in inverse proportion to the flow ratio.

Figure 65. Relative size of intake ports at throat

Determination of Throat Areas

191. The curves of Figure 65 are based on a design where all ports have the same height at the throat as the culvert, and the sum of the throat widths being greater than the culvert width by the factor selected for $\Sigma A_p/A_c$. Thus port widths may then be used to designate port areas. With reference to Figure 65, n represents any port in the manifold, A_n, the area of the nth port, A_1, the area of port number 1, and N_p the total number of ports. The area for any port, n, under consideration is expressed as a percent of the area of port number 1 (A_n/A_1) and is plotted versus the ratio of port n minus 1 to the total number of ports ($n - 1/N_p$). When $n = 1$, there is no difference in areas and $A_n/A_1 = 1.0$. Proceedings to port number 2, $n - 1/N_p = (2-1)/8 = 0.125$ and $A_n/A_1 = 0.76$. The procedure is continued for all ports. Continuing on with the explanation of Figure 65, an example gives:

Culvert size 16.25 × 16.25 feet	Area = 264 square feet
Ports at throat, $A_p/A_c = 1.41$	Area = 372 square feet
Ports at wall, $A_{p_w}/A_c = 2.65$	Area = 700 square feet

Using an eight-port manifold and a height of port at the wall face of 12.5 feet gives the port width at the wall of $700/(8 \times 12.5 \text{ feet}) = 7.0$ feet. The ports will have the same height at the throats as the culvert, 16.25 feet, and the top of the port throat will be at the same elevation as the top of the culvert. Using Figure 65 and these data gives the following computations:

(1) Port No.	(2) $n - 1/N_p$	(3) Percent of A_1, A_n/A_1	(4) Area A_n
1	0.000	1.00	5.10
2	0.125	0.76	3.88
3	0.250	0.62	3.16
4	0.375	0.53	2.70
5	0.500	0.46	2.35
6	0.625	0.41	2.09
7	0.750	0.37	1.89
8	0.875	0.34	1.73
		$\Sigma = 4.49$	

The values in column (4) are obtained as follows:

Total port area, $\Sigma A_p = 1.41 \times 16.25 = 22.91$ square feet

$A_1 = 22.91/4.49 = 5.10$ square feet

The values for ports 2 through 8 are computed by multiplying the percentage factors in column 3 by 5.10 square feet, the area of port 1.

Vortexes

192. Vortex action causes considerable concern due to the inherent hazards to personnel and small craft, loss of efficiency in the filling system, and the potential danger of damage to the intake grates by debris engulfed in the whirling currents. Basic design procedures that will ensure vortex-free approach flow are not known but in general the solution is to strive for symmetrical flow conditions, minimum velocities, and maximum submergence. Tests have indicated that intake manifolds located in the upper gate sill are more susceptible to vortex action than intakes located in the approach walls. Among the aggravating circumstances which cannot readily be avoided with sill intakes are the following: (1) concentration of high velocity in the approach to the intakes and in the port entrances because the width of flow is restricted to that of the lock sill, (2) due to the proximity of the miter gate V's, stagnation levels are raised in the acute corners which results in reverse flow toward the intakes, and (3) the miter gate recesses on either side of the intake manifold are breeding places for small whirlpools which stimulate development of larger vortexes. Contributing elements which should be avoided as far as practicable in future designs for side wall as well as sill intakes are unequal distribution of flow in the intakes ports, openings in the guide or guard walls which induce diagonal currents, and breaks in the alignment of the approach walls, all of which distort uniform flow patterns in the approach. Vortexes are difficult to avoid in high-lift locks designed for barge traffic where the depth above the upper sill is shallow and where the approach floor is near the elevation of the upper sill. Where a vortex problem is anticipated it should be investigated in a scale model of the structure.

Elevation of Intakes

193. The proper elevation of the intakes may be determined according to the following example. Using the port design of the previous analysis and an assumed peak inflow rate (discharge into the lock) of 12,750 cfs, the average maximum flow through each port is 12,750/16 = 800 cfs. It is assumed that the maximum velocity in the throat of port 8 equals about 10 percent above the average velocity at the throat section. Then, with an A_p of port 8 equal to 1.73×16.25

$$\text{maximum } V = 1.10\ q_p/A_p = \frac{1.10 \times 800}{1.73 \times 16.25} = 31.3 \text{ feet per second}$$

$$\text{velocity head} = \frac{(31.3)^2}{64.4} = 15.2 \text{ feet}$$

The tops of the ports should be submerged by a depth at least equal to the maximum velocity head occurring in the port to assure positive pressures. Then the elevation of the top of the intake ports should be at least 15.2 feet below the upper port level.

PART IX: OUTLET DESIGN

194. Discharge manifolds are designed to obtain an efficient emptying operation and to distribute the outflow from the lock at locations and velocities which will not imperil any craft in the immediate area of the lower approach. Turbulence and strong adverse currents in the lower lock entrance should be avoided in order to safeguard tows or boats navigating or moored in the area during an emptying operation. By gradually diverging the flow sections of the discharge system both the emptying time and the velocity characteristics can be improved. The conditions for obtaining these objectives are not as favorable as in the case of the filling system discharging into the lock chamber. The chamber manifold can occupy one third or more of the lock length and the cushion depth is constantly increasing during the filling operation, whereas, the discharge manifold is kept as short as possible for reasons of cost and the tailwater depth remains essentially constant throughout the emptying operation.

195. Emptying systems have been designed to discharge all the flow into the lower approach or to divert part or all of it outside of the approach. Where all the flow is discharged into the approach directly from manifold ports the degree of turbulence is usually too severe to permit vessels to be moored in the immediate area even though the expansion of the port area over the culvert area is large. An example of a recent typical design for a discharge manifold is shown in Figure 66.

Discharge Laterals

196. Discharge laterals can be used to reduce turbulence and to obtain a more uniform distribution of flow across the lower approach, and they are particularly effective in preventing the spiral movement set up by imbalanced discharge from a one-culvert system. The single-culvert discharge lateral system adopted for the St. Anthony Falls Lower Lock is shown in Figure 67. The laterals are reduced in width in the downstream direction by a series of steps at the successive ports and the outside walls of the laterals are parallel. Ports in adjacent laterals are staggered. Inasmuch as discharge laterals carry flow in only one direction, the outlet end of the ports need not be rounded. The recent discharge lateral design for the two-culvert system of

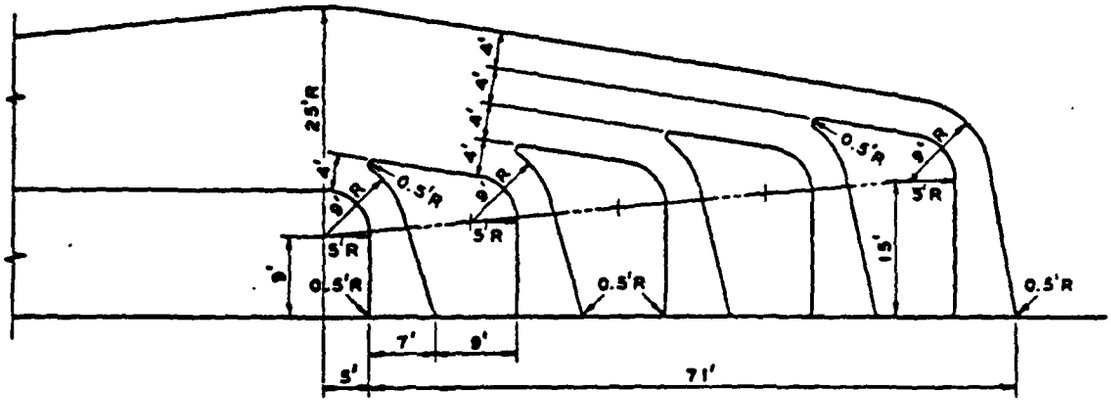

Figure 66. Discharge manifold, new second lock, St. Marys Falls Canal, Michigan

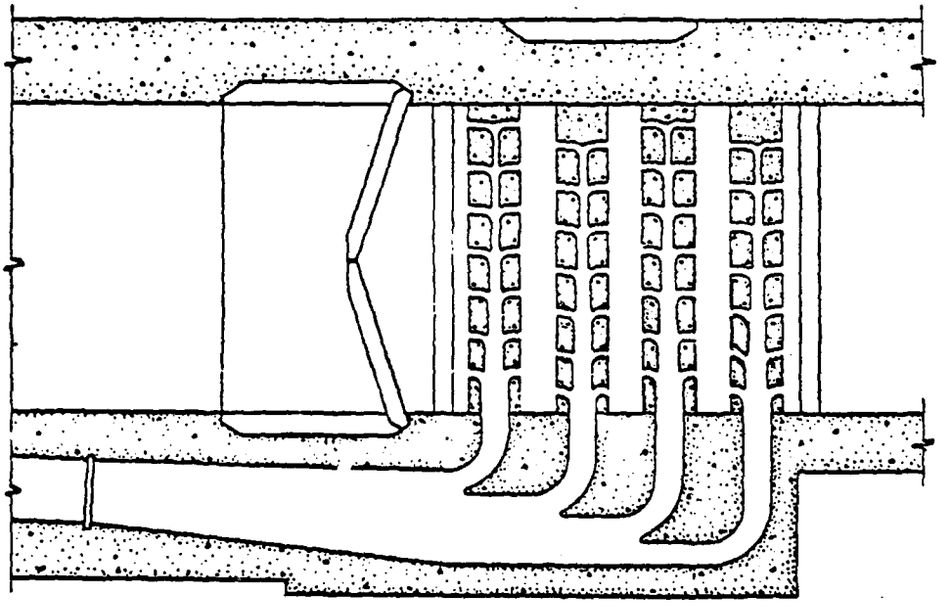

Figure 67. Discharge laterals, St. Anthony Falls Lower Lock, Mississippi River

the Snell Lock has extensions on all ports to direct the jets perpendicularly across the trenches and thus effect a better flow distribution in the lower approach.

Discharge Manifolds

197. Figure 68 indicates the arrangement of the discharge manifolds for the New Cumberland Main Lock. This system was designed to divert two-thirds of the lock discharge outside the approach area. With the wider spacing the ports in the lock approach could be staggered to reduce the interference of opposing jets. The depth of water in the lower approach of the New Cumberland Main Lock is 24 feet at the discharge manifolds. Cushion depths measured to the bottom of the trenches between discharge laterals are 22.2 feet for the St. Anthony Falls Lower Lock and 48 feet for the Snell Lock. Observations in the prototypes indicate that the turbulence in the discharge area at the New Cumberland Main Lock is less than that at the St. Anthony Falls Lower Lock but more severe than in the lower approach to the Snell Lock.

Single-Port Outlets

198. Cannelton Lock, Ohio River, tested in the WES Hydraulics Laboratory,[7] is provided with a discharge system which diverts the entire flow

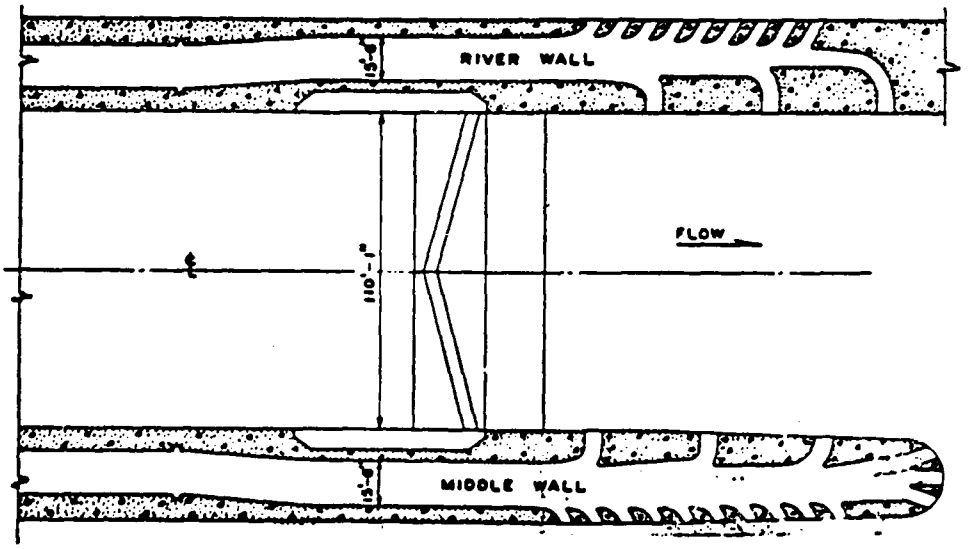

Figure 68. Discharge manifolds, New Cumberland Lock, Ohio River

outside of the lock approach. Such an emptying system, as shown in Figure 69, affords the opportunity for efficient expansion of the culverts to decrease head losses. This was not done at Cannelton, because additional culvert length would have been needed. This is particularly desirable (expanded outlet) since the longer emptying system tends to unbalance the filling and emptying time. Additional head losses occur in the landward wall culvert because of its additional length. Stilling basins are usually provided at such outlets to reduce turbulence. If this type of emptying system results in a head differential between the water levels in the lock chamber after emptying and the lower approach, the design of the lower miter gates may be affected, and in extreme cases, it may be necessary to provide an auxiliary emptying device to equalize the residual differential of head. In addition to Ohio River locks, several other locks constructed recently in the US Army Corps of Engineers South Atlantic Division and North Pacific Division and in the Tennessee River by the Tennessee Valley Authority, have been provided with discharge systems of this type which divert the outflow into the river outside of the lower lock approach. By so doing, the lock entrance is entirely free of disturbance during emptying operations and it permits the full use of the guide wall for mooring tows.

Outlet Ports with Baffle Blocks

199. Another type of outlet that has been used on some of the Arkansas River locks is shown in Figure 70. This type is suitable at some locations that have low-lift locks.

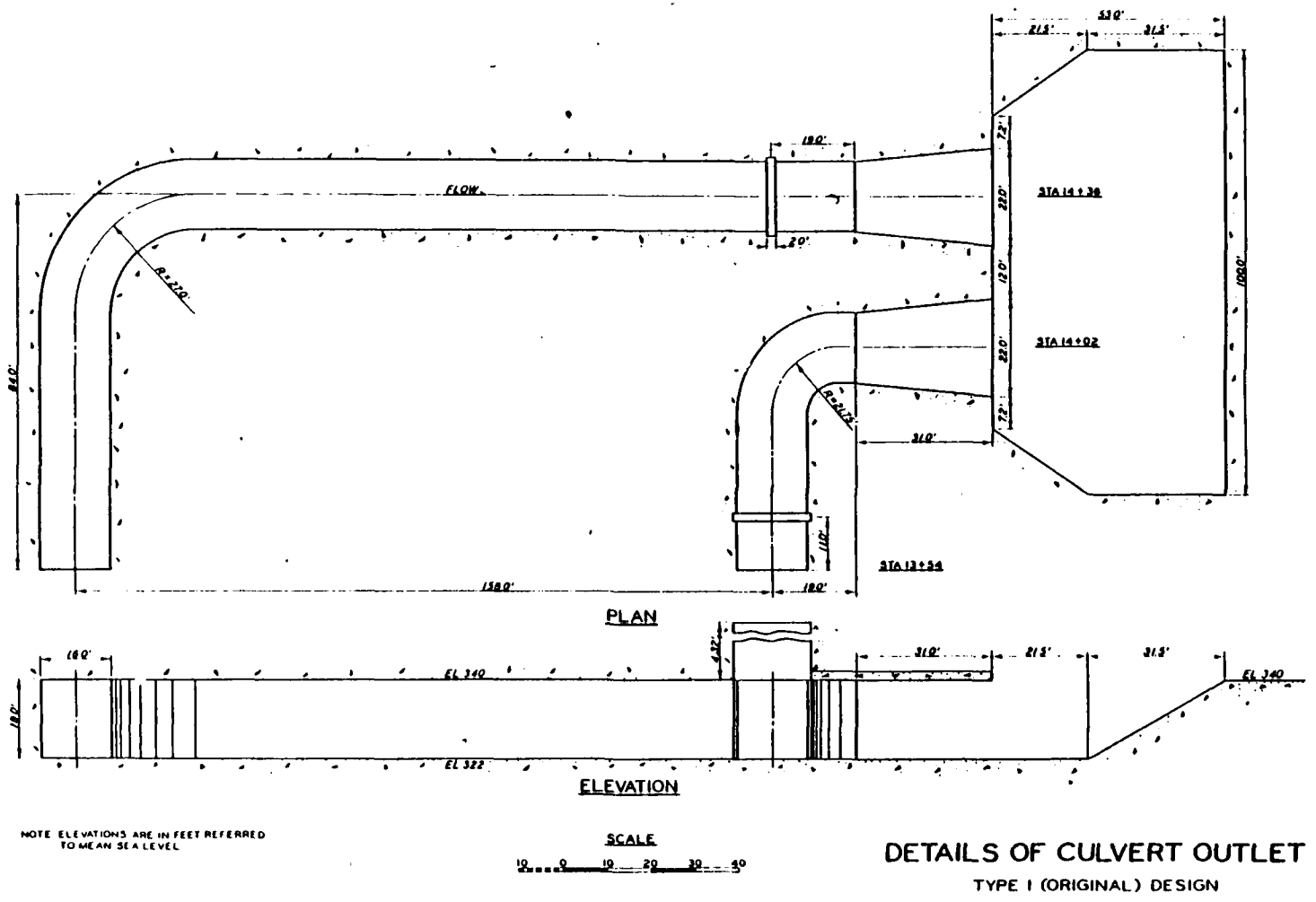

Figure 69. Details of culvert outlet, single-port design

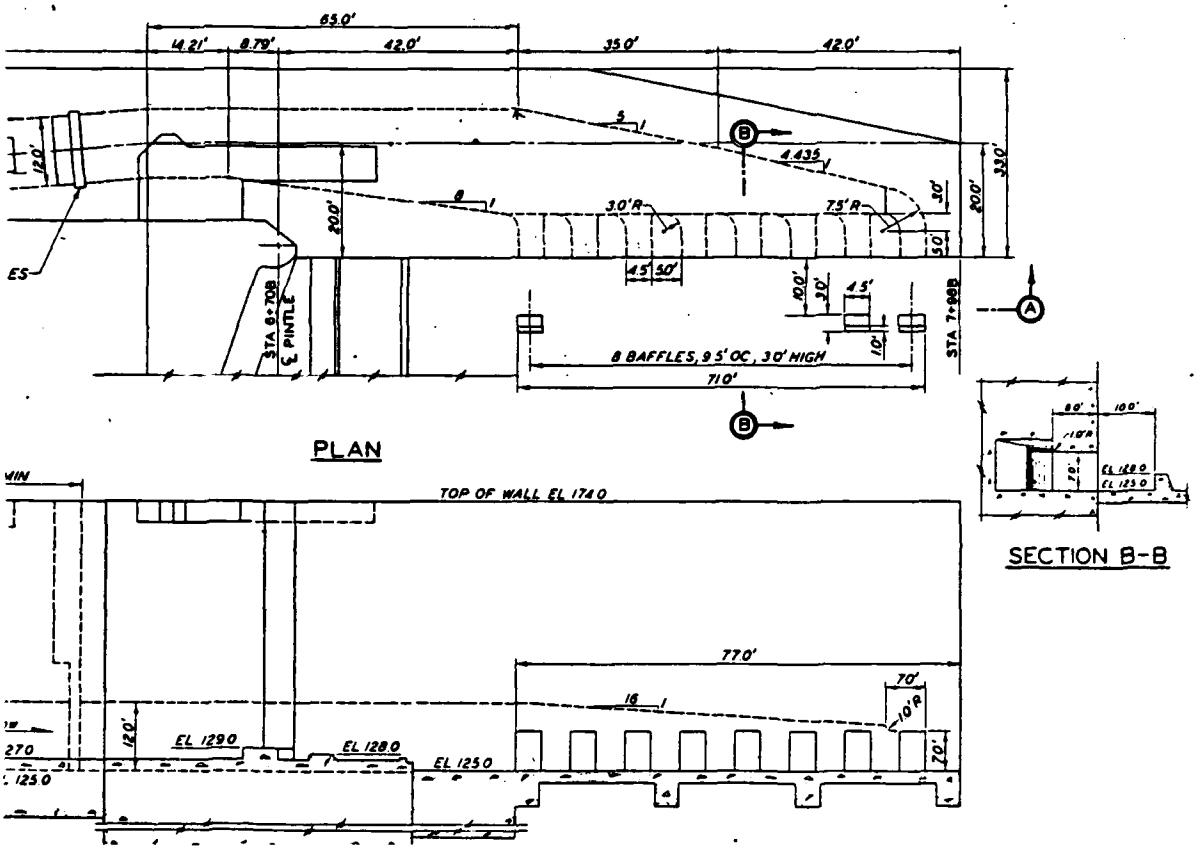

Figure 70. Outlet with baffle blocks

PART X: DESIGN OF WALL CULVERT SIDE PORT FILLING AND EMPTYING SYSTEM

200. Design of a lock with wall culverts and ports extending from the culverts to the lock chamber is presented to illustrate the procedures described in the foregoing chapters. While design curves in the preceding chapters have been developed for three different sizes of low-lift locks, the following example uses a size different from the three sizes previously covered to show how the existing data can be used for other lock sizes. Also, the example includes the treatment that is necessary when lengthened culverts between the intake and the lock manifolds are required. The design example makes use of some of the conditions that exist at the site of the proposed new locks on the Ohio River at Gallipolis, Ohio.

Location

201. The lock will be located in a canal through the left bank abutment of an existing dam, generally similar to the plan for the proposed locks at Gallipolis. In this example only one 800-foot by 110-foot lock has been considered instead of the 1,200- and 600-foot locks in the current Gallipolis plan. Figure 71 shows the general arrangement of the upstream end of the lock with respect to the river bank, the canal, and the axis of the dam. The following tabulation shows the basic conditions:

Size	
Length (pintle to pintle)	870.0 feet
Width (clear width)	110.0 feet
Pool elevations	
Upper pool	538.0 feet
Lower pool	510.5 feet
Maximum lift	27.5 feet
Minimum depth of sills	15.0 feet
Submergence	25.0 feet

Use of Existing Design Data

202. Since no design curves from model tests are available for this size lock that gives hawser stress, lift, operation time, and submergence, the

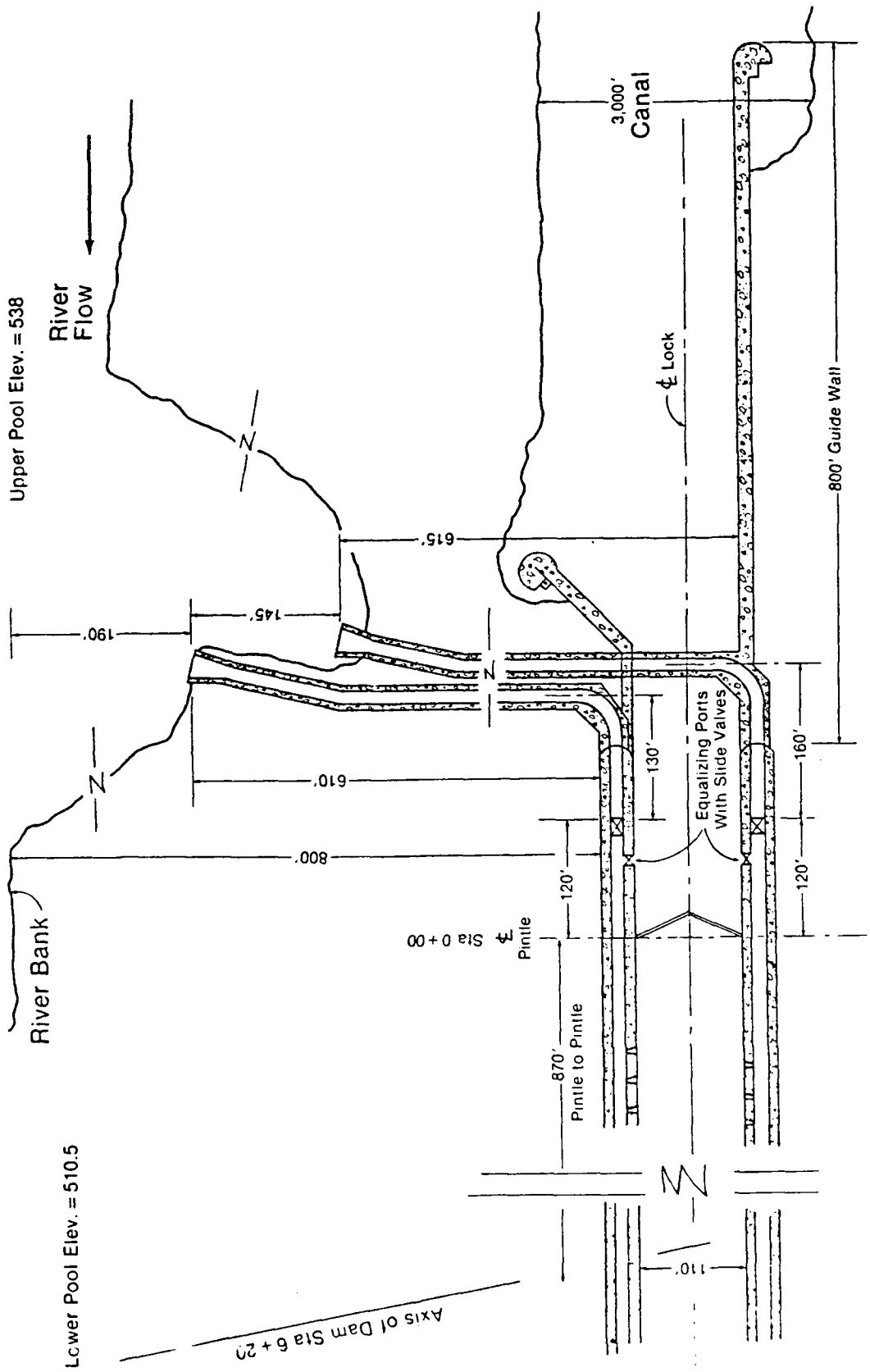

Figure 71. Filling system layout for design for side port lock

data for Cannelton Locks and Arkansas River Locks will be used. Based on these data, values of other parameters involved would be expected to be

Port size	10.0 to 11.0 square feet
Port spacing	28.0 feet
Length of port manifold	50 to 60 percent of lock length

Arkansas River low-lift locks

203. From Plate 17 of Reference 6, Port "D" is 4.10 by 2.54 feet with an area of 10.41 square feet, culvert size is 12 by 12 feet. On Plate 52 (Reference 6), design curves for Type 56 system, utilizing Port "D", show

Hawser stress	= 5 tons
Submergence	= 25 feet
Lift	= 27.5 feet
T_f	= 8.0 minutes
t_v (from Plate 53, Reference 6)	= 3.2 minutes
N_p (Table 28, Type 56, Reference 6)	= 13 ports
Area of ports = 13 × 10.41 feet	= 135.38 square feet
A_p/A_c	= 0.94
Length of manifold	= 52.2 percent of lock

Cannelton Locks

204. From Reference 7, Type A Port is 4.07 by 2.75 feet with an area of 11.19 square feet and culverts are 18 by 16 feet with an area of 288 square feet. From Plate 50 (Reference 7), Arrangement Type 100 design curves show

Hawser stress	= 5 tons
Submergence	= 25 feet
Lift	= 27.5 feet
T_f	= 8.5 minutes
t_v	= 4.8 minutes
Number of ports	= 24
Area of ports = 24 × 11.19 feet	= 268.63 square feet
A_p/A_c = 268.63/288	= 0.93
Length of manifold	= 52 percent of lock

Interpolating for an 870-foot lock

205. Using a 1,270-foot lock (Cannelton) and 670-foot lock (Arkansas) as a basis:

T_f (1,270-foot lock)	= 8.6 minutes
T_f (670-foot lock)	= 8.0 minutes
Difference	= 0.6 minutes

870 - 670 feet = 200 feet
1,270 - 670 feet = 600 feet

$\frac{200}{600} \times 0.6$ minutes = 0.2 minutes

T_f for 870-foot lock = 8.0 + 0.2 minutes	= 8.2 minutes
Length of port manifold = 52 percent of 870 feet	= 452 feet
At 28-foot spacing, number of spaces	= 16.5
With 16 spaces, number of ports	= 17
With 17 ports, length of manifold	= 462 feet
Length of manifold, percent of lock	= 53 percent
Use port size 4.10 by 2.54 feet, area	= 10.41 square feet
Area of ports, 17 × 10.41 feet	= 177.0 square feet
For ratio, A_p/A_c = 0.93; A_c	= 190.0 square feet
Consider culvert size 15 × 13 feet, A_c	= 195.0 square feet
Then A_p/A_c	= 0.91

Note: This value should be larger.

Reconsider number of ports

206. Using 18 ports (17 spaces):

Try 18 ports (17 spaces)	
Length of manifold = 17 × 28 + 14 feet	= 490.0 feet
Length of manifold, percent of lock	= 56 percent
Area of ports, 18 × 10.41 feet	= 187.38 square feet
For A_p/A_c of 0.93, A_c	= 201.48 square feet
Use 15.0 × 13.5-foot culvert	= 202.50 square feet
and A_p/A_c (187.38/202.5)	= 0.93

Prototype filling time

207. From curve of Figure 40 (T_f versus T_f''):

Prototype filling time = 7.1 minutes

Tentative Layout of Lock

208. The lock is to be located in a canal that bypasses the left bank abutment of an existing dam. The lock will be situated about 840 feet to the left of the left river bank with the downstream gate pintle about 300 feet downstream from the axis of the dam. A separate intake and culvert for each main wall culvert will convey flow from an embayment area cut into the left riverbank, directly riverward from the upstream end of the lock. Figures 71 and 72 show the general layout, and the following tabulation shows the culvert lengths.

Section of Culvert	Right Culvert Length feet	Left Culvert Length feet
Intake to wall culverts	610	615
Junction intake and wall culverts to upstream side valve well	130	160
Length of valve well	20	20
Upstream side of valve well to gate pintle	120	120
Gate pintle to first port	190	204
Length, intake to first port (minus valve well length)	1,050	1,099
Average length to first port 1,074.5 feet		
Length, first port to middle of manifold	245	231
Length for inertia head	1,295	1,330
Average length for inertia head 1,312.5 feet		

Determination of Head Losses

209. The culvert size based solely on port to culvert dimensions and ratios was

$$15.0 \times 13.5 \text{ feet} = 202.50 \text{ square feet}$$

This size must be increased because of the losses in the long culverts from

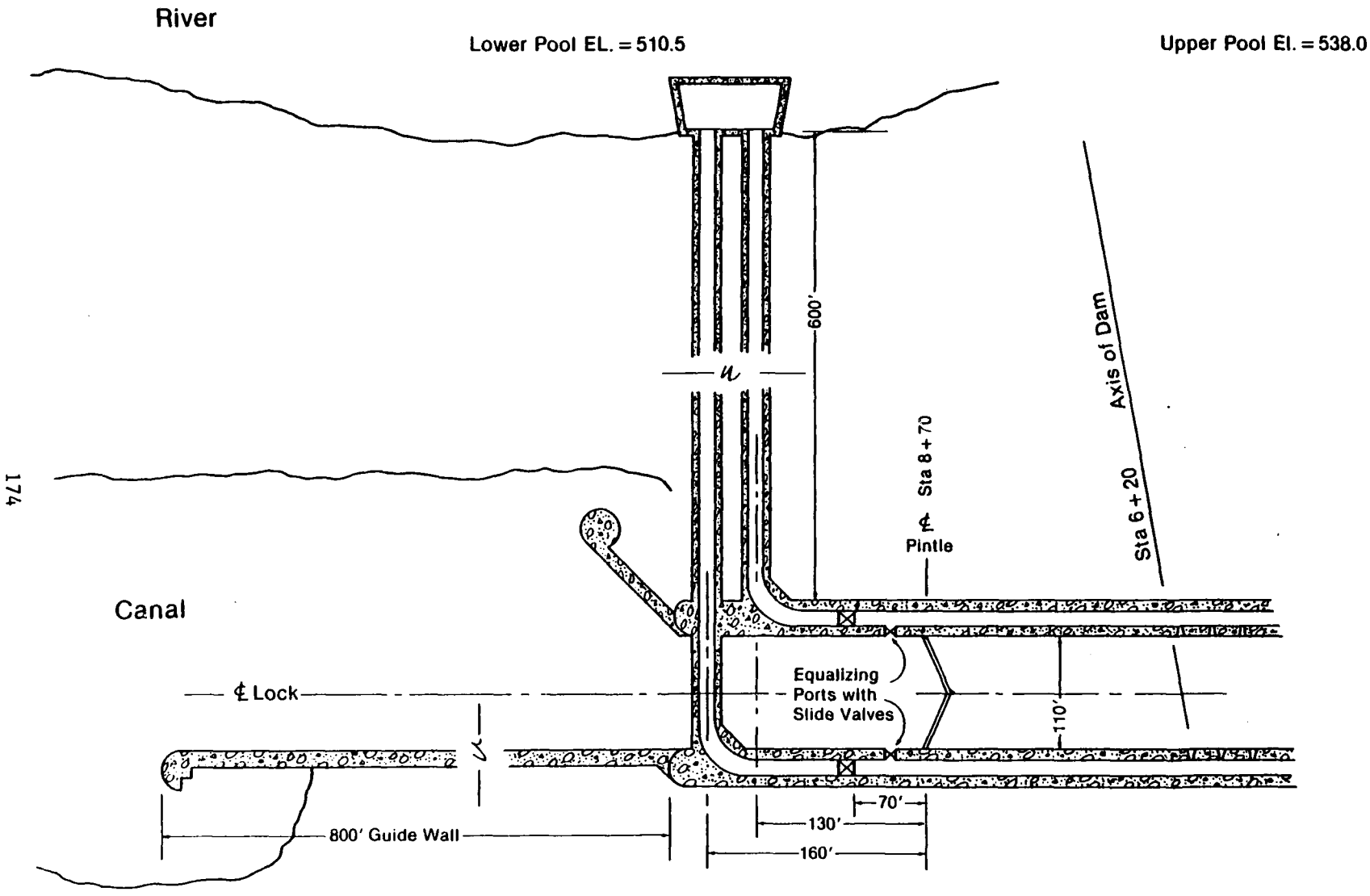

Figure 72. Emptying system layout for design of side port lock

intake to the junction with the wall culverts. Therefore, as a first trial, the culvert area of 202.50 square feet will be increased by about 15 percent. Then A_c would be $202.5 \times 1.15 = 232.38$ square feet. The following culvert dimensions are considered:

$$15.0 \times 15.0 \text{ feet} = 225 \text{ square feet}$$
$$16.0 \times 14.0 \text{ feet} = 224 \text{ square feet}$$
$$16.0 \times 15.0 \text{ feet} = 240 \text{ square feet}$$
$$15.5 \times 15.0 \text{ feet} = 232.5 \text{ square feet}$$

Since the last of the above sizes, 15.5 by 15.0 feet, gives an area very close to the above size of 232.88 square feet, this size will be adopted for further study.

Intake loss

210. Consider a single rectangular bell mouth type intake for each culvert. Design calculations are presented later. For head loss determination, the loss coefficient is

$$k_i = 0.07$$

$$H_{L_i} = 0.07 \, V_c^2/2g$$

Manifold loss

211. Originally 18 ports were selected that had a total throat area of 187.45 square feet (18 × 10.414 feet). This area, with the original culvert, 15.0 × 13.5 feet, gave $A_p/A_c = 0.93$. However, since the culvert was made larger, because of the length to the intakes, the A_p/A_c ratio with the larger culverts will be only (187.45/232.5) = 0.81. This value is low and would not be an efficient design. In order to partially compensate for this change, another port will be added to each culvert manifold. The A_p/A_c ratio then becomes $197.87/232.5 = 0.851$. From Figure 48 for an A_p/A_c ratio of 0.851, the manifold loss coefficient $k_{m_f} = 1.26$. Adding another port to the manifold will decrease the culvert lengths for resistance determination, but will not change the lengths for inertia head. With 19 ports, the changed lengths are:

	Right Culvert Length Feet	Left Culvert Length Feet
Length intake to first port (Minus valve well length)	1,036	1,085
Average length to first port 1,060.5 feet		
Length for inertia head	1,295	1,330
Average length for for inertia head 1,312.5 feet		

Resistance loss

212. Using $f = 0.009$ and $L = 1{,}060.5$ feet as follows:

$$D_h = 4R \quad \text{where} \quad R = \frac{232.5}{2(15.5 + 15)} = 3.81$$

$$D_h = 15.25$$

$$k_r = \frac{0.009 \times 1{,}060.5}{15.25} = \underline{0.63}$$

Bend loss

213. From Figure 9.7 in Appendix B, for a 90-degree bend:

$$k_b^* = 0.14 \quad \text{for} \quad r/w = 2.5$$

then $$r = 2.5 \times 15.00 = 37.50 \text{ feet.}$$

To calculate Reynolds number, R_e :

$$Q_{ave} = \frac{110 \times 870 \times 27.5}{60 \times 7.1} = 6{,}178 \text{ cfs}$$

$$v_c = \frac{6{,}178}{2 \times 232.5} = 13.286 \text{ feet per second}$$

$$R_e = \frac{13.286 \times 15.25}{0.0000121} = 16{,}744{,}282$$

where kinematic viscosity = 0.0000121 ft^2/sec . From Figure 9.3 in Appendix B, for r/D_h greater than 2, $C_{R_e} = 0.70$. Refer to paragraph 9.2.4, Appendix B, and to Colebrook-White diagram on Hydraulic Design, Chart 224-1 (Reference 14).

For $R_e = 16,744,282$, f value on "smooth curve" = 0.0075.

$$C_f = \frac{0.009}{0.0075} = 1.20$$

Refer to Figure 9.4 in Appendix B, outlet pipe length correction using outlet length = 145 feet (average length bend to valve).

$$145/15.25 = 9.51$$

From Figure 9.4 in Appendix B, $C_o = 0.70$.

Then $k_b = k_b^* \times C_o \times C_{R_e} \times C_f$

$$k_b = 0.14 \times 0.7 \times 0.7 \times 1.2 = \underline{0.082}$$

The vertical bends in the culverts will be so flat that losses would be negligible. This will be shown in design of the intake later.

214. Horizontal bends in the intake culverts, as shown in Figure 71, are approximately 12-degree bends. It is considered that they could be reduced or possibly eliminated. For these reasons no loss will be included for them.

Bulkhead slot loss

215. Use $k_s = 0.02$, as discussed previously in paragraph 135.

Valve loss (valve open)

216. Use $k_v = 0.05$, as discussed previously in paragraph 135.

Total losses

217. Coefficient values are listed and totaled in the following tabulation:

Culvert Section	Symbol	Value
Intake	k_i	0.070
Resistance	k_r	0.630
90-degree bend	k_b	0.082
Bulkhead slot	k_s	0.020
Valve	k_v	0.050
Bulkhead slot	k_s	0.020
Manifold	k_{m_f}	1.260
Total	k_c	= 2.132

Discharge coefficient

218. The discharge coefficient corresponding to k_c is

$$C''_f = \sqrt{1/k} = \sqrt{1/2.132} = 0.685$$

Then the lock coefficient C''_{L_f} is obtained from Figure 43. For $C''_f = 0.685$, $C''_{L_f} = 0.670$.

Overfill

219. Overfill can be estimated by using Figure 31, overfill (model values) versus j factor. The j factor versus overfill is an empirical relationship that utilizes culvert length, area, and the area of the lock water surface:

$$j = \frac{L \times 2A_c}{A_s} \tag{14}$$

Using the values of

$L = 1{,}312.5$ feet

$A_c = 232.5$ square feet

$A_s = 95{,}700$ square feet (870 × 110 feet)

then

$$j = \frac{1{,}312.5 \times 2 \times 232.5}{95{,}700} = 6.377$$

From Figure 31, $d_f = 1.4$ feet (model value). The value of the overfill for

the prototype lock, d''_f, is obtained from Figure 32, d_f versus d''_f, so that $d''_f = 2.9$ feet.

Check on culvert area

220. With prototype values of $C''_{L_f} = 0.67$, $d''_f = 2.9$ feet, $T''_f = 7.1$ minutes, and with a t''_v value of 4 minutes and a U value of 0.54, the value of A''_c of 232.5 square feet can be checked:

$$A''_c = \frac{2 \times 95{,}700\left(\sqrt{27.5 + 2.9} - \sqrt{2.9}\right)}{2 \times \sqrt{2g} \times 0.67\ (426 - 0.54 \times 240)} = 228.994$$

Since the 228.99-square-foot value is less than the trial value of 232.5 square feet, the trial value is satisfactory. The culvert might be reduced from 15.5 by 15.0 feet to a smaller size, but it is considered desirable to hold the 232.5-square-foot area. Other head losses may develop in final design.

221. Checking the operation time T''_f (with the 232.5-square-foot culvert)

$$T''_f = \frac{2 \times 95{,}700\left(\sqrt{27.5 + 2.9} - \sqrt{2.9}\right)}{2 \times 232.5 \times 0.67 \times 8.02} + 0.54 \times 240 = 421.580 \text{ seconds}$$
$$= \underline{7.026 \text{ minutes}}$$

Calculation of Lock Filling Curve

222. The procedures to be used in calculating a lock filling curve were described in detail in Part VII. Valve loss coefficients must be determined before the filling curve computation can be started. For this example, valve motion will be patterned after the Arkansas low-lift locks. Since the Arkansas lock valves are 12.0 by 12.0 feet and the valves for this design example are 15.5 by 15.0 feet, the Arkansas valve opening curve cannot be used directly. Development of a curve of opening versus time for the larger valve is given in Tables 5 and 6. Figure 73 is the valve opening curve of Table 6. Valve loss coefficient for the 15.5- by 15-foot valve were read from Figure 54 for values of b/B (from Table 6) at 10-second intervals and are shown on Table 7. These values have been entered in Table 8 to calculate the lock filling curve. The calculations for the filling curve proceed across Table 8, one column at a time. Each line begins with an assumed value Δz and

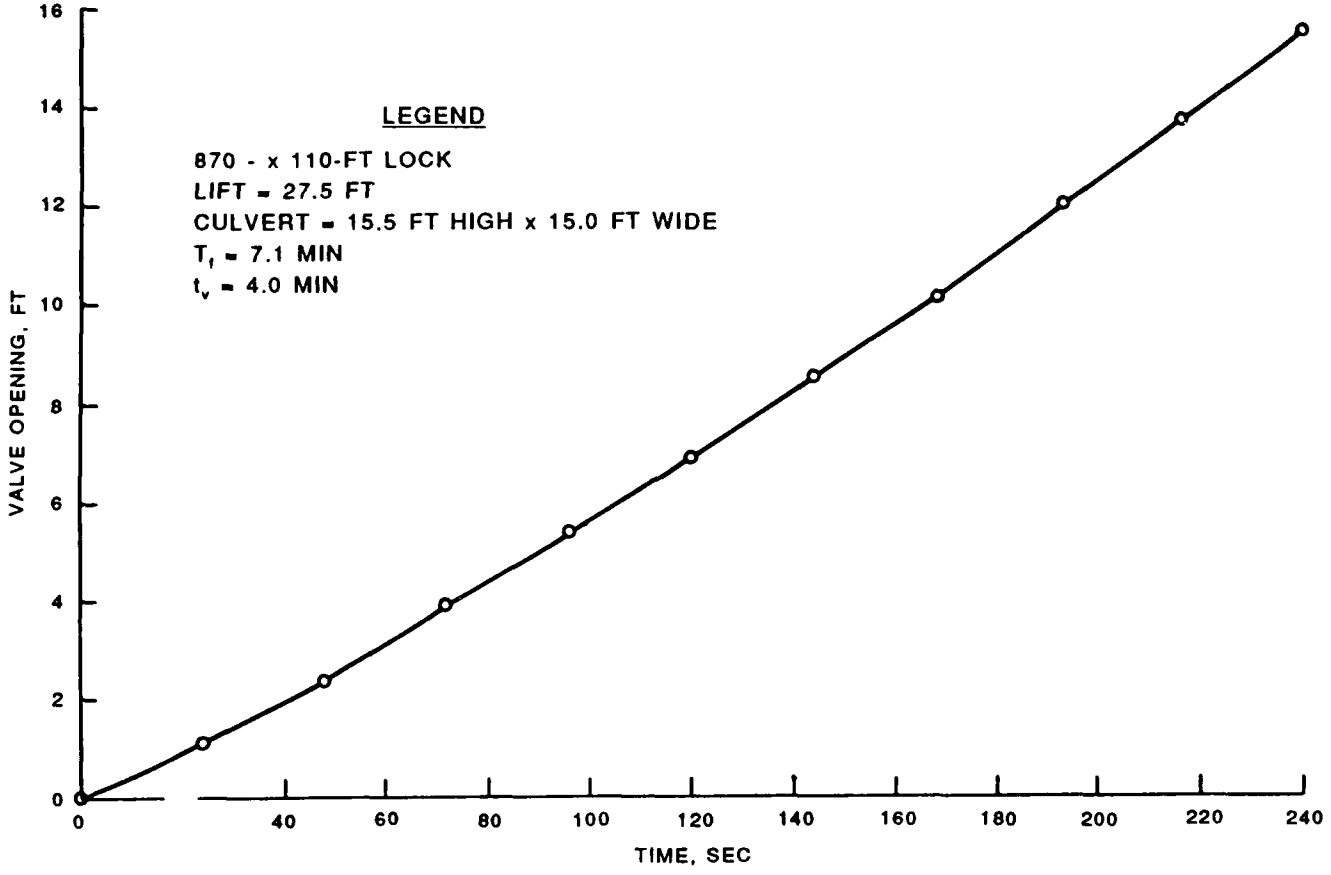

Figure 73. Design of Wallport Lock, valve schedule developed from Arkansas Lock in Reference 6 (see Table 5)

proceeds to calculate a value of V_{c_n} by two methods as explained in Part VII. It is usually necessary to make several trial calculations with different assumed values of Δz before the two values of velocity, V_{c_n} and V_{c_n}, are in close agreement. Curves of water-surface elevation, discharge into the lock chamber, inertia head, and valve opening versus time are shown in Figure 74.

Intake Design

223. In the foregoing studies, the submergence of the lock floor (depth below lower pool) was determined to be 25 feet. With a lower pool elevation of 510.5 feet,* the lock floor would be at el 485.5. The floor of the culverts will be placed very near to the elevation of the lock floor. The thalweg of the riverbed opposite the intake entrance is at or below el 500.0. The intake for each culvert will consist of a single flared opening with an area at the face of the structure 2.15 times the area of the culvert (2.15 × 232.5 square feet = 499.88 square feet). The entrance area can be approximated very closely by an opening 22.0 feet high by 23 feet wide which has an area of 506.00 square feet. A transition section 65 feet in length is provided to reduce the area at the entrance to the dimension of the culvert (15.5 by 15.0 feet). The maximum discharge into each culvert entrance (assuming an even distribution of flow between the culverts) would occur 210 seconds from beginning of valve opening and would be 9,924/2 cfs. The maximum average velocity would be

$$4{,}962/506 = 9.81 \text{ fps}$$

Assuming that the maximum velocity is 10 percent greater than the average, the maximum velocity would be

$$1.10 \times 9.81 = 10.79 \text{ fps}$$

and $$V^2/2g = \frac{10.79^2}{64.4} = 1.81 \text{ feet}$$

* All elevations (el) cited herein are in feet referred to the National Geodetic Vertical Datum (NGVD).

The lip along the bottom entrance will be at el 505.0 and with an entrance height of 22.0 feet, the entrance opening will be at el 527.0. This elevation provides a submergence below the upper pool level of 11.0 feet (538.0 - 527.0 = 11 feet). Since the velocity head is only 1.81 feet, there should be no problem with vortices. The floor of the intake transition and culvert would have a downward slope of 1 percent for 500 feet. Over the next 100 feet (approximately) the culvert floor would drop from el 500.0 to el 487.5. From that point the culvert would drop to el 486.5 at the bulkhead slot located 30 feet upstream from the valve (a length of about 110 feet).

224. The value of the loss coefficient of 0.07 that was shown earlier is appropriate for this type intake as is shown by Figure 47.

Outlet Design

225. On the emptying cycle, the ports of the manifold serve as an intake, and since their number, arrangement, and size are governed almost entirely by the filling requirements, the manifolds will be used without change as intakes for emptying. The emptying time must be determined, and the general layout and arrangement of the culverts leading from the manifold to the outlet must be developed. Figure 72 shows a layout where the outlets discharge into the river channel riverward from the lower lock approach. This layout avoids creating turbulence and adverse currents in the lower approach, but (depending on river flow conditions) may create a situation where the lock cannot be completely emptied. The water level immediately downstream from the downstream miter gates will normally be the same as the level at the downstream end of the lower riverward guidewall. In this example the outlet will terminate in a stilling basin structure about 800 feet upstream from the downstream end of the lower guidewall. Thus, when high river flow conditions occur, the water surface slope (in the river) between the outlet structure and the downstream end of the lower guidewall may be significant. The water level in the lock chamber will be approximately the same as it is at the outlet structure, and since it will be higher than the level on the downstream side of the lower miter gates, it may become difficult to open the miter gates against this head. With reference to Figure 72, equalizing valves (slide valves) will be provided as shown. Then, at the end of the emptying operation, if the level in the chamber is higher than the water level downstream

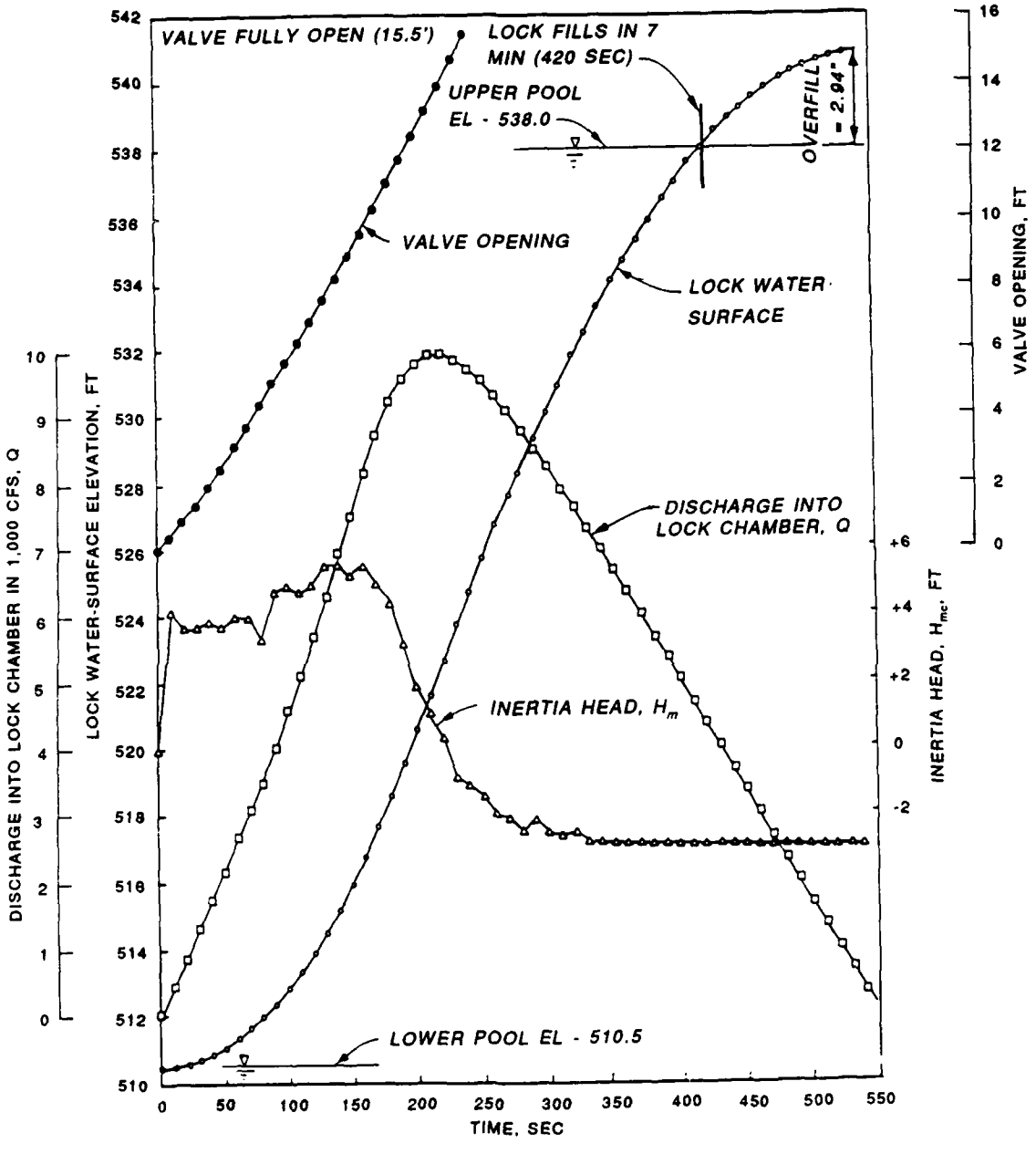

Figure 74. Design of side port lock, lock filling curves

from the miter gates, the main culvert emptying valves will be closed and the equalizing valves will be opened to permit complete emptying of the lock. Such an operation can be set up to function automatically when it is needed.

Head losses

226. The head loss coefficients for the emptying system include:

k_{m_e}	1.310
k''_r	0.443
k''_s	0.020
k''_{vw}	0.050
k''_s	0.020
k''_b	0.082
k''_{o_e}	1.000
k''_e	2.925

227. The value of k_{m_e} is obtained from Figure 51, using the ratio of A_p/A_c of 0.85 that was established in design of the manifold. Figure 51 is based on model data, and it is recognized that prototype values would probably be different. However, no prototype data are available, and it is believed that use of the model curve will not introduce really serious error. The average length of the culverts from the last port to the outlet is 750 feet, and with $f'' = 0.009$ and $D_h = 15.25$,

$$k''_r = \frac{750 \times 0.009}{15.25} = 0.443$$

The values of k''_s , k''_v , and k''_b determined earlier in this example are applicable for the outlet. There is not sufficient data available at this time to establish a curve relating outlet loss k''_{o_c} to other parameters. Values of k''_{o_e} developed in this study ranged from 0.60 to 1.19 depending on the arrangement and design used. By gradually expanding the culvert leading to the outlet structure, k''_{o_e} values can be significantly reduced. A value of $k''_{o_e} = 1.00$ has been adopted for this design because it is representative of values for this type of outlet and because a gradual expansion of the

culverts over an appreciable length may be undesirable from the standpoint of structural requirements. Expansion of the outlet culverts by flaring the sidewalls outward on a 1 on 7 or 8 flare angle is satisfactory. The distance over which the flare is to extend depends on the increase in culvert area considered desirable. In the Cannelton model tests each culvert was expanded symmetrically from a width of 16 feet to a width of 22 feet in a horizontal length of 31.0 feet. This gives an area ratio of $396/288 = 1.38$.

228. Using the total head loss coefficient $k''_e = 2.925$, the discharge coefficient C''_e is computed from Equation 30.

$$C''_e = \frac{1}{\sqrt{2.925}}$$

From Figure 45, with $C''_e = 0.585$, $C''_{L_e} = 0.550$.

Underfill

229. Using Equation 14, $j = \frac{2A_c L}{A_s}$, with a culvert length (from the midpoint of the manifold to outlet) of 1,002 feet, the value of j is

$$j = \frac{2 \times 232.5 \times 1{,}002}{870 \times 110} = 4.869$$

From Figure 31, $d_e = 1.23$ feet and from Figure 32, $d''_e = 2.40$.

Emptying time

230. The data on head loss, underfill, valve time, valve time coefficient, and culvert area may be used with Equation 9a to compute the emptying time:

$t''_v = 240$

$U = 0.58$

$C''_{L_e} = 0.55$

$d''_e = 2.40$ feet

$A_c = 232.5$ square feet

$A_s = 95{,}700$ square feet

$H = 27.5$ feet

$$T''_e = \frac{2 \times 95{,}700 \left(\sqrt{27.5 + 2.40} - \sqrt{2.40} \right)}{0.55 \times \sqrt{2g} \times 232.5 \times 2} + 0.58 \times 240 = 504.89 \text{ seconds}$$

$$= 8.4 \text{ minutes}$$

From Figure 40, for $T''_e = 8.4$ minutes, $T_e = 9.8$ minutes (model) . This value of emptying time, T_e , will meet requirements for minimum permissible emptying time for a 1,270-foot lock (27.5-foot lift and 25-foot submergence) as shown by Plates 28 and 36 of Reference 7. The type of outlet to be used in this example is similar to Cannelton's outlet, and since the emptying requirements are more severe for a 1,270-foot lock than for an 870-foot structure, model emptying time, T_e , of 9.8 minutes is considered a safe value. Even though the prototype emptying time, T''_e , will be only 8.4 minutes, experience has shown that when model values meet hawser stress criteria, the prototype lock performance will be satisfactory.

Pressure Downstream from Valves

231. Pressure downstream from the filling valves is calculated by Equation 46:

$$Z_{vc} = Z_u - \frac{k_{uv} V_c^2}{2g} - \frac{V_{vc}^2}{2g} \pm H_{m_{uv}} + \Psi \left(\frac{V_c^2}{2g} - \frac{V_{ec}^2}{2g} \right) \qquad (46)$$

In this example, the following values which were developed earlier are applicable:

$Z_u = 538.0$ feet
$L'_{uv} = 760.0$ feet
$D_h = 15.25$ feet
$\Psi = 0$
$f = 0.009$

$k_i = 0.070$
$k_s = 0.020$
$k_{vw} = 0.050$
$k_b = 0.082$
$\frac{k_r}{k_{uv}} = \frac{0.449}{0.671} \cdot = \left(\frac{760 \times 0.009}{15.25} \right)$

232. From several trial computations, the critical low pressure will occur when $b/B = 0.571$ at $t = 150$ seconds . At this time,

$C_c = 0.73$ — Figure 58

$H_m = 5.18$ feet — Table 8, column 13

$H_{m_{uv}} = 3.02$ feet — $(L'_{uv}/L') \times H_m = (760/1{,}305) \times 5.18$

$V_c = 16.16$ fps — Table 8, column 10

$V_c^2/2g = 4.06$ feet

$V_{vc} = 38.77$ fps — $V_{vc} = \frac{V_c B}{C_c b} = 16.16/0.571 \times 0.73$

$V_{vc}^2/2g = 23.34$ feet

$Z_{vc} = 538.00 - 0.67 \times 4.06 - 23.34 - 3.02 = 508.92$

Pressure on culvert roof = 508.92 - 502.00 = 6.92 feet

233. This computed amount of positive pressure is considered satisfactory, but it must be recognized that instantaneous high and low pressures can be several feet greater or lower than an average value. The cavitation index, σ, which is defined by:

$$\sigma = \frac{P + (P_a - P_v)}{V^2/2g} \tag{53}$$

will be computed to determine if low pressures might cause cavitation problems. In Equation 53:

P = gauge pressure over vena contracta

P_a = atmospheric pressure

P_v = vapor pressure of water

V = mean velocity (for vena contracta V_{vc})

A value of 33 feet is a reasonably accurate value of $(P_a - P_v)$ will be used here. To be absolutely certain that cavitation will not develop, the value of σ should not be very much less than 1.00. Utilizing the data developed earlier,

$b/B = 0.571$ where $B = 15.25$ feet and $b = 8.85$ feet

$C_c = 0.73$

$D_1 = 8.85 \times 0.73 = 6.46$ feet (depth at vena contracta)

$V_{vc} = 38.77$ fps

$V_{vc}^2/2g = 23.34$ feet

$$P = 6.92 + 15.5 - 6.46 = 15.96 \text{ feet}$$

$$\sigma = \frac{15.96 + 33.00}{23.34} = 2.10$$

Since the value of σ is over two times the value considered absolutely safe, there is no need to lower the culvert or to provide air vents. However, it is recommended that the bulkhead slots downstream from the filling valves be closed approximately 3 to 4 feet above the top of the culvert.

PART XI: DESIGN OF BOTTOM LONGITUDINAL FILLING AND EMPTYING SYSTEM

234. An example of the design procedures that are necessary to develop a filling system for a high-lift lock is presented in the following paragraphs. This design will be similar to, but not exactly the same as, the design used on the Lower Granite Lock. Full use is made of data from model tests on Millers Ferry, Lower Granite, Bankhead, and Bay Springs Locks. Prototype tests on Lower Granite, Bankhead, and McNary locks have also been used.

Location and Basic Conditions

235. In this example the lock is located in a dam that forms a deep reservoir. The upper miter gate pintles are located on the axis of the dam in deep water near the bluff side of the reservoir. Deep water exists on both sides of the lock chamber in the upper and lower pools. Figure 75 shows the general arrangement and locations of the lock. Pertinent dimensions are as follows:

Size	
Length (pintle to pintle)	670.0 feet
Width (clear width)	110.0 feet
Pool elevations	
Upper pool	424.00
Lower pool	330.00
Maximum lift	94.00 feet
Lower sill elevation	312.00
Upper sill elevation	400.00
Top of lock wall	432.00

236. Since the upstream end of the lock is situated in deep water, the intakes for the wall culverts will be placed in the back side (not entrance side) of the lock walls, upstream from the gate blocks. This arrangement will prevent occurrence of adverse currents in the lock entrance.

237. The discharge outlet is located on the riverward side of the downstream gate block. Floating guidewalls will be provided at the upstream end of the lock.

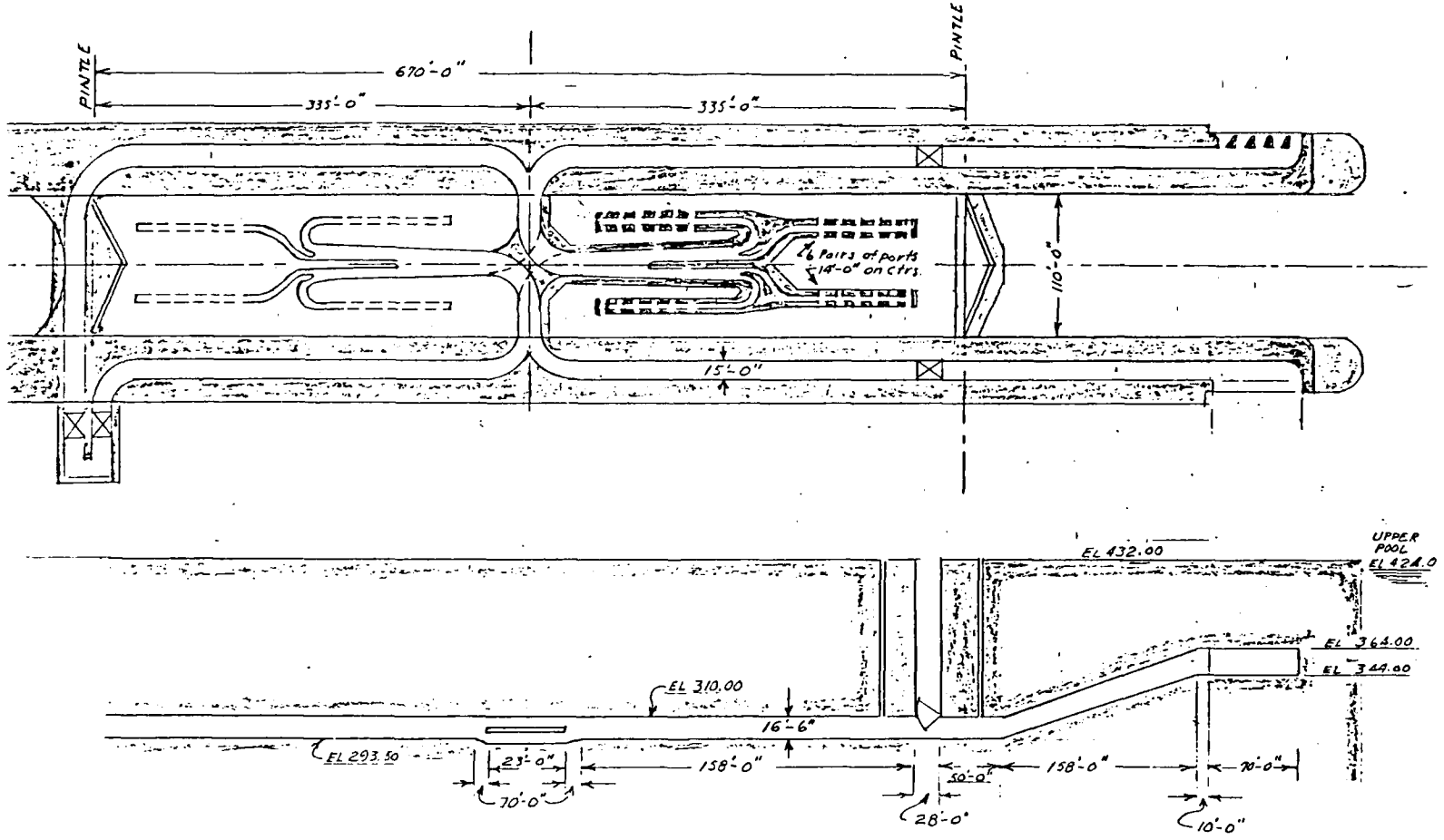

Figure 75. Design of bottom longitudinal filling and emptying system, sectional plan and elevation

Preliminary Considerations

238. The size of the main culverts must be established as a first step in design of the filling system. Equation 9c can be used as shown:

$$2A_c = \frac{2A_s(\sqrt{H + d_f} - \sqrt{d_f})}{C_{L_f}\sqrt{2g}\ (T_f - Ut_{v_f})} \qquad (9c)$$

but the five variables, C_{L_f}, T_f, t_{v_f}, U, and d_f must be evaluated or estimated before the a value of A_c can be determined.

239. A preliminary estimate of filling time can be obtained by use of Figure 39. In this example:

a. Lock volume is 670 × 110 × 94 feet = 6,927,800 cubic feet

b. From Figure 39, average discharge Q = 11,500 cfs

c. Average discharge per culvert q_c = 5,750 cfs

d. Filling time (model value) T_f = 6,977,800/11,500 = 10.04 minutes or 602.4 seconds

e. From Figure 40, prototype filling time T_f'' = 8.6 minutes or 516 seconds

240. In Table 2, values of C_f and C_f'' for Lower Granite Lock computed by three different methods are presented for comparison. These values are as follows:

Prototype	Model	Source
0.621	0.539	From summation of loss coefficients
0.633	0.534	From Equation 8b
0.645	0.535	From Test 10 studies, using computed q_c values and Equation 30.

For this study, the value of C_f = 0.534 will be used, and from Figure 42, a value of C_{L_f} = 0.520 is obtained.

241. Based on performance of Lower Granite, Bay Springs, and Bankhead Locks, a filling valve time of 1.00 minute will be satisfactory.

242. From Table 1, a value of the valve time coefficient, U, of 0.58 is selected.

243. Equation 14 and Figures 31 and 32 can be utilized to obtain a

value of d_f'' when preliminary estimate of the "equivalent length" of a uniform culvert and a trial value of culvert area are computed. In Table C-6 (Appendix C) the total length of culvert from intake to midpoint of a manifold culvert for Lower Granite Lock is given as 889 feet. The equivalent length of uniform culvert, L', with the same cross section as the cross section at the valve, is calculated by Equation 11a to be only 627 feet. The equivalent length of 627 feet is only 0.71 of the 889 foot total culvert length. The Lower Granite culverts have widely varying cross sections, and the cross sectional areas upstream and downstream from the valve are much greater than the area at the valve.

244. In the present design problem the culverts will be made more nearly uniform in cross section, with the section at the valve being relatively larger in comparison with the Lower Granite design. With a more uniform cross section the ratio of L'/L would be larger--falling between 1.00 and the 0.71 value of Lower Granite. As a first trial, a value of 0.90 is used along with the total length of 877 feet obtained from Figure 75. The trial value of L' then becomes

$$L' = 877 \times 0.9 = 789.3 \text{ feet}$$

This value will be used later to determine d_f''.

245. Estimating a value of d_f'' for use in Equation (9c) requires the use of an assumed trial value of A_c to calculate a value of j in Equation 14. At this stage of the study, values of t_v and U have been established and preliminary values of C_{L_f} and T_f have been estimated. In Equation 9c, the only remaining variable needed to calculate a trial value of A_c is the overfill, d_f. Of the five variables of Equation 9c, the one that has the least effect is d_f. Therefore, a value of d_f will be assumed based on the model value of Lower Granite Lock. The model value of d_f for Lower Granite Lock is 1.4 feet. However, since the equivalent culvert length, L', of Lower Granite Lock is greater than the design example, a value of 1.3 feet will be tentatively assumed for this example. The trial value of A_c, using model data, is

$$2A_c = \frac{2 \times 73{,}700 \left(\sqrt{94 + 1.3} - \sqrt{1.3}\right)}{0.52 \times 8.02 \left(602.4 - 0.58 \times 60\right)} = 537.27 \text{ square feet}$$

Then, using this value of $2A_c$ in Equation 14,

$$j = \frac{537.27 \times 789.3}{73,700} = 5.75$$

and from Figure 31, $d_f = 1.3$ feet. Since this d_f value is the same as the assumed value, it will be used in Figure 32 to obtain a prototype value of d''_f of 2.65 feet.

Culvert Area at Valve

246. A tentative value of the culvert area at the valve, based on prototype data, can be calculated with the values of the following five variables using Equation 9c.

$T''_f = 516.00$ second

$d''_f = 2.65$ feet

$C''_{L_f} = 0.62$ (from Figure 43, with $C''_f = 0.633$)

$U'' = 0.58$

$t''_{v_f} = 60.00$ seconds

$$2A_c = \frac{2 \times 73,700\ (\sqrt{94.00 + 2.65} - \sqrt{2.65})}{0.62 \times 8.02\ (516.0 - 0.58 \times 60)} = 505.34 \text{ square feet}$$

$A_c = 252.67$ square feet

247. This value of A_c appears to be a reasonable value and will be adopted for further consideration. Culvert dimensions that give areas close to the 252.67 square feet are listed in the following tabulation:

Height feet	Width feet	Area feet
16.00	16.00	256.00
16.50	15.00	247.50
17.00	14.50	246.50

The 16.50- by 15.00-foot size gives an area slightly less than the calculated value of 252.67, but the calculated value is probably conservative and therefore the size of 16.50 by 15.00 feet is adopted for further detailed consideration.

Other Components of Culvert System

Intake

248. In order to reduce intake loss, the combined area of the throats of all of the ports should be from 1.5 to 2.0 times the culvert area. In this example, where there is a depth in excess of 100 feet at the upper end of the lock, a less costly and more efficient intake can be developed with a small number of high intake ports than with a greater number of lower ports. Accordingly, the intake will have five ports, 20.00 feet high with a combined throat area of 410.00 square feet. The ports at the wall face will be 8.00 feet wide by 20.00 feet high and will have a combined area of 800.00 square feet. The area ratios are as follows:

$$A_i/A_c = 410.00/247.5 = 1.657$$

$$A_w/A_c = 800.00/247.5 = 3.23$$

From Figure 47, the head loss coefficient k_i'' is 0.140. The top of the intake ports will be at elevation 364.00 which is 60.00 feet below the upper pool level. Shape of the ports and dividers between ports will be developed by procedures in Part VIII.

Culvert from intake to valve

249. Figure 75 shows a sectional plan and profile of a tentative layout of the culvert system. The culvert cross section is reduced from a height of 20.00 feet to 16.50 feet in a downward sloping section that begins the downward slope at a miter bend 10.00 feet downstream from the edge of the intake. The downward sloping transition section ends at a miter bend 150 feet (horizontal distance) from the upper miter bend. The top of the culvert at the lower miter bend is at elevation 310.00--a fall of 54 feet in the 150-foot horizontal length. This results in two miter bends with deflection angles of about 19.55 degrees.

Culvert from valve to end of manifold culverts

250. Culvert dimensions of 16.50 by 15.00 feet are maintained from the valve downstream to a point 10.00 feet upstream from the beginning of the horizontal divider at the curving section where the culvert enters the lock

chamber. As is indicated in Figure 75, in a 10-foot transition section the culvert floor is lowered 2.00 feet so that at the beginning of the horizontal divider two 8.25- by 15-foot passages are provided that have the same net area (247.50 square feet) as the single passage upstream from the divider. The arrangement is exactly the same from the upstream edge of the divider on to the end of the manifold culverts as the system developed for Lower Granite Lock. Table 9 shows the lengths and dimensions of each section of the culvert. Table 10 contains the calculations for equivalent culvert lengths that are required to determine inertia head.

251. Half of the flow from each of the two wall culverts discharge into four manifold culverts in each half of the lock. Data on the manifolds are listed as follows:

Manifold culvert dimensions	12.00 feet high ×	5.00 feet wide
Area of each manifold		= 60.00 square feet
Area of four manifolds		= 240.00 square feet
Number of ports per manifold		= 12
Dimensions of ports	3.58 feet high ×	1.25 feet wide
Area of each port		= 4.48 square feet
Area of ports per each half of lock		= 214.80 square feet
Port to manifold culvert ratio $\frac{214.80}{240.00}$		= 0.90

Estimates of Head Losses

252. Head losses for the system consist of loss at intake, miter bends, bulkhead slots, valve well, 180- and 90-degree bends at midpoint of lock, bends at the manifold branches, resistance loss, and exit loss from manifold to lock chamber. No attempts have been made to analyze or determine specific losses in the culvert transition sections. An intake loss coefficient of 0.140 has already been determined from the A_i/A_c ratio with Figure 47.

253. Loss coefficients for the two 19.55-degree miter bends are determined as follows:

From Figure 9.9 in Appendix B:

$$k_b^* = 0.055$$

Ave q_c = 5,750.00 cfs

V_c = 5,750.00/247.5 = 23.232 fps

R = 247.5/2 (15 + 16.5) = 3.93 feet

D_h = 4 × 3.93 = 15.71 feet

ν = 0.0000121 ft^2/sec

$$R_e = \frac{23.23 \times 15.71}{0.0000121} = 30,168,831$$

From Figure 9.3 in Appendix B:

C_{R_e} = 1.00

$$C_f = \frac{0.009}{0.007} = 1.286$$

f = 0.009 as compared to smooth curve f = 0.007

From Figure 9.4 in Appendix B:

C_o = 0.70

From Figure 10.2 in Appendix B:

C_{b-b} = 1.00

$k_{b_1} = 0.055 \times 1.00 \times 1.286 \times 0.70 \times 1.00 = 0.0495$

$k_{b_2} = k_{b_1} = 0.0495$

254. Loss for circular bends at midpoint of lock are determined with same general procedure as is used above, and as outlined in Appendix B. Computations made for Lower Granite Lock that gave an average of 0.182 for that portion of the culvert that turns through 180 degrees and the part that turns through two 60-degree reverse bends will be used in this example.

255. Loss for resistance is calculated by

$$k_r = \frac{f \times L}{D_h}$$

$f = 0.009$

$L = 877.00$ feet

$D_h = 15.71$ feet

$$k_r = \frac{0.009 \times 877.0}{15.71} = 0.502$$

The value of D_h of 15.71 is based on the assumption that the culvert has uniform dimensions throughout its entire length, which is not strictly true. In a more detailed analysis, the resistance coefficient would be determined for each section of the culvert system and head loss for the average culvert discharge would be computed. The summation of all of the head losses, Σh_L, could then be divided by $V_c^2/2g$ to obtain an average overall resistance loss coefficient. Preliminary computations have indicated that where wide variations in culvert dimensions do not occur, determination of a single value of k_r using a representative cross section as an average does not introduce serious error.

256. The bends from the central culverts into the manifold culverts are so nearly identical to the Lower Granite system that it is considered satisfactory to use the value of k_b that has been computed earlier in studies for this report. This value is: $k_b = 0.120$.

257. In the section, "Other Components of Culvert System," the port area to manifold area ratio was established as 0.90, which is approximately the same as the A_p/A_m ratio of Lower Granite Lock. From Figure 49, the manifold head loss coefficient, k_{m-m}, is shown to be 1.37 in terms of the velocity head in the manifold culverts. Since the total manifold culvert area (for one wall culvert) is less than the wall culvert area at the reference section, the loss coefficient of 1.37 must be converted to the reference section by Equation 37.

$$k_{m_c} = \left(\frac{A_c}{A_m}\right)^2 \times k_{m-m} \qquad (37)$$

In this case, k_{m_c} is the head loss coefficient for the reference section and k_{m-m} is the loss coefficient based on manifold area. Then

$$k_{m_c} = \left(\frac{247.5}{240}\right)^2 \times 1.37 = 1.457$$

258. The total head loss for the system, k_f, is tabulated as follows:

Value	Culvert Section
0.140	Intake
0.050	Miter bend
0.050	Miter bend
0.020	Bulkhead slot
0.050	Valve well (valve open)
0.020	Bulkhead slot
0.182	Bend at midpoint of lock
0.120	Bend at manifold
0.502	Resistance in culvert
1.457	Manifold (in terms of culvert V_c)
k_f = 2.591	(Loss for system with valves open)
C_f'' = 0.621	

In the section, "Preliminary Considerations," values of prototype and model discharge coefficients C_f'' from Table 2 for Lower Granite Lock were compared and respective values of 0.633 and 0.534 were adopted for further study. Use of these values resulted in a computed culvert size of 16.50 by 15.00 feet, which was tentatively selected to continue the design study. Since the computed value of C_f'' of 0.621 (corresponding to a k_f of 2.591) is very close to the 0.633 C_f'' value from the same section, it is concluded that the culvert size of 16.50 by 15.00 feet with an area of 247.50 square feet will be satisfactory.

Conclusion of Bottom Longitudinal Design

259. The intake has been designed, the arrangement and size of the culvert system established, and head losses estimated. There remain development of a valve opening curve, calculation of a filling curve, and determination of pressures downstream from the valves, which will affect the final design elevation of culverts. Calculation of a valve curve and a filling curve will follow identical procedures explained in Part X for the wall culvert side port system and Appendix C. Since two examples of these calculations have already been presented, it is not necessary to repeat the calculations again.

260. Pressure downstream from the valve can be calculated with Equation 46. The cavitation index σ can be determined by

$$\sigma = \frac{P - 33}{V_{v_c}^2 / 2g} \tag{53}$$

To calculate pressure downstream from the valve and the corresponding cavitation index number requires values of culvert discharge. Since the discharge at any instant can only be determined from a lock filling curve, actual computation of pressure and cavitation number will not be presented in this example. All procedures involved have already been explained and demonstrated. It must be noted, however, that the final selection of the elevation of the culvert at the valve will depend on the determination of pressures and cavitation number, and cannot be "assumed." In this example, an elevation for the culvert roof of 310.00 was tentatively adopted in order to proceed with the example. With the lower pool at el 330.00, a submergence of 20.00 feet is provided. Since a negative pressure of at least 5.0 feet is desirable, the culvert may have to be raised by 5.0 feet or perhaps more. In any high-lift lock, the bulkhead slots downstream from the filling valves should be sealed, and adjustable opening air vents should be provided, similar to the arrangement at Lower Granite Lock. Admission of enough air through the vents to eliminate or cushion cavitation can then be accomplished when the lock is placed in operation.

REFERENCES

1. Kooman, C. 1973. Navigation Locks for Push Tows, RIJKSWATERSTAAT Communications No. 16, Government Publishing Office, The Hague, The Netherlands.

2. US Army Coastal Engineering Research Center. 1977. Shore Protection Manual, Fort Belvior, VA.

3. Miller, D. S. Internal Flow Systems (290 pp, 352 graphs and figures, 21 tables), Price $69.00, available from British Hydromechanics Research Association, BHRA Fluid Engineering, Cranfield, Bedford MK43 OAJ, England.

4. Dodge, Russel A., and Thompson, Milton J. 1937. Fluid Mechanics, McGraw-Hill, New York.

5. Pillsbury, G. B. 1915. "Excess Head in the Operation of Large Locks Through the Momentum of the Water in the Culverts," US Army Corps of Engineers Professional Memoirs, Vol 7, No. 31, pp 206-212.

6. Ables, J. H., Jr., and Boyd, M. B. 1966 (Nov). "Filling and Emptying Systems, Low-Lift Locks, Arkansas River Project; Hydraulic Model Investigation," Technical Report No. 2-743, US Army Engineer Waterways Experiment Station, Vicksburg, MS.

7. _____. 1966 (Feb). "Filling and Emptying Systems, Cannelton Main Lock, Ohio River, and Generalized Tests of Sidewall Port Systems for 110- by 1200-ft Locks; Hydraulic Model Investigation," Technical Report No. 2-713, US Army Engineer Waterways Experiment Station, Vicksburg, MS.

8. Oswalt, N. R., Ables, J. H., Jr., Boyd, M. B., and Murphy, T. E. 1965 (Jun). "Filling and Emptying System, Jonesville Lock, Ouachita-Black Rivers, Louisiana; Hydraulic Model Investigation," Technical Report No. 2-678, US Army Engineer Waterways Experiment Station, Vicksburg, MS.

9. O'Brien, Morrough P., and Hickox, George H. 1937. Applied Fluid Mechanics, McGraw-Hill, New York.

10. US Army Engineer Waterways Experiment Station. 1960 (Jun). "Hydraulic Prototype Tests of Tainter Valve, McNary Lock, Columbia River, Washington," Technical Report No. 2-552, Vicksburg, MS.

11. St. Anthony Falls Hydraulic Laboratory. 1964 (Dec). "Filling and Emptying Systems for St. Anthony Falls Locks, Mississippi River, Minnesota; Hydraulic Model Investigation," Hydraulic Laboratory Report No. 76, St. Paul, MN; University of Minnesota, Minneapolis, MN; performed for the US Army Engineer District, St. Paul, St. Paul, MN.

12. Neilson, Frank M. 1975 (Jun). "Barkley Lock Prototype Tests, Cumberland River, Kentucky," Technical Report H-75-11, US Army Engineer Waterways Experiment Station, Vicksburg, MS.

13. Gibson, A. H. 1952. Hydraulics and Its Applications, 5th ed., Constable & Co., Ltd., London.

14. US Army Corps of Engineers. "Hydraulic Design Criteria," prepared for Office, Chief of Engineers, by US Army Engineer Waterways Experiment Station, Vicksburg, MS, issued serially since 1952.

15. Hebler, Martin T., and Neilson, Frank M. 1976 (Jun). "Lock Filling and Emptying--Symmetrical Systems," Miscellaneous Paper H-76-13, US Army Engineer Waterways Experiment Station, Vicksburg, MS.

SELECTED BIBLIOGRAPHY

Ables, J. H., Jr., and Boyd, M. B. 1966 (Mar). "Filling and Emptying Systems, Millers Ferry and Jones Bluff Locks, Alabama River, Alabama; Hydraulic Model Investigation," Technical Report No. 2-718, US Army Engineer Waterways Experiment Station, Vicksburg, MS.

McNown, J. S. 1950. "Surges and Water Hammer," Engineering Hydraulics, Proceedings, Fourth Hydraulics Conference, Iowa Institute of Hydraulic Research, June 12-15, 1949, p 453, Wiley, New York.

Parker, Phillip A. Morley. 1952. The Control of Water, 2nd ed., Routledge & Kegan Paul, Ltd., London.

Rouse, Hunter. 1946. Elementary Mechanics of Fluids, Wiley, New York.

US Army Engineer Waterways Experiment Station. 1959 (May). "Filling and Emptying System, Port Allen Navigation Lock, Gulf Intracoastal Waterway, Louisiana; Hydraulic Model Investigation," Technical Report No. 2-500, Vicksburg, MS.

_____. 1960 (Jun). "Filling and Emptying System, Old River Navigation Lock, Louisiana; Hydraulic Model Investigation," Technical Report No. 2-549, Vicksburg, MS.

Table 1

Valve Time Coefficients

Lock	Model Value of U	Prototype Value of U	Source
Holt	0.70		Model Report
Ice Harbor	0.66		Model Report
McNary	0.70		Manual Study
Barkley	0.60	0.54	Manual Study
John Day	0.56		Manual Study
Lower St. Anthony	0.44		Manual Study
Jonesville	0.47		Manual Study
Jones Bluff	0.50		Manual Study
Bankhead	0.57	0.57	Manual Study
Lower Granite	0.58		Manual Study
Bay Springs	0.60		Manual Study
Cannelton	0.53		Manual Study
New Cumberland	0.62		Model Report
Arkansas (Type 6)	0.50		Model Report

Table 2

Comparative data on head losses for components of lock filling s

Name of Lock	(1) Lift (ft)	(2) M. or P.	(3) "f"	(4) k_i	(5) k_r	(6) k_b	(7) k_s	(8) k_v	(9) k_s	(10) k_j
New Cumberland	22.6	M	0.015	0.243	0.225	0.030	0.030	0.050	0.000	0.2
New Cumberland	22.6	P	0.009	[a]0.185	0.136	0.030	0.030	0.050	0.000	0.1
size: 1,265' x 110'	22.6									
Cannelton	26.0	M	0.015	[a]0.260	0.177	0.000	0.030	0.050	0.000	0.1
Cannelton	26.0	P	No data							
size: 1,270' x 110'										
Arkansas	20.0	M	0.015	[a]0.225	0.120	0.070	0.030	0.050	0.030	0.1
Arkansas	20.0	P	No data							
size: 670' x 110'										
Jackson	34.0	M	0.017	a0.280	0.157	0.020	0.030	0.030	0.030	0.1
Jackson	34.0	P	0.009	[a]0.210	0.083	0.020	0.030	0.030	0.030	0.1
size: 670' x 110'										
Jonesville	30.0	M	0.017	[a]0.245	0.228	0.020	0.030	0.030	0.030	0.2
Jonesville	30.0	P	No data							
size: 655' x 84'										
McNary	92.0	M	0.014	0.125	0.188	0.096	0.030	0.030	0.030	0.
McNary	92.0	P	0.009	0.070	0.121	0.080	0.030	0.030	0.030	0.
size: 724' x 86'										
Lower Granite	105.0	M	0.014	0.145	0.198	0.180	0.066	0.110	0.000	0.(
Lower Granite	105.0	P	0.009	0.067	0.119	0.160	0.061	0.102	0.000	[e]0..
size: 730' x 86'										

Explanation of column headings

1 Lift in ft.
2 Model or prototype data
3 Resistance factor "f"
4 Intake loss
5 "f" loss upstream of valve
6 Bend loss upstream of valve
7 Bulkhead slot loss
8 Loss for fully open valve
9 Bulkhead slot loss (downstream)
10 f loss downstream of valve
11 Bend loss downstream of valve
12 Manifold loss - includes exit loss
13 Summation of all losses (3) thru (12)
14 Discharge coefficient by eq. 30, $C = 1/\sqrt{\Sigma k}$
15 Discharge coefficient by eq. 8b, $C = \frac{2A_s[\sqrt{H_1+d} - \sqrt{H_2+d}\,]}{2A_c\sqrt{2g}(t_2 - t_1)}$

Table 2

ponents of lock filling systems calculated by 3 different methods with valves open

(7) k_s	(8) k_v	(9) k_s	(10) k_r	(11) k_b	(12) k_m	(13) Σk	(14) C	(15) C Eq. 8b	(16) k Eq. 29	(17) k up to LS	(18) C up to LS
30	0.050	0.000	0.273	0.000	1.111	1.962	0.714	0.723	1.913	1.892	0.727
030	0.050	0.000	0.164	0.000	1.111	1.706	0.766	0.728	1.887	1.815	0.742
030	0.050	0.000	0.107	0.000	1.145	1.769	0.752	0.778	1.652	1.734	0.759
										No data	
030	0.050	0.030	0.135	0.000	1.186	1.846	0.736	0.741	1.821	1.859	0.733
										No data	
030	0.030	0.030	0.192	0.000	[i]1.100	1.839	0.737	0.742	1.816	1.914	0.723
030	0.030	0.030	0.101	0.000	[i]1.100	1.604	0.790	0.791	1.598	1.631	0.783
030	0.030	0.030	0.226	0.000	1.069	1.878	0.730	0.733	1.861	1.796	0.746
										No data	
030	0.030	0.030	0.173	0.000	0.865	1.537	0.807	0.823	1.476	1.496	0.818
030	0.030	0.030	0.111	0.000	0.863	1.335	0.865	[c]0.879	[c]1.294	[d]1.342	[d]0.863
066	0.110	0.000	0.654	0.426	1.663	3.442	0.539	0.534	3.507	3.492	0.535
061	0.102	0.000	[e]0.387	0.302	[b]1.895	2.593	0.621	[g]0.633	[g]2.496	[h]2.407	[h]0.645

ss

(12)

$$C = 1/\sqrt{\Sigma k}$$

$$C = \frac{2A_s[\sqrt{H+d} - \sqrt{H_2+d}\ ]}{2A_c\sqrt{2g}(t_2 - t_1)}$$

16 Loss coeff. by eq. 29, $k=1/C^2$

17 Loss coeff. by eq. 32, $k=H_{L_2}/V_c^2/2g$

18 Discharge coeff. by eq. 30

Notes

a Value from Fig. 47
b Value from Fig. 49
c Values from Test 4 study
d Data from Test 4
e "f" = 0.008
g Value from Test 10 study, not eq. 8b
h Data from Test 10
i Values from Fig. 48

Table 3

Comparative Data on Observed and Computed Pressures

Downstream from Valves at Four Locks

Lock	Lift ft	Percent Valve Open	Observed Elevation of Hydraulic Gradient ft	Computed Elevation of Hydraulic Gradient ft	Difference in Elevation ft
Lower Granite	98	0.636	595.2	594.9	-0.3
McNary		0.558	225.5	225.18	-0.3
Barkley	50	0.63	307.8	307.5	-0.3
			308.8		-1.3
Barkley	50	0.30	296.0	295.9	-0.1
			297.0		-1.1
Lower St. Anthony Falls	25	0.42	720.45	725.75	+5.3

(1) Step No (i)	(2) Time t (secs)	(3) b/B %	(4) k_v	(5) $C_n = \frac{1}{\sqrt{k_v + k_c}}$	(6) $\Delta z_n = z_n - z_{n-1}$ (ft)	(7) $q_{a_n} = \frac{\Delta z_n \times A_s}{2\Delta t}$ (cfs)	(8) $V_{c_{a_n}} = q_{a_n}/A_c$ (ft/sec)	(9) $V_{c_{n-1}}$ (ft/sec)
1	0	0	0	0	0	0	0	0
2	10	0.054	445.0	0.047	0.073	227.3	1.72178	0
3	20	0.075	260.0	0.062	0.171	532.4	4.0332	3.4436
4	30	0.121	111.0	0.094	0.245	762.8	5.7785	4.6229
5	40	0.146	82.0	0.110	0.321	999.4	7.5711	6.9343
6	50	0.150	77.0	0.113	0.352	1,095.9	8.3023	8.2079
7	60	0.154	73.0	0.116	0.363	1,130.2	8.5617	8.3966
8	70	0.167	65.0	0.123	0.380	1,183.1	8.9627	8.7268
9	80	0.167	65.0	0.123	0.390	1,214.2	9.1985	9.1985
10	90	0.175	57.0	0.131	0.400	1,245.4	9.4344	9.1985
11	100	0.183	53.0	0.136	0.419	1,304.5	9.8825	9.6703
12	110	0.188	50.5	0.139	0.431	1,341.8	10.1656	10.0948
13	120	0.196	46.5	0.145	0.444	1,382.3	10.4772	10.2363
14	130	0.200	44.0	0.149	0.458	1,425.9	10.8024	10.7080
15	140	0.204	42.5	0.151	0.465	1,447.7	10.9675	10.8967
16	150	0.208	40.5	0.155	0.475	1,478.8	11.2033	11.0382
17	160	0.213	39.0	0.158	0.486	1,513.1	11.4628	11.3685
18	170	0.217	38.0	0.160	0.491	1,528.7	11.5807	11.5571
19	180	0.225	36.0	0.164	0.496	1,544.2	11.6986	11.6043
20	190	0.233	32.5	0.172	0.510	1,587.8	12.0288	11.7930
21	200	0.238	31.0	0.176	0.530	1,650.1	12.5006	12.2647
22	210	0.250	28.2	0.184	0.548	1,706.1	12.9251	12.7364
23	220	0.250	28.2	0.184	0.557	1,734.1	13.1374	13.1138
24	230	0.254	27.0	0.188	0.562	1,749.7	13.2553	13.1610
25	240	0.258	26.3	0.190	0.568	1,768.4	13.3968	13.3497
26	250	0.267	24.8	0.196	0.578	1,799.5	13.6327	13.4440
27	260	0.275	23.0	0.203	0.596	1,855.6	14.0592	13.8214
28	270	0.283	21.5	0.209	0.612	1,905.4	14.4346	14.2931
29	280	0.288	20.5	0.214	0.624	1,942.7	14.7176	14.5761
30	290	0.292	19.6	0.219	0.637	1,983.2	15.0243	14.8592
31	300	0.296	19.3	0.220	0.647	2,014.3	15.2601	15.1894
32	310	0.296	19.3	0.220	0.649	2,020.6	15.3073	15.3309
33	320	0.308	17.6	0.230	0.655	2,039.2	15.4488	15.2837
34	330	0.321	15.9	0.241	0.677	2,107.7	15.9677	15.6139
35	340	0.325	15.4	0.245	0.697	2,170.0	16.4394	16.3215
36	350	0.333	14.9	0.248	0.708	2,204.3	16.6989	16.5574
37	360	0.338	14.1	0.255	0.723	2,251.0	17.0527	16.8404
38	370	0.358	12.2	0.272	0.747	2,325.7	17.6187	17.2649

Table 4

Calculation of filling curve, McNary Lock (prototype test 4 conditions)

(9) $V_{c_{n-1}}$ (ft/sec)	(10) $V_{c_n} = 2V_{c_{a_n}} - V_{c_{n-1}}$ (ft/sec)	(11) $\Delta V_{c_n} = V_{c_n} - V_{c_{n-1}}$ (ft/sec)	(12) $\frac{\Delta V_{c_n}}{\Delta t}$	(13) $H_{m_n} = \frac{\Delta V_{c_n}}{\Delta t} \times \frac{L'_c}{g}$ (ft)	(14) $H_n = z_u - z_{n-1} - \Delta z_n$ (ft)	(15) $H_{L_n} = H_n \pm H_{m_n}$ (ft)
					88.540	
0	0	0	0	0	88.467	83.4500
0	3.4436	3.4436	0.3444	5.0171	88.296	86.5778
3.4436	4.6229	1.1793	0.1179	1.7182	88.051	84.6834
4.6229	6.9343	2.3114	0.2311	3.3676	87.730	85.8744
6.9343	8.2079	1.2736	0.1274	1.8556	87.378	87.1031
8.2079	8.3966	0.1887	0.0189	0.2749	87.015	86.5339
8.3966	8.7268	0.3302	0.0330	0.4811	86.635	85.9477
8.7268	9.1985	0.4717	0.0472	0.6873	86.245	86.2450
9.1985	9.1985	0.0000	0.0000	0.0000	85.845	85.1577
9.1985	9.6703	0.4717	0.0472	0.6873	85.426	84.8075
9.6703	10.0948	0.4245	0.0425	0.6185	84.995	84.7888
10.0948	10.2363	0.1415	0.0142	0.2062	84.551	83.8637
10.2363	10.7080	0.4717	0.0472	0.6873	84.093	83.8181
10.7080	10.8967	0.1887	0.0189	0.2749	83.628	83.4218
10.8967	11.0382	0.1415	0.0142	0.2062	83.153	82.6719
11.0382	11.3685	0.3302	0.0330	0.4811	82.667	82.3921
11.3685	11.5571	0.1887	0.0189	0.2749	82.176	82.1072
11.5571	11.6043	0.0472	0.0047	0.0688	81.680	81.4051
11.6043	11.7930	0.1887	0.0189	0.2749	81.170	80.4828
11.7930	12.2647	0.4717	0.0472	0.6872	80.640	79.9528
12.2647	12.7364	0.4717	0.0472	0.6872	80.092	79.5422
12.7364	13.1138	0.3774	0.0377	0.5498	79.535	79.4664
13.1138	13.1610	0.0471	0.0047	0.0686	78.973	78.6981
13.1610	13.3497	0.1887	0.0189	0.2749	78.405	78.2676
13.3497	13.4440	0.0943	0.0094	0.1374	77.827	77.2772
13.4440	13.8214	0.3774	0.0377	0.5498	77.231	76.5438
13.8214	14.2931	0.4717	0.0472	0.6872	76.619	76.2067
14.2931	14.5761	0.2830	0.0283	0.4123	75.995	75.5827
14.5761	14.8592	0.2830	0.0283	0.4123	75.358	74.8769
14.8592	15.1894	0.3302	0.0330	0.4811	74.711	74.5048
15.1894	15.3309	0.1415	0.0142	0.2062	74.062	74.1307
15.3309	15.2873	-0.0472	-0.0047	-0.0687	73.407	72.9259
15.2837	15.6139	0.3302	0.0330	0.4811	72.730	71.6991
15.6139	16.3215	0.7076	0.0708	1.0309	72.033	71.6894
16.3215	16.5574	0.2358	0.0236	0.3436	71.325	70.9126
16.5574	16.8404	0.2831	0.0283	0.4124	70.602	69.9835
16.8404	17.2649	0.4245	0.0425	0.6185	69.855	68.8241
17.2649	17.9725	0.7076	0.0708	1.0309		

(Continued)

4 conditions)

(13) $x\frac{L'_c}{g}$ t)	(14) $H_n = Z_u - Z_{n-1} - \Delta z_n$ (ft)	(15) $H_{L_n} = H_n \pm H_{m_n}$ (ft)	(16) $V_{c_n} = C_n x \sqrt{2gH_{L_n}}$ (ft/sec)	(17) % Diff. from V_{c_n}	(18) $z_n = z_{n-1} + \Delta z_n$ (ft)	(19) $Q_n = V_{c_n} x 2A_c$ (cfs)
	88.540		0		251.80	
0171	88.467	83.4500	3.4439	0.0102	251.87	909
7182	88.296	86.5778	4.6274	0.0980	252.04	1,220
3676	88.051	84.6834	6.9386	0.0613	252.29	1,830
8556	87.730	85.8744	8.1765	-0.3834	252.61	2,166
2749	87.378	87.1031	8.4593	0.7469	252.96	2,217
4811	87.015	86.5339	8.6555	-0.8173	253.33	2,304
6873	86.635	85.9477	9.1467	-0.5539	253.71	2,428
0000	86.245	86.2450	9.1625	-0.3921	254.10	2,428
6873	85.845	85.1577	9.6967	0.2735	254.50	2,553
6185	85.426	84.8075	10.0461	-0.4827	254.91	2,665
2062	84.995	84.7888	10.2666	0.2954	255.35	2,702
6873	84.551	83.8637	10.6511	-0.5314	255.79	2,827
2749	84.093	83.8181	10.9420	0.4153	256.25	2,877
2062	83.628	83.4218	11.0626	0.2208	256.71	2,914
4811	83.153	82.6719	11.3045	-0.5626	257.19	3,001
2749	82.667	82.3921	11.5038	-0.4616	257.67	3,051
.0688	82.176	82.1072	11.6292	0.2148	258.16	3,064
.2749	81.680	81.4051	11.8689	0.6437	258.66	3,113
.6872	81.170	80.4828	12.3771	0.9166	258.17	3,238
.6872	80.640	79.9528	12.6232	-0.8889	259.70	3,362
.5498	80.092	79.5422	13.1631	0.3755	260.25	3,462
.0686	79.535	79.4664	13.1568	-0.0317	260.80	3,476
.2749	78.973	78.6981	13.3777	0.2097	261.37	3,524
.1374	78.405	78.2676	13.4830	0.2898	261.94	3,549
.5498	77.827	77.2772	13.8204	-0.0069	262.51	3,649
.6872	77.231	76.5438	14.2460	-0.3299	263.11	3,773
.4123	76.619	76.2067	14.6347	0.4016	263.72	3,849
.4123	75.995	75.5827	14.9233	0.4318	264.34	3,923
.4811	75.358	74.8769	15.2005	0.0734	264.98	4,010
.2062	74.711	74.5048	15.2320	-0.6453	265.63	4,047
.0687	74.062	74.1307	15.1936	-0.5894	266.28	4,076
.4811	73.407	72.9259	15.7547	0.9015	266.93	4,122
.0309	72.730	71.6991	16.3687	0.2891	267.61	4,309
.3436	72.033	71.6894	16.6393	0.4947	268.31	4,371
.4124	71.325	70.9126	16.7515	-0.5279	269.02	4,446
.6185	70.602	69.9835	17.1111	-0.8909	269.74	4,558
.0309	69.855	68.8241	18.1000	0.7095	270.49	4,745

(1) Step No (i)	(2) Time t (secs)	(3) b/B %	(4) k_v	(5) $C_n = \frac{1}{\sqrt{k_v + k_c}}$	(6) $\Delta z_n = z_n - z_{n-1}$ (ft)	(7) $q_{a_n} = \frac{\Delta z_n \times A_s}{2\Delta t}$ (cfs)	(8) $V_{c_{a_n}} = q_{a_n}/A_c$ (ft/sec)	(9) $V_{c_{n-1}}$ (ft/se
39	380	0.375	10.6	0.290	0.786	2,447.1	18.5386	17.972
40	390	0.392	9.4	0.306	0.831	2,587.2	19.6000	19.104
41	400	0.425	8.49	0.343	0.893	2,780.2	21.0623	20.095
42	410	0.458	5.55	0.382	0.979	3,048.0	23.0907	23.029
43	420	0.492	4.10	0.431	1.087	3,384.2	25.6380	24.152
44	430	0.575	1.94	0.556	1.280	3,985.1	30.1901	27.123
45	440	0.625	1.09	0.648	1.520	4,732.3	35.8507	33.256
46	450	0.733	0.280	0.797	1.780	5,541.8	41.9831	38.445
47	460	0.833	0.072	0.856	2.025	6,304.5	47.7616	45.521
48	470	0.917	0.025	0.871	2.147	6,684.4	50.6391	50.002
49	480	1.000	0	0.879	2.180	6,787.1	51.4174	51.275
50	490	1.000	0	0.879	2.180	6,787.1	51.4174	51.559
51	500	1.000	0	0.879	2.152	6,699.9	50.7570	51.275
52	510	1.000	0	0.879	2.115	6,584.7	49.8844	50.238
53	520	1.000	0	0.879	2.080	6,475.8	49.0588	49.530
54	530	1.000	0	0.879	2.035	6,335.7	47.9975	48.587
55	540	1.000	0	0.879	1.990	6,195.6	46.9361	47.407
56	550	1.000	0	0.879	1.950	6,071.0	45.9927	46.464
57	560	1.000	0	0.879	1.908	5,940.3	45.0021	45.521
58	570	1.000	0	0.879	1.864	5,803.3	43.9643	44.483
59	580	1.000	0	0.879	1.820	5,666.3	42.9265	43.445
60	590	1.000	0	0.879	1.775	5,526.2	41.8651	42.407
61	600	1.000	0	0.879	1.725	5,370.5	40.6858	41.322
62	610	1.000	0	0.879	1.675	5,214.9	39.5065	40.049
63	620	1.000	0	0.879	1.630	5,074.8	38.4452	38.964
64	630	1.000	0	0.879	1.585	4,934.7	37.3838	37.926
65	640	1.000	0	0.879	1.540	4,794.6	36.3224	36.841
66	650	1.000	0	0.879	1.495	4,654.5	35.2610	35.803
67	660	1.000	0	0.879	1.453	4,523.7	34.2704	34.718
68	670	1.000	0	0.879	1.410	4,389.8	33.2562	33.822
69	680	1.000	0	0.879	1.340	4,252.6	32.2163	32.690
70	690	1.000	0	0.879	1.300	4,125.6	31.2547	31.742
71	700	1.000	0	0.879	1.255	3,982.8	30.1728	30.766
72	710	1.000	0	0.879	1.210	3,840.0	29.0909	29.578
73	720	1.000	0	0.879	1.167	3,703.5	28.0571	28.60
74	730	1.000	0	0.879	1.124	3,567.1	27.0232	27.51
75	740	1.000	0	0.879	1.081	3,430.6	25.9895	26.53
76	750	1.000	0	0.879	1.037	3,291.0	24.9316	25.44

Table 4 (Continued)

)	(9)	(10)	(11)	(12)	(13)	(14)	(15)
= n /A_c	$V_{c_{n-1}}$	$V_{c_n} = 2V_{c_{a_n}} - V_{c_{n-1}}$	$\Delta V_{c_n} = V_{c_n} - V_{c_{n-1}}$	$\frac{\Delta V_{c_n}}{\Delta t}$	$H_{m_n} = \frac{\Delta V_{c_n}}{\Delta t} \times \frac{L'_c}{g}$	$H_n = z_u - z_{n-1} - \Delta z_n$	$H_{L_n} = H_n \pm H_{m_n}$
ec)	(ft/sec)	(ft/sec)	(ft/sec)		(ft)	(ft)	(ft)
86	17.9725	19.1046	1.1321	0.1132	1.6494	69.069	67.41
00	19.1046	20.0953	0.9906	0.0991	1.4433	68.238	66.79
23	20.0953	22.0293	1.9340	0.1934	2.8178	67.345	64.52
07	23.0293	24.1521	2.1228	0.2123	3.0927	66.366	63.27
80	24.1521	27.1239	2.9718	0.2972	4.3298	65.279	60.94
01	27.1239	33.2562	6.1324	0.6132	8.9346	63.999	55.06
07	33.2562	38.4451	5.1889	0.5189	7.5599	62.479	54.91
31	38.4451	45.5210	7.0758	0.7076	10.3091	60.699	50.38
16	45.5210	50.0023	4.4813	0.4481	6.5290	58.674	52.14
91	50.0023	51.2759	1.2737	0.1274	1.8557	56.527	54.67
74	51.2759	51.5590	0.2830	0.0283	0.4123	54.347	53.93
74	51.5590	51.2759	-0.2831	-0.0283	-0.4123	52.167	52.5
70	51.2759	50.2381	-1.0378	-0.1038	-1.5120	50.015	51.5
44	50.2381	49.5306	-0.7076	-0.0708	-1.0309	47.900	48.9
88	49.5306	48.5871	-0.9435	-0.0944	-1.3733	45.820	47.1
75	48.5871	47.4078	-1.1793	-0.1179	-1.7181	43.785	45.5
61	47.4078	46.4643	-0.9434	-0.0943	-1.3745	41.795	43.1
27	46.4644	45.5210	-0.9434	-0.0943	-1.3745	39.845	41.2
21	45.5210	44.4832	-1.0378	-0.1038	-1.5120	37.937	39.4
43	44.4832	43.4454	-1.0378	-0.1038	-1.5120	36.073	37.5
65	43.4454	42.4076	-1.0378	-0.1038	-1.5120	34.253	35.7
51	42.4076	41.3227	-1.0849	-0.1085	-1.5807	32.478	34.0
58	41.3227	40.0490	-1.2737	-0.1274	-1.8557	30.753	32.6
65	40.0490	38.9641	-1.0849	-0.1085	-1.5807	29.078	30.6
52	38.9641	37.9263	-1,0378	-0.1038	-1.5120	27.448	28.9
38	37.9263	36.8413	-1.0849	-0.1085	-1.5807	25.863	27.4
24	36.8413	35.8035	-1.0378	-0.1038	-1.5120	24.323	25.8
10	35.8035	34.7186	-1.0849	-0.1085	-1.5807	22.828	24.4
04	34.7186	33.8223	-0.8963	-0.0896	-1.3058	21.375	22.6
62	33.8223	32.6901	-1.1321	-0.1132	-1.6494	19.965	21.6
63	32.6902	31.7425	-0.9477	-0.0948	-1.3807	18.625	20.0
47	31.7425	30.7668	-0.9757	-0.0976	-1.4215	17.325	18.
28	30.7668	29.5787	-1.1881	-0.1188	-1.7310	16.070	17.
09	29.5787	28.6030	-0.9757	-0.0976	-1.4215	14.860	16.
71	28.6030	27.5111	-1.0919	-0.1092	-1.5909	13.693	15.
32	27.5111	26.5354	-0.9757	-0.0976	-1.4215	12.569	13.
95	26.5354	25.4435	-1.0919	-0.1092	-1.5909	11.488	13.
16	25.4435	24.4197	-1.0238	-0.1024	-1.4916	10.451	11.

(Continued)

(13) $x\frac{L'_c}{g}$ (ft)	(14) $H_n = Z_u - z_{n-1} - \Delta z_n$ (ft)	(15) $H_{L_n} = H_n \pm H_{m_n}$ (ft)	(16) $V_{c_n} = C_n x \sqrt{2gH_{L_n}}$ (ft/sec)	(17) % Diff. from V_{c_n}	(18) $z_n = z_{n-1} + \Delta z_n$ (ft)	(19) $Q_n = V_{c_n} x 2A_c$ (cfs)
5494	69.069	67.4196	19.0999	-0.0247	271.27	5,044
5433	68.238	66.7947	20.0601	-0.1750	272.10	5,305
5178	67.345	64.5272	22.1007	0.3241	273.00	5,816
4927	66.366	63.2733	24.3733	0.9159	273.97	6,376
4298	65.279	60.9492	26.9899	-0.4938	275.06	7,161
4346	63.999	55.0644	33.0941	-0.4875	276.34	8,780
4599	62.479	54.9191	38.5192	0.1926	277.86	10,150
4091	60.699	50.3899	45.3806	-0.3083	279.64	12.018
4290	58.674	52.1450	49.5816	-0.8413	281.67	13,201
4557	56.527	54.6713	51.6581	0.7453	283.81	13,537
4123	54.347	53.9347	51.7802	0.4290	285.99	13,612
4123	52.167	52.5793	51.1254	-0.2935	288.17	13,537
5120	50.015	51.5270	50.6112	0.7427	290.32	13,263
0309	47.900	48.9309	49.3198	-0.4256	292.44	13,076
3733	45.820	47.1946	48.4368	-0.3094	294.52	12,827
7181	43.785	45.5031	47.5609	0.3229	296.56	12,516
8745	41.795	43.1695	46.3253	-0.2993	298.54	12,267
8745	39.845	41.2195	45.2667	-0.5581	300.50	12,018
5120	37.937	39.4490	44.2841	-0.4476	302.40	11,744
5120	36.073	37.5850	43.2251	-0.5070	304.27	11,470
5120	34.253	35.7650	42.1656	-0.5705	306.09	11,196
5807	32.478	34.0587	41.1475	-0.4239	307.86	10,909
8557	30.753	32.6087	40.2621	0.5320	309.59	10,573
5807	29.078	30.6587	39.0397	0.7941	311.26	10,215
5120	27.448	28.9600	37.9428	0.0435	312.89	10,013
5807	25.863	27.4437	36.9361	0.2572	314.48	9,726
5120	24.323	25.8350	35.8372	0.0940	316.02	9,452
5807	22.828	24.4087	34.8389	0.3321	317.51	9,166
3058	21.375	22.6808	33.5783	-0.7213	318.96	6,929
6494	19.965	21.6144	32.7794	0.2730	320.38	8,630
3807	18.625	20.0057	31.5360	-0.6505	321.72	8,380
4215	17.325	18.7465	30.5274	-0.7982	323.02	6,122
7310	16.070	17.8010	29.7476	0.5709	324.27	7,809
4215	14.860	16.2815	28.4496	-0.5363	325.48	7,551
5909	13.693	15.2839	27.5642	0.1931	326.65	7,263
4215	12.569	13.9905	26.3722	-0.6150	327.77	7,005
5909	11.488	13.0789	25.4985	0.2162	328.85	6,717
4916	10.451	11.9426	24.3657	-0.2212	329.89	6,447

(1) Step No (i)	(2) Time t (secs)	(3) b/B %	(4) k_v	(5) $C_n = \frac{1}{\sqrt{k_v + k_c}} =$	(6) $\Delta z_n = z_n - z_{n-1}$ (ft)	(7) $q_{a_n} = \frac{\Delta z_n \times A_s}{2\Delta t}$ (cfs)	(8) $V_{c_{a_n}} = q_{a_n}/A_c$ (ft/sec)	(9) $V_{c_{n-1}}$ (ft/sec
77	760	1.000	0	0.879	0.993	3,151.3	23:8738	24.4197
78	770	1.000	0	0.879	0.948	3,008.5	22.7919	23.3278
79	780	1.000	0	0.879	0.904	2,868.9	21.7340	22.2559
80	790	1.000	0	0.879	0.860	2,729.3	20.6762	21.2121
81	800	1.000	0	0.879	0.818	2,596.0	19.6664	20.1402
82	810	1.000	0	0.879	0.777	2,465.8	18.6807	19.1926
83	820	1.000	0	0.879	0.734	2,329.4	17.6469	18.1688
84	830	1.000	0	0.879	0.691	2,192.92	16.6131	17.1249
85	840	1.000	0	0.879	0.648	2,056.46	15.5792	16.1012
86	850	1.000	0	0.879	0.605	1,920.00	14.5454	15.0573
87	860	1.000	0	0.879	0.562	1,783.54	13.5116	14.0335
88	870	1.000	0	0.879	0.519	1,647.07	12.4778	12.9897
89	880	1.000	0	0.879	0.476	1,510.61	11.4440	11.9659
90	890	1.000	0	0.879	0.433	1,374.15	10.4102	10.9221
91	900	1.000	0	0.879	0.3905	1,239.28	9.3884	9.8983
92	910	1.000	0	0.879	0.3480	1,104.40	8.3666	8.8785
93	920	1.000	0	0.879	0.3055	969.52	7.3448	7.8547
94	930	1.000	0	0.879	0.2630	834.64	6.3231	6.8349
95	940	1.000	0	0.879	0.2203	699.13	5.2965	5.8112
96	950	1.000	0	0.879	0.1775	563.31	4.2675	4.7818
97	960	1.000	0	0.879	0.13465	427.32	3.237261	3.7532
98	970	1.000	0	0.879	0.09179	291.30	2.20682	2.7213

Explanation of column headings

1. Computation step number.
2. Time, in seconds from start of valve opening.
3. Percent of valve opening (see Fig. 27).
4. Valve loss coefficient (see Fig. 54, valve loss for McNary valve).
5. Discharge coefficient C_n, where k_c is loss for culvert system with valve open. Value of k_c is 1.294 (Table C-12, Appendix C).
6. Assumed rise in lock water surface in 10 seconds.
7. Ave discharge thru one culvert during 10 seconds.
8. Ave Velocity over 10 seconds in one culvert.
9. Vel at start of 10 sec interval. V_{c_n} is 0 at start of computation (when t=0). V_{c_n} is also 0 at start of 2nd step (i=2).

Table 4 (Concluded)

(9) $V_{c_{n-1}}$	(10) $V_{c_n} = 2V_{c_{a_n}} - V_{c_{n-1}}$	(11) $\Delta V_{c_n} = V_{c_n} - V_{c_{n-1}}$	(12) $\frac{\Delta V_{c_n}}{\Delta t}$	(13) $H_{m_n} = \frac{\Delta V_{c_n}}{\Delta t} \times \frac{L'_c}{g}$	(14) $H_n = Z_u - z_{n-1} - \Delta z_n$	(15) $H_{L_n} = H_n \pm H_{m_n}$
(ft/sec)	(ft/sec)	(ft/sec)		(ft)	(ft)	(ft)
24.4197	23.3278	-1.0919	-0.1092	-1.5909	9.458	11.048
23.3278	22.2559	-1.0719	-0.1072	-1.5617	8.510	10.071
22.2559	21.2120	-1.0438	-0.1044	-1.5208	7.606	9.126
21.2121	20.1402	-1.0719	-0.1072	-1.5617	6.746	8.307
20.1402	19.1926	-0.9477	-0.0948	-1.3807	5.928	7.308
19.1926	18.1688	-1.0238	-0.1024	-1.4916	5.151	6.642
18.1688	17.1249	-1.0438	-0.1044	-1.5208	4.417	5.93
17.1249	16.1012	-1.0238	-0.1024	-1.4915	3.726	5.21
16.1012	15,0573	-1.0438	-0.1044	-1.5208	3.078	4.59
15.0573	14.0335	-1.0238	-0.1024	-1.4916	2.473	3.96
14.0335	12.9897	-1.0438	-0.1044	-1.5208	1.911	3.43
12.9897	11.9659	-1.0238	-0.1024	-1.4916	1.392	2.88
11.9659	10.9221	-1.0438	-0.1044	-1.5208	0.914	2.43
10.9221	9.8983	-1.0238	-0.1024	-1.4916	0.481	1.97
9.8983	8.8785	-1.0198	-0.1020	-1.4858	0.0895	1.57
8.8785	7.8547	-1.0238	-0.1024	-1.4916	-0.2585	1.23
7.8547	6.8349	-1.0198	-0.1020	-1.4858	-0.5640	0.92
6.8349	5.8112	-1.0238	-0.1024	-1.4916	-0.8230	0.66
5.8112	4.7818	-1.0294	-0.1029	-1.4998	-1.0433	0.45
4.7818	3.7531	-1.0286	-0.10287	-1.49872	-1.2175	0.28
3.7532	2.721323	-1.031877	-0.103188	-1.50339	-1.35465	0.14
2.721323	1.692339	-1.02896	-0.102896	-1.49914	-1.44179	0.05

10. Calculated from columns (8) and (9).
11. Calculated from columns (9) and (10).
12. Accel. or decel. of culvert Vel. Δt has a constant value of 10 secs, and is difference between successive time steps. Col. 12 is col. 11/col. 10.
13. Computer value of inertia head.
14. Head loss, difference between upper pool and lock water surface.
15. Total head loss. Col. 14 plus or minus col. 13.
16. Culvert Vel computer by $V = C\sqrt{2gh}$, where $C=C_n$ and $H=H_{L_n}$ at any step, i.
17. Percent difference from value in col. (10). Note If value in col. (16) differs from col. (10) by more than 1%, a new value of Δz_n is assumed and the computations in the step must be repeated.
18. Lock water surface at end of any step.
19. Total discharge, Q, into lock at end of any step.

(13) $\frac{L'_c}{g}$	(14) $H_n = Z_u - z_{n-1} - \Delta z_n$	(15) $H_{L_n} = H_n \pm H_{m_n}$	(16) $V_{c_n} = C_n \times \sqrt{2gH_{L_n}}$	(17) % Diff. from V_{c_n}	(18) $z_n = z_{n-1} + \Delta z_n$	(19) $Q_n = V_{c_n} \times 2A_c$
ft)	(ft)	(ft)	(ft/sec)		(ft)	(cfs)
5909	9.458	11.0489	23.4363	0.4650	330.88	6,159
9617	8.510	10.0717	22.3759	0.5389	331.83	5,876
5208	7.606	9.1268	21.3005	0.4166	332.73	5,864
5617	6.746	8.3077	20.3221	0.9030	333.59	5,317
3807	5.928	7.3087	19.0612	-0.6846	334.41	5,067
4916	5.151	6.6426	18.1718	0.0167	335.19	4,797
5208	4.417	5.9378	17.1808	0.3260	335.92	4,521
4915	3.726	5.2176	16.1051	0.0247	336.61	4,251
5208	3.078	4.5988	15.1200	0.4163	337.26	3,975
4916	2.473	3.9646	14.0388	0.0372	337.87	3,705
5208	1.911	3.4318	13.0614	0.5522	338.43	3,429
4916	1.392	2.8836	11.9728	0.0576	338.95	3,159
5208	0.914	2.4368	11.0063	0.7708	339.42	2,883
4916	0.481	1.9746	9.9076	0.0938	339.86	2,613
4858	0.0895	1.5753	8.8493	-0.3291	340.25	2,344
4916	-0.2585	1.2331	7.8294	-0.3228	340.60	2,074
4858	-0.5640	0.9218	6.7693	-0.9604	340.90	1,804
4916	-0.8230	0.6686	5.7652	-0.7918	341.16	1,534
4998	-1.0433	0.4565	4.7637	-0.3768	341.38	1,262
.49872	-1.2175	0.28122	3.7390	0.3757	341.56	991
.50339	-1.35465	0.14874	2.719221	-0.0772	341.69	718
.49914	-1.44179	0.05735	1.688518	-0.2258	341.78	447

Notes

Z_u

z_n

t value of 10 secs,
Col. 12 is col. 11/col. 10.

A_s

L'_c

water surface.

k_c

A_c

$H = H_{L_n}$ at any step, i.

ave

secs

vel

col

acce

If value in col. (16)
e of Δz_n is assumed and

Notes:

Z_u = 340.34

z_n = 251.80 (when t=0)

A_s = 62,267 sq. ft. (lock water surface area)

L'_c = 468.7 ft.

k_c = 1.294

A_c = 132.0 sq. ft.

ave = average
secs = seconds
vel = velocity
col = column
accel = acceleration decel = deceleration

Table 5

Determination of Valve Opening Curve for 15.5- by 15.0-foot Valve from 12.0- by 12.0-foot Arkansas Valve (Reference 6)

Lift = 27.5 feet

Valve = 15.5 × 15.0 feet

Use Arkansas Low Lift Curve

(1) Percent of Time	(2) Valve Opening feet	(3) Percent of Valve Opening	(4) Valve Opening For 15.5- by 15.0-foot Valve, feet	(5) Time seconds
0	0	0	0	0
10	0.90	0.075	1.163	24
20	1.85	0.154	2.387	48
30	3.00	0.250	3.875	72
40	4.20	0.350	5.425	96
50	5.32	0.443	6.867	120
60	6.55	0.546	8.463	144
70	7.80	0.650	10.075	168
80	9.15	0.763	11.827	192
90	10.55	0.879	13.625	216
100	12.00	1.000	15.500	240

Notes: Filling time T''_f = 7.1 minutes (426 seconds)
Valve time t''_v = 4.0 minutes (240 seconds)
Values in columns 1 and 2 were read from Plate 7 (Reference 6).
Column 3 is column 2 values divided by 12.0.
Column 4 is column 3 values multiplied by 15.5.
Column 5 is column 1 values multiplied by 240.
Values in columns 4 and 5 are plotted in Figure 73.

Table 6

Calculation of Percent Valve Opening Versus Time

(1) Time seconds	(2) Valve Opening feet	(3) Valve Opening b/B percent
0	0	0
10	0.40	0.026
20	0.87	0.056
30	1.38	0.089
40	1.92	0.124
50	2.50	0.161
60	3.10	0.200
70	3.72	0.240
80	4.32	0.279
90	4.98	0.321
100	5.60	0.361
110	6.21	0.401
120	6.85	0.442
130	7.51	0.485
140	8.19	0.528
150	8.85	0.571
160	9.54	0.615
170	10.24	0.661
180	10.96	0.707
190	11.67	0.753
200	12.41	0.801
210	13.15	0.848
220	13.90	0.897
230	14.68	0.947
240	15.50	1.000

Notes: Values in column 2 were read from Figure 73.
Values in column 3 are column 2 values divided by 15.5.

Table 7

Valve Loss Coefficient (from Figure 54)

(1) Time seconds	(2) Valve Opening b/B feet	(3) Valve Loss Coefficient k_v
0	0	1,510
10	0.026	420
20	0.056	193
30	0.089	102
40	0.124	67
50	0.161	44
60	0.200	30
70	0.240	24
80	0.279	15.9
90	0.321	11.7
100	0.361	8.60
110	0.401	6.10
120	0.442	4.30
130	0.485	2.92
140	0.528	1.96
150	0.571	1.22
160	0.615	0.76
170	0.661	0.380
180	0.702	0.200
190	0.753	0.100
200	0.801	0.052
210	0.848	0.033
220	0.897	0.018
230	0.947	0.000
240	1.000	

Notes: Column 2 values are from Table 6.
Column 3 values were read from Figure 54.

(1) Step No (i)	(2) Time t (secs)	(3) b/B %	(4) k_v	(5) $C_n = \frac{1}{\sqrt{k_v + k_c}}$	(6) $\Delta z_n = z_n - z_{n-1}$ (ft)	(7) $q_{a_n} = \frac{\Delta z_n \times A_s}{2\Delta t}$ (cfs)	(8) $V_{c_{a_n}} = q_{a_n}/A_c$ (ft/sec)	(9) $V_{c_{n-1}}$ (ft/sec)
1	0	0		0	0	0	0	0
2	10	0.026	1,510	0.026	0.024	117.2	0.5042	0
3	20	0.056	420	0.049	0.071	339.7	1.4612	1.0085
4	30	0.089	193	0.072	0.115	550.3	2.3668	1.9140
5	40	0.124	102	0.098	0.160	765.6	3.2929	2.8195
6	50	0.161	67	0.120	0.205	980.9	4.2190	3.7663
7	60	0.200	44	0.147	0.251	1,201.0	5.1657	4.6718
8	70	0.240	30	0.176	0.299	1,430.7	6.1536	5.6597
9	80	0.279	24	0.196	0.343	1,641.3	7.0592	6.6475
10	90	0.321	15.9	0.236	0.391	1,870.9	8.0470	7.4708
11	100	0.361	11.7	0.269	0.448	2,143.7	9.2201	8.6233
12	110	0.401	8.60	0.305	0.505	2,416.4	10.3932	9.8170
13	120	0.442	6.10	0.348	0.562	2,689.2	11.5663	10.9695
14	130	0.485	4.30	0.394	0.624	2,985.8	12.8423	12.1632
15	140	0.528	2.92	0.445	0.690	3,301.6	14.2006	13.5215
16	150	0.571	1.96	0.494	0.754	3,607.9	15.5178	14.8798
17	160	0.615	1.22	0.546	0.818	3,914.1	16.8350	16.1558
18	170	0.661	0.76	0.588	0.880	4,210.8	18.1110	17.5141
19	180	0.707	0.380	0.630	0.935	4,474.0	19.2429	18.7078
20	190	0.753	0.200	0.655	0.980	4.689.3	20.1690	19.7780
21	200	0.801	0.100	0.669	1.010	4,832.8	20.7865	20.5601
22	210	0.848	0.052	0.677	1.027	4,914.2	21.1363	21.0128
23	220	0.897	0.033	0.680	1.035	4,952.5	21.3010	21.2598
24	230	0.947	0.018	0.682	1.032	4,938.1	21.2392	21.3421
25	240	1.000	0	0.685	1.020	4,880.7	20.9923	21.1363
26	250	1.000	0	0.685	1.004	4,804.1	20.6630	20.8482
27	260	1.000	0	0.685	0.983	4,703.7	20.2308	20.4777
28	270	1.000	0	0.685	0.958	4,584.0	19.7163	19.9838
29	280	1.000	0	0.685	0.930	4,450.1	19.1400	19.4487
30	290	1.000	0	0.685	0.902	4,316.1	18.5637	18.8313
31	300	1.000	0	0.685	0.874	4,182.1	17.9875	18.2962
32	310	1.000	0	0.685	0.843	4,033.8	17.3495	17.6788
33	320	1.000	0	0.685	0.812	3,885.4	16.7115	17.0202
34	330	1.000	0	0.685	0.780	3,732.3	16.0529	16.4028
35	340	1.000	0	0.685	0.746	3,569.6	15.3532	15.7030
36	350	1.000	0	0.685	0.712	3,406.9	14.6434	15.0033
37	360	1.000	0	0.685	0.678	3,244.2	13.9537	14.3035
38	370	1.000	0	0.685	0.644	3,081.5	13.2539	13.6038

Table 8

Calculation of filling curve, design example (870 X 110 ft lock)

(9) $V_{c_{n-1}}$ (ft/sec)	(10) $V_{c_n} = 2V_{c_{a_n}} - V_{c_{n-1}}$ (ft/sec)	(11) $\Delta V_{c_n} = V_{c_n} - V_{c_{n-1}}$ (ft/sec)	(12) $\frac{\Delta V_{c_n}}{\Delta t}$	(13) $H_{m_n} = \frac{\Delta V_{c_n}}{\Delta t} \times \frac{L'_c}{g}$ (ft)	(14) $H_n = Z_u - z_{n-1} - \Delta z_n$ (ft)	(15) $H_{L_n} = H_n \pm H_{m_n}$ (ft)
0	0	0	0	0	28.500	
0	1.0085	1.0085	0.1008	4.0924	27.476	23.383
1.0085	1.9140	0.9055	0.0906	3.6748	27.404	23.729
1.9140	2.8195	0.9055	0.0906	3.6748	27.290	23.614
2.8195	3.7663	0.9467	0.0947	3.8418	27.130	23.287
3.7663	4.6718	0.9055	0.0906	3.6748	26.924	23.249
4.6718	5.6597	0.9879	0.0988	4.0089	26.674	22.664
5.6597	6.6475	0.9879	0.0988	4.0089	26.374	22.365
6.6475	7.4708	0.8232	0.0823	3.3407	26.032	22.690
7.4708	8.6233	1.1525	0.1153	4.6770	25.640	20.963
8.6233	9.8170	1.1937	0.1194	4.8441	25.192	20.348
9.8170	10.9695	1.1525	0.1153	4.6770	24.688	20.010
10.9695	12.1632	1.1937	0.1937	4.8441	24.126	19.281
12.1632	13.5215	1.3583	0.1358	5.5122	23.501	17.988
13.5215	14.8798	1.3583	0.1358	5.5122	22.812	17.299
14.8798	16.1558	1.2760	0.1276	5.1781	22.058	16.879
16.1558	17.5141	1.3583	0.1358	5.5122	21.240	15.727
17.5141	18.7078	1.1937	0.1194	4.8441	20.360	15.515
18.7078	19.7780	1.0702	0.1070	4.3429	19.424	15.081
19.7780	20.5601	0.7821	0.0782	3.1737	18.445	15.271
20.5601	21.0128	0.4528	0.0453	1.8374	17.435	15.597
21.0128	21.2598	0.2470	0.0247	1.0022	16.408	15.405
21.2598	21.3421	0.0823	0.0082	0.3341	15.373	15.038
21.3421	21.1363	-0.2058	-0.0206	-0.8352	14.341	15.176
21.1363	20.8482	-0.2881	-0.0288	-1.1693	13.321	14.490
20.8482	20.4777	-0.3704	-0.0370	-1.5033	12.317	13.820
20.4777	19.9838	-0.4939	-0.0494	-2.0044	11.334	13.338
19.9838	19.4487	-0.5351	-0.0535	-2.1715	10.377	12.548
19.4487	18.8313	-0.6174	-0.0617	-2.5056	9.447	11.952
18.8313	18.2962	-0.5351	-0.0535	-2.1715	8.790	10.961
18.2962	17.6788	-0.6174	-0.0617	-2.5056	7.916	10.421
17.6788	17.0202	-0.6586	-0.0659	-2.6726	7.073	9.745
17.0202	16.4028	-0.6174	-0.0617	-2.5056	6.261	8.766
16.4028	15.7030	-0.6997	-0.0700	-2.8396	5.481	8.320
15.7030	15.0033	-0.6997	-0.0700	-2.8396	4.735	7.574
15.0033	14.3035	-0.6997	-0.0700	-2.8396	4.023	6.862
14.3035	13.6038	-0.6997	-0.0700	-2.8396	3.344	6.183
13.6038	12.9041	-0.6997	-0.0700	-2.8396	2.700	5.539

(Continued)

110 ft lock)

(13) $\Delta z_n = C_n \times \frac{L'_c}{g}$ (ft)	(14) $H_n = Z_u - z_{n-1} - \Delta z_n$ (ft)	(15) $H_{L_n} = H_n \pm H_{m_n}$ (ft)	(16) $V_{c_n} = C_n \times \sqrt{2gH_{L_n}}$ (ft/sec)	(17) % Diff. from V_{c_n}	(18) $z_n = z_{n-1} + \Delta z_n$ (ft)	(19) $Q_n = V_{c_n} \times 2A_c$ (cfs)
	28.500		0		510.50	0
1.0924	27.476	23.3831	1.0085	0.0022	510.52	467
1.6748	27.404	23.7297	1.9029	-0.5800	510.60	890
2.6748	27.290	23.6147	2.8065	-0.4630	510.71	1,311
3.8418	27.130	23.2877	3.7934	0.7209	510.87	1,751
4.6748	26.924	23.2497	4.6412	-0.6594	511.08	2,172
5.0089	26.674	22.6646	5.6135	-0.8163	511.33	2,689
4.0089	26.374	22.3656	6.6764	-0.4342	511.63	3,091
3.3407	26.032	22.6908	7.4890	0.2428	511.97	3,474
4.6770	25.640	20.9635	8.6673	0.5104	512.36	4,010
5.8441	25.192	20.3484	9.7333	-0.8525	512.81	4,565
4.6770	24.688	20.0105	10.9438	-0.2344	513.31	5,101
5.8441	24.126	19.2814	12.2572	0.7668	513.87	5,656
6.5122	23.501	17.9888	13.4041	-0.8757	514.50	6,288
5.5122	22.812	17.2993	14.8462	0.2260	515.19	6,919
5.1781	22.058	16.8794	16.2797	-0.7666	515.94	7,512
5.5122	21.240	15.7273	17.3684	-0.8319	516.76	8,144
4.8441	20.360	15.5154	18.5780	-0.6937	517.64	8,699
4.3429	19.424	15.0816	19.6248	-0.7748	518.58	9,197
3.1737	18.445	15.2713	20.5315	-0.1391	519.56	9,560
1.8374	17.435	15.5976	21.1932	0.8581	520.56	9,771
1.0022	16.408	15.4058	21.3143	-0.2563	521.59	9,886
0.3341	15.373	15.0389	21.1523	0.8824	522.63	9,924
0.8352	14.341	15.1762	21.3111	-0.8269	523.66	9,828
1.1693	13.321	14.4903	20.9155	-0.3231	524.68	9,694
1.5033	12.317	13.8203	20.4263	-0.2511	525.68	9,522
2.0044	11.334	13.3384	20.0671	0.4166	526.66	9,292
2.1715	10.377	12.5485	19.4637	0.0773	527.62	9,044
2.5056	9.447	11.9526	18.9960	0.8745	528.55	8,756
2.1715	8.790	10.9615	18.1914	-0.5729	529.45	8,508
2.5056	7.916	10.4216	17.7377	0.3334	530.32	8,221
2.6726	7.073	9.7456	17.1528	0.7791	531.17	7,914
2.5056	6.261	8.7666	16.2664	-0.8190	531.98	7,627
2.8396	5.481	8.3206	15.8493	0.9311	532.76	7,302
2.8396	4.735	7.5746	15.1221	0.7917	533.51	6,976
2.8396	4.023	6.8626	14.3938	0.6311	534.22	6,651
2.8396	3.344	6.1836	13.6637	0.4367	534.90	6,325
2.8396	2.700	5.5396	12.9322	0.2177	535.54	6,000

(1) Step No (i)	(2) Time t (secs)	(3) b/B %	(4) k_v	(5) $C_n = \frac{1}{\sqrt{k_v+k_c}}$	(6) $\Delta z_n = z_n - z_{n-1}$ (ft)	(7) $q_{a_n} = \frac{\Delta z_n \times A_s}{2\Delta t}$ (cfs)	(8) $V_{c_{a_n}} = q_{a_n}/A_c$ (ft/sec)	(9) $V_{c_{n-1}}$ (ft/sec)
39	380	1.000	0	0.685	0.610	2,918.8	12.5542	12.9041
40	390	1.000	0	0.685	0.576	2,756.2	11.8545	12.2043
41	400	1.000	0	0.685	0.542	2,593.5	11.1547	11.5046
42	410	1.000	0	0.685	0.5075	2,428.4	10.4447	10.8048
43	420	1.000	0	0.685	0.4725	2,260.9	9.7244	10.0845
44	430	1.000	0	0.685	0.4375	2,093.4	9.0040	9.3642
45	440	1.000	0	0.685	0.4025	1,926.0	8.2837	8.6439
46	450	1.000	0	0.685	0.3675	1,758.5	7.5634	7.9235
47	460	1.000	0	0.685	0.3325	1,591.0	6.8431	7.2032
48	470	1.000	0	0.685	0.2973	1,422.6	6.1186	6.4829
49	480	1.000	0	0.685	0.2620	1,253.7	5.3921	5.7544
50	490	1.000	0	0.685	0.2267	1,084.8	4.6656	5.0299
51	500	1.000	0	0.685	0.19135	915.6	3.9381	4.3014
52	510	1.000	0	0.685	0.15602	746.6	3.2110	3.5749
53	520	1.000	0	0.685	0.12069	577.5	2.4839	2.8471
54	530	1.000	0	0.685	0.08535	408.5	1.7570	2.1206
55	540	1.000	0	0.685	0.05002	239.4	1.0295	1.3933

Explanation of column headings

1. Computation step number.
2. Time, in seconds from start of valve opening.
3. Percent of valve opening (see Fig. 27).
4. Valve loss coefficient, k_v vs time (see Fig. 54).
5. Discharge coefficient C_n, where k_c is loss for culvert system with valve open. Value of k_c is 2.132 (Paragraph 217).
6. Assumed rise in lock water surface in 10 seconds.
7. Ave discharge thru one culvert during 10 seconds.
8. Ave Velocity over 10 seconds in one culvert.
9. Vel at start of 10 sec interval. V_{c_n} is 0 at start of computation (when t=0). V_{c_n} is also 0 at start of 2nd step (i=2).

Table 8 (Concluded)

(9) $V_{c_{n-1}}$ (ft/sec)	(10) $V_{c_n} = 2V_{c_{a_n}} - V_{c_{n-1}}$ (ft/sec)	(11) $\Delta V_{c_n} = V_{c_n} - V_{c_{n-1}}$ (ft/sec)	(12) $\frac{\Delta V_{c_n}}{\Delta t}$	(13) $H_{m_n} = \frac{\Delta V_{c_n}}{\Delta t} \times \frac{L'_c}{g}$ (ft)	(14) $H_n = Z_u - z_{n-1} - \Delta z_n$ (ft)	(15) $H_{L_n} = H_n \pm H_{m_n}$ (ft)
12.9041	12.2043	-0.6997	-0.0700	-2.8396	2.090	4.929
12.2043	11.5046	-0.6997	-0.0700	-2.8396	1.514	4.353
11.5046	10.8048	-0.6997	-0.0700	-2.8396	0.972	3.811
10.8048	10.0845	-0.7203	-0.0720	-2.9231	0.464	3.387
10.0845	9.3642	-0.7203	-0.0720	-2.9231	-0.0080	2.915
9.3642	8.6439	-0.7203	-0.0720	-2.9231	-0.4455	2.477
8.6439	7.9235	-0.7203	-0.0720	-2.9232	-0.8480	2.075
7.9235	7.2032	-0.7203	-0.0720	-2.9231	-1.2230	1.700
7.2032	6.4829	-0.7203	-0.0720	-2.9232	-1.5480	1.375
6.4829	5.7544	-0.7286	-0.0729	-2.9566	-1.8453	1.111
5.7544	5.0299	-0.7244	-0.0724	-2.9399	-2.1073	0.832
5.0299	4.3014	-0.7285	-0.0728	-2.9566	-2.3340	0.622
4.3014	3.5749	-0.7265	-0.0726	-2.9482	-2.5235	0.422
3.5749	2.8471	-0.7277	-0.0728	-2.9531	-2.68137	0.271
2.8471	2.1206	-0.7265	-0.0726	-2.9482	-2.80206	0.146
2.1206	1.3933	-0.7273	-0.0727	-2.9515	-2.88743	0.064
1.3933	0.6658	-0.7276	-0.0728	-2.9524	-2.93745	0.014

10. Calculated from columns (8) and (9).
11. Calculated from columns (9) and (10).
12. Accel. or decel. of culvert Vel. Δt has a constant value of 10 secs, and is difference between successive time steps. Col. 12 is col. 11/col. 10.
13. Computer value of inertia head.
14. Head loss, difference between upper pool and lock water surface.
15. Total head loss. Col. 14 plus or minus col. 13.
16. Culvert Vel computer by $V = C\sqrt{2gh}$, where $C=C_n$ and $H=H_{L_n}$ at any step, i.
17. Percent difference from value in col. (10). Note If value in col. (16) differs from col. (10) by more than 1%, a new value of Δz_n is assumed and the computations in the step must be repeated.
18. Lock water surface at end of any step.
19. Total discharge, Q, into lock at end of any step.

(13)	(14)	(15)	(16)	(17)	(18)	(19)
$\times\frac{L'_c}{g}$	$H_n = Z_u - z_{n-1} - \Delta z_n$	$H_{L_n} = H_n \pm H_{m_n}$	$V_{c_n} = C_n \times \sqrt{2gH_{L_n}}$	% Diff. from V_{c_n}	$z_n = z_{n-1} + \Delta z_n$	$Q_n = V_{c_n} \times 2A_c$
)	(ft)	(ft)	(ft/sec)		(ft)	(cfs)
8396	2.090	4.9296	12.1994	-0.0403	536.15	5,675
8396	1.514	4.3536	11.4645	-0.3482	536.73	5,350
8396	0.972	3.8116	10.7272	-0.7185	537.27	5,024
9231	0.464	3.3876	10.1130	0.2822	537.78	4,689
9231	-0.0080	2.9152	9.3813	0.1825	538.25	4,354
9231	-0.4455	2.47763	8.6487	-0.5550	538.69	4,019
9232	-0.8480	2.07516	7.9151	-0.1065	539.09	3,684
9231	-1.2230	1.70012	7.1643	-0.5410	539.46	3,350
9232	-1.5480	1.37516	6.4433	-0.6111	539.79	3,014
9566	-1.8453	1.11123	5.7921	0.6553	540.09	2,676
9399	-2.1073	0.83257	5.0135	-0.3263	540.35	2,339
9566	-2.3340	0.62253	4.3352	0.7870	540.58	2,000
9482	-2.5235	0.42287	3.573021	-0.0513	540.77	1,662
9531	-2.68137	0.27181	2.864615	0.6141	540.93	1,324
9482	-2.80206	0.14616	2.100646	-0.9422	541.05	986
9515	-2.88743	0.06408	1.390856	-0.1763	541.13	648
9524	-2.93745	0.01495	0.671796	0.9034	541.18	310

es

value of 10 secs,
1. 12 is col. 11/col. 10.

ter surface.

$=H_{L_n}$ at any step, i.

f value in col. (16)
of Δz_n is assumed and

s

el

Notes:

Z_u = 538.0
z_n = 510.5 (when t=0)
A_s = 95,700 sq. ft. (lock water surface area)
L'_c = 1,305.5
k_c = 2.132
A_c = 232.5 sq. ft.
ave = average
secs = seconds
vel = velocity
col = column
accel = acceleration decel = deceleration

383

Table 9

Culvert Dimension, Bottom Longitudinal Lock

	Description and Location	Length ft	Upper End Height ft	Upper End Width ft	Lower End Height ft	Lower End Width ft	Average End Area sq ft
L_1	Downstream intake port to start of downward slope	10.00	20.00	15.00	20.00	15.00	300.00
L_2	Transition section	150.00	20.00	15.00	16.50	15.00	273.75
L_3	End of transition to valve well	50.00	16.50	15.00	16.50	15.00	247.50
L_4	Valve well	28.00	16.50	15.00	16.50	15.00	247.50
L_5	Valve well to divider	258.00	16.50	15.00	16.50	15.00	247.50
L_6	Transition	10.00	16.50	15.00	18.50	15.00	262.50
L_7	Curve at divider	120.00	2 × 8.25	15.00	2 × 8.25	15.00	247.50
L_8	Central culvert	60.00	18.50	15.00	12.00	26.00	294.75
L_9	Vertical divide section	80.00	12.00	2 × 12.00	12.00	2 × 12.00	288.00
L_{10}	Curve section to manifold	31.00	12.00	4 × 5.00	12.00	4 × 5.00	240.00
L_{11}	Manifold to first port	80.00	12.00	4 × 5.00	12.00	4 × 5.00	240.00

Table 10

Equivalent Culvert Lengths, Bottom Longitudinal Lock

Area No.	Area A sq ft	Length L ft	$\frac{A_v}{A}$	$L \times \frac{A_v}{A} = L'$
1	300.00	10.00	0.825	8.25
2	273.75	150.00	0.904	135.60
3	247.50	50.00	1.000	50.00
4	247.50	28.00	1.000	28.00
5	247.50	258.00	1.000	258.00
6	262.50	10.00	0.943	9.43
7	247.50	120.00	1.000	120.00
8	294.75	60.00	0.84	50.38
9	288.00	80.00	0.86	68.75
10	240.00	31.00	1.03	31.96
11	240.00	80.00	1.03	82.40
		L = 877.00		L' = 842.77

Note: $L'/g = 26.17$; $L'_{uv}/g = 6.89$.

APPENDIX A: NOTATION AND SYMBOLS

a	Acceleration
A	Area of opening or orifice
A_c	Area of one culvert at valve
A_c^*	Trial value of A_c
A_{ec}	Area of culvert of expanded section
A_m	Manifold-culvert area
A_p	Port area
A_s	Area of lock water surface, square feet
A_v	Area of valve opening
A_{vc}	Area of vena contracta
b	Height of valve opening
B	Height of culvert at valve
B_{ec}	Height of culvert at expanded section
C	Discharge coefficient
C_c	Contraction coefficient
C_L	Overall lock coefficient
C_n	Discharge coefficient during valve opening
d	Depth of overfill or overempty
d_e	Depth of overempty
d_f	Depth of overfill
D_1	Depth of flow at vena contracta
D_h	Hydraulic diameter (4R)
f	Resistance factor
F	Force
g	Acceleration of gravity (32.2 feet per second per second)
H	Head on a lock
H_L	Total head loss in culvert, valve and at exit
H_{L_c}	Total head loss through culvert excluding valve loss
H_{L_i}	Head loss for intake
H_{L_m}	Head loss for manifold for filling
$H_{L_{m_e}}$	Head loss for manifold for emptying
H_{L_v}	Head loss at partially open valve
$H_{L_{uc}}$	Head loss for intake plus culvert upstream from valve well
$H_{L_{uv}}$	Head loss upstream from valve face

H_m	Inertia head
H_{m_c}	Inertia head for entire lock culvert
$H_{m_{uc}}$	Inertia head for culvert upstream from valve well
$H_{m_{uv}}$	Inertia head for culvert upstream from valve face section
j	Inertia parameter
k	Head loss coefficient for a culvert system
k_c	Loss coefficient for all culvert losses, including exit with valve open
k_e	Loss coefficient for all losses for emptying, valve open
k_f	Same as k_c ; the f indicates filling operation
k_i	Loss coefficient for intake
k_b	Loss coefficient for bends in culvert
k_r	Loss coefficient for resistance in culvert
k_s	Loss coefficient for bulkhead slots
k_{ic}	Loss coefficient for culvert upstream of valve well
k_{uc}	Loss coefficient for intake plus culvert from intake valve to valve well
k_{uv}	Loss coefficient for all losses upstream of valve face
k_v	Loss coefficient for valve
k_{vw}	Loss coefficient for valve well
k_{m_f}	Loss at manifold for filling based on A_c
k_{m-m}	Loss at manifold for filling based on area at manifold culvert
k_{m_e}	Loss at manifold for emptying
k_{o_e}	Loss at outlet
L	Length
L_c	Length of culvert
L'_c	Equivalent length of culvert having section the same as reference section
L'_{uc}	Equivalent length of uniform culvert upstream from valve well
L'_{uv}	Equivalent length of uniform culvert upstream from valve face
M	Mass
n	Single value integer
N_p	Total number of ports
N_R	Reynolds number
P	Pressure; gauge pressure over vena contracta

P_a	Atmospheric pressure
P_v	Vapor pressure of water
q	Discharge in one culvert (cfs) at any instant
q_a	Average discharge of one culvert over Δt time period
Q	Discharge
r	Rate of rise of lock water surface, feet per minute; radius
r*	Radius of bend in a culvert
R	Hydraulic radius
R_e	Reynolds number
s	Submergence
t	Time
t_v	Valve opening time
T	Lock operation time
U	Valve time coefficient
V	Velocity
V_c	Mean velocity in reference section (culvert at valve)
V_{ec}	Mean velocity in expanded culvert
V_{vc}	Mean velocity in vena contracta
w	Weight
w*	width of a culvert
W	Width of culvert at valve
z	Elevation of lock water surface at any instant
Z	Elevation above some reference datum
Z_r	Elevation of culvert roof
Z_u	Elevation of upper pool water surface
Z_{vc}	Elevation of piezometric level over vena contracta
Z_{vw}	Elevation of valve well water surface
Δt	Time increment
Δz	Increment of change in lock water surface
σ	Cavitation index number
Ψ	Pressure reduction factor for expanded culvert
ν	Kinematic viscosity

$$H = Z_u - z \tag{1}$$

$$V = C\sqrt{2gH} \tag{2a}$$

$$Q = CA\sqrt{2gH} \tag{2b}$$

$$CA\sqrt{2gH}\,dt = -A_s dH \tag{3}$$

$$dt = \frac{-A_s dH}{CA\sqrt{2gH}} \tag{4}$$

$$t = \frac{2A_s}{CA\sqrt{2g}}\left(\sqrt{H_1} - \sqrt{H_2}\right) \tag{5}$$

$$T = \frac{2A_s}{C_L A\sqrt{2g}}\sqrt{H} + Ut_v \tag{6}$$

$$U = \frac{\Delta T}{\Delta T_v} \tag{7}$$

$$t = \frac{2A_s}{C2A_c\sqrt{2g}}\left(\sqrt{H_1 + d} - \sqrt{H_2 + d}\right) \tag{8a}$$

$$C = \frac{2A_s\left(\sqrt{H_1 + d} - \sqrt{H_2 + d}\right)}{2A_c\sqrt{2g}\;\;t_2 - t_1}. \tag{8b}$$

$$T = \frac{2A_s}{C_L 2A_c\sqrt{2g}}\left(\sqrt{H + d} - \sqrt{d}\right) + Ut_v \tag{9a}$$

$$T - Ut_v = \frac{2A_s}{C_L 2A_c\sqrt{2g}}\left(\sqrt{H + d} - \sqrt{d}\right) \tag{9b}$$

$$2A_c = \frac{2A_s\,(\sqrt{H + d} - \sqrt{d})}{C_L\sqrt{2g}\,(T - Ut_v)} \tag{9c}$$

$$C_L = \frac{2A_s(\sqrt{H + d} - \sqrt{d})}{2A_c\sqrt{2g}\,(T - Ut_v)} \tag{9d}$$

$$2A_c^* = \frac{2A_s\sqrt{H}}{\sqrt{2g}\,(T - Ut_v)} \tag{9e}$$

$$H_m = \frac{L}{g}\,\frac{dV}{dt} \tag{10}$$

$$L_c' = L_1\,\frac{A_c}{A_{c_1}} + L_2\,\frac{A_c}{A_{c_2}} + L_3\,\frac{A_c}{A_{c_3}} \cdots L_n\,\frac{A_c}{A_{c_n}} \tag{11a}$$

$$L_{uc}' = L_{uc_1}\,\frac{A_c}{A_{c_1}} + L_{uc_2}\,\frac{A_c}{A_{c_2}} \cdots L_{uc_n}\,\frac{A_c}{A_{c_n}} \tag{11b}$$

$$L_{uv}' = L_{uc_1}'\,\frac{A_c}{A_{c_1}} + {}^*L_{uc_2}\,\frac{A_c}{A_{c_2}} \tag{11c}$$

${}^*L_{uc_2}$ includes length of valve well.

$$H_{m_c} = \frac{\Delta V_c}{\Delta t}\,\frac{L_c'}{g} \tag{12a}$$

$$H_{m_{uc}} = \frac{\Delta V_c}{\Delta t}\,\frac{L_{uc}'}{g} \tag{12b}$$

$$H_{m_{uv}} = \frac{\Delta V_c}{\Delta t}\,\frac{L_{uv}'}{g} \tag{12c}$$

$$\Delta V_c = V_{c_n} - V_{c_{n-1}} \tag{13}$$

$$j = \frac{2A_c L}{A_s} \tag{14}$$

$$H_L = H \mp H_m \tag{15a}$$

$$H_{L_c} = H \mp H_m \text{ (when valve is fully open } H_L = H_{L_c}) \tag{15b}$$

$$H_{L_c} = H \mp H_m - H_{L_V} \text{ (during valve opening)} \tag{16}$$

$$H_{L_V} = H \mp H_m - H_{L_c} \tag{17}$$

$$H_{L_V} = H_L - H_{L_c} \tag{18}$$

$$H_{L_c} = (k_i + k_r + k_b + k_s + k_{vw} + k_m) \frac{V_c^2}{2g} \tag{19}$$

Note: Above equation includes exit loss and is applicable when valve is fully open.

$$H_{L_c} = k_c \frac{V_c^2}{2g} \text{ where } k_c = \sum \text{of loss factors in equation (19)} \tag{20}$$

$$\Delta Z_{vw} = Z_u - Z_{vw} \tag{21}$$

$$H_{L_{uc}} = \Delta Z_{vw} - V_c^2/2g \mp H_{m_{uc}} \tag{22}$$

$$H_{L_{uc}} = k_{uc} \frac{V_c^2}{2g} \quad (\text{where } k_{uc} = k_i + k_{ic}) \tag{23}$$

$$k_{u_c} = H_{L_{uc}} / V_c^2/2g \tag{24}$$

$$H_{L_{uv}} = H_{L_{uc}} + H_{L_{vw}} \tag{25}$$

$$H_{L_{uv}} = k_{uc} \frac{V_c^2}{2g} + k_{vw} \frac{V_c^2}{2g} \tag{26}$$

$$H_{L_{uv}} = k_{uv} \frac{V_c^2}{2g} \tag{27}$$

$$k_c = \frac{H \mp H_m}{V_c^2/2g} \quad (k_f \text{ is used for filling, valve open; } k_e \text{ is used for emptying, valve open}) \tag{28}$$

$$k = \frac{1}{C^2} \tag{29}$$

$$C = \frac{1}{\sqrt{k}} \tag{30}$$

$$k = k_c + k_v \quad (\text{Note: } k = k_c \text{ when valve is open}) \tag{31}$$

$$k_c = \frac{H_{L_c}}{V_c^2/2g} \tag{32}$$

$$k_v = \frac{H_{L_v}}{V_c^2/2g} \tag{33}$$

$$k_i = \frac{H_{L_i}}{V_c^2/2g} \text{ (from curves on Figure 47)} \tag{34}$$

$$k_r = \frac{Lf}{D_h} \tag{35}$$

$$k_{m_f} = \frac{H_{L_m}}{V_c^2/2g} \text{ (from curves on Figures 48, 49, and 50)} \tag{36}$$

$$k_{m_c} = \left(\frac{A_c}{A_m}\right)^2 k_{m-m} \tag{37}$$

$$k_{m_e} = \frac{H_{L_{m_e}}}{V_c^2/2g} \text{ (from curve on Figure 51)} \tag{38}$$

$$\Delta z = z_n - z_{n-1} \tag{39a}$$

$$z_n = z_{n-1} + \Delta z \tag{39b}$$

$$r = \frac{\Delta z}{\Delta t} 60 \tag{40}$$

$$q_{a_n} = \frac{\Delta z A_s}{2\Delta t} \tag{41}$$

$$V_{c_{a_n}} = \frac{q_{a_n}}{A_c} \tag{42}$$

$$V_{c_n} = 2V_{c_{a_n}} - V_{c_{n-1}} \tag{43}$$

$$V_{c_n} = 0 \text{ at } t = 0 \tag{44}$$

$$V_{c_{n-1}} = 0 \text{ at } t = 0 + \Delta t \tag{45}$$

$$Z_{vc} = Z_u - k_{uv}\, V_c^2/2g - V_{vc}^2/2g \mp H_{m_{uv}} + \psi\left(\frac{V_c^2}{2g} - \frac{V_{ec}^2}{2g}\right) \tag{46}$$

$$V_{vc} = \sqrt{2g\left[Z_u - k_{uv}\, V_c^2/2g - Z_{vc} + H_{m_{uv}} + \psi\left(\frac{V_c^2}{2g} - \frac{V_{ec}^2}{2g}\right)\right]} \tag{47}$$

$$C_c = \frac{V_c}{b/B\ V_{vc}} \tag{48}$$

$$V_{vc} = \frac{V_c}{C_c\ b/B} \tag{49}$$

Equations for loss at sudden expansion (valve)

$$H_{L_v} = \left(\frac{B}{bC_c} - 1\right)^2 \left(\frac{V_c^2}{2g}\right) \tag{50}$$

$$k_v = \left(\frac{B}{bC_c} - 1\right)^2 \tag{51}$$

$$C_c = \frac{B}{b(\sqrt{k_v} + 1)} \tag{52}$$

Cavitation index

$$\sigma = \frac{P + (P_a - P_v)}{V^2/2g} \tag{53}$$

APPENDIX B: EXCERPT FROM INTERNAL FLOW SYSTEMS BY DONALD S. MILLER

The material in this Appendix is an exact reproduction of Chapters 8 (9) (10) of the work Internal Flow Systems by Donald S. Miller (290 pp, 352 graphs and figures, 21 tables), 1978 c Copyright BHRA Fluid Engineering and Donald S. Miller of BHRA Fluid Engineering, Cranfield, Bedford, UK, and is used with permission.

Symbols, Non-dimensional Ratios and Pressure Definitions

Flow distribution parameters

In fluid mechanics the practice is to reduce all geometric and flow parameters to non-dimensional form by the selection of appropriate and generally accepted non-dimensionalising factors. It is only when a calculation for a particular flow situation is required that dimensional quantities are involved.

Present understanding of internal flows is not sufficient to develop non-dimensional parameters which describe flow distributions in such a manner that they can be used for component performance predictions. In order to have some general and 'engineeringly' useful descriptions of flow distributions the following are used in the text:

Thin boundary layer	- A flow which is nearly one-dimensional, such as that observed in the first diameter of pipe following a smooth contraction.
Thick Boundary layer	- A non-swirling flow which has a velocity and turbulence distribution appropriate to a pipe flow 10 diameters after a component such as a contraction, orifice plate, sudden expansion, screen or other device which does not create strong swirl.
Developed flow	- A flow which has traversed 30 or more diameters of straight pipe.

Symbols

The general practice is to define symbols as they occur in each chapter. Only the principle symbols are listed below.

		Units			Units
A	cross-sectional area	m^2	N	diffuser length	m
A	constant		P	total pressure	N/m^2 (Pa)
a	pressure wave velocity	m/s	ΔP	total pressure loss	N/m^2 (Pa)
B	constant		P_r	perimeter (wetted perimeter)	m
b	width or breadth	m	p	static pressure	N/m^2 (Pa)
C	correction factor		Q	flow rate	m^3/s
C	constant		Q^*	non-dimensional flow	
C_p	pressure recovery coefficient		R	radius	m
			Re	Reynolds number	
D	hydraulic diameter		r	radius	m
	$(4A/P_r)$	m	t	time	s
d	pipe diameter	m	Δt	time step	s
f	friction coefficient		U	mean velocity	m/s
g	gravity	m/s^2	ΔU	velocity change	m/s
H	total head	m	W	width	m
H^*	non-dimensional head				
ΔH	total head loss	m	γ	specific weight	N/m^3
h	head	m	θ	angle	degrees
K	loss coefficient		μ	absolute viscosity	Ns/m^2
k	roughness coefficient	m	ν	kinematic viscosity	m^2/s
L	length	m	ρ	density	kg/m^3
l	length	m	σ	cavitation parameter	

Pressure definitions

Hydraulic engineers often deal with fluids flowing from one level to another, for example from one reservoir to another. In describing system performance it is appropriate to use differences in levels or heads expressed in metres of fluid. Low speed air and gas flows are usually measured using manometers which register pressures as a displacement of a fluid column. For these and other reasons it has become common, in certain branches of fluid mechanics, to use the term total head and velocity head in preference to total pressure and velocity pressure. This practice is followed in the present text as it reduces the monotonous use of pressure terms and follows the convention adopted with SI units of continuing, where appropriate, to express pressures in terms of "pressure heads". It should always be remembered that although heads are taken as the height of a liquid column the units of head are those of pressure, N/m^2 (height of liquid column (m) X density (kg/m^3) X gravity (m/s^2)).

static pressure	- the pressure acting equally in all directions at a point in a fluid.
velocity pressure	- given by $1/2\rho U^2$, also called the kinematic pressure.
total pressure	- the sum of the static and velocity pressures.
total pressure loss	- the difference in total pressures between two points related to a common datum. As all pressure losses in the text are total pressure losses the words total and pressure are often dropped.
gauge pressure	- the pressure above or below local atmospheric pressure, if the gauge pressure is less than atmospheric pressure it is also called the vacuum pressure.
absolute pressure	- the pressure above zero, given by the sum of the local atmospheric pressure and the gauge pressure.
atmospheric (barometric) pressure	- the local pressure measured with a barometer.
standard atmospheric pressure	- equal to 101.325 kN/m^2
vapour pressure	- the pressure exerted when a liquid is in equilibrium with its own vapour.
piezometric or hydraulic head	- the head above a datum to which fluid rises in a tube connected to a tapping in a pipe or passage, or the water level in a reservoir.
velocity head	- given by $U^2/2g$
total head	- the sum of the piezometric and velocity head.
total head loss	- the difference in total head between two points related to a common datum. As all head losses in the text are total head losses the words total and head are often dropped.
pump head	- head generated by a pump given by the piezometric head difference across the pump plus the difference in velocity heads between outlet and inlet.
vapour head	- the head in fluid exerted when a liquid is in equilibrium with its own vapour.

8. Friction in Pipes and Passages

8.1. INTRODUCTION

In this chapter the procedures for determining friction losses in straight pipes and passages are outlined. Except for section 8.5. on laminar flow, Reynolds numbers are assumed to be above 5×10^3, which normally guarantees turbulent flow in engineering systems. If the Reynolds number is less than 2×10^3 the flow will be laminar and if disturbed will return to the laminar condition. Between Reynolds numbers of 2×10^3 and 5×10^3 is an area of uncertainty. If the Reynolds number exceeds 2.5×10^3 and the flow at inlet to the pipe is disturbed by a sharp edged inlet, partially open valve or other high loss component, the turbulence generated is likely to persist.

Due to the development of the velocity profile in the initial section of a pipe or passage, higher losses occur than with developed flow. Losses in the initial section of a pipe, over and above developed flow friction losses, are accounted for in the losses attributed to the upstream component.

The pressure loss in a length of pipe is given by:

$$\Delta H = f \frac{L}{D} \frac{U^2}{2g} \text{ (m of fluid)} \qquad 8.1a$$

$$\Delta P = f \frac{L}{D} \rho \frac{U^2}{2} \text{ (N/m}^2\text{)} \qquad 8.1b$$

where f is the friction coefficient

L is the pipe or passage length (m)

D is the pipe diameter or the hydraulic diameter (m) given by:

$$D = \frac{4 \times \text{cross-sectional area}}{\text{wetted perimeter}} \qquad 8.2$$

U is the mean velocity

In calculating system losses it is desirable to treat pipes in the same manner as components and use a pipe loss coefficient given by:

$$K_f = f \frac{L}{D} \qquad 8.3$$

Friction coefficients are dependent on Reynolds number, on relative roughness and on cross-sectional shape. Friction coefficients for circular cross-sections are presented in terms of Reynolds number, Re, and relative roughness, k/D. Friction coefficients for non-circular cross sections are obtained by applying a correction factor to the circular cross-section values.

Warning: Two definitions for friction coefficients are in widespread use which differ by a factor of four. The definition adopted here is the most appropriate for use in a consistent method for calculating system head losses.

8.1.1. ROUGHNESS VALUES

The main difficulty in calculating friction losses is the uncertainty in selecting a value of pipe roughness. Suggested roughness values are given in Table 8.1. An allowance must be added to new pipe values to account for deterioration in service brought about by surface deposits, erossion, corrosion, bacterial slimes and growths and marine and fresh water fouling. Experience of similar systems is the best guide to selecting roughness values and deterioration allowances. Pipes conveying water pose particular problems because of wide variation of pH, dissolved gasses and chemical content. If the water is not aggressive, scale forming, treated or chlorinated a roughness value of 1mm is appropriate after several years service, otherwise a roughness of 2 mm is suggested. For chlorinated, untreated, clear, filtered water, that is not scale forming or aggressive, a roughness value of 0.5 mm is suggested after several years service.

Table 8.1. Roughness Values, k

		mm
1. Smooth pipes*		
	Drawn brass, copper, alluminium, etc.	0.0025
	Glass, plastic, perspex, fibre glass, etc.	0.0025
2. Steel pipes		
	New smooth pipes	0.025
	Centrifugally applied enamels	0.025
	Light rust	0.25
	Heavy brush ashphalts, enamels and tars	0.5
	Water mains with general tuberculations	1.2
3. Concrete pipes		
	New, unusually smooth concrete with smooth joints	0.025
	Steel forms first class workmanship with smooth joints	0.025
	New, or fairly new, smooth concrete and joints	0.1
	Steel forms average workmanship smooth joints	0.1
	Wood floated or brushed surface in good condition with good joints	0.25
	Eroded by sharp material in transit, marks visible from wooden forms	0.5
	Precast pipes good surface finish average joints	0.25
4. Other pipes		
	Sheet metal ducts with smooth joints	0.0025
	Galvanised metals normal finish	0.15
	Galvanised metals smooth finish	0.025
	Cast iron uncoated and coated	0.15
	Asbestos cement	0.025
	Flexible straight rubber pipe with a smooth bore	0.025
	Corrugated plastic pipes+ (apparent roughness)	3.5
	Mature foul sewers	3.0

*extruded, cast and pipes formed on mandrels may have imperfections that can increase roughness by a factor of 10.

+ commercial corrugated plastic pipes in the 40 to 100 mm diameter size range have corrugation crest length to depth ratios of about 1.5. Increasing the crest length to depth ratio from 1.5 to 5 may double the friction coefficient.

Precautions against deterioration in service are:

1. Good initial surface finish to minimise areas of low velocity where deposits can begin to form in the wakes caused by roughness.

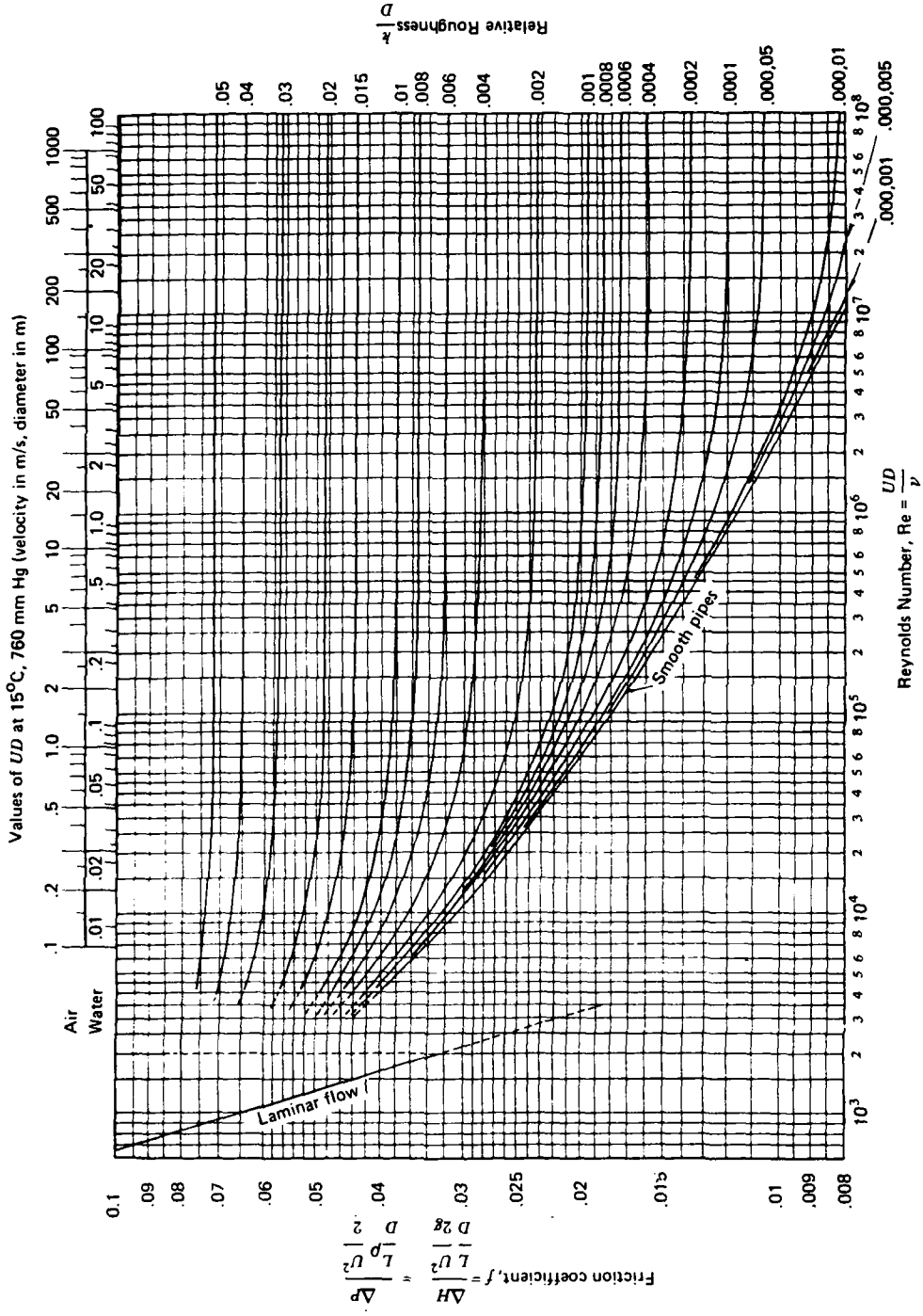

Fig. 8.1. Moody Chart

2. Adequate initial protection to prevent corrosion and erosion.
3. Chlorination of water to prevent slimes and the growth of both fresh and salt water mussels and other fouling. Continuous water velocities in excess of 2 m/s are usually required in order that the wall shear stress is sufficiently high to discourage settlement and to hinder feeding of barnacles and other marine organisms.
4. When corrosion is a severe problem in pipes carrying untreated water it may be necessary to de-oxygenate the water. Similarly if hydrogen sulphide is present it may be necessary to remove it.

8.1.2. ACCURACY OF FRICTION CALCULATIONS

Friction calculations involve an element of judgement in selecting roughness values. At high Reynolds numbers an error of 100 percent in a roughness value causes about a 10 percent error in friction coefficient. As head losses vary inversely with at least the fourth power of the diameter, actual not nominal pipe diameters must be used.

For new pipes with estimated friction coefficients less than 1.2 times the smooth pipe friction coefficient, in which there is no fouling or deterioration of the walls, the head loss can be predicted with an accuracy of 5 percent, provided the pipe diameter is known to within 0.5 percent. Friction coefficients for similar pipes, but with estimated friction coefficients less than 1.5. times the smooth pipe values, can be predicted with an accuracy of about 10 percent.

Typical allowances, where deterioration in service is expected, are 25 to 50 percent of new pipe values, but much higher allowances may be necessary where growths, deposits or slimes are expected.

8.2. PIPES OF CIRCULAR CROSS SECTION (CLASS 1 SUBJECT TO THE RESTRICTIONS OF 8.1.2.)

The accepted presentation of friction coefficients is the Moody Chart, Fig. 8.1. which is a plot of the Colebrook-White equation. The Colebrook-White equation requires an itterative solution and is not recommended for computer or calculator calculations. An equation of similar accuracy to the Colebrook-White equation which allows the friction coefficient to be obtained directly is:

$$f = \frac{0.25}{\left[\log\left(\frac{k}{3.7D} + \frac{5.74}{Re^{0.9}}\right)\right]^2} \qquad 8.4$$

8.3. NON-CIRCULAR CROSS-SECTIONS

8.3.1. RECTANGULAR CROSS-SECTIONS

Using the hydraulic diameter in equations 8.1 and 8.3 allows friction coefficients from Fig. 8.1 and equation 8.4 to be used for rectangular passages of aspect ratio less than 10 (class 1 subject to the restrictions of 8.1.2). At higher aspect ratios there are indications that the hydraulic diameter concept may result in underestimation of friction losses. For aspect ratios above 10 the hydraulic diameter used in the Reynolds number equation should correspond to an aspect ratio of 10 passage (- from equation 8.3 the hydraulic diameter for an aspect ratio 10 passage is 1.82 times the passage height) but the true hydraulic diameter should be used in calculating the head loss (class 2).

8.3.2. CONCENTRIC ANNULI (CLASS 2)

Using the hydraulic diameter concept, friction coefficients for concentric annuli lie within about 1.05 of those given by equation 8.4 and Fig. 8.1, so:

$$f_{annular} = 1.05 f_{circular} \qquad 8.5$$

The perimeter in equation 8.2 for the hydraulic diameter is given by $(d_2 - d_1)$ where d_1 and d_2 are the inner and outer annulus diameters.

8.3.3. ECCENTRIC ANNULI (CLASS 2)

Correction factors to apply to equation 8.5 to account for eccentricity are given in Fig. 8.2.

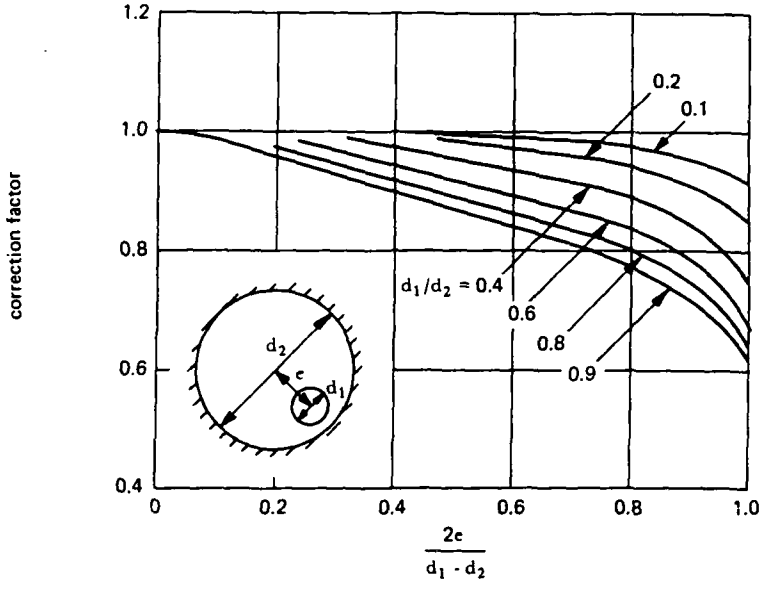

Fig. 8.2.

8.3.4. PASSAGES OF OTHER CROSS-SECTIONAL SHAPES (CLASS 3)

Replacing U in equation 8.1a by Q/A and D by $4A/P_r$, where Q is the total flow, A is the cross-sectional area and P_r is the perimeter, gives:

$$\Delta H = \frac{fLQ^2}{8g} \frac{P_r}{A^3} \qquad 8.6$$

Within passages having shapes that depart significantly from circular or rectangular it is possible to fit another cross-sectional shape with a ratio of P_r/A^3 smaller than for the full cross-section. In the areas not encompassed by the minimum P_r/A^3 shape there is little flow and these areas can be neglected in calculating head losses. Example 4 in the next section demonstrates the method of calculation.

8.4. CALCULATION OF HEAD, FLOW OR PIPE SIZE

When the pipe size, flow rate and roughness are known the Reynolds number and roughness ratio can be calculated and a friction coefficient found from equation 8.4 or Fig. 8.1, example 1. A direct solution for flow rate or pipe diameter is possible if only pipe friction is involved, but the calculations are much more involved and prone to error than a simple trial and successive approximation approach. Head loss in pipes and components vary approximately with the square of the flow rate and inversely as the fourth to fifth power of the diameter. Small changes in flow or pipe size have, therefore, a large effect on head losses, leading to rapid convergence in a trial and a successive approximation solution; examples 2 and 3 demonstrate the procedure. Estimates of head loss, or flow or pipe size obtained from pipe manufacturers' catalogues and from direct solution charts should always be checked by solving equation 8.1.

Example 1

Given Q, L, D, ν, k; find head loss.
Calculate the head loss for air flowing in a 0.2 m square cross-section passage 25 m long given:

$Q = 0.8\ m^3/s$ air density= $1.23\ kg/m^3$
Kinematic viscosity = $1.45 \times 10^{-5}\ m^2/s$ surface roughness k = 0.025 mm

Solution

from equation 8.2. $$D = \frac{4A}{P_r} = \frac{4 \times 0.2^2}{4 \times 0.2} = 0.2\ m$$

relative roughness $$= \frac{k}{D} = \frac{0.025 \times 10^{-3}}{0.2} = 1.2 \times 10^{-4}$$

mean velocity $$U = \frac{Q}{A} = \frac{0.8}{0.2 \times 0.2} = 20\ m/s$$

Reynolds number $$\mathrm{Re} = \frac{DU}{\nu} = \frac{0.2 \times 20}{1.45 \times 10^{-5}} = 2.8 \times 10^5$$

From equation 8.4.

$$f = \frac{0.25}{\left[\log\left(\frac{k}{3.7D} + \frac{5.74}{\mathrm{Re}^{0.9}}\right)\right]^2} = \frac{0.25}{\left[\log\left(\frac{1.2 \times 10^{-4}}{3.7} + \frac{5.74}{(2.8 \times 10^5)^{0.9}}\right)\right]^2}$$

$$= 0.0158$$

For a Reynolds number of 2.8×10^5 and a relative roughness of 1.2×10^{-4} the friction coefficient from Fig. 8.1 is also 0.0158.

From equation 8.3.

$$K_f = f\frac{L}{D} = 0.0158 \times \frac{25}{0.2} = 1.975$$

Head loss $$\Delta H = K_f\frac{U^2}{2g} = \frac{1.975 \times 20^2}{2 \times 9.81} = 40.3\ m \text{ of air}$$

$$= 49.6\ mm \text{ of water}$$

Example 2

Given ΔH, L, D, ν, k, find the flow rate Q.
Water at 15°C flows by gravity between two tanks in a system consisting of 50mm diameter pipes and components. The combined loss coefficient for the components is $K_t = 6.5$ for Reynolds numbers above 10^5. If the total length of the straight pipes is 40 m, determine the flow for a head differential between the tanks of 6 m. Assume the pipe is smooth.

kinematic viscosity = 1.14×10^{-6} m^2/s

Solution

First trial

Assume $f = 0.015$ which lies in the middle of the smooth curve in Fig. 8.1.

pipe loss coefficient $\quad K_f = f\frac{L}{D} = \frac{0.015 \times 40}{50 \times 10^{-3}} = 12$

head loss $\quad \Delta H = 6 \text{ m} = (K_f + K_t)\frac{U^2}{2g}$

mean velocity $\quad U = \sqrt{\frac{6 \times 2 \times 9.81}{(12 + 6.5)}} = 2.52 \text{ m/s}$

Reynolds number $\quad \text{Re} = \frac{UD}{\nu} = \frac{2.52 \times 50 \times 10^{-3}}{1.14 \times 10^{-6}} = 0.111 \times 10^6$

from Fig. 8.1. $\quad f = 0.0178$

Second trial

Assume $\quad f = 0.0178$

$$K_f = \frac{12 \times 0.0178}{0.015} = 14.2$$

$$U = 2.52\sqrt{\frac{12 + 6.5}{14.2 + 6.5}} = 2.38 \text{ m/s}$$

$$\text{Re} = 0.111 \times 10^6 \times \frac{2.38}{2.52} = 0.105 \times 10^6$$

from Fig. 8.1 $f = 0.0179$ which agrees with the assumed value to within the accuracy of Fig.8.1.

Flow $\quad Q = UA = 2.38 \times 0.785 \times 50^2 \times 10^{-6}$

$= 4.68 \times 10^{-3}$ m^3/s

Example 3

Given ΔH, Q, L, ν, k, find the diameter.

0.58 m^3 of water at 15°C has to flow through a constant diameter system with a head loss of not more than 3 m of w.g. The system consists of a number of sections of straight new steel pipe with a total length of 145 m and a number of components. The estimated total loss coefficient for the components is $K_t = 2.9$ at Reynolds numbers above 10^6. Determine the minimum pipe and component diameter required.

kinetic viscosity = 1.14×10^{-6} m^2/s

From Table 8.1. hydraulic roughness $k = 0.025$ mm

Solution

First trial

Assume diameter $D = 0.6$ m

mean velocity $U = \dfrac{Q}{A} = \dfrac{0.58}{0.785 \times 0.6^2} = 2.052$ m/s

Reynolds number $\mathrm{Re} = \dfrac{UD}{\nu} = \dfrac{2.052 \times 0.6}{1.14 \times 10^{-6}} = 1.08 \times 10^6$

relative roughness $= \dfrac{k}{D} = \dfrac{0.025}{600} = 0.000{,}042$

From Fig. 8.1. friction coefficient $f = 0.0123$

pipe loss coefficient $K_f = f\dfrac{L}{D} = 0.0123 \times \dfrac{145}{0.6} = 2.973$

head loss $\Delta H = (K_t + K_f)\dfrac{U^2}{2g}$

$= \dfrac{(2.973 + 2.9)}{2 \times 9.81} \times 2.052^2$

$= 1.260$ m of w.g.

Second trial

Assume diameter $D = 0.5$ m

mean velocity $U = 2.052 \times \left(\dfrac{0.6}{0.5}\right)^2 = 2.955$ m/s

Reynolds number $\mathrm{Re} = 1.08 \times 10^6 \times \dfrac{0.6}{0.5} = 1.3 \times 10^6$

relative roughness $\dfrac{k}{D} = 0.000{,}05$

From Fig. 8.1. friction coefficient $f = 0.0123$

pipe loss coefficient $K_f = f\dfrac{L}{D} = 0.0123 \times \dfrac{145}{0.5} = 3.567$

head loss $\Delta H = 6.467 \times \dfrac{2.9552}{2 \times 9.81} = 2.878$ m of w.g.

Minimum pipe and component size is 0.5 m.

Example 4

Determine the approximate head loss per metre for a flow of 10^{-3} m^3/s of water in the triangular cross-section shown in Fig. 8.3. Assume the walls are smooth and the water temperature is 15°C with a kinetic viscosity of 1.14×10^{-6} m^2/s.

Cross-sections similar to that shown in Fig. 8.3. have a long perimeter for their area compared to a circular cross-section, and have very non-uniform velocities around the perimeter. Parts of the passage with a long perimeter surrounding a small part of the cross-section, such as the shaded area, are filled with slow moving fluid and can be neglected in calculating head loss.

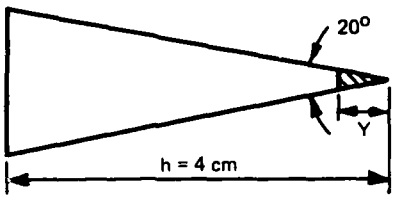

Fig. 8.3

Equation 8.6. shows that if within the cross-section a shape can be drawn that has a smaller geometric ratio P_r/A^3 it will have a lower friction loss. By filling in the shaded area of Fig. 8.3 in steps of $y = 0.05h$, and plotting the ratio of P_r/A^3 filled in to P_r/A^3 for the complete section against y, it is found that the ratio is a minimum at about $y = 0.15h$.

Solution

Area $A = 40 \times 40 \times \tan 10^\circ \times (1-0.15^2) = 275.8 \text{ mm}^2$

Perimeter $P_r = \dfrac{40 \times 2}{\cos 10^\circ} \times 0.85 + 40 \times 2 \times \tan 10^\circ \times 1.15 = 85.27 \text{ mm}$

Hydraulic diameter $D = \dfrac{4A}{P_r} = \dfrac{4 \times 275.8}{85.27} = 12.94 \text{ mm}$

Mean velocity $U = \dfrac{Q}{A} = \dfrac{10^{-3}}{275.8 \times 10^{-6}} = 3.626 \text{ m/s}$

Reynolds number $\text{Re} = \dfrac{UD}{\nu} = \dfrac{3.626 \times 0.01294}{1.14 \times 10^{-6}} = 4.12 \times 10^4$

From Fig. 8.1. or equation 8.4. friction coefficient, $f = 0.0218$

Head loss per metre $\Delta H = f\dfrac{L}{D}\dfrac{U^2}{2g}$

$$= 0.0218 \times \frac{1}{0.0129} \times \frac{3.626^2}{2 \times 9.81} = 1.13 \text{ m of w.g.}$$

Note: In practice the ratio P_r/A^3 would be a minimum if the corners were filled in using circular arcs, the minimum value of P_r/A^3 being found by calculation. However, for the present illustrative purposes the small error is not important.

8.5. LAMINAR FLOW

Developed laminar flow loss coefficients can be expressed as:

$$f = \frac{C_f}{\mathrm{Re}} \qquad 8.7$$

where C_f = 64 for circular cross-sections
= 56 for square cross-sections
= 96 for an infinitely wide two-dimensional passage

C_f values for a number of cross-sectional shapes are given in Figs. 8.4. to 8.6.

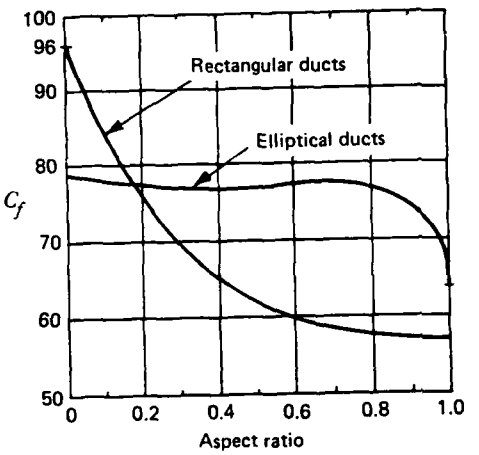

Fig. 8.4. Laminar flow coefficients - rectangular and elliptical cross-section

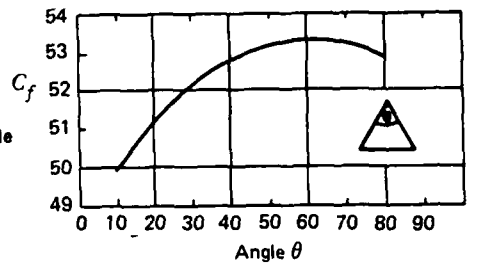

Fig. 8.5. Laminar flow coefficients - isoscles triangle

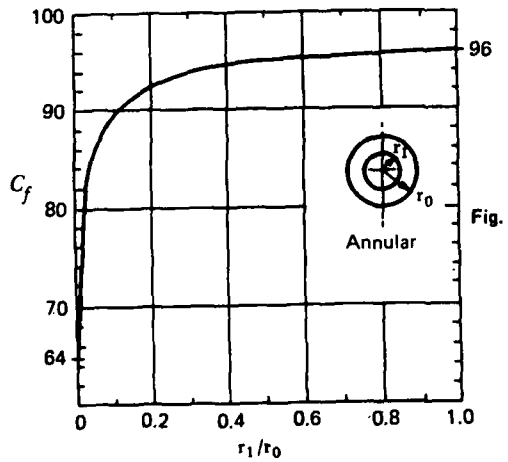

Fig. 8.6. Laminar flow coefficients - annular cross-sections

Notes on Chapter 8

Equation 8.4. for calculating friction coefficients is due to:

1. Swamee, P.K. and Jain, A.K., *Explicit Equations for Pipe-Flow Problems*, Proc. A.S.C.E. J. Hydraul. Div. **102**, HY5, pp. 657-664. (May 1976)

This equation is one of a number of explicit and exponential equations proposed for calculating friction coefficients instead of the implicit Colebrook-White equation. Although historically the Colebrook-White equation was the first equation to provide friction coefficients that are reasonable approximations to experimental sand roughness and commercial pipe data, it is extremely unfortunate that it was not shortly followed by the adoption of an explicit formula. The continued use of Colebrook-White equation by the fluid mechanics community has undoubtably resulted in a number of easier to use, but dimensionally incorrect equations, remaining in widespread engineering use. The challenge provided by the implicit form of the Colebrook-White equation has involved much academic ingenuity in devising methods of direction solution for pipe size or flow rate. It is to be hoped that the fluid mechanics community will standardise on equation 8.4. or a similar equation and halt the proliferation of explicit equations.

Much of the literature of flow in non-circular pipes is contained in:

2. Zanker, K.J. and Barratt, G.M., *Data on the correlation of pressure losses in straight non-circular pipes flowing full*, BHRA report TN 909, 33 pp. (January 1968).

More recent work on rectangular passages can be found in:

3. Jones, O.C., *An improvement in the calculation of turbulent friction in rectangular ducts*, Tran. A.S.M.E. J. Fluids Eng., series I, **98**, 2, pp. 173-181. (June 1976)

The eccentric annuli correction factors are based upon:

4. Jonsson, V.K. and Sparrow, E.M. *Experiments on turbulent-flow phenomena in eccentric annular ducts*, J. Fluid Mech., **25**, 1, pp. 65-86. (May 1966)

The calculation method for passages with a large perimeter compared to a circular cross-section of equal area is taken from:

5. Miller, D.S., *Internal flow: a guide to losses in pipe and ducts systems*, Cranfield, Bedford: BHRA. 329 pp. (1971)

The literature on flow in corrugated pipes can be accessed through references in:

6. Shipton, R.J. and Grange, A.M., *Flow in corrugated pipes*, Proc. A.S.C.E. J. Hydraul. Div., **102**, HY9, pp.1343-1351. (September 1976)

9. Turning Flow-Bends

9.1. INTRODUCTION

The presentation of loss coefficient data is made using circular cross-section bends of constant area. Data for other cross-sections and bend geometries is referred back to circular cross-section bends where this is appropriate. It is recommended that the text and example in Section 9.2. be worked through before using other sections.

Bend loss coefficients, K_b, vary markedly with Reynolds number and, usually to a lesser extent, with inlet and outlet pipe arrangements and with surface roughness.

Basic loss coefficients, K_b^*, are defined at a Reynolds number of 10^6 for bends with long and hydraulically smooth inlet and outlet pipes or passages. Correction factors are given to correct the loss coefficient to any other Reynolds number and outlet pipe or passage length. Allowance is made for roughness by multiplying the smooth pipe loss coefficient by the ratio of the rough to smooth friction coefficients as found from the data in Chapter 8. When the roughness correction exceeds 1.4 the validity of the correction is questionable but so will be the accuracy to which the friction coefficient is known.

When a bend is located in close proximity to other components corrections for interaction effects are necessary. For bend-bend and bend-diffuser interactions, see Chapters 10 and 12.

Except for data on commercial bends in Section 9.10., the loss coefficients given are for accurately manufactured bends matched to their inlet and outlet pipes or passages.

9.2. CIRCULAR CROSS-SECTION BENDS OF CONSTANT AREA

Geometric parameters for circular arc bends are shown in Fig. 9.1. The important bend parameters are the radius ratio, r/d, and the bend deflection angle, θ_b.

Head losses due to a bend are made up of losses within the bend and losses associated with flow redevelopment after the bend. The head loss and Reynolds number equations are:

$$\Delta H = K_b \frac{U^2}{2g}$$

$$\mathrm{Re} = \frac{Ud}{\nu}$$

where U is the mean inlet velocity
and ν is the kinematic viscosity

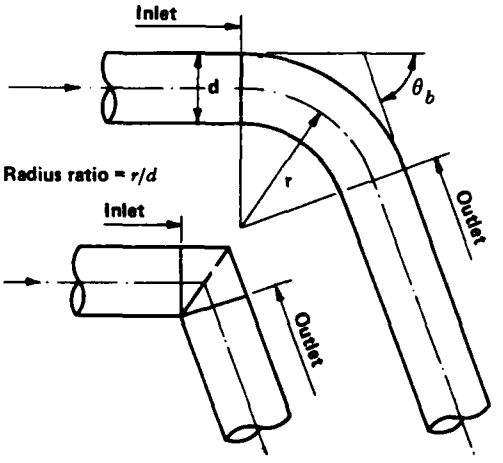

Fig. 9.1. Circular cross-section bend geometries

9.2.1. BASIC COEFFICIENTS K_b^* (CLASS 1)

Basic loss coefficients at a Reynolds number of 10^6 are given in Fig. 9.2.

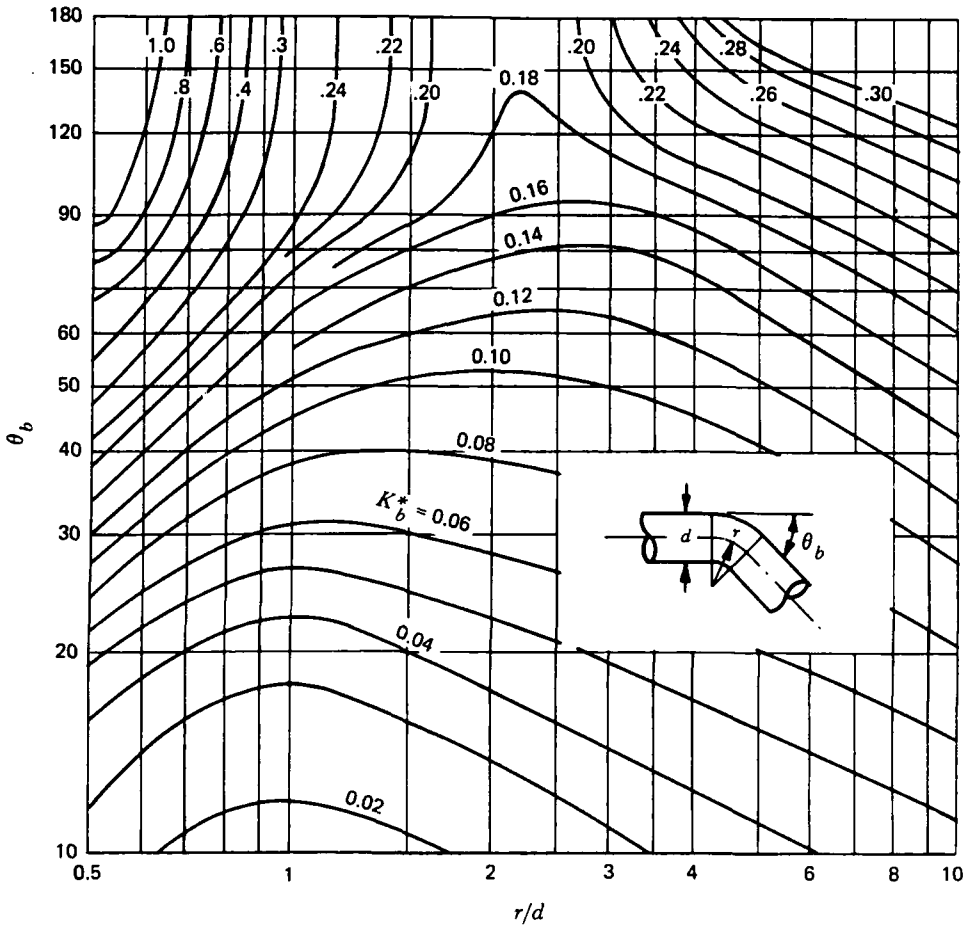

Fig. 9.2. Loss coefficients, K_b^* for circular cross-section bends (Re = 10^6)

9.2.2. REYNOLDS NUMBER CORRECTION C_{Re} (CLASS 2 FOR $Re > 10^6$, CLASS 1 FOR $Re < 10^6$)

The Reynolds number correction C_{Re} to be applied to the basic coefficients K_b^* are given in Fig. 9.3. Only part of the loss due to bends of $r/d < 1$ is strongly Reynolds number dependent. For $r/d > 0.7$ or $K_b^* < 0.4$ use the correction factors for $r/d = 1$ bends (class 2), otherwise the correction factor is given by (class 3):

$$C_{Re} = \frac{K_b^*}{K_b^* - 0.2\,(C_{Re} \text{ from Fig 9.3 for } r/d = 1) + 0.2}$$

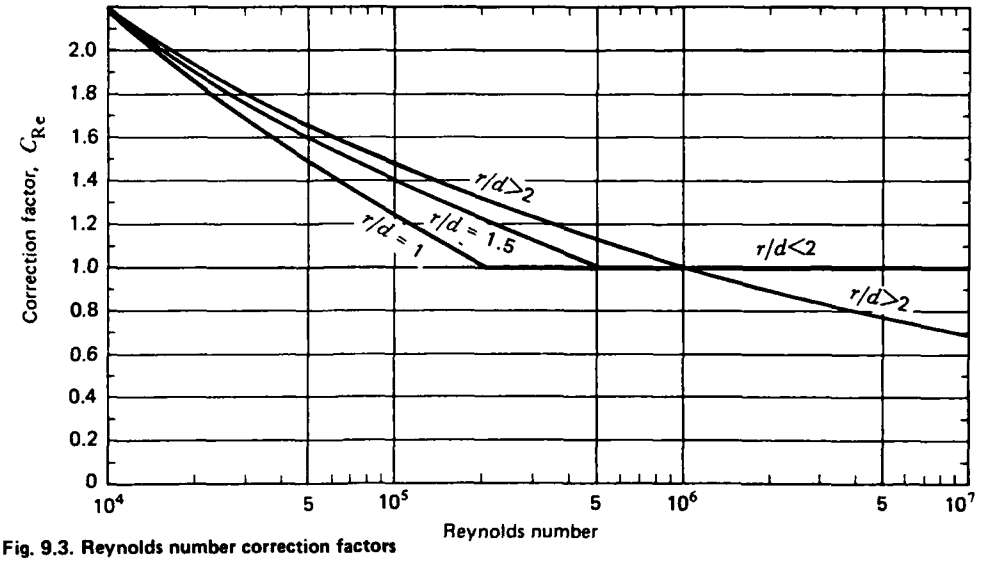

Fig. 9.3. Reynolds number correction factors

9.2.3. OUTLET PIPE LENGTH CORRECTION C_o (CLASS 3)

Outlet pipe length correction factors to be used with the basic coefficients are given in Fig.9.4. Using the basic coefficient K_b^* from Fig. 9.2. along with the outlet tangent length obtain outlet correction from Fig. 9.4. If $r/d > 3$ and/or $\theta_b > 100^o$ outlet tangent correction factors are closer to unity.

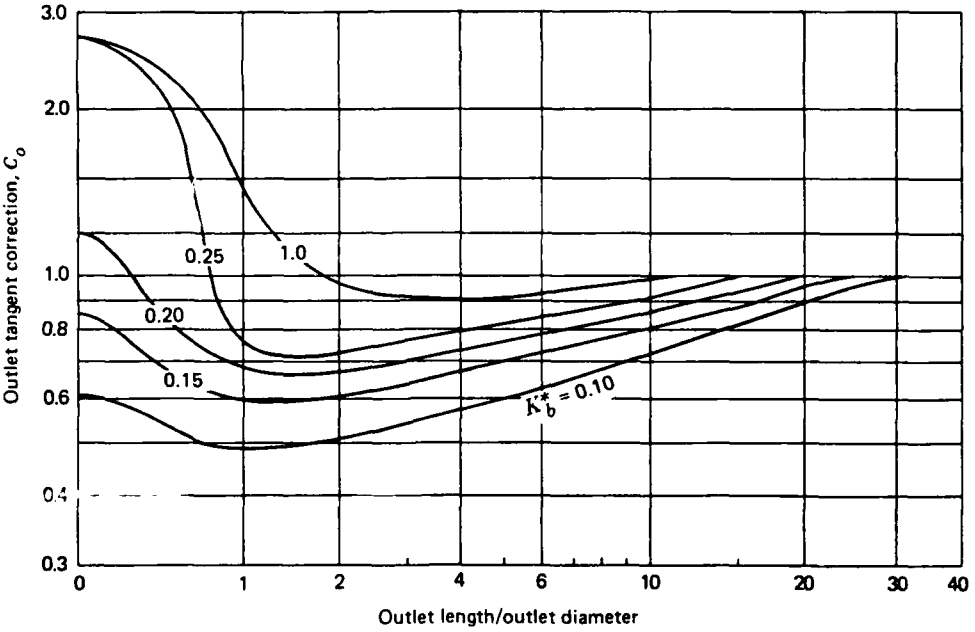

Fig. 9.4. Outlet tangent correction

Note: If the bend or pipe discharges to a large space there is a loss of one velocity head from the system so the loss coefficient must be increased by 1.0.

Tabulated in Table 9.1. are loss coefficients for r/d = 1 and 2 bends of 90° with short outlet pipes. Values are given for thick and thin inlet boundary layers. Separation is responsible for the high coefficient of the r/d = 2 bend with no outlet pipe and a thin boundary layer. The same bend with a thick inlet boundary layer has strong secondary flows which prevent separation.

Table 9.2.1.
Loss coefficients for 90° bends with short outlet pipes at Reynolds number of 10^6 (Class 1)

r/d	outlet length (pipe diameters)	Loss coefficients*	
		thin boundary layer	thick boundary layer
1	0	0.64	0.70
1	1	-	0.22
1	4	-	0.18
2	0	0.31	0.19
2	1	0.12	0.11

*excludes loss in pipe and one velocity head loss if pipe discharges to a large space.

9.2.4. ROUGHNESS CORRECTION C_f (CLASS 3)

The roughness correction is given by:

$$C_f = \frac{f_{rough}}{f_{smooth}}$$

where f_{smooth} is the friction coefficient for a hydraulically smooth pipe

f_{rough} is the friction coefficient found using the assumed pipe and bend roughness

Friction coefficients are found from Chapter 8 using the bend inlet Reynolds number and the assumed roughness for the pipe and bend.

9.2.5. CORRECTED LOSS COEFFICIENT K_b

The corrected bend loss coefficient is given by:

$$K_b = K_b^* \times C_{Re} \times C_o \times C_f$$

and the head loss is given by:

$$\Delta H = K_b \times \frac{U^2}{2g}$$

9.2.6. EFFECT OF INLET PIPE LENGTH (CLASS 2)

Provided inlet pipe lengths comply with the following requirements the loss coefficients in Section 9.2.5. will not normally underestimate head losses:

1. More than two inlet pipe diameters when the bend follows another component which has a loss coefficient of less than 0.25 at Re = 10^6
2. More than four pipe diameters when the bend follows another component which has a loss coefficient greater than 0.5 at Re = 10^6.

9.2.7. EXAMPLE

Estimate the system loss between the inlet to a 90^{o} bend of $r/d = 2$ and the end of the outlet pipe for the following outlet conditions:

a) an outlet pipe of 30 diameters

b) with the bend directly discharging into an infinite expansion chamber

c) with a 2 diameter outlet pipe connected to another component

The pipe diameter is 0.6m, and the mean velocity 4 m/s, the kinematic viscosity is 1.14×10^{-6} m^2/s and the pipe and bend roughness is 0.02mm.

$$\text{Reynolds number } Re = \frac{Ud}{\nu} = \frac{4 \times 0.6}{1.14 \times 10^{-6}} = 2.1 \times 10^{6}$$

Basic coefficient from Fig. 9.2. $K_b^* = 0.16$

Reynolds number correction from Fig. 9.3. $C_{Re} = 0.89$

Outlet tangent correction from Fig. 9.4. for $K_b^* = 0.16$

a) $L/d = 30$, $C_o = 1.0$

b) $L/d = 0$, $C_o = 0.9$

c) $L/d = 2$, $C_o = 0.62$

Roughness correction from Section 9.2.4.

$$C_f = \frac{f_{rough}}{f_{smooth}} = \frac{0.0114}{0.0103} = 1.11$$

Corrected loss coefficient from Section 9.2.5.

a) $K_b = 0.16 \times 0.89 \times 1.0 \times 1.11 = 0.158$

b) $K_b = 0.16 \times 0.89 \times 0.9 \times 1.11 = 0.142$

c) $K_b = 0.16 \times 0.89 \times 0.62 \times 1.11 = 0.098$

Total head loss = bend loss + friction loss

a) $\Delta H = (0.158 + 30 \times 0.0114) \frac{4^2}{2 \times 9.81} = 0.41\text{m}$

b) $\Delta H^{\dagger} = (0.142 + 1) \frac{4^2}{2 \times 9.81} = 0.93\text{m}$

c) $\Delta H = (0.098 + 2 \times 0.0114) \frac{4^2}{2 \times 9.81} = 0.10\text{m}$

† included in the head loss is the one velocity head associated with a discharge into an infinite space.

9.3. RECTANGULAR CROSS-SECTION BENDS OF CONSTANT AREA

Geometric parameters for circular arc bends of rectangular cross section are shown in Fig. 9.5. The important geometric parameters are the radius ratio r/W, the bend deflection angle θ_b and the aspect ratio b/W. The length of the inlet and outlet passage is always referred to in terms of hydraulic diameters D where:-

$$D = \frac{4 \times \text{cross sectional area}}{\text{perimeter}} = \frac{4 \times b \times W}{2(b + W)}$$

The Reynolds number is given by:-

$$\text{Re} = \frac{UD}{\nu}$$

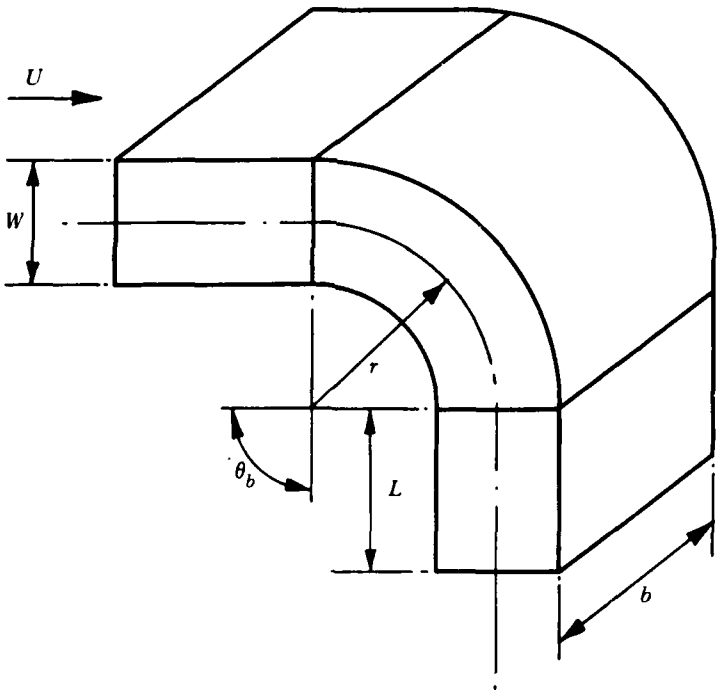

Fig. 9.5. Rectangular cross-section bend geometries

9.3.1. BASIC COEFFICIENTS K^*_b (CLASS 1)

Basic loss coefficients at a Reynolds number of 10^6 are plotted on Fig. 9.6. for rectangular bends of aspect ratio 0.5, Fig. 9.7. for rectangular bends of aspect ratio 1.0, and Fig. 9.8. for bends of aspect ratio 2.0.

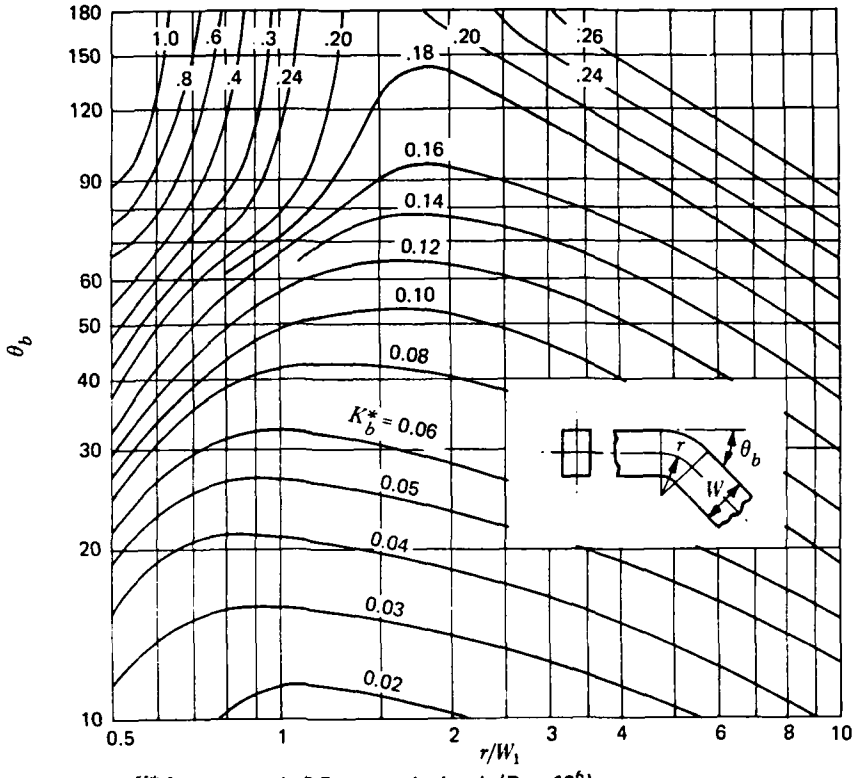

Fig. 9.6. Loss coefficient K_b^* for aspect ratio 0.5 rectangular bends (Re = 10^6)

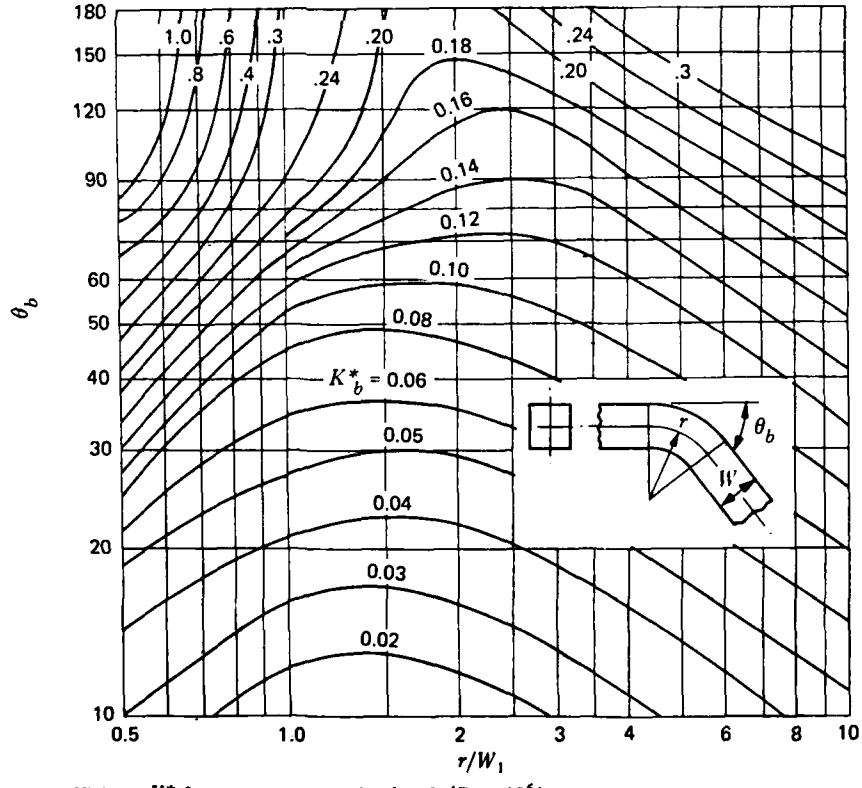

Fig. 9.7. Loss coefficients K_b^* for square cross-section bends (Re = 10^6)

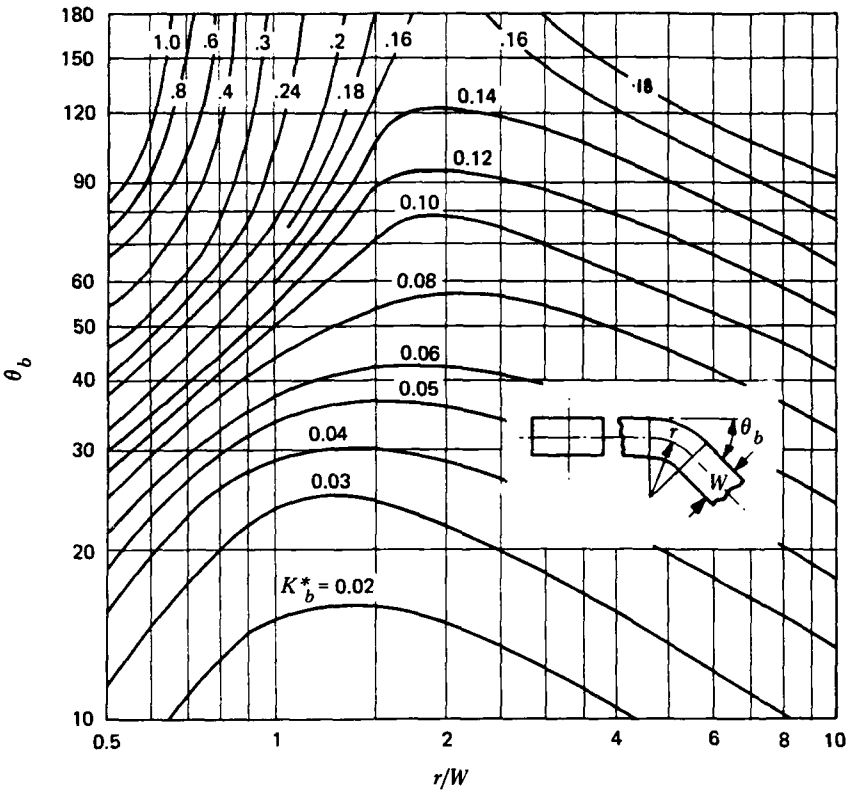

Fig. 9.8. Loss coefficients K^*_b for aspect ratio 2 rectangular bends (Re = 10^6)

9.3.2. REYNOLDS NUMBER CORRECTION C_{Re} (CLASS 2)

Use the circular cross-section Reynolds number correction from Section 9.2.2. replacing r/d by r/W.

9.3.3. OUTLET DUCT LENGTH CORRECTION C_o (CLASS 2)

Use the circular cross-section outlet duct correction from Fig. 9.4. but modified as follows:

1. Aspect ratios $b/W < 0.7$ and $L/D > 1$, use $C_{o\ rectangular} = 1 - (1 - C_{o\ circular})/2$
2. Aspect ratios $b/W < 0.7$ and $L/D < 1$, use $C_{o\ rectangular} = C_{o\ circular}$
3. Aspect ratios $b/W > 1.0$ and $L/D > 1$, use $C_{o\ rectangular} = C_{o\ circular}$
4. Aspect ratios $b/W > 1.0$ and $L/D < 1$, use values of C_o for circular cross-sections except for bends of r/W between 1.5 and 3 when the basic coefficient K^*_b should be multiplied by 2.

A number of loss coefficients for rectangular bends with short outlet tangents are given in Tables 9.2 and 9.3. The loss coefficients do not include the friction loss in the outlet pipe or the loss of one velocity head if the outlet pipe discharges to a large space.

Table 9.2.
90^{o} bend loss coefficients with short outlet pipes at a Reynolds number of 10^{6}

r/W	outlet passage length in passage widths W	Aspect ratio	
		0.5	2.0
1	0	0.75	0.74
1	0.5	0.59	0.73
1	1.0	0.34	0.36
1	2.0	0.20	0.22
2	0	0.17	0.25
2	0.5	-	0.20
2	1.0	0.14	0.11

Table 9.3.
45^{o} bend loss coefficients aspect ratio = 2 at a Reynolds number of 10^{6}

r/W	outlet passage length in passage widths W	Loss coefficient
1	0	0.28
1	0.5	0.18
1	1.0	0.07
2	0	0.11
2	0.5	0.07
2	1.0	0.06

9.3.4. ROUGHNESS CORRECTION C_f (CLASS 3)

Use the same correction as for circular cross-sections (see Section 9.2.4.).

9.3.5. CORRECTED LOSS COEFFICIENTS K_b

Corrected loss coefficients are given by:-

$$K_b = K^*_b \times C_{\mathrm{Re}} \times C_o \times C_f$$

9.3.6. EFFECT OF INLET PASSAGE LENGTH (CLASS 2)

Using the loss coefficient found in Section 9.3.5. it is unlikely that head losses will underestimate provided the inlet passage length exceeds $4D$.

9.4. SINGLE MITRE BENDS (CIRCULAR CROSS-SECTION CLASS 1, RECTANGULAR CROSS-SECTION CLASS 2)

9.4.1. BASIC COEFFICIENT K_b^*

Basic loss coefficients, K_b^*, are plotted against angle in Fig. 9.9. for circular and rectangular cross-section mitre bends.

9.4.2. CORRECTION TO BASIC COEFFICIENTS (CLASS 3)

Use the Reynolds number correction from Section 9.2.2. for $r/d < 0.7$ and the outlet pipe length corrections of Fig. 9.4. Roughness corrections should be made using Section 9.2.4. and the inlet pipe limitations as in Section 9.2.6.

9.5. 90° COMPOSITE MITRE BENDS

9.5.1. BASIC COEFFICIENTS K_b^* (CIRCULAR CROSS-SECTION CLASS 1, RECTANGULAR CROSS-SECTION CLASS 2)

Basic loss coefficients K_b^* are plotted against r/d or r/W in Fig. 9.10.

9.5.2. CORRECTIONS TO BASIC COEFFICIENTS (CLASS 3)

Use the Reynolds number corrections from Fig. 9.3. and the outlet pipe corrections from Fig. 9.4. Roughness corrections should be made using Section 9.2.4. and the inlet pipe limitations as in Section 9.2.6.

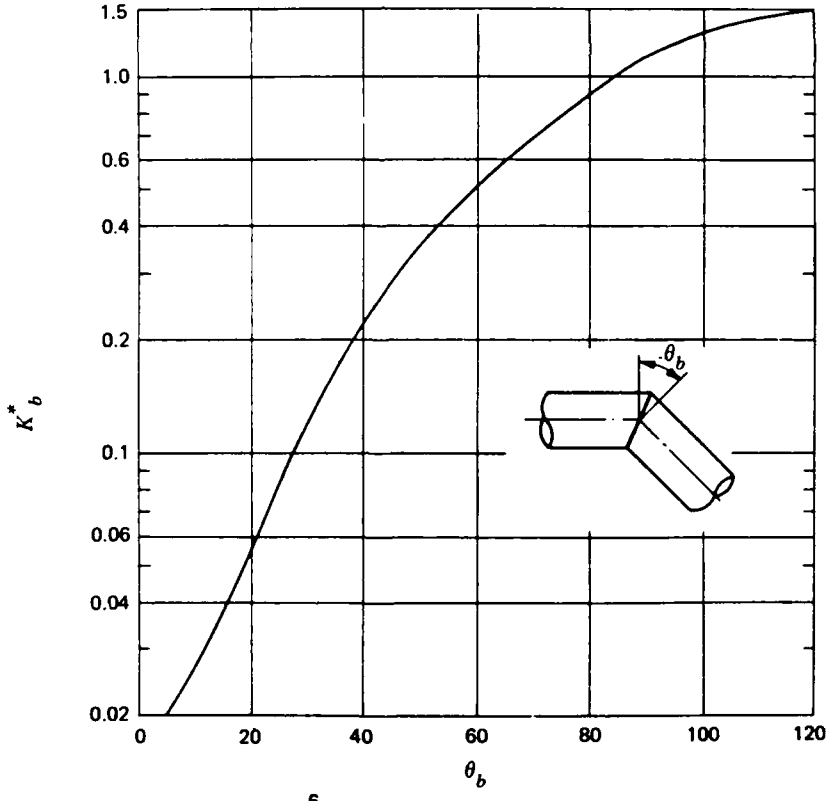

Fig. 9.9. Mitre bend loss coefficients (Re = 10^6)

9.6. VARIABLE AREA AND VARIABLE RADIUS RATIO BENDS BETWEEN PIPES OR PASSAGES OF EQUAL AREA

9.6.1. BENDS OF VARIABLE AREA (CLASS 2)

When it is necessary to use a bend having a variable area, minimum losses will be achieved if the inner radius is made as large as possible and the area through the bend is never less than the pipe or passage area. Typical examples of loss coefficients for variable area bends are shown in Fig. 9.11. for a Reynolds number of 10^6. To correct for Reynolds number use the $r/d < 1$ curve of Fig. 9.2.3. (class 3). These values can be used for rectangular and circular bends.

9.6.2. BENDS OF VARYING RADIUS RATIO

Loss coefficients are least if the rate of turning is reduced towards the outlet of a bend, as in the arrangement shown on Fig. 9.12. Two examples of 90^o bends made up of two 45^o bends of different radius ratios are compared in Table 9.4. with a 90^o bend of $r/d = 1.5$.

Table 9.4.
90^o composite bend loss coefficients for bends of circular cross-section

bend configuration	K^*_b
45^o $r/d = 1$ + 45^o $r/d = 2$	0.16
45^o $r/d = 2$ + 45^o $r/d = 1$	0.20
90^o $r/d = 1.5$	0.18

These values can be corrected for Reynolds number, outlet tangent and roughness using Section 9.2.

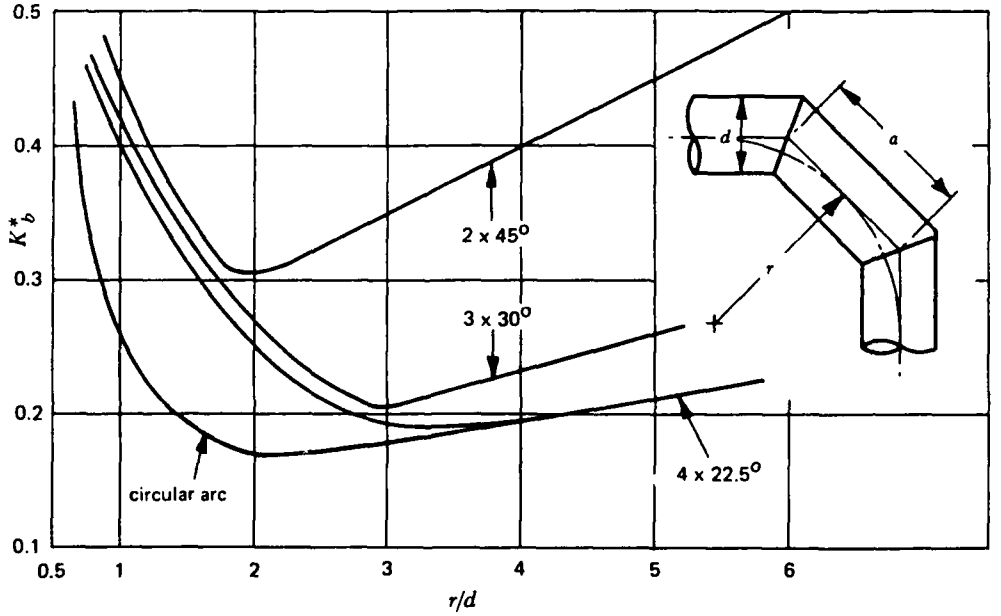

Fig. 9.10 Composite mitre bends – calculations are made using the equivalent circular arc r/d values where:

$r = \frac{a}{2} \cot \frac{90^o}{2n}$ **and n = number of individual bends**

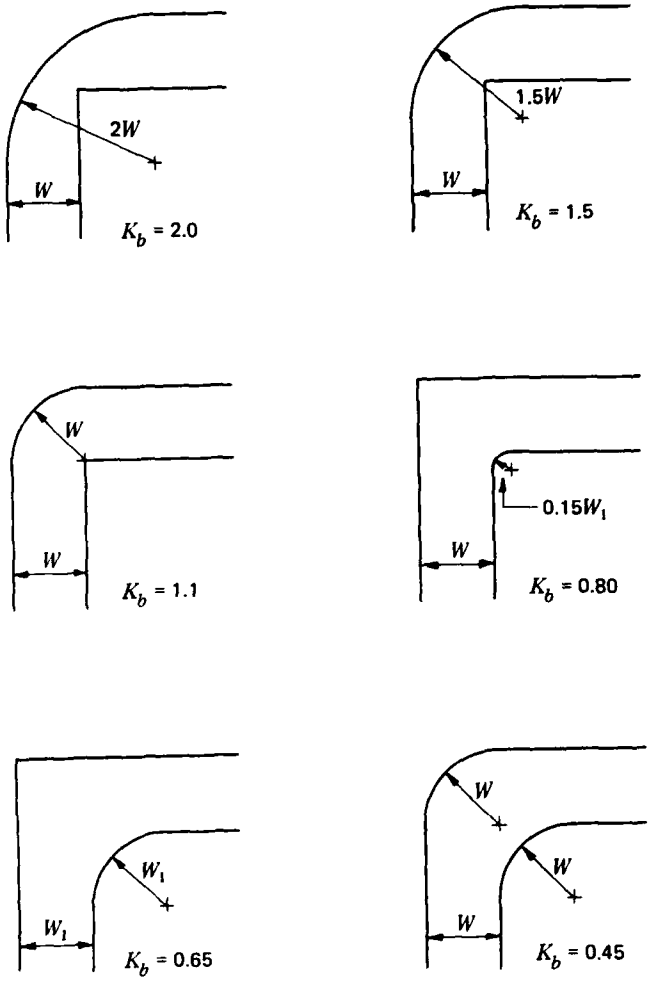

Fig. 9.11. Variable area bend loss coefficients K^*_b

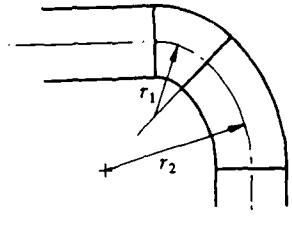

Fig. 9.12. Variable radius ratio bends

9.7. 180° ANNULAR BENDS (CLASS 2)

The geometric arrangement of the annular bends considered is shown on Fig. 9.13.

The loss coefficients for flow from the pipe to the annulus and flow from the annulus to the pipe are based upon the pipe velocity. The head loss is given by:

$$\Delta H = K_b \frac{U^2}{2g}$$

where, U, is the mean pipe velocity

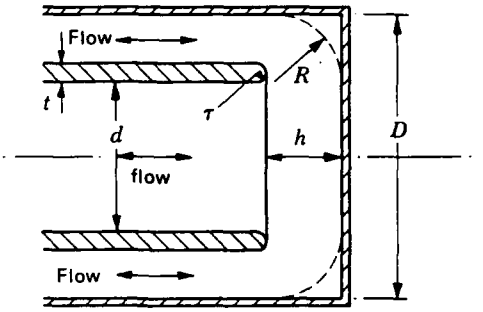

Fig. 9.13. Annular bend geometries

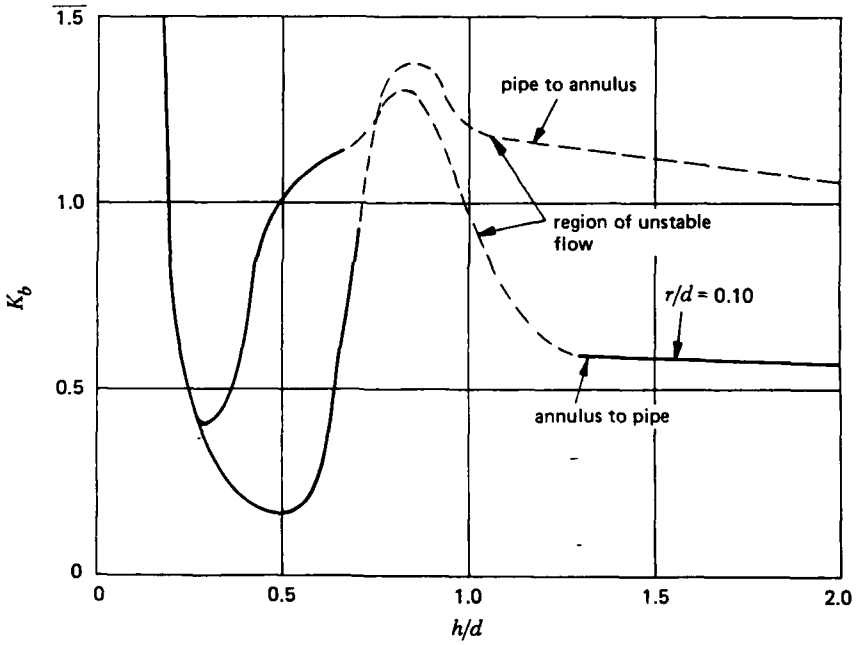

Fig. 9.14. Annular bend loss coefficient variation with h/d for equal areas

Fig. 9.14 is a plot of loss coefficient against h/d ratio for the two flow directions with equal pipe and annulus areas.

The shape of the curves in Fig. 9.14 shows that:

1. If h/d is small losses are high due to contraction of the flow.
2. There is an optimum range h/d for minimum losses.
3. Losses rise rapidly as h/d is increased above the optimum. This is due to flow remaining attached to the end wall and not turning immediately into the pipe or annulus. The flow in this region is extremely unstable and loss coefficients may vary by a factor of 2.
4. In the case of flow from the annulus to the pipe, when h/d is sufficiently large for the end wall to no longer influence the main flow, coefficients fall to values close to those at optimum h/d.

9.7.1. PIPE TO ANNULUS

Basic loss coefficients, K^*_b , are tabulated in table 9.5. for flow from the pipe to the annulus with the optimum h/d.

Table 9.5.
Pipe to annulus loss coefficients

Area ratio annulus/pipe	optimum h/d range	r/d	t/d	Loss coefficient K^*_b
0.75	0.4 - 0.8	0.05	0.1	0.19
1.08	0.5 - 0.8	0.05	0.1	0.43
2.05	0.6 - 0.9	0.05	0.1	0.34
0.75	0.4 - 0.6	0	0.1	0.24
1.08	0.5 - 0.6	0	0.1	0.40
2.05	0.8 - 1.0	0	0.1	0.34
0.76	0.3 - 0.5	0.1	0.2	0.16
1.06	0.3 - 0.5	0.1	0.2	0.23
2.07	0.6 - 1.0	0.1	0.2	0.32
0.76	0.4 - 0.5	0	0.2	0.22
1.06	0.4 - 0.5	0	0.2	0.26
2.07	0.7 - 0.9	0	0.2	0.40
0.8	0.2 - 0.5	0.2	0.4	0.30
1.07	0.3 - 0.5	0.2	0.4	0.20
2.10	0.2 - 1.0	0.2	0.4	0.40
0.8	0.3 - 0.5	0	0.4	0.36
1.07	0.3 - 0.4	0	0.4	0.26
2.10	0.5 - 0.9	0	0.4	0.30

Loss coefficients are mildly dependent on the t/d ratio and on the R/D ratio. Loss coefficients are about 0.05 higher for an R/D = 0 compared to an R/D = 0.3 which is the optimum R/D ratio.

9.7.2. ANNULUS TO PIPE

Basic loss coefficients K^*_b are tabulated in table 9.6. for flow from the annulus to the pipe with the optimum h/d. The values also apply to h/d values greater than 1.5.

Loss coefficients vary markedly with t/d. For t/d less than 0.1, the minimum value for which loss coefficients are given in Table 9.6., the coefficients may be double the t/d = 0.1 value. Local thickening and rounding of the pipe can halve the loss coefficient.

Loss coefficients are only mildly dependent on r/d for values less than about 0.4., with an optimum at 0.3.

Table 9.6.
Annulus to pipe loss coefficients

Area ratio annulus/pipe	optimum h/d range	r/d	t/d	Loss coefficient K^*_b
0.75	0.18 - 0.22	0.5	0.10	1.90
1.08	0.24 - 0.33	0.5	0.10	1.04
2.05	0.33 - 0.66	0.5	0.10	0.50
0.75	0.23 - 0.27	0	0.10	1.70
1.08	0.27 - 0.34	0	0.10	1.0
2.05	0.35 - 0.45	0	0.10	0.44
0.76	0.18 - 0.23	0.10	0.20	0.96
1.06	0.20 - 0.29	0.10	0.20	0.40
2.07	0.28 - 0.40	0.10	0.20	0.20
0.76	0.22 - 0.28	0	0.20	1.10
1.06	0.23 - 0.33	0	0.20	0.45
2.07	0.22 - 0.48	0	0.20	0.50
0.80	0.22 - 0.30	0.20	0.40	0.70
1.07	0.18 - 0.28	0.20	0.40	0.32
2.10	0.17 - 0.50	0.20	0.40	0.16
0.8	0.30 - 0.38	0	0.40	0.72
1.07	0.26 - 0.36	0	0.40	0.40
2.1	0.20 - 0.40	0	0.40	0.40

9.8. VANED BENDS

By using vanes the loss coefficient of a mitre bend can be reduced to that of the lowest loss circular arc bend. The general arrangement of a vaned bend and details of the vanes are given in Fig. 9.15.

The number of vanes N is given by:

$$N = \frac{1.8W}{R} - 1 \text{ to the nearest whole number}$$

where W = the duct height (mm) shown in Fig. 9.15.
R = the vane radius given in Table 9.7.

Table 9.7.

Pipe diameter or passage width (mm)	Vane radius (mm)
100 - 200	20 - 30
200 - 400	30 - 50
500 - 800	60 - 80

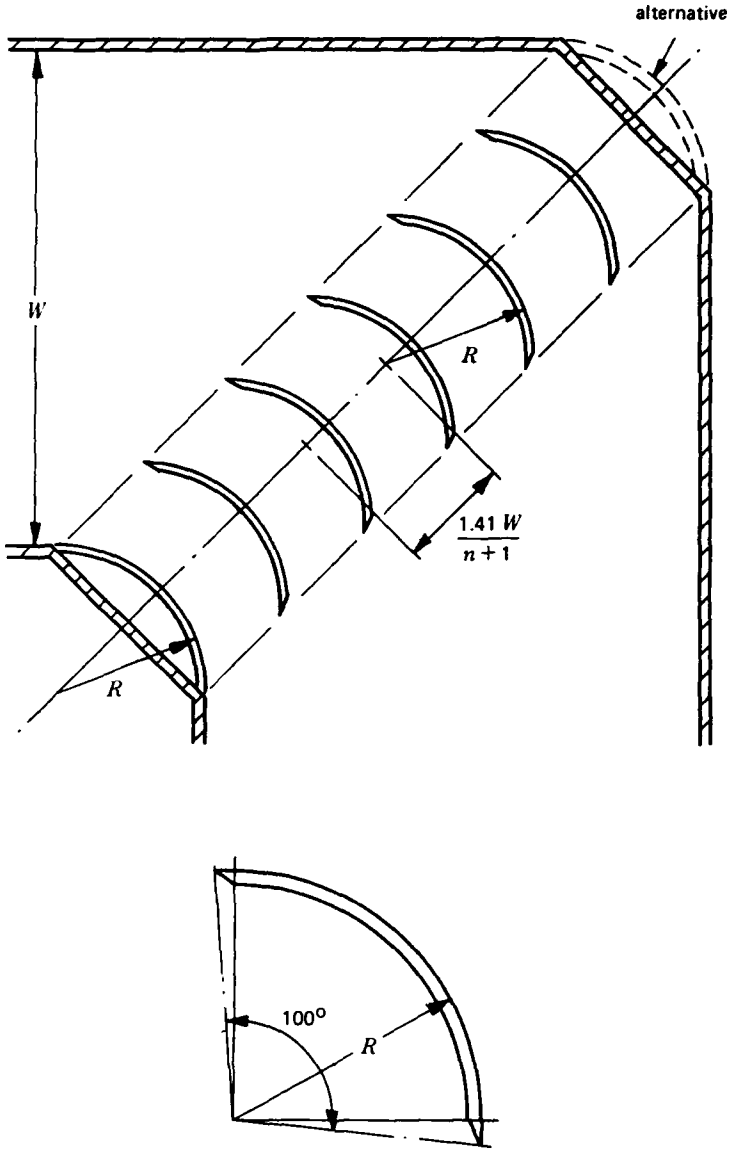

Fig. 9.15. Vaned bend geometry

The vanes can usually be cut from standard tube. Ideally vanes should be closer together on the inside of the bend, but because of strength requirements the vane thickness may be such as to cause excessive blockage on the inside of the bend. Fluctuating forces occur in vaned bends which may exceed the calculated steady dynamic loads. Allowance should be made for fluctuating forces in strength calculations.

Vanes within circular arc bends are only justified if the bend radius ratio, r/d, is less than 1 and the vanes are thin and occupy less than 5 percent of the cross-sectional area. For radius ratios greater than 0.7 a single vane located at $R = \sqrt{r_i r_o}$ should be used. r_i and r_o being the inner and outer bend radius respectively. A vane at this location reduces the loss coefficient of a $r/d = 0.7$. bend by half and a $r/d = 1$ bend by 20 percent.

9.9. COILS (CLASS 2)

The geometric parameters of the coils considered are shown in Fig. 9.16. The coil is assumed to be hydraulically smooth.

The length of the coil excluding the inlet and outlet pipe is given by:-

$$L = \pi D.n \left[1 + P^2/4D^2\right]^{0.5}$$

where D is the coil diameter
P is the mean pitch
n is the number of turns

For a Reynolds number range of 1.5×10^4, to 10^5, the loss coefficient K_b is given by:-

$$K_b = (0.32\mathrm{Re}^{-0.25} + 0.048\ (d_i/D)^{0.5}) \times L/d_i$$

where $\mathrm{Re} = \dfrac{d_i U}{\nu}$

and d_i is the inside diameter

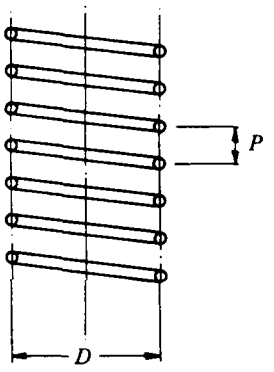

Fig. 9.16. Coil geometry

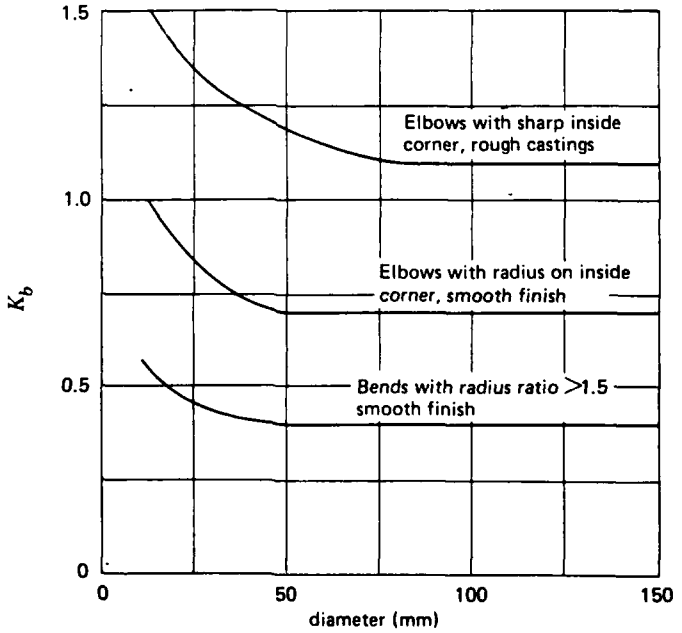

Fig. 9.17. Commercial pipe bend loss coefficients

9.10. COMMERCIAL BENDS - SCREWED, FLANGED, COMPRESSION AND CAPILLARY (CLASS 3)

Approximate loss coefficients are given in Fig. 9.17 for single bends with angles $\geqslant 90^{o}$. For bends of less than 90^{o} use a percentage of the 90^{o} loss coefficient e.g. for a 60^{o} bend use 2/3 of the 90^{o} loss coeficient.

9.11. LAMINAR FLOW IN BENDS (CLASS 2)

Approximate loss coefficients for laminar flow through 90^{o} bends with radius ratio between 1.5 and 3 are shown on Fig. 9.18.

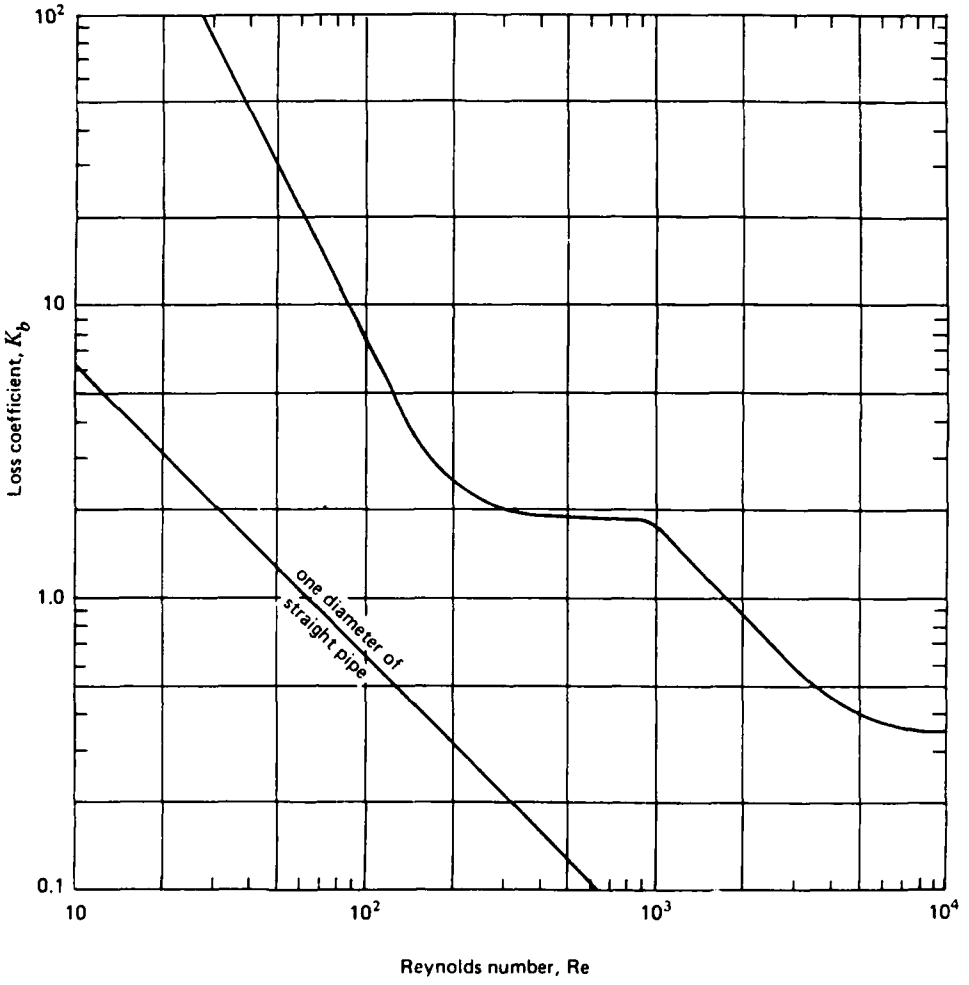

Fig. 9.18. Approximate loss coefficients for bends of r/d between 1.5 and 3.0 at low Reynolds numbers

Notes on Chapter 9

The loss coefficients for cicular arc bends are taken from:

1. Miller, D.S., *Internal flow: a guide to losses in pipe and duct systems*, Cranfield, Bedford. BHRA, 329 pp. (1971).
2. Ito, H, *Pressure losses in smooth pipe bends*, Rep. Inst. High Speed Mechanics, Tohoku Univ., **12**, 99. 41-62, (1960/61).

Variable area bend data is based upon:

3. Sprenger, H., *Pressure head losses in 90° bends for tubes or ducting of rectangular cross-section*, BHRA report T1027, 17 pp. (October, 1969). (Translated from Schweiz. Bauzeit. **87**, 13, pp. 223-231, 27 March 1969)

The information in 180° annular bends is due to:

4. Idel'chik, I.E. and Ginzburg, Ya.L., *The hydraulic resistance of 180° annular bends*, Thermal Eng., **15**, 4, pp. 109-114. (1968)

References and formula for flow in coils are given in:

5. Srinvasan, P.S., Nandapukar, S.S. and Holland, F.A., *Friction factors for coils*, Trans. Instn. Chem. Engrs., **48**, 4-6, pp. T156-T161 (July/August 1970)

10. Correcting for Bend-Bend Interactions

10.1. INTRODUCTION

This chapter is concerned with correcting the bend loss coefficients of Chapter 9 to account for interaction between bends. If the bends are separated by a spacer of more than 30 diameters interaction effects are not important. Neglecting interaction effects will usually result in an overestimate of head losses, except for mitre and radius ratio less than one bends which require a 4 diameter spacer to guarantee a correction factor less than unity.

The procedure is to multiply the combined loss coefficients for two bends by an interaction correction factor $C_{b\text{-}b}$:

$$K_{b\text{-}b} = (K_{b_1} + K_{b_2})\, C_{b\text{-}b} \qquad 10.1$$

where K_{b_1} and K_{b_2} are bend loss coefficients from Chapter 9.

Friction losses within spacers are calculated as for pipes or passages.

The correction factors apply to bend - spacer - bend combinations with a long pipe after the second bend. When the outlet pipe is less than 30 diameters long an estimate of the effect of the short outlet pipe can be made using an outlet pipe correction from Chapter 9.2.

10.1.1. REYNOLDS NUMBER (CLASS 2)

Interaction correction factors for bends of circular cross-section apply to Reynolds number above 10^4.

10.1.2. CROSS-SECTIONAL SHAPE

The interaction correction factors given are for circular cross-section bends. Limitations on applying the loss coefficients to other cross-sections are outlined.

10.2. COMBINATIONS OF 90° BENDS (CLASS 1)

The notation used for combinations of 90° bends is shown in Fig. 10.1.

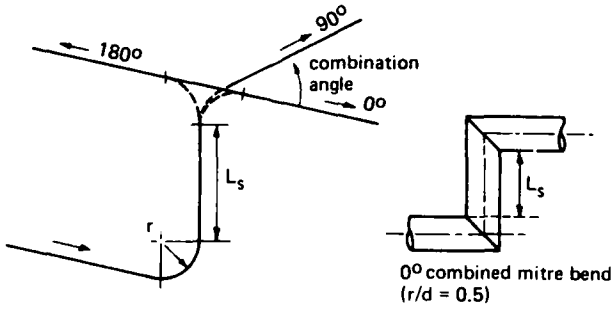

Fig. 10.1. Notation for combinations of two 90° degree bends

Table 10.1 contains interaction correction factors for bend - spacer - bend combinations with spacer lengths of 0, 1, 4 and 8 diameters and bend radius ratios of 1, 2, and 3. Interaction correction factors for combinations of two bends of the same radius ratio are plotted in Figs. 10.2, 10.3, and 10.4.

Table 10.1

Interaction correction factors for combinations of two 90 degree bends

Spacer*	0	1	4	8	0	1	4	8	0	1	4	8
θ_c†	r/d = 1 + spacer + r/d = 1				r/d = 1 + spacer + r/d = 2				r/d = 1 + spacer + r/d = 3			
0	1.00	.86	.71	.81	1.06	.91	.74	.83	1.02	.93	.78	.87
30	1.16	1.04	.94	.83	1.15	1.05	.85	.84	1.06	1.05	.83	.83
60	1.04	.93	.76	.82	1.01	.96	.82	.84	.97	.92	.83	.83
90	.81	.79	.74	.82	.81	.86	.80	.82	.86	.90	.82	.83
120	.69	.69	.72	.81	.71	.78	.79	.81	.78	.82	.82	.83
150	.60	.63	.73	.81	.64	.71	.78	.81	.72	.78	.81	.84
180	.53	.58	.71	.80	.60	.64	.77	.81	.67	.72	.81	.85
θ_c†	r/d = 2 + spacer + r/d = 1				r/d = 2 + spacer + r/d = 2				r/d = 2 + spacer + r/d = 3			
0	.76	.74	.69	.74	.86	.83	.72	.77	.88	.85	.74	.83
30	.73	.72	.73	.79	.79	.79	.71	.81	.84	.83	.77	.82
60	.71	.70	.74	.80	.77	.74	.70	.81	.81	.81	.79	.83
90	.67	.68	.74	.80	.73	.71	.70	.80	.78	.79	.81	.84
120	.64	.66	.75	.81	.68	.68	.69	.80	.76	.77	.82	.85
150	.60	.64	.75	.81	.63	.65	.69	.80	.72	.75	.82	.86
180	.57	.62	.75	.81	.58	.62	.72	.80	.69	.73	.83	.87
θ_c†	r/d = 3 + spacer + r/d = 1				r/d = 3 + spacer + r/d = 2				r/d = 3 + spacer + r/d = 3			
0	.79	.76	.70	.76	.85	.83	.72	.77	.86	.87	.82	.85
30	.76	.75	.73	.81	.83	.81	.74	.81	.83	.85	.81	.85
60	.73	.73	.75	.81	.80	.79	.75	.80	.81	.83	.81	.85
90	.70	.72	.77	.81	.76	.76	.76	.80	.78	.79	.80	.85
120	.68	.70	.78	.82	.73	.74	.77	.80	.76	.77	.80	.85
150	.65	.69	.78	.82	.69	.71	.77	.80	.74	.75	.79	.85
180	.64	.68	.79	.82	.65	.68	.77	.80	.71	.73	.79	.85

*Spacer lengths in diameters

†θ_c combination angle, Fig. 10.1.

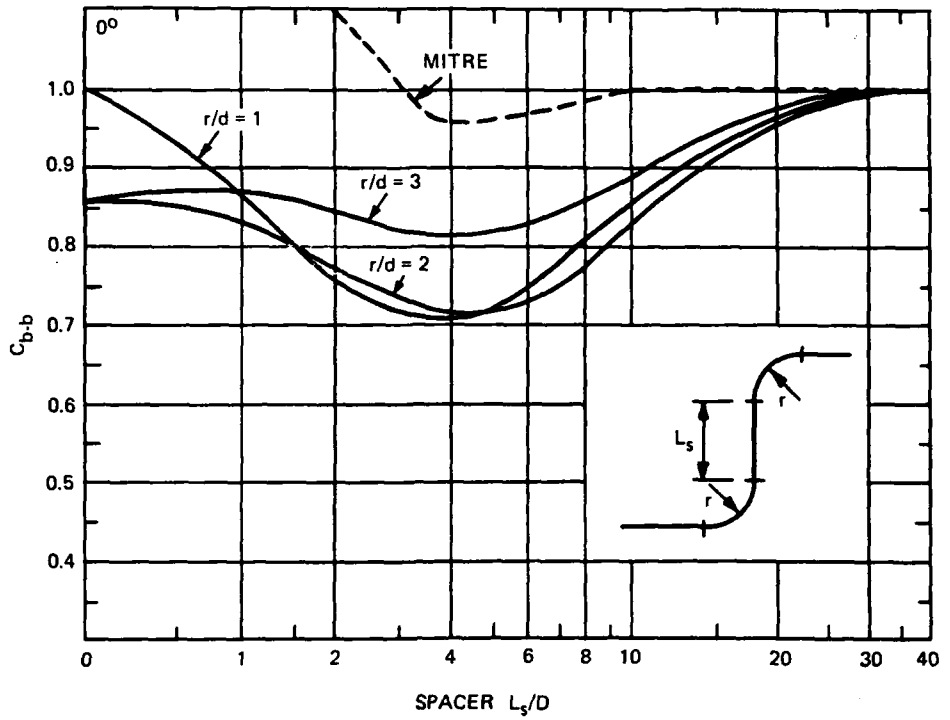

Fig. 10.2. Correction factors for 0° combined bends

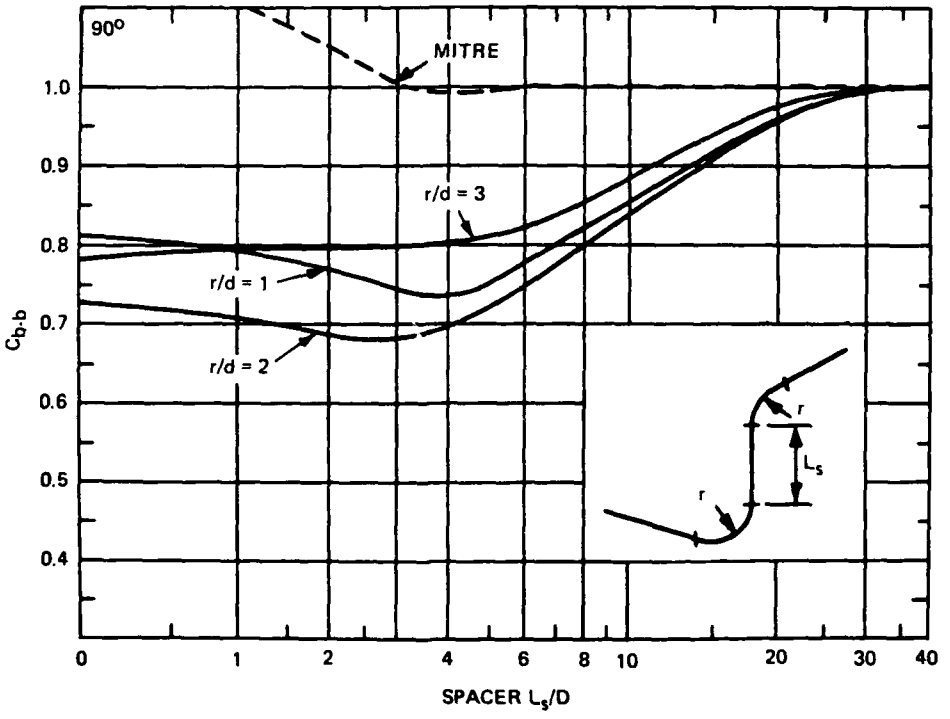

Fig. 10.3. Correction factors for 90° combined bends

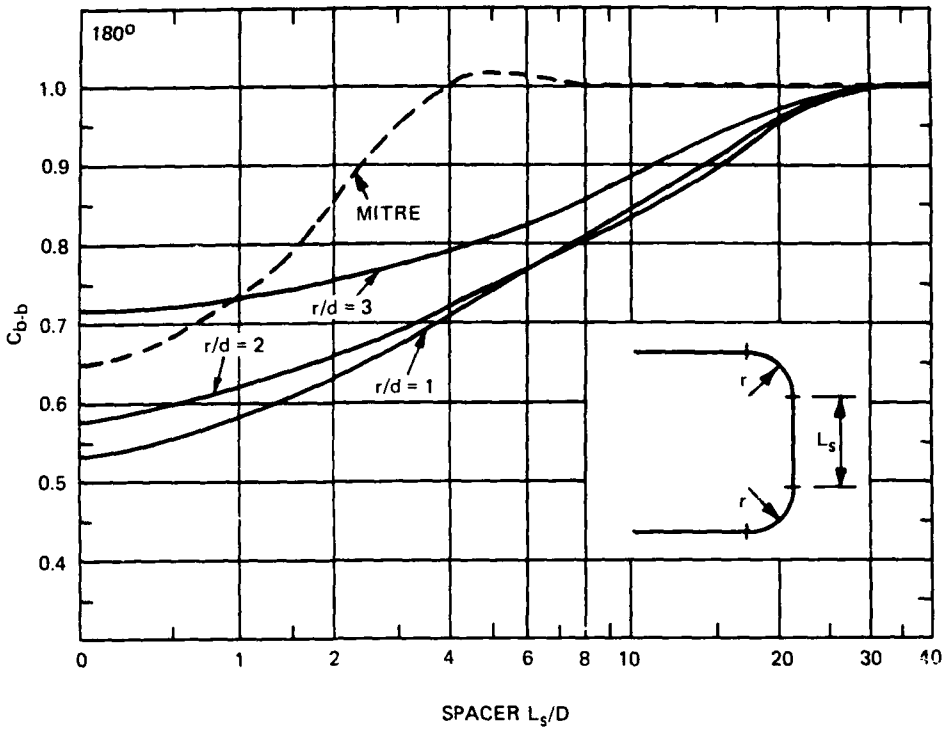

Fig. 10.4. Correction factors for 180° combined bends

Mitre bend interaction correction factors for 0° combined bends exceed 3 at zero spacer length.

Bend interaction correction factors are at a maximum at a combination angle of about 30° This arrangement gives rise to a strong secondary rotation that can be detected 100 diameters or more after the second bend.

10.2.1. EXAMPLE

Determine the head loss between station 1 and 6 in Fig. 10.5. for water flowing at 2 m/s. The 0.5 m diameter pipe can be taken as hydraulically smooth and the kinematic viscosity is 1.14×10^{-6} m^2/s.

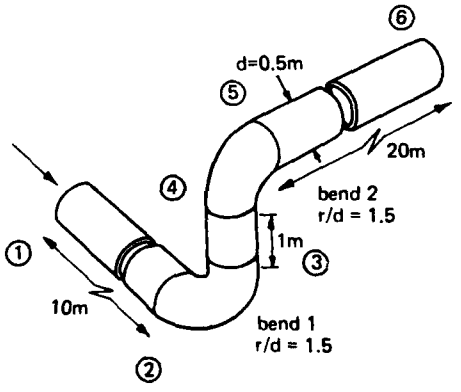

Fig. 10.5. 90° combined bend

$$\text{Re} = \frac{UD}{\nu} = \frac{2 \times 0.5}{1.14 \times 10^{-6}} = 0.88 \times 10^6$$

2. From Fig. 8.1. the friction coefficient for a hydraulically smooth pipe with a Reynolds number of 0.88×10^6 is:

$$f = 0.0118$$

3. From Fig. 9.2. the basic loss coefficient for a $r/d = 1.5$ bend is:

$$K_b^* = 0.185$$

The Reynolds number correction factor for a $r/d = 1.5$ bend at Re = 0.88×10^6 from Fig. 9.3. is 1.0.

4. Interpolating between the r/d = 1 and 2 curves of Fig. 10.2. the interaction factor for the two $r/d = 1.5$ bends with a 2 diameter spacer is 0.74.

5. From equation 10.1.

$$K_{b\text{-}b} = (0.185 + 0.185) \times 0.74$$

$$= 0.274$$

6. Loss coefficient for the three sections of pipe between stations 1 and 6

$$K_f = f\frac{L}{D} = 0.0118 \frac{(10 + 1 + 20)}{0.5} = 0.732$$

7. Total head loss between 1 and 6

$$\Delta H = K_{total} \times \frac{U^2}{2g} = (0.274 + 0.732) \times \frac{2^2}{2 \times 9.81}$$

$$= 0.21\text{m}$$

10.3. COMBINATIONS OF TWO SIMILAR BENDS OF LESS THAN 90° (CLASS 2)

Combinations of two similar bends with individual angles greater than 70 degrees have similar correction factors to bends of 90 degrees so the data in Section 10.2. can be used.

Combinations of two similar circular arc bends with angles less than 70 degrees have interaction correction factors similar to those for 0 degree combinations of two 90 degree bends. For combinations of two similar circular arc bends with angles less than 70 degrees use correction factors from Fig. 10.2.

The variation in correction factors for combinations of similar mitre bends with spacers of under 4 diameters is complex. If the individual mitre bend angles are less than 45 degrees and the spacer is >1 diameter, then use the curve for $r/d = 1$ bends in Fig. 10.2. for all combination angles.

10.4 COMBINATIONS OF NON-CIRCULAR CROSS-SECTION BENDS (CLASS 3)

For rectangular bends of aspect ratio less than 0.7 use correction factors from Fig. 10.4. for all combination angles, but reduce their difference from unity by half. That is to say:

$$\text{correction factor} = 1 - \frac{(1 - C_{b\text{-}b})}{2}$$

For rectangular bends of aspect ratios greater than 1.5 use correction factors from Fig. 10.2 for all combination angles.

Between aspect ratios of 0.7 and 1.5 use circular cross-section data.

When bends of different aspect ratios are connected together, such as an aspect ratio 2 to an aspect ratio 0.5, use correction factors from Fig. 10.2.

10.5. COMBINATION OF 90° VANED BENDS (CLASS 2)

An interaction correction factor of unity applies to two 90° bends arranged to form a 0° or an 180° bend.

Notes on Chapter 6

The bend interaction correction factors are based upon experimental work and correlations in:

1. Ito, H., *Experimental and theoretical studies on the flow in curved pipes*, Mem. Inst. of High Speed Mech., Tohoku Univ., Sendai, Japan, 15, paper 142 (1959). (In Japanese)
2. Miller, D.S., *Internal flow: a guide to losses in pipe and duct systems*, Cranfield, Bedford: BHRA, 329pp. (1971)

APPENDIX C: DATA ON PROTOTYPE STUDIES, McNARY AND LOWER GRANITE LOCKS

Table of Contents

Table C1

Observed Lock Water Surface Elevations, Lower Granite Lock, Test 10 Filling Operation

Upper pool elevation = 736.2
Lower pool elevation = 638.1

All air vents closed.
Two filling valves opened in 80 seconds.

Time In Minutes and Seconds	Lock Water Surface Elevation feet	Time In Minutes and Seconds	Lock Water Surface Elevation feet
0:00	638.1	4:15	703.8
0:15	638.4	4:30	706.2
0:30	639.6	4:45	709.5
0:45	641.5	5:00	712.4
1:00	644.5	5:15	715.4
1:15	648.7	5:30	718.1
1:30	653.9	5:45	720.8
1:45	659.0	6:00	723.1
2:00	664.3	6:15	725.4
2:15	669.1	6:30	727.3
2:30	674.0	6:45	729.3
2:45	678.6	7:00	730.9
3:00	683.0	7:15	732.5
3:15	687.3	7:30	733.9
3:30	691.5	7:45	735.0
3:45	695.4	8:00	736.2
4:00	699.3	8:15	737.0

Table C2

Observed Pressures Upstream From Valve, Lower Granite Lock,

Test 10 Filling Operation

Upper pool elevation = 736.2
Lower pool elevation = 638.1
Piezometer elevation = 606.0
Manometer with air bubbler

All vents closed.
Two filling valves opened in 80 seconds.

Time seconds	Pressure Above Piezometer, feet	Time seconds	Pressure Above Piezometer, feet
00	130.3	125	58.8
05	128.0	130	61.1
10	125.7	135	63.4
15	128.0	140	63.4
20	130.3	145	65.7
25	123.4	150	65.7
30	121.1	155	68.0
35	121.1	160	70.4
40	118.8	165	70.4
45	111.9	170	72.7
50	104.9	175	75.0
55	98.0	180	75.0
60	93.4	185	77.3
65	86.5	190	79.6
70	77.3	195	81.9
75	65.7	200	84.2
80	58.8	205	84.2
85	54.2	210	84.2
90	54.2	215	86.5
95	54.2	220	86.5
100	54.2	225	88.8
105	54.2	230	88.8
110	54.2	235	91.1
115	56.5	240	91.1
120	56.5		

Table C3

Observed Pressures Downstream From Valve, Lower Granite Lock, Test 10 Filling Operation

Upper pool elevation = 736.2
Lower pool elevation = 638.1
Pressure cell elevation = 606.0

All air vents closed.
Two filling valves opened in 80 seconds.

Time seconds	Pressure Above Cell feet
0	32.1
10	25.1
20	19.8
30	10.8
40	1.4
50	-7.8
60	-10.8
70	+0.5
80	42.2
90	44.3
100	47.5
110	48.9
120	52.6
130	57.4
140	60.2
150	63.7
160	66.4
170	69.7
180	73.1

Note: Instantaneous minimum pressure is -24.0 feet and occurred 49 seconds after valves started to open.

Table C4

Computation of Discharge, Lower Granite Lock, Prototype Test 10

Filling Operation, Two Valves

(1) Time t sec	(2) Lock Water Surface Elevation, z ft	(3) Δz in Δt ft	(4) Rate of Rise, r, ft per min	(5) q For One Culvert cfs	(6) q_c For One Culvert From Curve cfs	(7) Velocity V_c, ft per sec
0	638.10					
3	638.12	0.03	0.6	314	250	1.488
6	638.13					
9	638.20	0.15	1.5	785	850	5.060
12	638.28					
15	638.40	0.31	3.1	1,623	1,500	8.929
18	638.59					
21	638.80	0.43	4.3	2,251	2,170	12.917
24	637.02					
27	639.31	0.56	5.6	2,931	2,860	17.024
30	639.58					
33	639.90	0.67	6.7	3,507	3,570	21.250
36	640.25					
39	640.68	0.80	8.0	4,187	4,300	25.595
42	641.05					
45	641.48	0.95	9.5	4,972	5,110	30.417
48	642.00					
51	642.58	1.18	11.8	6,176	6,030	35.893
54	643.18					
57	643.89	1.35	13.5	7,066	7,050	41.964
60	644.53				7,590	45.179

(Continued)

Note: Δz = change in lock water surface in 6 seconds
$q = A_s/(2 \times 60) \times r$, where A_s = length × width of lock
q_c = values read from smooth curve through values of column 3
$V_c = q_c/A_c$, where A_c = area of 1 culvert at valve
$A_s = 730.2 \times 86 = 62{,}797$ sq ft
r = rate of rise of lock water surface, ft per min

(Sheet 1 of 6)

Table C4 (Continued)

(1) Time t sec	(2) Lock Water Surface Elevation, z ft	(3) Δz in Δt ft	(4) Rate of Rise, r, ft per min	(5) q For One Culvert cfs	(6) q_c For One Culvert From Curve cfs	(7) Velocity V_c, ft per sec
63	645.30	1.52	15.2	7,956	8,120	48.333
66	646.05				8,650	51.488
69	647.00	1.77	17.7	9,264	9,220	54.881
72	647.82				9,780	58.814
75	648.80	1.96	19.6	10,259	10,160	60.576
78	649.78				10,410	61.964
81	650.79	2.02	20.2	10,573	10,580	62.976
84	651.80					
87	652.82	2.06	20.6	10,782	10,780	64.167
90	653.86					
93	654.91	2.10	21.0	10,991	10,850	64.583
96	655.96					
99	657.00	2.07	20.7	10,834	10,860	64.643
102	658.03					
105	659.07	2.08	20.8	10,887	10,820	64.425
108	660.11					
111	661.16	2.05	20.5	10,780	10,740	63.929
114	662.20					
117	663.21	2.02	20.2	10,573	10,610	63.155
120	664.22					
123	665.23	2.01	20.1	10.520	10,480	62.381
126	666.23					
129	667.21	1.91	19.1	9,997	10,330	61.438
132	668.14					
135	669.10	1.91	19.1	9,997	10,180	60.595
138	670.05					
141	671.01	1.91	19.1	9,997	10,030	59.702
144	671.96					

(Continued)

Table C4 (Continued)

(1) Time t sec	(2) Lock Water Surface Elevation, z ft	(3) Δz in Δt ft	(4) Rate of Rise, r, ft per min	(5) q For One Culvert cfs	(6) q_c For One Culvert From Curve cfs	(7) Velocity V_c, ft per sec
147	672.91	1.89	18.9	9,892	9,890	58.869
150	673.85					
153	674.81	1.90	19.0	9,945	9,750	58.036
156	675.75					
159	676.70	1.86	18.6	9,735	9,610	57.202
162	677.61					
165	678.51	1.80	18.0	9.421	9,470	56.369
168	679.41					
171	680.29	1.73	17.3	9,055	9,330	55.536
174	681.14					
177	682.01	1.74	17.4	9,107	9,190	54.702
180	682.88					
183	683.76	1.74	17.4	9,107	9,040	53.810
186	684.63					
189	685.50	1.72	17.2	9,002	8,900	52.976
192	686.36					
195	687.22	1.73	17.3	9,055	8,760	52.143
198	688.09					
201	688.98	1.72	17.2	9,002	8,610	51.250
204	689.81					
207	690.65	1.69	16.9	8,845	8,470	50.417
210	691.50					
213	692.31	1.61	16.1	8,427	8,330	49.583
216	693.11					
219	693.90	1.58	15.8	8,270	8,190	48.750
222	694.69					
225	695.48	1.56	15.6	8,165	8,050	47.917
228	696.25					

(Continued)

Table C4 (Continued)

(1) Time t sec	(2) Lock Water Surface Elevation, z ft	(3) Δz in Δt ft	(4) Rate of Rise, r, ft per min	(5) q For One Culvert cfs	(6) q_c For One Culvert From Curve cfs	(7) Velocity V_c, ft per sec
231	697.01	1.52	15.2	7,956	7,910	47.083
234	697.77					
237	698.51	1.48	14.8	7,746	7,760	46.190
240	699.25					
243	699.98	1.46	14.6	7,642	7,620	45.357
246	700.71					
249	701.42	1.45	14.5	7,589	7,480	44.524
252	702.16					
255	702.88	1.41	14.1	7,380	7,340	43.690
258	703.57					
261	704.26	1.35	13.5	7,066	7,200	42.857
264	704.92					
267	705.60	1.36	13.6	7,118	7,050	41.964
270	706.28					
273	706.94	1.32	13.2	6,909	6,910	41.131
276	707.60					
279	708.23	1.29	12.9	6,752	6,770	40.298
282	708.87					
285	709.49	1.26	12.6	6,595	6,630	39.464
288	710.05					
291	710.62	1.16	11.6	6,071	6,490	38.631
294	711.21					
297	711.80	1.17	11.7	6,124	6,350	37.798
300	712.38					
303	712.99	1.19	11.9	6,228	6,210	36.964
306	713.57					
309	714.14	1.14	11.4	5,967	6,070	36.131
312	714.71					

(Continued)

Table C4 (Continued)

(1) Time t sec	(2) Lock Water Surface Elevation, z ft	(3) Δz in Δt ft	(4) Rate of Rise, r, ft per min	(5) q For One Culvert cfs	(6) q_c For One Culvert From Curve cfs	(7) Velocity V_c, ft per sec
315	715.30	1.18	11.8	6,176	5,930	35.298
318	715.89					
321	716.45	1.11	11.1	5,810	5,790	34.464
324	717.00					
327	717.54	1.11	11.1	5,810	5,650	33.631
330	718.11					
333	718.66	1.10	11.0	5,757	5,500	32.738
336	719.21					
339	719.73	1.01	10.1	5,286	5,370	31.964
342	720.22					
345	720.73	0.99	9.9	5,182	5,220	31.071
348	721.21					
351	721.70	0.99	9.9	5,182	5,090	30.298
354	722.20					
357	722.69	0.99	9.9	5,182	4,950	29.464
360	723.13					
363	723.60	0.90	9.0	4,711	4,800	28.571
366	724.03					
369	724.47	0.87	8.7	4,554	4,670	27.798
372	724.90					
375	725.33	0.83	8.3	4,344	4,510	26.845
378	725.73					
381	726.12	0.79	7.9	4,135	4,360	25.952
384	726.52					
387	726.91	0.79	7.9	4,135	4,250	25.298
390	727.31					
393	727.70	0.79	7.9	4,185	4,090	24.345
396	728.11					

(Continued)

Table C4 (Concluded)

(1) Time t sec	(2) Lock Water Surface Elevation, z ft	(3) Δz in Δt ft	(4) Rate of Rise, r, ft per min	(5) q For One Culvert cfs	(6) q_c For One Culvert From Curve cfs	(7) Velocity V_c, ft per sec
399	728.49	0.79	7.9	4,185	3,970	23.681
402	728.90					

(Sheet 6 of 6)

Table C5

Culvert Dimensions, Lower Granite Lock

	Description and Location	Length ft	Upper End Height ft	Upper End Width ft	Lower End Height ft	Lower End Width ft	Average Areas End Area sq ft	Average Areas Less Fillets sq ft
L_1	Downstream intake port to beginning of vertical curve	72*	30	12.0	30	12.0	360	355.5
L_2	Vertical curve section (transition section)	129	30	12.0	14	12.0	264	259.5
L_3	End of vertical curve to valve shaft	28	14	12.0	14	12.0	168	168.0
L_{vw}	Upstream edge of valve shaft to downstream edge of shaft	22	14	12.0	14	12.0	168	168.0
L_5	Downstream edge of valve shaft to start of expansion	56	14	12.0	14	12.0	168	168.0
L_6	Transition section to upward expansion	75	14	12.0	22	12.0	216	211.5
L_7	Start of expanded section to start of horizontal divide	139	22	12.0	22	12.0	264	259.5
L_8	Curved section at horizontal divider	122	20	12.0	20	12.0	240	235.5
L_9	Transition section in central culvert	67	22	12.0	17	15.9	267	262.5
L_{10}	Transition section at vertical divide to curve	87	17	13.9	15	18.0	253	248.5
L_{11}	Transition on curve to center line of ports	92	15	16.0	12	20.0**	240	235.5

* Average length for riverward and landward culverts.
** Combined area of 4 manifolds for 1 culvert.

Table C6

Equivalent Culvert Length, Lower Granite Lock

(For Inertia Correction)

Area No.	Area, A sq ft	Length, L ft	$\frac{A_v^{**}}{A}$	$\frac{L \times A_v}{A}$
A_1	355.5	72*	0.473	34.056
A_2	259.5	129	0.647	83.463
A_3	168.0	28	1.000	28.000
A_v	168.0	22	1.000	22.000
A_5	168.0	56	1.000	56.000
A_6	211.5	75	0.794	59.550
A_7	259.5	139	0.647	89.933
A_8	235.5	122	0.713	86.986
A_9	262.5	67	0.640	42.880
A_{10}	248.5	87	0.676	58.812
A_{11}	235.5	92	0.713	65.596
				$L' = 627.276$

Note:

$$L' = L_1 \frac{A_v}{A_1} + L_2 \frac{A_v}{A_2} + L_3 \frac{A_v}{A_3} + \cdots L_n \frac{A_v}{A_n}$$

$$L' = 627.276 \qquad \frac{L'}{g} = \frac{627.276}{32.2} = 19.481$$

$$L'_{uc} = 145.519 \qquad \frac{L'_{uc}}{g} = \frac{145.519}{32.2} = 4.519$$

$$L'_{uv} = 167.519 \qquad \frac{L'_{uv}}{g} = \frac{167.519}{32.2} = 5.202$$

* Average of landside and riverside culverts

** $A_v = 12 \times 14$ ft = 168 sq ft

Table C7

Valve Opening Versus Time, Lower Granite Lock, Test 10

(1) Time seconds	(2) Valve Opening feet	(3) Time seconds	(4) Valve Opening b/B percent
6	0.65	0	0
11	1.86	3	0.023
17	2.11	6	0.048
22	2.81	9	0.074
28	3.76	12	0.102
40	5.62	15	0.131
46	6.65	18	0.163
53	7.75	21	0.196
61	8.94	24	0.228
67	10.24	27	0.260
74	11.70	30	0.293
80	13.40	33	0.324
83	14.84	36	0.356
		39	0.390
		42	0.424
		45	0.457
		48	0.491
		51	0.526
		54	0.560
		57	0.597
		60	0.686
		63	0.674
		66	0.715
		69	0.760
		72	0.810
		75	0.861
		78	0.919
		81	0.980
		84	1.000

Table C8

Calculation of Culvert Loss Coefficient, k_c, With Valves Fully Open, Lower Granite Lock, Test 1[illegible]

Time, t sec	b/B	Q_c cfs	V_c ft/sec	ΔV_c ft/sec	$\Delta V_c/\Delta t$ ft/sec^2	H_m ft	z	$H = Z_u - z$ ft	$H + H_m$ ft	$V_c^2/2g$ ft	k_c
11[illegible]		10,6[illegible]	63.15[illegible]								
120	1.00										
123		10,480	62.381	-0.774	-0.129	2.513	665.23	70.97	73.483	60.425	1.216
126							666.23				
129		10,330	61.488	-0.893	-0.149	2.903	667.21	68.99	71.893	58.708	1.225
132							668.14				
135		10,180	60.595	-0.893	-0.149	2.903	669.10	67.10	70.003	57.015	1.228
138							670.05				
141		10,030	59.702	-0.893	-0.149	2.903	671.01	65.19	68.093	55.347	1.230
144							671.96				
147		9,890	58.869	-0.833	-0.139	2.708	672.91	63.29	65.998	53.813	1.226
150							673.85				
153		9,750	58.036	-0.833	-0.139	2.708	674.81	61.39	64.098	52.301	1.226
156							675.75				
159		9,610	57.202	-0.834	-0.139	2.708	676.70	59.50	62.208	50.809	1.224
162							677.61				
165		9,470	56.369	-0.833	-0.139	2.708	678.51	57.69	60.398	49.340	1.224
168							679.41				
171		9,330	55.536	-0.833	-0.139	2.708	680.29	55.91	58.618	47.892	1.224
174							681.14				
177		9,190	54.702	-0.834	-0.139	2.708	682.01	54.19	56.898	46.464	1.225
180							682.88				
183		9,040	53.810	-0.892	-0.149	2.903	683.76	52.44	55.343	44.961	1.231
186							684.63				
189		8,900	52.976	-0.834	-0.139	2.708	685.50	50.70	53.408	43.579	1.226
192							686.36				
195		8,760	52.143	-0.833	-0.139	2.708	687.22	48.98	51.688	42.219	1.224
198							688.09				
201		8,610	51.250	-0.893	-0.149	2.903	688.98	47.22	50.123	40.785	1.229
204							689.81				
207	1.00	8,470	50.417	-0.833	-0.139	2.708	690.65	45.55	48.258	39.470	1.223
210	1.00						691.50				
213		8,330	49.583	-0.834	-0.139	2.708	692.31	43.89	46.598	38.175	1.221
216							693.11				
219		8,190	48.750	-0.833	-0.139	2.708	693.90	42.30	45.008	36.903	1.220
222							694.69				
225		8,050	47.917	-0.833	-0.139	2.708	695.48	40.72	43.428	35.653	1.218
228							696.25				
231		7,910	47.083	-0.834	-0.139	2.708	697.01	39.19	41.898	34.422	1.217
234							697.77				
237		7,760	46.190	-0.893	-0.149	2.903	698.51	37.69	40.593	33.129	1.225
240							699.25				
243		7,620	45.357	-0.833	-0.139	2.708	699.98	36.22	38.928	31.945	1.219
246							700.71				
249		7,480	44.524	-0.833	-0.139	2.708	701.42	34.78	37.488	30.782	1.218
252							702.16				
255		7,340	43.690	-0.834	-0.139	2.708	702.88	33.32	36.023	29.640	1.216
258							703.57				
261		7,200	42.857	-0.833	-0.139	2.708	704.26	31.94	34.648	28.521	1.215
264							704.92				
267		7,050	41.964	-0.893	-0.149	2.903	705.60	30.60	33.503	27.344	1.225
270							706.28				
273		6,910	41.131	-0.833	-0.139	2.708	706.94	29.26	31.968	26.270	1.217
276							707.60				
279		6,770	40.298	-0.833	-0.139	2.708	708.23	27.97	30.678	25.216	1.217
282	1.00						708.87				
285		6,630	39.464	-0.834	-0.139	2.708	709.49	26.71	29.418	24.183	1.216
288							710.08				
291		6,490	38.631	-0.833	-0.139	2.708	710.62	25.58	28.288	23.173	1.221
294							711.21				
297		6,350	37.798	-0.833	-0.139	2.708	711.80	24.40	27.108	22.185	1.222
300							712.38				
303		6,210	36.964	-0.834	-0.139	2.708	712.99	23.21	25.918	21.216	1.222
306							713.57				
309		6,070	36.131	-0.833	-0.139	2.708	714.14	22.06	24.768	20.271	1.222
312							714.71				
315		5,930	35.298	-0.833	-0.139	2.708	715.30	20.90	23.608	19.347	1.220
318							715.89				
321		5,790	34.464	-0.834	-0.139	2.708	716.45	19.75	22.453	18.44[illegible]	1.21[illegible]
324							717.00				
327	1.00	5,650	33.631	-0.833	-0.139	2.708	717.54	18.66	21.368	17.56[illegible]	1.217

Average value = 1.22[illegible]

Notes: Values of Q_c and z are from Table C[illegible]

$L/B = 627.28/32.2 = 19.481$

$H_m = 19.481 * \Delta V_c/\Delta t$

z = elevation of lock water surface

Z_u = elevation of upper pool = 736.2

$H = Z_u - z$

$H_{L_c} = H + H_m$

$k_c = H_{L_c}/V_c^2/2g$

t_Δ = 80 seconds

Table C9

Calculation of Loss Coefficient, k_{uc}, of Culvert Upstream From Valve

Lower Granite Lock, Test 10, Two Valves Fully Open

Time t sec	b/B	q cfs	V_c fps	ΔV_c fps	$\Delta V_c/\Delta t$ ft/sec^2	$H_{m_{uc}}$ feet	Z_{vw}	ΔZ_{vw} feet	$\Delta Z_{vw}+H_{m_{uc}}$ feet	$\frac{V_c^2}{2g}$ feet	$H_{L_{uc}}$ feet	k_{uc}
135	1.00	10,180	60.595	-0.893	-0.149	0.673	668.5	67.7	68.373	57.015	11.358	0.199
165		9,470	56.369	-0.833	-0.139	0.628	677.6	58.6	59.228	49.340	9.888	0.200
183		9,040	53.810	-0.892	-0.149	0.673	683.0	53.2	53.873	44.961	8.912	0.198
201		8,610	51.250	-0.893	-0.149	0.673	688.7	47.5	48.173	40.785	7.388	0.181
213		8,330	49.583	-0.834	-0.139	0.628	691.9	44.3	44.928	38.175	6.753	0.177
219		8.190	48.750	-0.833	-0.139	0.628	693.5	42.7	43.328	36.903	6.425	0.174
225		8,050	47.917	-0.833	-0.139	0.628	694.9	41.3	41.928	35.653	6.275	0.176
237		7,760	46.190	-0.893	-0.149	0.673	697.5	38.7	39.373	33.127	6.246	0.189
243		7,620	45.357	-0.833	-0.139	0.628	698.6	37.6	38.228	31.945	6.283	0.197
123		10,480	62.381	-0.774	-0.129	0.583	664.8	71.4	71.983	60.425	11.558	0.191
147	1.00	9,890	58.869	-0.835	-0.139	0.628	672.2	64.0	64.628	53.813	10.815	0.201
										Average value =		0.189

Notes: ΔV_c values were taken from Table C8 and represent the difference between V_c at the time shown and the V_c value 6 seconds earlier.

$H_{m_{uc}} = 4.519\ \Delta V_c/\Delta t$

Z_{vw} is taken from curve plotted from data in Table C2

$\Delta Z_{vw} = Z_u - Z_{vw} = (736.6 - Z_{vw})$

$H_{L_{uc}} = \Delta Z_{vw} + H_{m_{uc}} - V_c^2/2g$

$k_{uc} = H_{L_{uc}}/V_c^2/2g$

Table C10

Computation of Valve Loss Curve, k_v, Versus Percent of Valve Opening, b/B

Lower Granite Lock, Test 10, Two Valve Filling Operation

Time t sec	b/B	q cfs	V_c ft/sec	ΔV_c ft/sec	$\Delta V_c/\Delta t$ ft/sec^2	H_m ft	z	$H=Z_u-z$ ft	$H_L=H-H_m$ ft	$V_c^2/2g$ ft	$H_{L_c}=k_c V_c^2/2g$ ft	$H_{L_v}=H_L-H_{L_c}$ ft	k_v
0	0						638.10	98.10					
3	0.023	250	1.488	1.488	0.496	9.663	638.12	98.08	88.417	0.034	0.042	88.375	2,599.000
6	0.048						638.13	98.07					
9	0.074	850	5.060	3.572	0.595	11.591	638.20	98.00	86.409	0.398	0.486	85.923	215.887
12	0.102	1,180	7.024				638.28	97.92					
15	0.131	1,500	8.929	3.869	0.645	12.565	638.40	97.80	85.235	1.238	1.513	83.722	67.627
18	0.163						638.59	97.61					
21	0.196	2,170	12.917	3.988	0.665	12.955	638.80	97.40	84.445	2.591	3.166	81.279	31.370
24	0.228						639.02	97.18					
27	0.260	2,860	17.024	4.107	0.685	13.344	639.31	96.89	83.546	4.500	5.499	78.047	17.344
30	0.293	3,210	19.107				639.58	96.62					
33	0.324	3,570	21.250	4.226	0.704	13.715	639.90	96.30	82.585	7.012	8.569	74.016	10.556
36	0.356						640.25	95.95					
39	0.390	4,300	25.595	4.345	0.724	14.104	640.68	95.52	81.416	10.172	12.430	68.986	6.782
42	0.424						641.05	95.15					
45	0.457	5,110	30.517	4.822	0.804	15.663	641.48	94.72	79.057	14.366	17.555	61.502	4.281
48	0.491						642.00	94.20					
51	0.526	6,030	35.893	5.476	0.913	17.786	642.58	93.62	75.834	20.005	24.446	51.388	2.569
54	0.560	6,530					643.18	93.02					
57	0.597	7,050	41.964	6.071	1.012	19.715	643.89	93.31	73.595	27.344	33.414	40.181	1.469
60	0.636	7,590	45.179	3.215	1.072	20.884	644.53	91.67	70.786	31.695	38.731	32.055	1.011
63	0.674	8,120	48.333	3.154	1.051	20.475	645.30	90.90	70.425	36.275	44.328	26.097	0.719
66	0.715	8,650	51.488	3.155	1.052	20.494	646.05	90.15	69.656	41.165	50.304	19.352	0.470
69	0.760	9,220	54.881	3.393	1.131	22.033	647.00	89.20	67.167	46.769	57.152	10.015	0.214
72	0.810	9,780	58.214	3.333	1.111	21.643	647.82	88.38	66.737	52.622	64.304	2.433	0.046
75	0.861	10,160	60.476	2.262	0.754	14.689	648.80	87.40	72.711	56.791	69.399	3.312	0.058
78	0.919	10,410	61.964	1.488	0.496	9.663	649.78	86.42	76.757	59.620	72.856	3.901	0.065
81	0.980	10,580	62.976	1.012	0.337	6.565	650.79	83.41	78.845	61.583	75.254	3.591	0.058
84	1.000						651.80	84.40					

Notes: Values of q and z are from Table C4

$L/g = 627.28/32.2 = 19.481$

$H_m = 19.481\ \Delta V/\Delta t$

z = elevation lock water surface

Z_u = elevation of upper pool = 736.2

$H_L = H - H_m$

$H_{L_c} = 1.222\ V_c^2/2g$

$H_{L_v} = H_L - H_{L_c}$

$$k_v = \frac{H_{L_v}}{V_c^2/2g}$$

Table C11

Valve Opening Versus Time, McNary Lock, Two Valve Filling Operation, Test 4

Time seconds	Valve Opening feet	Valve Opening b/B percent
0	0	0
10	0.65	0.054
20	0.90	0.075
30	1.45	0.121
40	1.75	0.146
50	1.80	0.150
60	1.85	0.154
70	2.00	0.167
80	2.00	0.167
90	2.10	0.175
100	2.20	0.185
110	2.25	0.188
120	2.35	0.196
130	2.40	0.200
140	2.45	0.204
150	2.50	0.208
160	2.55	0.213
170	2.60	0.217
180	2.70	0.225
190	2.80	0.233
200	2.85	0.238
210	3.00	0.250
220	3.00	0.250
230	3.05	0.254
240	3.10	0.258
250	3.20	0.267
260	3.30	0.275
270	3.40	0.283

(Continued)

Table C11 (Concluded)

Time seconds	Valve Opening feet	Valve Opening b/B percent
280	3.45	0.288
290	3.50	0.292
300	3.55	0.296
310	3.55	0.296
320	3.70	0.308
330	3.85	0.321
340	3.90	0.325
350	4.00	0.333
360	4.05	0.338
370	4.30	0.358
380	4.50	0.375
390	4.70	0.392
400	5.10	0.425
410	5.50	0.458
420	5.90	0.492
430	6.90	0.575
440	7.50	0.625
450	8.80	0.783
460	10.00	0.833
470	11.00	0.917
480	12.00	1.000

Table C12

Computation of Culvert Loss Coefficient, k_c, With Two Filling Valves Fully Open, McNary Lock, Test -

Time t sec	b/B -	q cfs	V_c ft/sec	ΔV_c ft/sec	$\Delta V_c/\Delta t$ ft/sec^2	H_m ft	z	$H=Z_u-z$ ft	$H+H_m$ ft	$V_c^2/2g$ ft	k_c
480	1.00	6,920	52.424				287.0				
490		6,900	52.273	-0.151	-0.015	+0.218	289.1	51.040	51.258	42.430	1.208
500		6,850	51.894	-0.379	-0.038	+0.553	291.5	48.640	49.19[illegible]	41.81[illegible]	1.17[illegible]
510		6,770	51.288	-0.606	-0.061	+0.888	293.3	46.840	47.72[illegible]	40.84[illegible]	1.16[illegible]
520		6,620	50.152	-1.136	-0.114	+1.659	295.6	44.540	46.19[illegible]	39.05[illegible]	1.18[illegible]
530		6,450	48.864	-1.288	-0.129	+1.878	297.4	42.740	44.118	37.076	1.190
540		6,250	47.348	-1.516	-0.152	+2.212	299.6	40.540	42.752	34.811	1.228
550		5,970	45.227	-2.121	-0.212	+3.087	301.8	38.440	41.527	31.762	1.307
560		5,280	43.788	-1.439	-0.144	+2.096	303.3	36.840	38.986	29.773	1.308
570		5,600	42.424	-1.364	-0.136	+1.979	305.8	34.340	36.319	27.947	1.300
580		5,400	40.909	-1.518	-0.152	+2.212	306.9	33.240	35.452	25.987	1.364
590		5,270	39.924	-0.985	-0.098	+1.441	308.7	31.440	32.881	24.750	1.329
600		5,100	38.636	-1.288	-0.128	+1.863	310.6	29.540	31.403	23.179	1.355
610		4,980	37.727	-0.909	-0.091	+1.325	312.4	27.740	29.065	22.101	1.315
620		4,830	36.591	-1.136	-0.114	+1.659	313.8	26.340	27.999	20.790	1.347
630		4,700	35.606	-0.985	-0.099	+1.441	315.4	24.740	26.181	19.686	1.330
640		4,590	34.773	-0.833	-0.083	+1.208	317.0	23.140	24.348	18.776	1.297
650		4,430	33.561	-1.212	-0.121	+1.761	318.1	22.040	23.801	17.490	1.361
660		4,300	32.576	-0.985	-0.099	+1.441	319.4	20.740	22.181	16.478	1.346
670		4,150	31.439	-1.137	-0.114	+1.659	321.2	18.940	20.599	15.348	1.342
680		4,030	30.530	-0.909	-0.091	+1.325	322.3	17.840	19.165	14.473	1.324
690		3,900	29.546	-0.984	-0.098	+1.426	324.0	16.140	17.566	13.555	1.296
700		3,760	28.488	-1.061	-0.106	+1.543	325.0	15.140	16.683	12.599	1.324
710		3,610	27.348	-1.137	-0.114	+1.659	326.2	13.940	15.599	11.614	1.343
720		3,480	26.364	-0.984	-0.098	+1.426	327.5	12.640	14.066	10.793	1.303
730		3,350	25.379	-0.985	-0.098	+1.426	328.6	11.540	12.966	10.001	1.296
740		3,220	24.394	-0.985	-0.098	+1.426	329.6	10.540	11.966	9.240	1.297

average = 1.294

Notes: Values of q and z are from Reference 10

$L/g = 468.66/32.2 = 14.555$

$H_m = 14.555\ \Delta V/\Delta t$

Z_u = elevation of upper pool - 340.14

$H = Z_u - z$

$H_{L_c} = H + H_m$

$k_c = H + H_m/V_c^2/2g$

t_v = 7 min and 56 sec

Table C-13

Computation of valve loss curve, k_v versus percent of valve opening, b/B

McNary Lock Test 4, two valve filling operation

Time t (sec)	b/B %	q (cfs)	V_c (ft/sec)	ΔV_c (ft/sec)	$\Delta V_c/\Delta t$ (ft/sec^2)	H_m (ft)	z	$H=Z_u-z$ (ft)	$H_L=H-H_m$ (ft)	$V_c^2/2g$ (ft)	$H_{L_c}=k_c V_c^2/2g$ (ft)	$H_{L_v}=H_L-H_{L_c}$ (ft)	k_v
0			0				251.8						
10	0.054	450	3.409	+3.409	+0.341	-4.963	251.9	88.24	83.277	0.180	0.233	83.044	461.356
20	0.075	650	4.924	+1.515	+0.152	-2.212	252.1	88.04	85.828	0.376	0.487	85.341	226.971
30	0.121	800	6.061	+1.137	+0.114	-1.659	252.3	87.84	86.181	0.570	0.738	85.443	149.900
40	0.146	960	7.273	+1.212	+0.121	-1.761	252.5	87.64	85.870	0.821	1.062	84.817	103.309
50	0.150	1090	8.258	+0.935	+0.099	-1.441	252.9	87.24	85.799	1.053	1.363	84.436	80.186
60	0.154	1190	9.0152	+0.759	+0.076	-1.105	253.4	86.74	85.635	1.262	1.633	84.002	66.563
70	0.167	1250	9.470	+0.455	+0.046	-0.670	253.4	86.74	86.070	1.393	1.803	84.267	60.493
80	0.167	1300	9.848	+0.378	+0.038	-0.533	254.2	85.94	85.387	1.505	1.947	83.440	53.442
90	0.175	1360	10.303	+0.455	+0.046	-0.670	254.6	85.540	84.870	1.648	2.133	82.737	50.204
100	0.183	1400	10.606	+0.303	+0.030	-0.437	254.9	85.24	84.803	1.747	2.261	82.456	47.199
110	0.188	1420	10.758	+0.152	+0.015	-0.218	255.3	84.84	84.622	1.797	2.325	82.297	45.797
120	0.196	1460	11.061	+0.303	+0.030	-0.437	255.5	84.64	84.203	1.900	2.459	81.744	43.023
130	0.200	1480	11.212	+0.151	+0.015	-0.218	256.3	83.84	83.662	1.952	2.526	81.136	41.566
140	0.204	1500	11.364	+0.152	+0.015	-0.218	256.9	83.24	83.022	2.005	2.594	80.428	40.114
150	0.208	1530	11.591	+0.227	+0.023	-0.335	257.3	82.84	82.505	2.085	2.698	79.807	38.277
160	0.213	1560	11.818	+0.227	+0.023	-0.335	257.2	82.44	82.105	2.169	2.807	79.298	36.560
170	0.217	1580	11.970	+0.152	+0.015	-0.218	258.1	82.04	81.822	2.225	2.879	78.943	35.480
180	0.225	1600	12.121	+0.151	+0.015	-0.218	258.7	81.44	81.222	2.281	2.952	78.270	34.314
190	0.233	1620	12.273	+0.152	+0.015	-0.218	259.2	80.94	80.722	2.339	3.027	77.695	33.217
200	0.238	1670	12.652	+0.379	+0.038	-0.553	259.8	80.34	79.787	2.485	3.216	76.571	30.813
210	0.250	1690	12.803	+0.151	+0.015	-0.218	260.2	79.94	79.722	2.545	3.293	76.429	30.031
220	0.250	1730	13.106	+0.303	+0.030	-0.437	260.9	79.24	78.803	2.667	3.451	75.352	28.253
230	0.254	1760	13.333	+0.227	+0.023	-0.335	261.4	78.74	78.405	2.760	3.571	74.834	27.114
240	0.258	1790	13.561	+0.228	+0.023	-0.335	262.0	78.14	77.805	2.856	3.696	74.109	25.948
250	0.267	1820	13.788	+0.227	+0.023	-0.335	262.5	77.64	77.305	2.952	3.820	73.485	24.893
260	0.275	1880	14.242	+0.452	+0.045	-0.655	263.1	77.04	76.385	3.150	4.076	72.309	22.955
270	0.283	1910	14.570	+0.328	+0.033	-0.480	263.7	76.44	75.068	3.296	4.265	71.703	21.755
280	0.288	1950	14.773	+0.203	+0.020	-0.291	264.4	75.74	75.449	3.389	4.385	71.064	20.969
290	0.292	2000	15.152	+0.379	+0.038	-0.553	265.0	75.14	74.587	3.565	4.613	69.974	19.628
300	0.296	2030	15.379	+0.227	+0.023	-0.338	265.8	74.34	74.005	3.673	4.753	69.252	18.854
310	0.296	2090	15.833	+0.454	+0.045	-0.655	266.3	73.84	73.185	3.893	5.038	68.148	17.505
320	0.308	2110	15.985	+0.152	+0.015	-0.218	267.2	72.94	72.722	3.968	5.135	67.587	17.033
330	0.321	2150	16.288	+0.303	+0.030	-0.437	267.7	72.44	72.003	4.120	5.331	66.672	16.183

(Continued)

Table C-13 (Continued)

Time t sec	b/B	q cfs	V_c ft/sec	ΔV_c ft/sec	$\Delta V_c/\Delta t$ ft/sec^2	H_m ft	z	$H=Z_u-z$ ft	$H_L=H-H_m$ ft	$v_c^2/2g$ ft	$H_{L_c}=k_c V_c^2/2g$ ft	$H_{L_v}=H_L-H_{L_c}$ ft	k_v
340	0.325	2,220	16.818	40.530	+0.053	-0.771	268.7	71.44	70.669	4.392	5.683	64.986	14.796
350	0.333	2,290	17.348	+0.530	+0.053	-0.771	269.2	70.94	70.169	4.673	6.049	64.122	13.722
360	0.338	2,380	18.030	+0.682	+0.068	-0.990	270.0	70.14	69.150	5.048	6.532	62.618	12.405
370	0.358	2,500	18.939	+0.909	+0.091	-1.325	270.8	69.34	68.015	5.570	7.208	62.445	11.211
380	0.375	2,640	20.000	+1.061	+0.106	-1.543	271.5	68.64	67.098	6.211	8.037	59.060	9.509
390	0.392	2,800	21.212	+1.212	+0.121	-1.761	272.6	67.54	65.779	6.987	9.041	56.738	8.121
400	0.425	3,000	22.727	+1.515	+0.152	-2.212	273.6	66.54	64.828	8.020	10.378	53.950	6.727
410	0.458	3,340	25.303	+2.576	+0.258	-3.755	274.7	65.44	61.685	9.942	12.865	48.820	4.910
420	0.492	3,750	28.409	+3.106	+0.311	-4.527	275.8	64.340	54.813	12.532	16.216	43.597	3.479
430	0.575	4,250	32.197	+4.148	+0.415	-6.040	277.1	63.040	57.000	16.097	20.830	36.170	2.247
440	0.625	5,000	37.879	+5.682	+0.568	-8.267	277.7	62.440	54.173	22.280	28.830	25.343	1.137
450	0.733	6,000	45.455	+7.576	+0.758	-11.033	280.3	59.840	48.807	32.083	41.515	7.293	0.227
460	0.833	6,740	51.061	+5.606	+0.561	-8.165	282.85	57.290	49.125	40.485	52.387		
470	0.917	6,900	52.273	+1.212	+0.121	-1.761	285.4	54.740	52.979	42.480	54.904		
480	1.000	6,920	52.424	+0.151	+0.015	-0.218	287.0	53.140	52.922	42.675	55.221		

Notes: Values of q and z are from Table A-4, Reference 10

L/g = 468.66/32.2 = 14.555

H_m = 14.555 $\Delta V/\Delta t$

Z_u = Elevation of upper pool = 340.14

z = Elevation lock water surface

$H = Z_u - z$

$H_L = H - H_m$

$H_{L_c} = 1.294^m V_c/2g$

$H_{L_v} = H_L - H_{L_c}$

$k_v = H_{L_v}^2/V_c/2g$

tv = 7 min and 56 sec